

# **INVESTIGATING INNATE LYMPHOID CELL FUNCTION IN PRIMARY LYMPHOID TISSUE**

By

**RHYS JONES**

A thesis submitted to the University of Birmingham for the degree of  
DOCTOR OF PHILOSOPHY

Institute of Immunology and Immunotherapy

College of Medical and Dental Sciences

University of Birmingham

December 2019

UNIVERSITY OF  
BIRMINGHAM

**University of Birmingham Research Archive**

**e-theses repository**

This unpublished thesis/dissertation is copyright of the author and/or third parties. The intellectual property rights of the author or third parties in respect of this work are as defined by The Copyright Designs and Patents Act 1988 or as modified by any successor legislation.

Any use made of information contained in this thesis/dissertation must be in accordance with that legislation and must be properly acknowledged. Further distribution or reproduction in any format is prohibited without the permission of the copyright holder.

## **ABSTRACT**

Lymphoid Tissue inducer (LTi) cells are part of the Innate Lymphoid Cell (ILC) family and have been implicated in the development of thymic microenvironments and support their recovery following damage. However, a detailed characterisation of other ILC subsets within the thymus is lacking. This study aimed to characterise the ILC composition of the thymus across ontogeny and investigate their function. Inhibitor of DNA-binding 2 (Id2) is a transcriptional regulator required for the development of ILC subsets. Several *in vivo* models, including Id2 fate mapping and Id2 reporter mice, were used to dissect ILC populations within the thymus. LTi cells, a subset of ILC3, were prominent in the embryo, but numbers reduced in the neonate and continued to decline in the adult, where ILC2 became the dominant population. ILC2 were capable of producing IL-5 and IL-13 *ex vivo*, and through confocal imaging we discovered ILC2 within the thymic medulla. Surprisingly, the majority of Id2 expressing cells in the thymus were not ILC but developing thymocytes, which are present in much greater numbers compared to the number of ILC2. Collectively, we have revealed changes in the ILC compartment of the thymus across ontogeny and started to characterise Id2 expression amongst other lymphocytes.

## **ACKNOWLEDGEMENTS**

I owe my gratitude to many people, both at the University of Birmingham and beyond, who have made a positive impact throughout my PhD. Firstly, I would like to thank my supervisor Dr David Withers, as without his support, submission of this thesis would not have been possible. I feel fortunate to have been able to complete my PhD as part of Dave's laboratory and will always be grateful for the support and encouragement I received.

I also owe thanks to the wonderful group of people within the Withers lab and other members of the department who made my PhD journey ultimately enjoyable. With special thanks to Dr Emma Dutton, Dominika Gajdasik, Dr Zhi "Speedy" Li and Dr Rémi Fiancette, of the Withers lab, for sharing their knowledge and laughter with me on a daily basis. I also thank Claire Willis who has been a fundamental part of my PhD – I thank Claire for always finding the time to help and for her endless supply of bakes. I would also like to thank Dr Fabrina Gaspal for providing the lab with a little "*je ne sais quoi*", and to Dr Emilie Cosway for sharing her expertise on all things thymus and for accompanying me on RACE getaways.

And, finally, I would like to express appreciation for my supportive network of friends and family who have been there for me from the very start of my studies. You will never know how invaluable you have been.



## **TABLE OF CONTENTS**

CHAPTER 1: GENERAL INTRODUCTION.....	1
1.1 Overview of the immune system.....	2
1.1.1 The innate and adaptive immune system.....	2
1.2 T cell development.....	5
1.2.1 Overview .....	5
1.2.2 The thymic microenvironment .....	6
1.2.3 Development through the cortex .....	8
1.2.4 Positive selection.....	9
1.2.5 CD4 CD8 lineage commitment.....	12
1.2.6 Development through the medulla .....	12
1.3 Unconventional T Cells .....	17
1.3.1 Overview .....	17
1.3.2 Invariant Natural Killer T (iNKT) cells .....	18
1.3.3 $\gamma\delta$ T cells .....	21
1.4 Innate Lymphoid Cells (ILC) .....	23
1.4.1 Overview .....	23
1.4.2 Overview of ILC Development.....	25
1.4.3 Transcriptional Control in the Context of Id2 .....	26
1.4.4 Plasticity of ILC.....	28
1.5 Functions of ILC at Peripheral Sites .....	30
1.5.1 Secondary Lymphoid Tissue .....	31
1.5.2 Lung .....	32
1.5.3 Small intestine .....	33
1.6 ILC within the thymus.....	34
1.7 Experimental Approaches for Studying ILC in the Thymus .....	37
1.7.1 Foetal Thymic Organ Culture .....	38
1.7.2 Sub-lethal Irradiation .....	40
1.8 Aims of this investigation .....	42
CHAPTER 2: MATERIALS AND METHODS .....	44
2.1 Mice .....	45

2.2 Medium and reagents .....	50
2.2.1 Medium.....	50
2.2.2 Gey's red blood cell lysis buffer.....	51
2.3 Preparation of single cell suspensions.....	52
2.3.1 Lymph nodes .....	52
2.3.2 Spleen .....	52
2.3.3 Thymus.....	53
2.3.4 Small intestine .....	53
2.3.5 Lung .....	54
2.4 Flow cytometry .....	55
2.5 Cell culture .....	60
2.5.1 <i>In vitro</i> .....	60
2.5.2 Foetal Thymic Organ Culture (FTOC) .....	61
2.6 Immunofluorescence microscopy .....	61
2.6.1 Preparation of frozen tissue .....	61
2.6.2 Immunolabelling of thymus sections .....	61
2.7 <i>In vivo</i> experiments .....	64
2.7.1 Sub-lethal irradiation .....	64
2.7.2 Tamoxifen preparation and administration .....	64
2.7.3 Immunisation with Lm-2W1S.....	64
2.8 Identification of 2W1S-specific T cells .....	65
2.9 Tissue preparation for CD4 <sup>+</sup> enrichment.....	65
2.10 Statistical analysis.....	66
CHAPTER 3: CHARACTERISING ILC POPULATIONS WITHIN THE THYMUS.....	68
3.1 Introduction .....	69
3.2 Results .....	72
3.2.1 Identification of ILCs within the developing thymus.....	72
3.2.2 Using fate-mapping of Id2 to track bona fide ILC populations in the thymus .....	83
3.2.3 Assessing plasticity amongst thymic ILC populations .....	95
3.2.4 ILC2 increase in mice lacking ILC3 .....	96
3.2.5 Characterisation of ILC populations in alternative transgenic mouse models.....	109

3.3 Discussion.....	119
CHAPTER 4: INVESTIGATING THE FUNCTION OF THYMIC ILC .....	130
4.1 Introduction .....	131
4.2 Results .....	135
4.2.1 Early evidence suggests recovery of the thymus is impaired in the absence of ROR $\gamma$ t following injury .....	135
4.2.2 ILC3 are not involved in thymic regeneration following thymic damage.....	139
4.2.3 LT $\alpha$ i cells of the neonatal thymus are capable of producing IL-22 .....	149
4.2.4 ILC3 is a source of RANKL within the neonatal thymus.....	152
4.2.5 ILC2 are capable of producing IL-5 following <i>ex vivo</i> culture .....	155
4.2.6 ILC2 reside in the thymic medulla .....	159
4.2.7 ILC2 within the neonatal thymus share functional similarities to those isolated from adult tissue .....	160
4.3 Discussion.....	164
CHAPTER 5: ASSESSMENT OF ID2 EXPRESSION AMONGST INNATE AND EFFECTOR POPULATIONS .....	173
5.1 Introduction .....	174
5.2 Results .....	178
5.2.1 Characterisation of Id2 expression amongst iNKT cells, $\alpha\beta$ T cells and $\gamma\delta$ T cells .....	178
5.2.2 Id2 is expressed by iNKT1, iNKT2 and iNKT17 cells in the thymus and is maintained in the periphery .....	183
5.2.3 $\gamma\delta$ T cells of multiple developmental lineages express Id2 .....	190
5.2.4 Id2 expression is restricted to an IL-17A-producing lineage in the neonatal thymus .....	200
5.2.5 Id2 expression is greater in T effector memory (Tem) cells when compared to their naïve counterparts.....	201
5.2.6 Id2 is expressed by $\alpha\beta$ and $\gamma\delta$ T cells in effector tissue .....	203
5.2.7 Investigation of Id2 expression following immunisation with Lm-2W1S .....	205
5.3 Discussion.....	220
CHAPTER 6: GENERAL DISCUSSION.....	229
6.1 Overview .....	230
6.2 ILC3 support epithelial development in the embryonic and neonatal thymus.....	233
6.3 Postnatal changes in thymic ILC3 populations .....	234

6.4 ILC2 is the dominant ILC population post-birth .....	236
6.5 Other lymphocytes .....	240
6.6 Further limitations .....	242
6.6 Concluding remarks .....	242
References .....	256

## **LIST OF FIGURES**

### **CHAPTER 1**

Figure 1.1: Overview of $\alpha\beta$ T cell development in the thymus.....	7
Figure 1.2: Pattern of CD4, CD8 and TCR expression during thymocyte development.....	13
Figure 1.3: Phenotypic and functional similarities of T helper subsets and ILC	24
Figure 1.4: Development of ILC.....	29

### **CHAPTER 2**

Figure 2.1: Schematic of frequently used tamoxifen-inducible Cre mouse models in our investigations.....	47
Figure 2.2: Mechanism of Cre induction following administration of tamoxifen in $Id2^{CreERT2} \times ROSA26^{mT/mG}$ .....	48
Figure 2.3: Figure 2.3 Mechanism of Cre induction following administration of tamoxifen in $Id2^{CreERT2} Tbx21^{F/F} \times ROSA26^{RFP}$ mice.....	49

### **CHAPTER 3**

Figure 3.1: Identification of ILC populations in foetal thymic organ cultures.....	77
Figure 3.2: The proportion of ILC in the thymus rapidly declines during neonatal development.....	79
Figure 3.3: The decline in the proportion of ILC coincides with an increase in T cell number.....	80
Figure 3.4: Tracking of ILC2 and ILC3 populations through neonatal development reveals a dramatic decline in ILC3 over time.....	82
Figure 3.5: ILC1 and ILCs lacking GATA-3, ROR $\gamma$ t and Tbet are found within the neonatal thymus .....	84
Figure 3.6: Analysis of thymic ILC populations through fate mapping $Id2$ expression.....	86

Figure 3.7: Analysis of thymic ILC populations through fate-mapping Id2 expression induced by a tamoxifen diet.....	88
Figure 3.8: Administration of tamoxifen by oral gavage results in reduction of double positive thymocytes.....	91
Figure 3.9: Analysis of ILC populations in the thymus of adult Id2-eGFP reporter mice.....	94
Figure 3.10: ILC3 plasticity does not account for the changes amongst ILC subsets post-birth.....	97
Figure 3.11: Analysis of ILC populations in the thymus of adult mice deficient in ROR $\gamma$ t reveal an increase in ILC2.....	99
Figure 3.12: The absence of ILC3 in neonatal mice leads to an increase in thymic ILC2 number.....	102
Figure 3.13: Phenotyping ILC2 populations within the neonatal thymus.....	105
Figure 3.14: Phenotyping ILC3 populations within the neonatal thymus.....	108
Figure 3.15: Assessment of ILC2 and ILC3 in the thymus of C57BL/6 and BALB/c mice identified a similar number of these cells in both mouse strains.	110
Figure 3.16: Comparison of ILC2 and ILC3 in thymus of C57BL/6 and TCR $\alpha^{-/-}$ identified an increase in these cells in TCR $\alpha^{-/-}$ mice.....	112
Figure 3.17: Phenotyping ILC2 in non-lymphoid and lymphoid tissues in TCR $\alpha^{-/-}$ mice.....	115
Figure 3.18: Phenotyping ILC3 in the mLN and thymus of TCR $\alpha^{-/-}$ mice.....	118

## **CHAPTER 4**

Figure 4.1: Recovery of thymus tissue following sub-lethal irradiation is impaired in mice lacking ILC3.....	137
Figure 4.2: Double-positive thymocytes are depleted following sub-lethal irradiation.....	140
Figure 4.3: ILC populations within the thymus of WT and <i>Rorc</i> <sup>-/-</sup> mice are depleted following sub-lethal irradiation.....	143
Figure 4.4: Assessment of IL-22 production by ILC3 in the adult thymus following sub-lethal irradiation using an alternative gating strategy.....	148
Figure 4.5: ILC3 isolated from the neonatal thymus are capable of producing IL-22 following <i>ex vivo</i> stimulation at 7 days post-birth.....	151
Figure 4.6: ILC3 are a source of RANKL in the neonatal thymus.....	154
Figure 4.7: RANKL expression by ILC2 is elevated in the thymus of <i>Rorc</i> <sup>-/-</sup> mice.....	156
Figure 4.8: ILC2 from the thymus of <i>TCRα</i> <sup>-/-</sup> mice are capable of producing IL-5 following <i>ex vivo</i> stimulation.....	158
Figure 4.9: ILC2 are located in the thymic medulla of <i>TCRα</i> <sup>-/-</sup> mice.....	161
Figure 4.10: ILC2 isolated from the neonatal thymus are capable of producing IL-5 and IL-13 following <i>ex vivo</i> stimulation.....	163

## **CHAPTER 5**

Figure 5.1: αβ T cells are the most abundant cells fate-mapped to Id2 in the thymus and mLN.....	180
--	-----

Figure 5.2: The proportion of iNKT cells fate-mapped to Id2 is comparable to that of ILC.....	182
Figure 5.3: Identification of iNKT1, iNKT2 and iNKT17 cells in the thymus and peripheral lymph nodes.....	185
Figure 5.4: Id2 is expressed by iNKT1, iNKT2 and iNKT17 cells in the thymus and is maintained in peripheral lymph nodes.....	188
Figure 5.5: The fate-mapping of iNKT cells to Id2 does not affect the ability of these cells to produce IL-4 or IFN $\gamma$ .....	191
Figure 5.6: $\gamma\delta$ T cells can be classified based on their commitment to IL-17A-producing or IFN $\gamma$ -producing lineages.....	194
Figure 5.7: Id2 is expressed in $\gamma\delta$ T cells of both the IL-17A-producing and IFN $\gamma$ -producing lineage.....	196
Figure 5.8: V $\gamma$ -segment usage amongst Id2 <sup>+</sup> $\gamma\delta$ T cells varies depending on location and effector function.....	199
Figure 5.9: $\gamma\delta$ T cells expressing Id2 in the neonatal thymus are predominantly of the IL-17A-producing lineage.....	202
Figure 5.10: Id2 expression is greater in T effector memory cells compared to naïve T cells in peripheral lymphoid tissue.....	204
Figure 5.11: Id2 is expressed by both $\alpha\beta$ and $\gamma\delta$ T cells in the small intestine.	206
Figure 5.12: Analysis of Id2 expression by effector CD4 <sup>+</sup> T cell subsets following immunisation with Lm-2W1S.....	208
Figure 5.13: Id2 expression is restricted to CXCR5 <sup>-</sup> Th1 effector CD4 <sup>+</sup> T cells 7 days post-immunisation with Lm-2W1S.....	210



Figure 5.14: Increasing Id2 expression corresponds with the increasing number of 2W1S <sup>+</sup> CD4 <sup>+</sup> T cells in response to Lm-2W1S immunisation.....	212
Figure 5.15: Experimental design for investigating Id2 expression amongst CD4 <sup>+</sup> effector T cells during a Th1 response.....	214
Figure 5.16: Id2 expression can be detected amongst CD4 <sup>+</sup> effector T cells in the spleen following immunisation with 2W1S.....	216
Figure 5.17: Tbet can be deleted amongst CD4 <sup>+</sup> effector T cells in the spleen and pLN following Cre induction with tamoxifen.....	218

## **LIST OF TABLES**

Table 2.1: Mouse strains used in this investigation.....	45
Table 2.2: Components used in staining buffer.....	50
Table 2.3: Components used in culture media.....	50
Table 2.4: Components used in staining solution for immunofluorescence microscopy.....	50
Table 2.5: Components of Gey's red blood cell lysis buffer.....	51
Table 2.6: List of antibodies.....	58
Table 2.7: List of Tetramers.....	60
Table 2.8: Primary antibodies used for immunofluorescence microscopy.....	63
Table 2.9: Additional antibodies and streptavidin for immunofluorescence microscopy.....	63

## **ABBREVIATIONS**

$\alpha$ -GalCer	$\alpha$ -Galactosylceramide
Aire	Autoimmune regulator
AP3	Adapter Protein Complex-3
APC	Antigen Presenting Cell
aTreg	Adipose regulatory T cells
BMP	Bone Morphogenetic Protein
CCL	Chemokine CC Ligand
ChILP	Common helper ILC Progenitor
CLP	Common Lymphoid Progenitor
CMJ	Corticomedullary Junction
cTEC	cortical Thymic Epithelial Cells
CXCL	Chemokine CXC Ligand
DC	Dendritic Cell
DL4	Delta-like 4
DN	Double Negative
DP	Double Positive
E	Embryonic day
ETP	Early Thymic Progenitor
FOXP1	Forkhead box protein N1
FoxP3	Forkhead box protein P3
FTOC	Foetal Thymic Organ Culture
GFP	Green Fluorescent Protein
GWAS	Genome-wide Association Studies
Id1	Inhibitor of DNA-binding domain 1
Id2	Inhibitor of DNA-binding domain 2
IFN	Interferon
IL	Interleukin
ILC	Innate Lymphoid Cells
ILC1	Group 1 ILC
ILC2	Group 2 ILC

ILC3	Group 3 ILC
iNKT	invariant Natural Killer T
iNKT1	Type 1 invariant Natural Killer T
iNKT2	Type 2 invariant Natural Killer T
iNKT17	Type 17 invariant Natural Killer T
KO	Knock-out
LTi	Lymphoid Tissue inducer
MAIT	Mucosal Associated Invariant T
mG	“membrane-Green”
mLN	Mesenteric lymph node
MHC	Major Histocompatibility Complex
mT	“membrane-Tomato”
mTEC	medullary Thymic Epithelial Cells
NK	Natural Killer
NKT	Natural Killer T
NKP	Natural Killer cell Precursor
OCT	Optimal Cutting Temperature compound
OVA	Ovalbumin
PAMPs	Pathogen Associated Molecular Patterns
PBS	Phosphate Buffered Saline
pLN	Pooled peripheral lymph nodes
PLZF	Promyelocytic Leukaemia Zinc Finger
PRRs	Pathogen Recognition Receptors
RAG	Recombination-Activating Genes
RANK	Receptor Activator of Nuclear factor $\kappa$ B
RANKL	Receptor Activator of Nuclear factor $\kappa$ B Ligand
RFP	Red Fluorescent Protein
SLI	Sub-lethal Irradiation
Tbet	T-box transcription Factor
TBI	Total-body Irradiation
Tcm	T-central memory
TCR	T-cell Receptor

tDC	thymic Dendritic Cell
TEC	Thymic Epithelial Cells
Tem	T-effector memory
Tfh	T-follicular helper
Th	T-helper
Th1	Type 1 helper T cell
Th2	Type 2 helper T cell
Th17	Type 17 helper T cell
TNF	Tumour Necrosis Factor
TRA	Tissue Restricted Antigens
Treg	T regulatory
TSP	Thymic Seeding Progenitor
VAT	Visceral Adipose Tissue
VDJ	Variable, Diversity and Joining
WT	Wild-type

## **CHAPTER 1: GENERAL INTRODUCTION**

## **1.1 Overview of the immune system**

The general function of the immune system is to provide the host with essential protection against invading pathogens that would otherwise cause damage. Host organisms are constantly under threat from invading pathogens that are inhaled, swallowed or inhabit the skin and mucous membranes.(1) The success of these pathogens to enter a host is dependent on both the pathogenicity of the invading pathogen and the robustness of host defences.(1) The integrity of these host defences relies on a highly structured network of lymphoid tissues, immune cells, cytokines and humoral factors that is reflective of the complex nature of foreign invaders. The importance, of which, is highlighted in cases of immune dysfunction. While immunodeficiency, and the absence or compromise of immune components, leaves the host susceptible to attack, the over activity of these defences can result in the development of autoimmune diseases.(2) Therefore, the regulation and maintenance of immune homeostasis is fundamental for successful host protection.

### **1.1.1 The innate and adaptive immune system**

The immune system has evolved into two distinct arms to ensure sufficient and effective protection against a range of invading pathogens, such as bacteria, viruses, fungi and parasites.(1) These two arms of protection are defined by the speed and specificity of their reactions and are referred to as innate and adaptive immunity.(1) Following breach of physical barriers that act as a first line of defence, mechanisms of immediate innate immunity occur and localised cells act quickly to clear the infection through cell mediators. This is followed by the detection of invading microorganisms based on their expression of pathogen-associated molecular patterns (PAMPs).(3) PAMPs are conserved amongst classes of microorganisms and

enable broad recognition by pathogen recognition receptors (PRRs) in the early innate immune response that occurs between 4-96 hours following infection. In this time, sentinels of the innate immune system, such as macrophages and other phagocytes, express PRRs and their activation leads to inflammation and the recruitment of other immune cells.(3) The non-specific and highly conserved nature of the innate immune system enables fast acting and broad recognition of invading pathogens that supplements their removal. However, cells of the innate immune system are sometimes unable to clear the host of the infection and require input from the adaptive immune response.(4)

The adaptive immune system is a function of higher organisms and enables a specialised and highly specific immune response that requires involvement from both B and T lymphocytes.(4) This side of the immune system initiates following proliferation of the invading pathogen and accumulation of its antigen. This antigen is detected and processed by specialised cells, known as antigen-presenting cells (APC), and presented on surface as part of a class I or class II a major histocompatibility complex (MHC). Naïve B and T cells circulate the blood and lymphatic systems until they encounter a cognate antigen for which they have specificity.(4) The interaction between naïve lymphocytes and antigen occurs within secondary lymphoid structures, such as the spleen or lymph nodes, and results in clonal expansion of lymphocytes with specificity for the encountered antigen. While these actions support an antigen specific immune response, the process takes several days to develop, which is much greater than it takes for the innate immune system to respond. However, the adaptive immune system encompasses immunological memory and enables an immediate response following exposure to



the same antigen.(4) Although innate and adaptive immunity are described as separate entities due their discrete functions, it is the interplay between these two sides that provide complete protection for the host.

The adaptive immune system has the advantage of generating effector populations towards a specific pathogen and the ability to generate immunological memory. However, its action relies on signals from the innate immune system to initiate and direct its response.(5) Dendritic cells are a prime example of how signals from the innate immune system dictate the effector response of the adaptive immune system. Following antigen processing, these cells are capable of loading antigenic peptides onto their surface in either MHC class I or MHC class II molecules. The ability of dendritic cells to present antigen in either of these molecules enables them to interact with both CD8<sup>+</sup> and CD4<sup>+</sup> T cells.(5) Innate lymphoid cells (ILC) represent a recently emerged class of lymphocytes that, in addition to dendritic cells, have been shown to influence the adaptive immune response. Specifically, a subclass of these cells has been shown to express MHC class II and present antigen to CD4<sup>+</sup> T cells. However, instead of promoting the proliferation of CD4<sup>+</sup> T cells and initiating an adaptive immune response, the interaction between ILC and T cells limited the activity of T cells in response to commensal bacteria.(6)

Since the recent discovery of ILC it has become apparent that these cells have greater diversity than first anticipated.(7) This is reflected in the tissue specificity of these cells where they have varied functions that are influenced by their surrounding microenvironments. This thesis seeks a greater understanding of ILC in the thymus; therefore we will first provide an overview of the thymus itself. This will be followed by a review of ILC, including how these cells develop, the functional plasticity that exists

between subsets and the functions of these cells at different peripheral sites. Finally, we will acknowledge the current evidence that supports a role for these cells within the thymus that lead into our own investigations.

## **1.2 T cell development**

### **1.2.1 Overview**

The thymus is a primary lymphoid organ with a fundamental role in generating a diverse repertoire of functional T cells.(8) Situated in the upper anterior thorax, just above the heart, the thymus consists of two lobes and comprises a unique microenvironment that consists predominantly of thymic epithelial cells (TEC).(8) These cells orchestrate the development of T cells from T cell progenitors following their migration from the bone marrow to the thymus.(8) This well coordinated process allows for the development of T cells of multiple lineages, including  $\alpha\beta$ -T cells,  $\gamma\delta$ -T cells, Natural Killer T (NKT) cells and Mucosal Associated Invariant T (MAIT) cells, which are categorised based on their specialist functions and differential expression of surface markers, cytokines and transcription factors. (9) Of these lineages, the  $\alpha\beta$ -T cells, which bear the  $\alpha\beta$ -T Cell Receptor (TCR), are the best studied and are often compared to Innate Lymphoid Cells (ILC) given their developmental and phenotypic similarities with the T-helper (Th) subsets.(10) Therefore, this section will focus on the development of  $\alpha\beta$ -T cells.

This process of  $\alpha\beta$ -T cell development involves key checkpoints that ensure T cells are tolerant of self-antigens prior to their emigration into the periphery.(8) Broadly, these checkpoints are mediated by interactions between thymocytes and epithelial cells of two distinct regions within the thymus, known as the cortex and the medulla,

and are responsible for positive and negative selection, respectively.(8,11) Given that this thesis will explore ILC within the thymus, it is important to understand the key aspects of T cell development, with particular interest in cell markers that will later be used to discriminate between ILCs and T cells. An overview of  $\alpha\beta$ -T cell development in the thymus is shown in Figure 1.1.

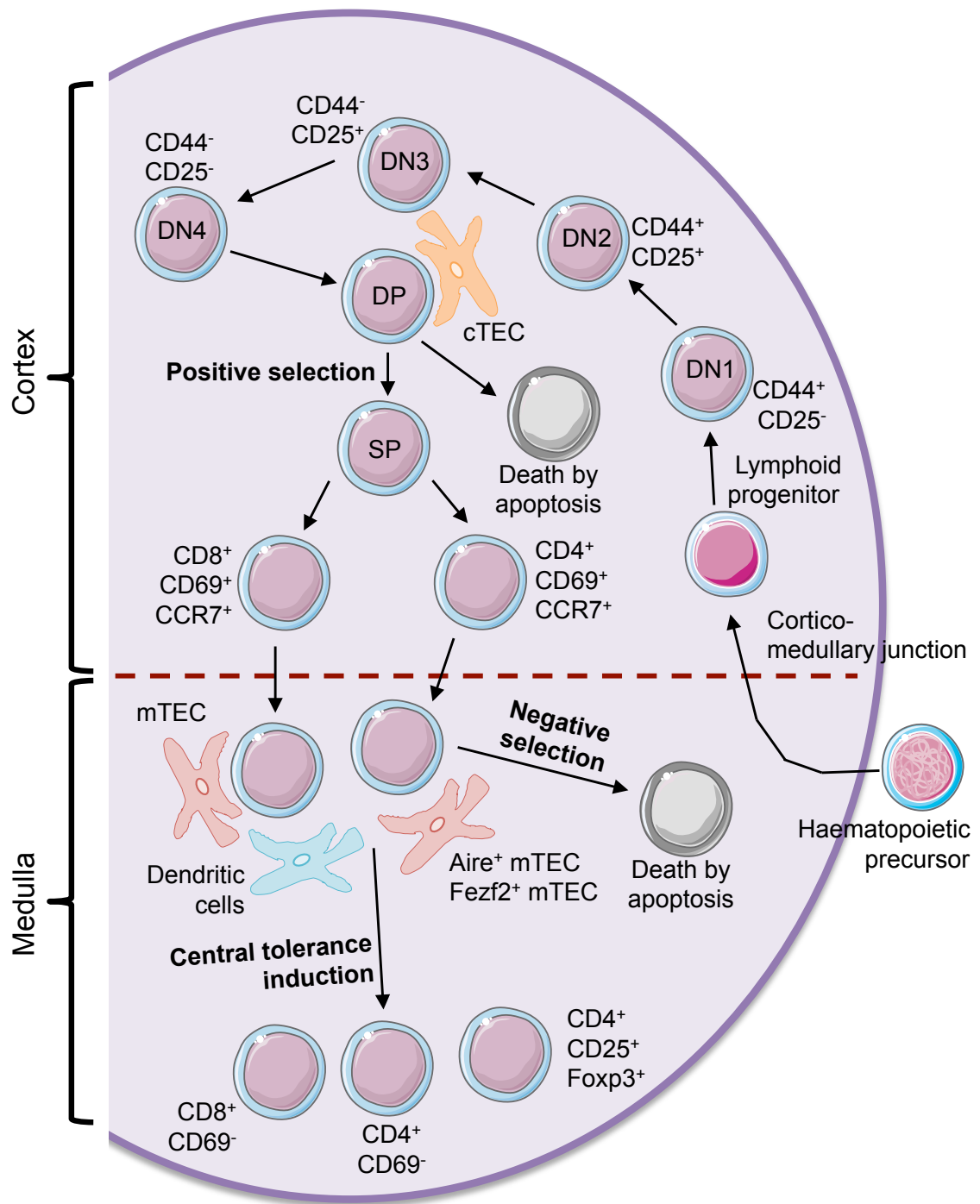
### **1.2.2 The thymic microenvironment**

As previously touched upon, the thymus has an important role in the development of a vast repertoire of functional T cells. This process relies on strict interactions between developing thymocytes and the thymic stroma, which itself consists of a variety of cell types, including mesenchymal cells, vascular endothelium, macrophages, dendritic cells, and specialised epithelial cells that provide structural and functional support to the tissue.(11) Of these, cortical thymic epithelial cells (cTEC) and medullary thymic epithelial cells (mTEC) which comprise the thymic cortex and medulla, respectively, are responsible for positive and negative selection processes. Therefore, the correct establishment of the thymic architecture is essential for the development of functionally diverse T cells.(11,12)

The thymic epithelium arises early in embryonic development from the endodermal cells of the third pharyngeal pouch and, together, these epithelial tissues form the thymic anlage.(8,13) Of importance to the thymic fate of the pharyngeal epithelium is expression of the gene encoding the forkhead box protein N1 (FOXN1), which is required for terminal differentiation of these epithelial cells.(11) Studies utilising *nude* (*nu/nu*) mice have been key in understanding the role of the FOXN1 transcription factor in this context. The *nude* phenotype is caused by a null mutation in the *FOXN1* gene and causes an arrest of initial primordial organ formation. This, in turn, prevents

### **Figure 1.1 Overview of $\alpha\beta$ T cell development in the thymus**

Haematopoietic precursors arise in the bone marrow and migrate in circulation to the thymus where they enter at the corticomedullary junction (CMJ). This Early Thymic Progenitor (ETP) population lacks the expression of CD4, CD8 and a T-cell Receptor (TCR), and is termed Double Negative (DN) cells. These DN cells are subdivided into 4 groups, DN1-DN4, based on the expression of CD25 and CD44. Development through the DN2 to DN4 stages requires the expression of a pre-TCR that consists of the non-rearranging pre- $\alpha$  chain and rearranged TCR $\beta$  chain. Pre-TCR $\alpha$  expression enables the successful transition from DN4 to CD4<sup>+</sup> CD8<sup>+</sup> (Double Positive; DP) thymocytes where the pre-TCR $\alpha$  is replaced with a newly rearranged TCR $\alpha$  chain; forming a complete TCR $\alpha\beta$ . DP cells undergo positive selection through interactions with cortical thymic epithelial cells (cTEC) where strength of TCR $\alpha\beta$  binding with peptide MHC molecules determines whether these cells transition to the Single Positive (SP) stage or die by apoptosis. Upregulation of C-C chemokine receptor type-7 (CCR7) by positively selected thymocytes supports their migration to the medulla where they undergo negative selection through interactions with medullary thymic epithelial cells (mTEC). Tissue Restricted Antigen (TRA) expression by mTEC is regulated by autoimmune regulator (Aire) and Fezf2. Positively selected thymocytes that successfully undergo tolerance induction are immunocompetent and migrate out of the thymus into the periphery while cells that fail are eliminated by apoptosis. Figure adapted from Germain (2002).(1)



the colonisation of the tissue with haematopoietic precursors; resulting in athymia and severe immunodeficiency due to the lack of functional T cells in these mice(11,14) Thus, demonstrating the requirement of input from the surrounding microenvironment for T cell development.(15)

### **1.2.3 Development through the cortex**

The importance of interleukin (IL)-7 in the development and survival of immune populations is widely accepted. Within the bone marrow, IL-7 acts to support the development of B and T cells from precursors within the bone marrow.(16). Initial attraction of these Thymic Seeding Progenitors (TSPs), or Early Thymic Progenitors (ETPs), from the bone marrow to the thymus is a fundamental first step for T cell development.(17,18) This movement is facilitated through the action of adhesion molecules and chemokines.(15,19–21) Adhesion molecules, such as P-selectin, are expressed by endothelial cells, while chemokines, such as chemokine C-C ligand (CCL) 21 and CCL25, and chemokine CXC ligand (CXCL) 12, are expressed by TECs; aiding entry through the corticomedullary junction (CMJ) and progenitor seeding.(15,19–21) IL-7 is an essential cytokine for T cell development with its action required during stages of thymocyte development, and promotes the survival and differentiation of these cells.(22,23) At this stage, cTEC provide IL-7, along with Delta-like 4 (DL4) ligands, to thymic progenitors where they induce cell proliferation and differentiation.(15)

The transition of Double Negative (DN) thymocytes is illustrated in Figure 1.1 where each DN stage is defined by the cellular expression of CD25 and CD44.(24) These actions require binding of IL-7 to its heterodimeric receptor interleukin-7 receptor- $\alpha$  (IL-7R $\alpha$ ) and the common gamma chain,  $\gamma_c$ , which cascades activation of the

tyrosine kinases, Jak1 and Jak3, and subsequent activation of STAT5-induced gene expression.(22,25,26) Further studies evidenced the importance of IL-7 using mice deficient in IL-7 (IL-7<sup>-/-</sup>) and IL-7Rα (IL-7Rα<sup>-/-</sup>).(22) Researchers observed the thymus to be smaller in these mice and quantification of T cells in the periphery demonstrated a reduction in the number of these cells. It was later shown that this was due to a blockage of thymocyte differentiation between the DN1 and DN2 stages of development.(22) Signalling through IL-7Rα is also important for ILC where it is required for the development and maintenance of these cells.(27) IL-7 and DL4 expression by cTEC is therefore absolutely pivotal to support the development of CD25<sup>+</sup> DN cells that are found in the subcapsular region of the cortex and orchestrate the initial stages of T-cell development.(15,18) The transition from the DN2 to DN3 stage of thymocyte development is where these cells become fully committed to the T cell lineage.(17,28) At this stage, DN3 cells, defined as CD44<sup>-</sup> CD25<sup>+</sup>, that have successfully rearranged their TCRβ chain associate with the pre-TCRα chain and CD3 signalling molecules.(17) Signalling through IL-7 is key in this process and ultimately supports the survival of these cells and their progression to the next developmental stage.(23) Collectively, this cascade of events is responsible for enforcing β-selection, saving cells from apoptosis and orchestrating continued development through the αβ lineage.(17,29)

#### **1.2.4 Positive selection**

The generation of a diverse repertoire of immunocompetent T cells relies on a series of checkpoints within the thymus to ensure T cells entering the periphery do not respond to self-antigens and thus cause harm.(8) The first of these selection processes occurs within the cortex where, following transition through the DN stages,

TCR-mediated positive selection of  $\text{TCR}\alpha\beta^{\text{low}} \text{CD4}^+ \text{CD8}^+$  cells takes place.(15) Initial activation of genetic programs in T cell progenitors induces the expression of  $\text{TCR}\beta$ , which provides the signals required for the up regulation of the co-receptors CD4 and CD8, and rearrangement of the  $\text{TCR}\alpha$ , which does not require ligand engagement.(30) The specificity of the  $\text{TCR}\alpha\beta$  complex is a result of variable, diversity and joining (VDJ) gene rearrangements of the  $\beta$ -chain, or for the  $\alpha$ -chain, V and J only undergo rearrangements. This process is orchestrated by the recombination-activating genes, RAG1 and RAG2.(15,30) This results in a process of random gene segment rearrangements ultimately allowing for the generation of a broad repertoire of thymocytes, each with an antigen-specific  $\alpha\beta$ -TCR.(31)

Given the diversity of these cells and the random nature in which they are generated, it is important that only functional and self-tolerant thymocytes are selected to move forward through the developmental program.(15) At the checkpoint of positive selection,  $\text{CD4}^+ \text{CD8}^+ \text{TCR}\alpha\beta^{\text{low}}$  T cells are exposed to self-peptide Major Histocompatibility Complex (MHC) complexes that are presented by cTEC in the microenvironment.(15,30,32) Overall, positive selection examines the affinity of individual TCRs for self-peptide and only those with low engagement of the TCR are able to progress to the subsequent stages of T cell development; accounting for 1-5% of developing thymocytes.(15,30,32) The remaining thymocytes are broadly divided into two categories: cells that bind with high affinity TCR engagement and those with no, or very low, TCR engagement. These cells undergo programmed cell death or die as a result of neglect, respectively.(15,32)

Efforts have been made to determine intracellular mechanisms that support the presentation of peptides by cTEC. It has been established that the capability of cTEC



to present MHC-associated peptides in this manner requires the action of intracellular proteolytic enzymes that are found in these epithelial cells.(15) Researchers have termed this uniquely expressed set of enzymes as the thymoproteosome, where the proteasome subunit,  $\beta 5t$ , in a complex with subunits  $\beta 1i$  and  $\beta 2i$ , is involved in proteolytic breakdown of intracellular proteins prior to the presentation of resulting peptides.(33) Interestingly, it is the  $\beta 5t$  subunit itself that has a pivotal role in this process and not its  $\beta 5$  or  $\beta 5i$  counterparts.(33) The importance of  $\beta 5t$  has been further demonstrated in  $\beta 5t$ -deficient mice where the proportion of  $CD8^+$  T cells was shown to be just 20% of that found in a wild type (WT) mouse.(34) Moreover, the TCR specificities in these mice were incompetent in supporting both allogeneic and antiviral immune responses.(15,35) As such, the evidence in this study supports the concept of thymoproteosome-dependent production of immunocompetent  $CD8^+$  T cells.(15,34)

The mechanisms that govern the presentation of peptide-MHC class II complexes required for  $CD4^+$  T cell development differs to those described above for peptide-MHC class I and subsequent  $CD8^+$  T cell commitment.(15) In this context, it is the function of the lysosomal proteases, thymic-specific serine protease (Tssp) and cathepsin L, which support peptide presentation by MHC class II molecules.(15) While these proteases are not exclusively expressed by cTEC, studies utilising mice deficient in these enzymes have concluded that both Tssp and cathepsin L are required for the positive selection of  $CD4^+$  T cells in the cortex.(36,37) Collectively, these studies support the requirement for specific proteolytic enzymes in peptide presentation by MHC class I and class II molecules, and subsequent development of

CD4<sup>+</sup> or CD8<sup>+</sup> restricted T cells, respectively. However, lineage commitment amongst developing thymocytes is not as straightforward as it first appears.

### **1.2.5 CD4 CD8 lineage commitment**

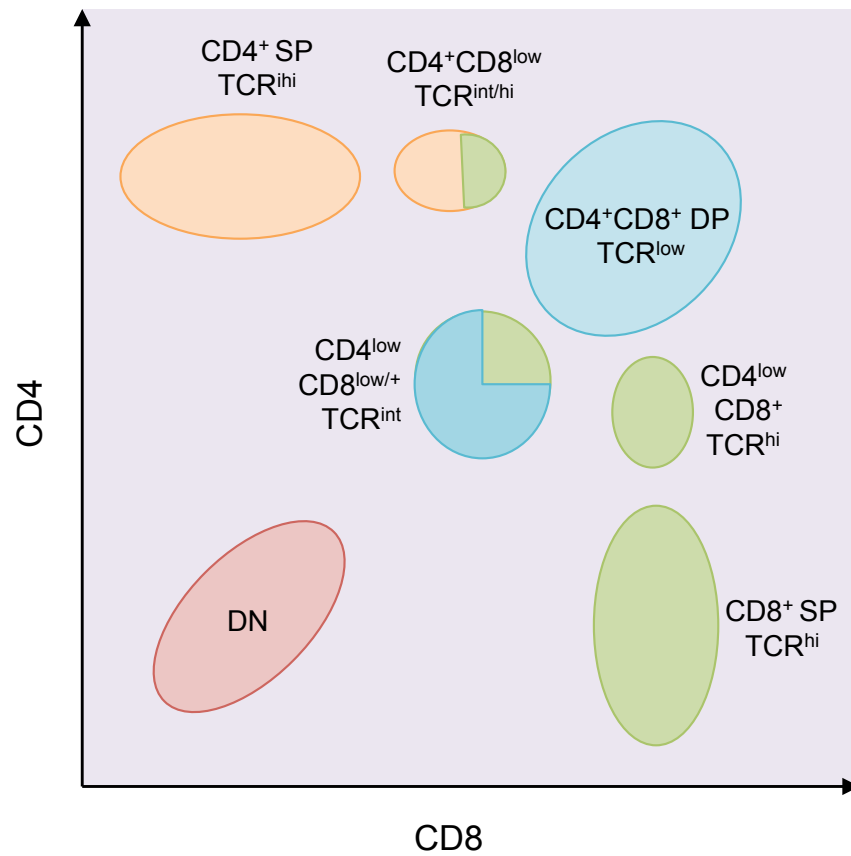
Following the discovery that CD4<sup>+</sup> and CD8<sup>+</sup> single-positive (SP) T cells arise from CD4<sup>+</sup> CD8<sup>+</sup> TCR<sup>low</sup> double-positive (DP) cells, it was hypothesised that the expression of single receptor, either CD4 or CD8, is a result of transcriptional silencing.(24) This notion suggested that the gene locus of the irrelevant receptor is silenced and is followed by gradual loss of the corresponding surface protein.(24) While this concept was widely accepted in the field of thymus biology, it also added confusion to whether the commitment of developing thymocytes to the CD4 or CD8 lineage resulted from instruction or stochastic choice.(24) Moreover, it was thought that disappearance of either CD4 or CD8 cells was a steady and uninterrupted process.(24) However, evidence has shown that this process is not as straightforward as first assumed. It is now understood that commitment to CD4 or CD8 T cell lineages involves a complex program of down regulation and asymmetric up regulation of CD4 and CD8, followed by selective loss of the unwanted receptor.(24,38) This concept is illustrated in Figure 1.2 and also highlights changes in TCR expression during this process.


### **1.2.6 Development through the medulla**

The proceeding stage of T cell development following CD4 or CD8 lineage commitment is negative selection and first requires thymocyte migration from the cortex into the medulla. C-C chemokine receptor type 7 (CCR7) expression is important in this process and is induced on positively selected thymocytes following peptide-MHC complex engagement with the TCR.(39) Interestingly, some cortical


## **Figure 1.2 Pattern of CD4, CD8 and TCR expression during thymocyte development**


The transition of DP cells to either CD4<sup>+</sup> or CD8<sup>+</sup> SP is a complex developmental program. Initial signalling through the positively selected TCR of DP cells results in partial loss of both CD4 and CD8 expression; yielding CD4<sup>low</sup> CD8<sup>low</sup> cells. This is followed by the re-expression of CD4 and then CD8 where CD4<sup>low</sup> CD8<sup>intermediate</sup> cells result. These initial processes occur no matter the strength of TCR engagement with MHC class I or MHC class II. Instead, the strength of TCR signalling determines the extent of CD4 and CD8 down-regulation in the initial phase. Eventually, cells that are committed to the CD4 SP lineage lose all expression of CD8. The process of CD8 SP lineage commitment varies slightly whereby these cells upregulate CD8 expression and lose expression of CD4. However, these cells upregulate CD4 once again to become DP cells but with higher levels of TCR expression than the previously immature DP cells. The final stage demonstrates the loss of all CD4 and the emergence of CD8<sup>+</sup> cells. Figure adapted from Germain (2002).(1)



 CD4 CD8 Double Negative (DN)

 Uncommitted

 CD8 committed

 CD4 committed

thymocytes that have not been positively selected also express CCR7 even though these cells will undergo apoptosis.(15) Specifically, the expression of CCR7 promotes the migration of positively selected thymocytes to the medulla, which has rich expression of CCR7 ligands, C-C chemokine ligand 19 and 20 (CCL19 and CCL20, respectively) by medullary thymic epithelial cells (mTEC).(15,39) Thus demonstrating the importance of CCR7 and associated ligands in the migration of positively selected thymocytes into the thymic medulla so that screening for tolerant TCR expressing thymocytes can take place.(39,40)

The expression of CCR7 on positively selected thymocytes is beneficial to their own development as it directs their migration to the medulla where subsequent selection processes take place.(15) However, these developing thymocytes are also of benefit to the medullary microenvironment. Positive selection of thymocytes in the cortex leads to the provision of several cytokines of the Tumour Necrosis Factor (TNF) superfamily, including Receptor Activator of Nuclear factor- $\kappa$ B Ligand (RANKL).(15) Interestingly, expression of the receptor for RANKL, termed RANK, is expressed on mTEC but not cTEC. Studies using RANKL-deficient mice demonstrated the interaction between RANKL and RANK in this context to support growth and maturation of mTEC.(15) Therefore contributing to the establishment of the microenvironment fundamental to the tolerising function of the thymic medulla.(15) In addition, positively selected thymocytes express another member of the TNF superfamily, known as CD40, which also supports medullary development.(15)

The strict architecture of the thymic medulla is fundamental to its role in negative selection procedures that acts to eliminate self-reactive T cells.(15,30) It is within this location that positively selected CD4 and CD8 T cells further encounter self-peptide-

MHC complexes that are presented by antigen-presenting cells (APC), such as mTEC but also dendritic cells (DC). Engagement of positively selected thymocytes with peptide-MHC complexes leads to clonal deletion of these reactive T cells. mTEC, in particular, have impressive capabilities whereby they present tissue-restricted antigens (TRA) that would otherwise be found in the in specific tissues in the periphery. Moreover, it is possible for mTEC to transfer TRA to dendritic cells to increase the frequency of self-antigens being presented to developing thymocytes and the chance of correct selection.(41) The autoimmune regulator (Aire) has a key role in the expression of TRA and is, itself, expressed by approximately 30% of mTEC yet absent from cTEC.(41) Studies using Aire-deficient mice have helped gain further understanding of the importance of this transcription factor. It was in Aire-deficient mice that a reduction in TRA resulted in an autoimmune phenotype.(15,30,42) This was characterised by autoantibody production and the infiltration of inflammatory cells to a multitude of tissues, such as the retina, pancreas and lacrimal gland.(30,42,43) Interestingly, the regulatory role of Aire exceeds that of TRA presentation and, most recently, has been described in the regulation of mTEC-derived IL-7 expression during the neonatal period of  $\gamma\delta$ -T cell development.(44) In the context of this study, a pool of  $\gamma\delta$  T cells with the  $V\gamma 6^+V\gamma 1^+$  TCR expanded in Aire-deficient mice due increased expression of IL-7 by mTEC.(44)

While the literature is predominantly focussed on the role of Aire in this process, there is also evidence to support a role for another transcriptional regulator, known as *Fezf2*, in the presentation of TRA by mTEC.(45) Analysis of GeneChip data on mRNA isolated from mTEC revealed *Fezf2* to be expressed at a similar level to Aire and prompted its further investigation. Although, much like Aire, *Fezf2* is responsible

for the presentation of TRA by mTEC yet it acts independently of Aire.(44) Unlike Aire, which functions through a RANK/CD40 axis, Fezf2 was initially suggested to act through the lymphotoxin beta receptor (LT $\beta$ R) pathway.(45) However, other researchers discovered that Fezf2 was in fact similarly induced by RANK signalling through stimulation experiments using embryonic mouse thymus lobes.(46) Nonetheless, the resulting phenotype of Fezf2-deficient mTEC is comparable to that in Aire-deficient mice.(45,46) On both accounts, mice deficient in either transcriptional regulator have a severe autoimmune phenotype characterised by autoantibody production and the infiltration of immune cells at peripheral sites.(45,46) While the pancreas and retina are common sites of inflammatory cell infiltration in Aire-deficient mice, these sites are largely unaffected in Fezf2-deficient mice.(45) Instead, inflammatory cells have been shown to infiltrate the lung, liver, kidney and small intestine.(45) Therefore it is thought that Aire and Fezf2 work together to present distinct TRA to developing thymocytes to guide development of a self-tolerant thymocyte repertoire and prevent development of autoimmunity.(30,45)

While the majority of CD4 T cells that demonstrate reactivity to self-antigens expressed in the context of a MHCII molecule by mTEC or DC are eliminated through negative selection, some of these cells go on to survive.(30,47) Under these circumstances, these cells are induced to develop into T regulatory (Treg) cells that are characterised by the expression of forkhead box P3 (FoxP3) and have a specific role in maintaining tolerance in the periphery.(30,47) Treg develop from two progenitor populations within the thymus either CD25<sup>+</sup>Foxp3<sup>-</sup> or Foxp3<sup>+</sup>CD25<sup>-</sup> but both develop into the Foxp3<sup>+</sup>CD25<sup>+</sup> thymically derived natural Treg cells.(48) In the periphery they have multiple mechanisms that allow them to control any escapee

non-tolerant T-cells such as by inhibiting the production of IL-2 that is needed for effector T-cell expansion, therefore preventing their ability to proliferate and potentially damage the host(49) While Treg cells are not studied in the context of this thesis it is important to have an appreciation for the existence of these cells.

As discussed, the process of T cell development within the thymus is complex and is followed by the emigration of these cells into the periphery. It is important that these cells are maintained throughout the lifespan of the organism to prevent the loss of unique antigen receptor specificities.(50) It is those cells which have recently arrived in the periphery that have the greatest capacity for proliferation. Given that the thymus begins to involute during puberty, and the capacity of this tissue to produce functional T cells reduces, it is important that existing T cells in the periphery are maintained. This process of is also reliant on IL-7.(50) Although ILC are the predominant focus of this thesis, it is important to appreciate the microenvironment in which these cells will be investigated. The knowledge shown here will be used to justify our robust methodology aimed at identifying ILC amongst thymocytes where defining marker expression changes across the landscape of development.

## **1.3 Unconventional T Cells**

### **1.3.1 Overview**

It is apparent from the descriptions so far presented within this thesis that T cell lineages are defined by their combination of surface antigen expression, capability to produce specific cytokines and the transcription factors they express.(9) This ultimately leads to functionally diverse cells with their own identifiable characteristics. While T cells of the  $\alpha\beta$  lineage are the best studied, there is a growing appreciation



for T cells of other lineages. These cells include NKT cells, Mucosal Associated Invariant T (MAIT) cells and  $\gamma\delta$  T cells, and are commonly referred to as unconventional T cells.(9) Together, it is estimated that these unconventional T cells make up approximately 10% of all circulating T cells.(9) The importance of these cells is demonstrated by their absence or defects in unconventional T cells that are associated with autoimmunity, chronic inflammation and cancer.(9) While the importance of MAIT cells should not be understated, these cells are not a focus of our own investigations and will not be introduced in this section. However, both NKT cells and  $\gamma\delta$  T cells are focal points within this thesis and will therefore be introduced here.

### **1.3.2 Invariant Natural Killer T (iNKT) cells**

NKT cells are defined by their ability to recognise lipid antigens in the context of CD1d.(9) Two broad classes of NKT cells exist and are termed type 1 and type 2 NKT cells.(9) Type 1 NKT cells, also termed invariant Natural Killer T (iNKT) cells, recognise the lipid antigen,  $\alpha$ -Galactosylceramide ( $\alpha$ -GalCer), and are the focus of our own investigations. Structurally, these cells express a CD1d-restricted semi-invariant  $\alpha\beta$  TCR that consists of an invariant  $\alpha$ -chain (V $\alpha$ 14-J $\alpha$ 18 in mice) and a limited choice of  $\beta$ -chains; namely V $\beta$ 8, V $\beta$ 7 and V $\beta$ 2 in mice.(9) This has been taken advantage of by researchers who have manufactured CD1d- $\alpha$ -GalCer tetramers for the study of the development, phenotype and function of these cells, and will later be used to aid our own investigations(9)

The iNKT lineage ascends from a small fraction of  $\alpha\beta$ -T cells and relies on the expression of CD1d by DP thymocytes in the cortex.(9,51) However, it was later discovered that the expression of CD1d alone is not sufficient for the survival of these

cells.(9,52) This is illustrated in mice whereby intracellular trafficking and antigen presentation in the context of CD1d was impaired.(52) Recent findings are consistent with this theory whereby mice lacking the Adapter Protein Complex-3 (AP3) have problems with iNKT cell development.(9,53) These findings provide evidence to support the idea that iNKT cells require endogenous lipid antigens by CD1d to continue through the developmental program.(9) Further insight into the development of iNKT cells was provided by studies in mice with a *nude* phenotype, where iNKT cell development was absent.(54) A similar effect was also observed in neonatal mice that underwent thymectomy following birth.(55) Collectively, these findings illustrated iNKT cell development to be thymus dependent and also occurred after birth.(9)

Historically, subclasses of iNKT cells were defined by their developmental stage, stages 0-3.(56) This classification model resulted from work in C57BL/6 mice and relies heavily on NK1.1, which is absent in many other mouse strains, such as BALB/c mice. The staging of iNKT cell maturation in this capacity is defined as follows: stage 0 ( $CD24^+ CD44^{lo} NK1.1^{lo}$ ), stage 1 ( $CD24^{lo} CD44^{lo} NK1.1^{lo}$ ), stage 2 ( $CD24^{lo} CD44^{hi} NK1.1^{lo}$ ) and stage 3 ( $CD24^{lo} CD44^{hi} NK1.1^{hi}$ ). Stages 0-2 of iNKT cell development occur within the thymus where stage 2 iNKT cells follow one of two routes. The majority of stage 2 iNKT cells migrate into the periphery where they rapidly up regulate NK1.1, but a small population of stage 2 iNKT cells remain in the thymus where they undergo terminal maturation.(56) Mature iNKT cells were later sub-divided into 3 main subsets based on the expression of PLZF, Tbet and ROR $\gamma$ t and follow the Th1, Th2 and Th17 paradigm. Using this nomenclature, iNKT subsets

can be classified as follows: iNKT1 (PLZF<sup>lo</sup> Tbet<sup>+</sup> RORγt<sup>-</sup>), iNKT2 (PLZF<sup>hi</sup> Tbet<sup>-</sup> RORγt<sup>-</sup>) and iNKT17 (PLZF<sup>lo</sup> Tbet<sup>-</sup> RORγt<sup>+</sup>).<sup>(57)</sup>

Further to the characterisation of iNKT subsets based on their transcription factor profile, iNKT subsets are associated with cytokine expression patterns.<sup>(58)</sup> This is demonstrated by iNKT1, iNKT2 and iNKT17 subsets that are associated with IFNγ, IL-4 and IL-17 production, respectively. However, recent studies have highlighted some of the overlap that exists in the cytokine producing capabilities of these cells.<sup>(58)</sup> Investigations at a molecular level have demonstrated IFNγ mRNA to be strongly expressed in iNKT1 cells and IL-17A mRNA to be expressed solely in iNKT17 cells, acting in concordance with our previous understanding. IL-4 mRNA, however, was shown to be expressed in both iNKT2 and iNKT17 cells.<sup>(58)</sup> The cytokine expression profile of these cells has also been assessed *in vitro* in the presence of PMA, ionomycin and BFA. While iNKT1 cells are mainly IFNγ-producing, cells capable of producing both IFNγ and IL-4 were also present. Concerning iNKT2 cells, greater than half of these cells were shown to produce IL-4 with some of the cells capable of producing both IL-4 and IL-17 or IL-4 and IFNγ. Further overlap was demonstrated by iNKT17 cells, which were a main source of IL-17 with some of these cells expressing both IL-4 and IL-17.<sup>(58)</sup>

Although these cells are coined invariant, they exhibit a wide range of functional capabilities.<sup>(58)</sup> This is perhaps due to the diversity amongst these cells, as demonstrated by their transcription factor and cytokine expression profiles. This is illustrated in the capability of these cells in activating both NK cells and B cells.<sup>(58–60)</sup> In addition to this, iNKT cells have been shown to influence T cell bias and actions of DC.<sup>(58,61)</sup> Furthermore, the importance of iNKT cells has been

demonstrated by their role in influencing disease outcomes, such as supporting the immune response in both bacterial and viral infections.(58,62,63) However, their role extends from basic immune functions and these cells have also been described in the context of autoimmune disease, allergy and cancer.(64) Therefore, understanding more about these cells in immune homeostasis and disease states is of great interest.

### **1.3.3 $\gamma\delta$ T cells**

Much like  $\alpha\beta$  T cells,  $\gamma\delta$  T cells develop in the thymus where they arise from a CD4<sup>+</sup> CD8<sup>-</sup> DN precursor.(65) In contrast to  $\alpha\beta$  T cells, which are involved solely in the adaptive immune response,  $\gamma\delta$  T cells have functions in both the innate and adaptive arm of the immune system.(66) While  $\gamma\delta$  T cells are capable of responding rapidly following stimulation, indicative of the innate immune system, they also express variable TCRs as a result of  $\gamma\delta$  TCR rearrangement, which is a feature of the adaptive immune system.(66) Moreover,  $\alpha\beta$  T cells exit the thymus in a naïve state and obtain their effector function in the periphery. However, many  $\gamma\delta$  T cells acquire their effector fate during development in the thymus and have limited plasticity following emigration from the thymus into the periphery.(65)

Minimally,  $\gamma\delta$  T cells can be categorised into three main subsets based on their effector function. These are IL-17A-producing  $\gamma\delta$  T cells, IFN $\gamma$ -producing  $\gamma\delta$  T cells and  $\gamma\delta$  T cells of an innate-like phenotype.(65) The function of these cells is thought to influence the anatomical location of these cells with the spleen containing a majority of IFN $\gamma$ -producing  $\gamma\delta$  T cells. While, on the other hand, IL-17A-producing  $\gamma\delta$  T cells are predominantly found within the lymph nodes.(65) Furthermore, the effector fate of these cells is dictated by their use of different  $\gamma$ -chains. There is an

enrichment of IL-17A producing cells amongst  $\gamma\delta$  T cells expressing the V $\gamma$ 2 chain. IFN $\gamma$ -producing cells, in contrast, consist mainly of  $\gamma\delta$  T cells using the V $\gamma$ 1 chain.(65)

The literature has documented a number of factors that contribute to the development of  $\gamma\delta$  T cells in the thymus. It has been established that the development of  $\gamma\delta$  T cells occurs in waves that are characterised by V $\gamma$  segment usage.(67,68) According to the Garman nomenclature, V $\gamma$ 1.1, V $\gamma$ 3 or V $\gamma$ 5 segment usage is associated with the development of IFN $\gamma$ -producing  $\gamma\delta$  T cells while V $\gamma$ 4 usage is linked to IL-17A-producing cells.(69) V $\gamma$ 2 segment usage, however, is capable to develop into either IFN $\gamma$ -producing or IL-17A-producing cells. The development of these subsets is also dictated by the strength of signaling at the TCR. For example, IFN $\gamma$ -producing  $\gamma\delta$  T cells result from a strong level of TCR signaling while IL-17A-producing  $\gamma\delta$  T cells arise when TCR signaling is weak or non-existent.(68) Other factors determining  $\gamma\delta$  T cell development include signaling through co-stimulatory receptors and signals from cytokines in the surrounding microenvironments. Signaling through CD27, for example, has been implicated in the development of IFN $\gamma$ -producing cells while development of  $\gamma\delta$  T cell in the absence of CD27 results in IL-17A-producing cells.(68,70) Instead, IL-17A-producing  $\gamma\delta$  T cells develop in response to TGF $\beta$ , IL-1, IL-6 and IL-23 signals.(68,71) The importance of how  $\gamma\delta$  T cells develop will become important in our final chapter of work where we investigate the role of Id2 amongst these developmental programs.

## **1.4 Innate Lymphoid Cells (ILC)**








### **1.4.1 Overview**

ILC are a recently emerged class of lymphocytes that are considered the innate counterparts of helper T cell subsets.(72) This comparison results from the shared phenotypic and functional qualities observed between these cells, as demonstrated in Figure 1.3. The most distinctive feature of these cells, and what makes them unique to T cells, is the absence of rearranged antigen receptors.(27) Furthermore, ILC have a lymphoid morphology and lack markers associated with cells of the myeloid lineage or dendritic cells; thus confirming the requirement of these cells to be classified on their own.(27)

There are several distinct subsets of ILC, which include the cytotoxic Natural Killer (NK) cells and the non-cytotoxic group 1 ILC (ILC1), group 2 ILC (ILC2) and the group 3 ILC (ILC3) that also encompass lymphoid tissue inducer (LTi) cells. Broadly speaking, ILC1 are defined by their expression of the T-box transcription factor (Tbet) and production of IFN $\gamma$ , ILC2 are defined by their expression of GATA-3 and production of interleukin (IL)-5 and IL-13, and ILC3 are defined by their expression of the nuclear receptor retinoic acid receptor-related orphan receptor gamma (ROR $\gamma$ t) and production of IL-17A and IL-22.(27) Owing to the variation in the phenotype of these cells across subsets, each group of ILC have distinct functions and are associated with at least some level of tissue specificity. Despite the diverse phenotypes of ILC subsets across tissues, each of these has a role to play in the maintenance of immune homeostasis.(27) This is demonstrated by the role of ILC at barrier surfaces, which provide first line defence to bacteria, viruses, fungi and parasites. Damage at these sites is detected by epithelial cells and cells of the

### **Figure 1.3 Phenotypic and functional similarities of T helper subsets and ILC**

Subsets of ILC have been described as innate-counterparts to T-helper (Th) subsets of the adaptive immune system. While ILC develop independent of the Recombination-Activating Genes (RAG) and thus do not express a TCR, they are otherwise functionally and phenotypically similar to Th cells. Th1 cells and ILC1 express Tbet and secrete the signature cytokine IFN $\gamma$ . Th2 cells and ILC2 express GATA-3 and secrete the type-2 cytokines IL-4, IL-5 and IL-13. Th17 cells and ILC3, alike, express ROR $\gamma$ t and secrete IL-22 and variants of IL-17. Regulatory T cells (Tregs) express the FoxP3 transcription factor and secrete IL-10 and TGF $\beta$ . The shared functions of Th cells and ILC are also shown. Figure adapted from Zhu, Yamane and Paul (2010), and Fang and Zhu (2017).(73,74)

T helper subsets	Immune functions	ILC subsets
<b>Th1</b>  Tbet TCR	IFN $\gamma$ Immunity to intracellular bacteria, viruses and protozoa Autoimmunity	IFN $\gamma$  Tbet <b>ILC1</b> Tbet <sup>+</sup>
<b>Th2</b>  GATA-3 TCR	IL-4 IL-5 IL-13 Immunity to helminths Asthma and allergic disease	IL-4 IL-5 IL-13  GATA-3 <b>ILC2</b>
<b>Th17</b>  RORyt TCR	IL-17A IL-17F IL-22 Immunity to extracellular bacteria and fungi Autoimmunity	IL-17A IL-22  RORyt <b>ILC3</b>
<b>Treg</b>  FoxP3 TCR	IL-10 TGF $\beta$ Immune suppression	



myeloid lineage, and results in the secretion of cytokines and alarmins that are detected by ILC and activate a signal specific response.(27)

#### **1.4.2 Overview of ILC Development**

The common lymphoid progenitor (CLP) is part of a discrete lineage that gives rise to T and B lymphocytes during haematopoiesis.(75) Until very recently, it was thought that only two other lymphocytes arose from CLP and these lacked antigen receptors.(75) These were the NK cells and LTi cells, which were functionally distinct from one another and when first discovered they were not known to be part of the much wider ILC family. NK cells are considered the cytotoxic cells of the ILC family and mediate early immune responses against viruses and have involvement in the elimination of cancerous cells. LTi cells, on the other hand, are important in the generation of lymphoid tissues during embryogenesis.(72)

It is now appreciated that these cells are developmentally related and both require the action of the common gamma chain ( $\gamma_c$ ) and the transcriptional regulator, inhibitor of DNA-binding 2 (Id2). It was later discovered that several other subsets of ILC depend on these modulators for their development.(74,76) ILC develop from the CLP that also give rise to B and T lymphocytes. This requires the action of several transcription factors that enable the differentiation of CLP to either a Natural Killer cell Precursor (NKP) or Common helper ILC precursor (chILP).(74,75) NKP can give rise to NK cells only while ChILP is able to give rise to all ILC subsets but not NK cells. In addition, the development of ILC subsets is influenced by the variable expression of the Promyelocytic Leukaemia Zinc Finger (PLZF) following differentiation from ChILP. Precursors of ILC that express PLZF are capable of developing into ILC1, ILC2 and

ILC3, but not LT $\alpha$ i cells. Given that PLZF is expressed following commitment to a ChILP rather than NKP, PLZF<sup>+</sup> cells are unable to develop into NK cells.(74,75)

Other transcription factors required for the development of ILC include GATA-3 and Nfil3. Together with Id2, these transcription factors have been described as critical in the development of CLP to either a NKP or ChILP that are restricted to ILC development.(74,75) However, our current understanding of how these transcription factors control cell fate is incomplete. Here, we review our understanding of Id2, which is a focal point of our investigations, in the context of transcriptional enhancement and repression.

#### **1.4.3 Transcriptional Control in the Context of Id2**

Basic Helix-Loop-Helix (bHLH) proteins represent a widely understood category of transcriptional regulators that are known to form heterodimers with many of the ubiquitously expressed E Proteins.(77,78) The term E protein originated during studies that demonstrated the bHLH domain to bind Ephrussi box (E box) sequences and regulate the IgG enhancer in B cells.(78,79) However, it is now understood that E box sequences have a much more general function.(78) E box sequences are short sequences of DNA found within the gene promoter or enhancer region and binding of the bHLH domain to this region regulates transcription of the gene. The Inhibitor of DNA-binding (Id) binding proteins are another class of bHLH proteins that act competitively to oppose the action of E proteins.(78) In contrast to other bHLH proteins, Id proteins do not contain a DNA binding domain and therefore act to inhibit the transcriptional activity of E proteins in a dominant manner.(77) As such, heterodimers of Id proteins with E proteins are unable to bind DNA and activate transcription.(78) Acting as a negative regulator of transcription, Id2 binds to and

inhibits the activity the E Proteins, E2A, E2-2 and HEB, which are critical for the development of B and T cells. Therefore, the increased activity of Id2 in this context forces CLP towards an ILC restricted lineage at the expense of B and T cell development.(75)

Similarly, GATA-3 restricts the development of B cells through the inhibition of Early B-cell Factor 1 (EBF). Together, these transcription factors facilitate the development of ILC by blocking the fundamental pathways required for development of B and T cells from CLP. Id2 is an important feature of this thesis whereby it is later used as a tool to identify ILC amongst T cell populations within the thymus. However, there is an incomplete understanding of how Id2 expression is controlled. It has previously been shown that Id2 is regulated by environmental cues, such as Bone Morphogenetic Protein (BMP) and Notch ligands, and therefore it is thought that Id2 might be controlled similarly in this context.(74) Moreover, Nfil3 is another transcription factors involved in the development of CLP to an ILC restricted fate and is modulated by soluble factors in the surrounding microenvironment, such as cytokines.(74) Figure 1.4 summarises this understanding of ILC development from the CLP.

While ILC precursors develop in the foetal liver and adult bone marrow, it is thought that these precursors mature in peripheral sites, much like the development of T helper subsets, and respond to tissue specific cues in the surrounding microenvironment. As previously mentioned, these ILC subsets share phenotypic and functional similarities to that of helper T cells. However, unlike T cells, which are activated following stimulation of their antigen receptors, ILC are activated by signals from the surrounding microenvironment. These signals are very similar to those that

activate innate T cell populations, such as iNKT cells and  $\gamma\delta$  T cells, including signals from stress, microbial products, and the cytokine milieu.(75) Furthermore, the mechanism by which ILC are activated enable a rapid response and secretion of effector cytokines that had previously been associated with T helper cells.(75).

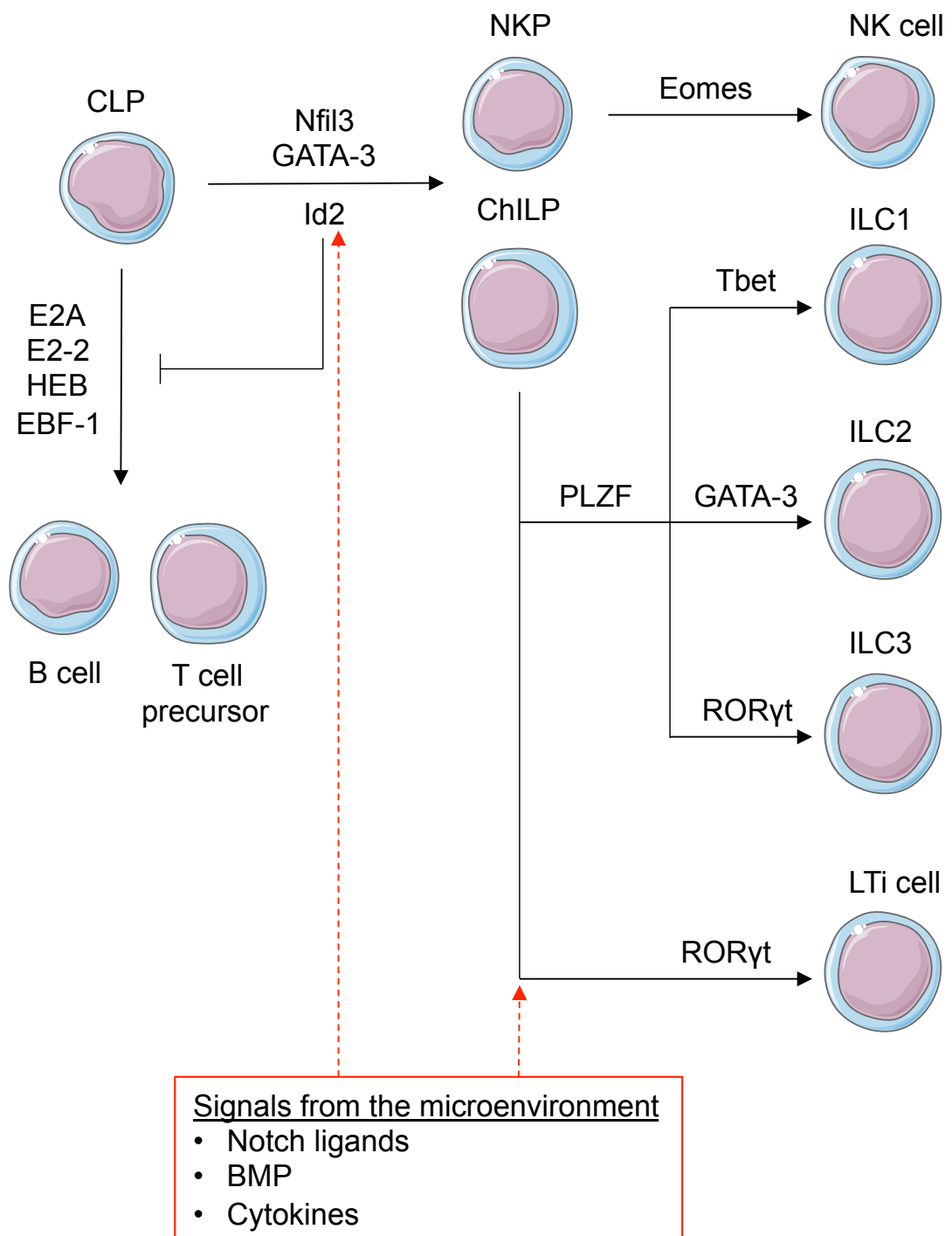
The discrete differences in the development of these cells result in subsets with widespread functions. ILC have been implicated in immunity, tissue development and remodelling, the early immune response against microorganisms, and the maintenance of epithelial layer integrity at barrier surfaces.(27) In addition to their valid contribution to immune homeostasis, these cells have also been shown to contribute to pathogenesis.(27)

#### **1.4.4 Plasticity of ILC**

Despite being classified as distinct subsets, there is evidence to suggest functional plasticity amongst ILC populations.(7) It has been suggested that it is this plasticity that enables ILC populations to adapt in different tissue microenvironments.(7) Heterogeneity amongst ILC1 has been widely reported where these cells arise through the canonical developmental pathway from ILC progenitors but also as a result of plasticity. For example, following the exposure of ILC2 to IL-12 and IL-1 $\beta$ , these cells down regulate their expression of GATA-3 and up regulate Tbet, adopting an ILC1-like phenotype.(7) Additionally, it has been shown that ILC3 down regulate ROR $\gamma$ t and up regulate Tbet in response to IL-2, IL-15 and IL-23. ROR $\gamma$ t is encoded by the *Rorc* gene and studies utilised *Rorc* reporter mice have illustrated the conversion of CCR6<sup>-</sup> NKp46<sup>+</sup> ILC3 into IFN $\gamma$ -producing ILC1; termed “ex-ILC3”.(7,80)

## **Figure 1.4 Development of ILC**

Much like B cells and T cells, ILC develop from the Common Lymphoid Progenitor (CLP). This occurs in the liver of the foetus and bone marrow in the adult. Suppression of the transcription factors E2A, E2-2, HEB and EBF-1 by Id2 is required to restrict the CLP to an ILC fate. Two distinct precursors, the Natural Killer cell Precursor (NKP) and Common helper ILC Precursor (ChILP), determine an Natural Killer (NK) cell or Innate Lymphoid Cell (ILC) fate. The expression of Eomes enables the differentiation of NKP cells into mature NK cells. The ILC pathway is further divided by PLZF into PLZF-dependent ILC1, ILC2 and ILC3, which require Tbet, GATA-3 or ROR $\gamma$ t, respectively, for their maturation. LTi cells also require ROR $\gamma$ t for their maturation and are encompassed within the ILC3 family but develop independently of PLZF. The development of mature ILC from ILC precursors is supported by signals in the microenvironment, such as notch ligands, cytokines, bone morphogenetic proteins (BMP) and changes that result from the circadian rhythm. Figure adapted from Eberl, Colonna, Di Santo and McKenzie (2015).(75)



Proceeding investigations demonstrated the inhibition of this conversion in *Txb21*<sup>-/-</sup> mice.(7,17) Furthermore, the conversion of ILC3 to ILC1 phenotype requires the action of the Notch signalling pathway. This was demonstrated in mice that lack Notch2 receptors or the downstream Notch signalling protein, RBPj.(82,83) Interestingly, the reverse conversion of ILC1 to ILC3 has not yet been identified.(7)

As mentioned above, ILC2 have the potential to adopt an ILC1 phenotype in response to signals from the surrounding microenvironment. There is also evidence to suggest ILC2 have the capability of adopting an inflammatory phenotype. In these studies, mice were injected with IL-25 and this resulted in the presence of ILC2 capable of producing IL-17 in addition to the associated type-2 cytokines.(7,84) It has also been shown that exposure of ILC2 to Notch ligands results in the up regulation of ROR $\gamma$ t and secretion of both IL-17 and IL-13.(7,85) Together, these data highlight the functional plasticity of amongst ILC subsets. However, studies using single cell RNA-sequencing (RNA-seq) technologies have proposed that the heterogeneity of ILCs exceeds the strict definitions of these cells that we currently use.(7,86)

### **1.5 Functions of ILC at Peripheral Sites**

Since the characterisation of ILC as their own family of immune cells, there has been growing evidence to support functional diversity amongst subsets. Studies in both mouse and human cohorts have demonstrated a non-redundant role for these cells in maintaining tissue homeostasis as well as driving pathology in disease.(10,27,87) The diversity of cell function amongst ILC subsets is owing to their presence at barrier sites and within lymphoid organs, where they can respond rapidly to signals in the surrounding microenvironment.(6) However, the proportion of specific subsets of ILC varies greatly amongst tissues.(88) Although our investigations are focussed on

understanding more about these cells within the thymus, it is important to have an appreciation of their function at peripheral sites. This understanding will be used when determining appropriate tissue for control samples in our own studies and also provide context to ILC in supporting tissue homeostasis. As such, we will provide an overview of ILC function in secondary lymphoid tissue, lung and small intestine.

### **1.5.1 Secondary Lymphoid Tissue**

Lymph nodes are important secondary lymphoid structures that provide a unique environment where antigen specific lymphocytes are able to engage with their cognate antigen.(89) The efficiency of this immune response is aided by the network of lymphatic vessels that enable the drainage of immune cells and antigen away from the site of infection.(89) The importance of ILC function in lymph nodes was first demonstrated by LT $\alpha$  cells where they were shown to provide key lymphotoxin signals to the developing cells of the stroma.(89,90) More recently studies from have sought to characterise ILC populations in different lymph nodes, comparing those that drain mucosal tissues with those that drain peripheral sites.(89) These investigations identified ILC3, known to be CCR6<sup>+</sup> LT $\alpha$  cells, to be enriched in the mesenteric lymph node (mLN) that drained mucosal tissues. Furthermore, it was demonstrated that these cells require CCR7 for their migration from the intestine to the mesenteric lymph node that drains this site.(89) Interestingly, these ILC3 were discovered in a specific location within the lymph node, known as the interfollicular space, where initial stages of the adaptive immune response occur.(89) This is highlighted by the migration of antigen-specific T and B cells into this space prior to movement into the follicle.(89,91) Interestingly, this microenvironment was not present in the brachial, inguinal or popliteal lymph nodes.(89) Although ILC3 express MHCII, they do not



express CD80 or CD86, and therefore it is unlikely that ILC3 initiate T cell proliferation.(6) However, it is suggested that ILC3 interact with effector T cells following priming, or engage with regulatory or memory CD4 T cells as they recirculate through the tissue.(89) Although ILC1 and ILC2 subsets have also been identified in the mLN, this is to a lesser extent.(88,89) As will become apparent further on in this thesis, the clear ILC populations present in the mLN are of interest in our own studies, providing a suitable control tissue for comparing ILC populations in the thymus.

### **1.5.2 Lung**

Evidence from our own laboratory has provided evidence that demonstrated few ILC3 to exist following isolation of ILC from lung tissue.(88) Instead, this tissue is enriched with ILC2.(88,89) It is well established that mouse ILC lack the PRRs that are broadly expressed by other immune cells and are therefore unable to respond to pathogens through the recognition of PAMPs.(87) Instead, these cells respond to environmental cues secreted by other cells, such as cytokines, alarmins and other inflammatory mediators.(87) ILC2 are able to respond to a variety of these signals, such as IL-33, IL-25, thymic stromal lymphopoietin (TSLP), IL-2 and IL-7, amongst others.(72,87) The action of ILC in response to these signals is held in a fine balance as chronic exposure to these signals result in a tissue protective response becoming an immune pathology.(87,92) This is highlighted in the genes associated with ILC2 responses, such as the genes encoding TSLP, IL-4, IL-5 and IL-13, which are also linked to susceptibility to atopic disease.(87,92) Detrimental ILC2 responses are of relevance to the lung where data obtained in mouse models has illustrated their role in asthma.(93) Papain and house dust mite are examples of protease allergens that

are commonly used to investigate non-infectious lung inflammation.(87,93) It has been shown in the literature than papain induced symptoms associated with asthma in *Rag*<sup>-/-</sup>. However, these effects were not observed in *Rag*<sup>-/-</sup> *IL2rg*<sup>-/-</sup> or *Rag*<sup>-/-</sup> that have undergone depletion of ILC2. Moreover, ILC-deficient mice that were reconstituted with ILC2 and challenged with allergen resulted in asthma-like symptoms.(87,93) Taken together, it is clear than ILC2 are an abundant population in the lung. While these cells are capable of supporting a protective immune function, they are also associated with immune pathology.

### **1.5.3 Small intestine**

The small intestine is an important site of interest in ILC biology due to the importance of ILC at this site in maintaining immune homeostasis. In this context, ILC have been shown to regulate CD4<sup>+</sup> T cell responses to commensal bacteria that are naturally found within this tissue.(6) In the context of the study, the loss of RORγt<sup>+</sup> ILC resulted in dysregulation of the adaptive immune response to commensal bacteria and low-grade systemic inflammation.(6) Much like all ILC subsets, ILC3 become activated by signals in their surrounding microenvironment, such as IL-23, and become activated to produce IL-17 or IL-22.(87) However, in the action of ILC3 in this study was shown to be independent to these processes.(6) It was discovered using genome-wide association studies (GWAS) that RORγt<sup>+</sup> ILC express MHCII and, in keeping with this, were capable of processing and presenting antigen.(6) Interestingly, this action limited the CD4<sup>+</sup> T cell response to commensal bacteria rather than inducing a response.(6) This role is supported by the ability of ILC3 to outcompete CD4<sup>+</sup> T cells for IL-2, and thus limit some of the signals required for T cell proliferation; resulting in apoptosis of these cells.(94) Further to this, ILC3 in the

small intestine are considered key sources of IL-22 that supports epithelial barrier integrity.(89,95) However, overproduction of this cytokine is associated with driving inflammation in the intestine.(95) Other supportive functions of ILC3 have been demonstrated in the adult where LT $\alpha$ i cells have been shown to express co-stimulatory molecules, CD30L and OX40L, which are associated with the survival of T cells.(89,96,97) This supports a role for these cells in the developed immune system in addition to supporting early lymphoid tissue development. Collectively, the evidence described here supports a role of ILC, namely ILC3, in maintaining tissue homeostasis in the small intestine.

### **1.6 ILC within the thymus**

Until recently, investigations concerning the function of ILC within the immune system have predominantly focussed on their role at peripheral locations, while our knowledge of ILC in primary lymphoid tissues is lacking. Although it is important to appreciate the bone marrow as a primary lymphoid organ that has a vital role in ILC production in the adult, this body research focuses solely on the characterisation of these cells within the thymus.

The earliest description of ILC within the thymus relays back to the work of Rossi *et al.* (2007) which identified a subset of CD4<sup>+</sup> CD3<sup>-</sup> inducer cells within the embryonic thymus.(98) It is now understood that these cells are LT $\alpha$ i cells and categorised within a much wider family of ILC. In this context, LT $\alpha$ i cells were shown to contribute to the establishment of the thymic microenvironment through the provision of Receptor Activator of Nuclear factor Kappa-B Ligand (RANKL) to the surrounding stroma. Specifically, the contribution of RANKL from LT $\alpha$ i cells enables the maturation of CD80<sup>-</sup> Aire<sup>-</sup> medullary Thymic Epithelial Cells (mTEC) progenitors to CD80<sup>+</sup> Aire<sup>+</sup>

mTEC. The expression of Autoimmune regulator (Aire) is crucial in the development of lifelong immune tolerance by presenting self-antigen to developing thymocytes in the thymic medulla and eliminating T cells whose T cell receptor (TCR) interacts with self-antigen. Furthermore, it has been reported that these RANKL signals are jointly provided by invariant V $\gamma$ 5<sup>+</sup> dendritic epidermal T cell (DETC) progenitors.(99)

The normal function of lymphoid tissue relies on mechanisms that govern the establishment, maintenance and recovery of these sites. In the adult thymus ILC3 have been implicated in the recovery of the thymic architecture following damage by providing key IL-22 signals.(100) In this model, it was proposed that the depletion of double-positive (DP) thymocytes following damage triggered the production of IL-23 by thymic dendritic cells (tDC) that acted upon LT $\alpha$ i cells via the IL-23 receptor (IL-23R). Following activation by IL-23, LT $\alpha$ i cells provided a key source of IL-22 and that signals through thymic epithelial cells (TEC) and promotes their proliferation and survival.(100) Together, this process stimulates the regeneration of the thymic microenvironment and recovery of thymopoiesis. This was later studied in the context of Graft versus Host Disease (GVHD) where the absence of ILC3 resulted in the depletion of IL-22. The absence of IL-22 in this context impaired the protection of the thymic stroma through interactions and resulted in impairment of thymic recover.(101)

In addition to ILC3, there has also been evidence to illustrate the presence of ILC2 within the thymus. With much of this work being published in the last couple of years, and importantly, later than the commencement of the work presented within this thesis. Following a review of the currently literature it was clear that ILC2 had been implicated in both the mouse and human thymus, however the location of function of

these cells within this tissue are not entirely clear.(102) Initially, uncommitted thymic progenitors of human donors demonstrated potential for developing into ILC2 and this was dependent on the strength of Notch signalling. This *in vitro* study demonstrated T cells to develop in response to low strength Notch signalling while high strength signalling resulted in the development of ILC2.(102)

More recent studies illustrated the potential for ILC2 to develop within the thymus whereby ILC precursors had an inverse relationship with the activity of the E proteins, E2A and HEB.(103) Moreover, E2A activity amongst ILC precursors derived from CLP was reduced while the expression of Id2 in these cells was greatly increased. The 4 E proteins expressed in lymphoid cells are E12m E47, HEB and E2-2. Of these, E12 and E47 are encoded by the E2A gene locus, *Tcf3*, while *Tcf12* encodes HEB. H2A and HEB proteins were deleted using *Tcf3*<sup>-/-</sup> and *Tcf12*<sup>-/-</sup> mice and resulted in the blockage of ETP in both the foetal and adult thymus. Moreover, this blockage was accompanied by the aberrant development of ILC2.(103) It was established through these investigations that the development of ILC2 did not require the action of Id2, thus indicating the sole function of Id2 in ILC development is to inhibit the action of E proteins.(103)

Similar studies have also shown a drastic increase in ILC2 in the thymus following deletion of 2 E proteins.(104) In the same context, it was shown that aberrant expression of inhibitor of DNA-binding 1 (Id1), which is not normally found in lymphocytes, had the same effect.(104) Interest in ILC2 of a thymic origin has gained significant momentum over recent years. Further to the potential of these cells to arise from multipotent progenitors in the thymus, more current research has suggested these cells also have the potential to arise from T cell precursors.(105) In

this context, the authors labelled the *p/ck* transgene, which is specifically turned on in the thymus at the DN3 stage, with tdTomato.(105,106) This approach identified ~30% of thymic ILC2 to express tdTomato while labelling was absent from either B or myeloid cells, or ILC progenitors in the bone marrow.(105) These data indicate that a proportion of ILC2 in the thymus are derived from thymic progenitors.(105) Overall, this evidence proposes the idea that ILC2 are capable of developing within the thymus but their potential to do so is restricted due to E protein activity. While these studies provide insight into the origin of ILC2 within the thymus, little development has been made in understanding the location or function of these cells within this tissue.

Taken together, the evidence reviewed here demonstrates our understanding of ILC within primary lymphoid structures, such as the thymus, to be lacking. While there is evidence to support the premise that ILC3 support the establishment of the thymic microenvironment, much work is required to fully understand the ILC composition within this tissue. As such, this thesis will seek to characterise ILC in thymus and attempt to gain further understanding of its function in this tissue.

## **1.7 Experimental Approaches for Studying ILC in the Thymus**

The study of ILC within the thymus is no simple task given the complexity of this primary lymphoid organ. However, over the years, researchers have established a variety of methods to gain a further understanding of this tissue and the cells that reside within it. Characterisation of ILC across ontogeny, including the embryonic stages of development, and the role of ILC in the recovery of the thymus following damage are just two examples where we have referred to established methods to gain a further understanding. Our investigations utilised Foetal Thymic Organ

Cultures (FTOC) to study ILC within the embryonic thymus while models of sub-lethal, total body irradiation were used to study the role of ILC in thymic recovery following damage. Here, we review these methods to provide context to our investigations.

### **1.7.1 Foetal Thymic Organ Culture**

FTOC were initially developed as a means for studying intrathymic T cell development *in vitro*.<sup>(107)</sup> This provided a system where progenitors from an early embryonic timepoint could be tracked and followed through T cell development.<sup>(107)</sup> Ultimately, this technique demonstrated that immunocompetent T cells could be generated from thymic tissue explant *in vitro* under controlled conditions, giving greater insight into how T cells develop in the thymus and through which stages.<sup>(107,108)</sup> Early investigations using thymic lobes dissected from an embryonic mouse at days 14 and 15 of gestation identified large, blast-like cells that were hypothesised to be lymphoid cell progenitors.<sup>(107,108)</sup> Furthermore, it was observed within these experiments that FTOC resulted in a significant increase in the size of the thymic lobes that correlated within increasing lymphocyte number.<sup>(108)</sup> It was soon demonstrated that FTOC supported the emergence of lymphocytes of a size comparable to those in the periphery. Moreover, these cells expressed Thy-1, which is largely associated with mouse thymocytes and peripheral T cells.<sup>(109)</sup> Importantly, B cells were not identified in these FTOC; providing evidence to support the specialised function of the thymus in generating the production of T cells could be mimicked *in vitro*.<sup>(107,108)</sup>

These early investigations documented the use of FTOC in studying intrathymic mechanisms of T cell development and have been widely used since their

introduction. One such example includes the use of FTOC in determining the role of peptide-MHC complexes in negative and positive selection processes.(108,110) In these investigations, FTOC provided the means by which the effects of individual peptides on thymocytes selection could be studied.(2,4) In addition to their use in understanding thymocyte development, FTOC have been adapted to study the supporting role of the thymic microenvironment, particularly the function of thymic epithelial cells. In this context, FTOC enable recombinant proteins, such as cytokines, to be added in a closed system where it is possible to study the effects on the thymus only without having systemic consequences.(108) However, this has its caveats, as there may be circumstances when understanding the systemic effects is important. Examples of this include the study of therapeutic agents and in this case *in vivo* studies may be more appropriate.

The addition of 2-deoxyguanosine is a useful model for understanding the factors controlling epithelial cell development.(111) As an agent toxic to haematopoietic cells, it is used to deplete the thymic lobes of these endogenous cells while maintaining the core of the thymus.(111) Additional reagents can subsequently be added to the culture to determine its effect on epithelial cell development. One example of this is the addition of RANKL that demonstrated an increase in mTEC and Aire<sup>+</sup> mTEC.(98) Furthermore, it was through the use of FTOC that CD4<sup>+</sup> CD3<sup>-</sup> lymphoid inducer cells, which we now know belong to the ILC family were identified in the embryonic thymus at E14 and E16.(98) Overall, demonstrating that FTOC can be used to study the development and function of a whole host of cells within the thymus without too much difficulty. However, the very nature of *in vivo* experiments means that the surrounding environment is artificial and cannot replicate *in vivo*



conditions entirely. Despite this, FTOC is deemed an appropriate model for studying the thymus during the embryonic stages of development and will later be used to characterise ILC populations in this context.

### **1.7.2 Sub-lethal Irradiation**

Recent evidence has emerged that suggests ILC3, defined as ROR $\gamma$ t<sup>+</sup> CCR6<sup>+</sup> NKp46<sup>-</sup> lymphoid inducer cells, have a role in restoring the thymic microenvironment in a model of damage.(100) In the context of these investigations, the authors induce thymic damage using total body irradiation and, in turn, this leads to the production of IL-22 by ILC3 that acts upon thymic epithelial cells, resulting in restoration of the thymic microenvironment.(100) While the specific details of these investigations are discussed elsewhere within this thesis, it does introduce the idea of using irradiation models to investigate tissue recovery.

The involution of the thymus is associated with the natural ageing process but, interestingly, the reason for this involution is under constant debate.(112,113) Some immunologists argue that this is a result of limited recruitment of ETP into the thymus to sustain the thymocyte pool. However, it is also believed that it is a result of a decline in TEC populations that are required to support thymocyte development.(112,113) While it is likely that both are contributing factors, this is difficult to pull apart due to the interdependence between TEC and thymocyte populations in maintaining thymus homeostasis and function. In addition to involution with age, the thymus is sensitive to acute insult where circumstances of treatment toxicity, such as chemotherapy, or infection have been shown to damage the thymus.(114) While the thymus is unable to self-renew as part of the ageing process, it is capable of some level of repair following injury.(113–115) Therefore,

understanding the mechanisms that govern tissue recovery in the thymus are of great interest and may provide insight into how these mechanisms can be manipulated for therapeutic gain.

Total body irradiation is a commonly used approach to investigate the recovery of the thymus in mice.<sup>(56)</sup> Cell DNA is targeted in total body irradiation and prevents cells from dividing and proliferating as they would under normal conditions.<sup>(116)</sup> Under this consensus, it is thought that actively proliferating cells, including haematopoietic cells such as thymocytes and peripheral lymphocytes, are sensitive to the effects of radiation while primitive haematopoietic precursors in the bone marrow are largely unaffected.<sup>(116,117)</sup> Exposure to sub-lethal, total body irradiation in mice has shown to cause immediate damage to most lymphoid progenitors and thymocytes, with DN and DP cells being most susceptible. This initiates apoptosis amongst these cells in rapid rates and, as a result, a relative increase in the number of CD4 and CD8 single positive cells is observed in the days following radiation.<sup>(116)</sup> More recently, a study investigating the long-term effects of irradiation on total thymocytes in mice demonstrated sex and irradiation dose to be influential factors in thymic recovery.<sup>(116)</sup> The authors illustrated that following an immediate, irradiation-induced loss of thymocytes, there is a transient increase in the total number of thymocytes by day 10, which is thought to be mediated by progenitors that are already in the thymus.<sup>(116)</sup> This transient increase is followed by another reduction in total thymocyte number that takes much longer to recovery. It is presumed that this second phase of recovery takes longer due to the requirement of the thymic to recruit new progenitors.<sup>(116,118)</sup> Interestingly, this research demonstrated that female mice reached this second peak of recovery at a much quicker rate than males.

Furthermore, male mice were much more sensitive to lower irradiation doses and exhibited more severe defects at a lower threshold.(116)

Overall, studies involving total body irradiation are widely accepted to understand more about thymic recovery following damage. Using this approach, it is possible to identify surviving populations following irradiation and interrogate the signals that they produce. In the context of this thesis, a model of sub-lethal irradiation will be used to investigate the role that ILC play in recovery of the thymus following damage.

### **1.8 Aims of this investigation**

The overall aim of this research was to investigate the role of ILCs in supporting thymic function, given the critical role of the thymus in controlling the generation of self-reactive T cells and the role of ILC in supporting tissue homeostasis. Furthermore, the initial description of LT<sub>i</sub> cells within the thymus preceded the identification of the ILC family and the formal definition of these cells. It is evident from the literature that ILC are involved in supporting epithelial barriers, such as the lung or gut. As such we sought to revisit the thymus, which has a rich epithelial network, in search of potential roles of ILCs in this microenvironment and whether this affected thymic epithelial populations and thus tolerance. We will test the hypothesis that LT<sub>i</sub> cells are the main population of cells amongst the ILC family within the thymus where they have a role in supporting tissue architecture.

In this investigation we aimed to:

1. Undertake a detailed characterisation of ILC populations in the thymus using different *in vivo* models and across ontogeny

2. Interrogate the potential role of ILC in normal thymic function and recovery post-injury.
3. Investigate similarities between ILC and iNKT populations in the thymus and the periphery

## **CHAPTER 2: MATERIALS AND METHODS**

## 2.1 Mice

Mice were obtained from the University of Birmingham Biomedical Services Unit (BMSU) and were used in accordance with Home Office regulations. Both wild type (WT) and transgenic mice were bred and maintained in the BMSU. Efforts were made to ensure mice were age and sex matched within each experiment. Adult mice between the ages of 6-12 weeks were used. Where embryonic or neonatal tissue was used, a timed mating was set up and a successful mating was indicated by the presence of a vaginal plug, noted as day 0 of gestation (embryonic day 0, E0). All transgenic mice used within this investigation were on a C57BL/6 background and are detailed in Table 2.1. A schematic illustrating frequently used conditional mouse strains in these investigations is shown in Figure 2.1. The intracellular mechanisms of two complex mouse strains used within our studies are shown in Figure 2.2 and Figure 2.3.

**Table 2.1 Mouse strains used in this investigation**

Mouse strain	Phenotype	Source
C57BL/6	Wild type	BMSU
B6.SJL- <i>Ptprc<sup>a</sup> Pepc<sup>b</sup></i> /BoyJ (BoyJ)	Congenic wild type mouse strain carrying the pan leukocyte marker, CD45.1	BMSU
BALB/c	Wild type	BMSU
B6.129S2- <i>Tcra</i> <sup>tm1Mom</sup> /J (TCR $\alpha$ <sup>-/-</sup> )	Mice deficient for the $\alpha$ and $\beta$ T cell receptor. As a result, these mice lack CD4 <sup>-</sup> CD8 <sup>+</sup> and CD4 <sup>+</sup> CD8 <sup>-</sup> T cells. CD4 <sup>+</sup> CD8 <sup>+</sup> and CD4 <sup>-</sup> CD8 <sup>-</sup> numbers are normal.(119)	The Jackson Laboratory

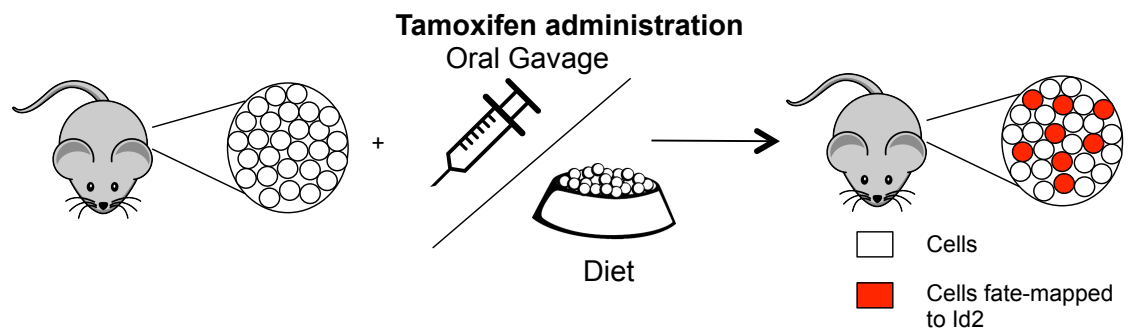
B6.129P2- <i>Rorc</i> <sup>tm1Litt/J</sup> ( <i>Rorc</i> <sup>-/-</sup> )	Immature CD4 <sup>+</sup> CD8 <sup>+</sup> require ROR $\gamma$ t for survival leading to impaired T cell development in mice lacking ROR $\gamma$ t. LTi cells, ROR $\gamma$ t <sup>+</sup> T cells and other cell types requiring this transcription factor are absent in these mice. Lymph nodes and Peyer's patches are also lacking.(120)	A kind gift from Daniela Finke. Originally donated by Dan Littman
B6.129S(Cg)- <i>Id2</i> <sup>tm1.1(cre/ERT2)Blh/ZhuJ</sup> x <i>Gt(ROSA)26Sor</i> <sup>tm4(ACTB-tdTomato,-EGFP)Luo/J</sup> ( <i>Id2</i> <sup>creERT2</sup> x <i>ROSA26</i> <sup>mT/mG</sup> )	Tamoxifen inducible fate-mapping mouse model whereby mT is expressed ubiquitously in all tissues. Administration of tamoxifen causes recombination in <i>Id2</i> -expressing cells where a cre-recombinase is present. mT gene is excised and allows for the expression of mG through the action of the promoter.(121,122)	The Jackson Laboratory
B6.129S(Cg)- <i>Id2</i> <sup>tm1.1(cre/ERT2)Blh/ZhuJ</sup> x <i>Gt(ROSA)26Sor</i> <sup>tm1Hjf</sup> ( <i>Id2</i> <sup>CreERT2</sup> x <i>ROSA26</i> <sup>RFP</sup> )	Tamoxifen inducible fate-mapping mouse model whereby cre-recombinase is present in cells expressing <i>Id2</i> . A floxed stop codon is present upstream of RFP under the control of the <i>ROSA26</i> promoter.(121,123)	A kind gift from Joerg Fehling
<i>Id2</i> <sup>tm1Gtbz</sup> ( <i>Id2</i> -eGFP)	<i>Id2</i> <sup>gfp/gfp</sup> reporter mouse strain whereby GFP is expressed in cells expressing <i>Id2</i> .(124)	Professor Gabrielle Belz, Walter and Eliza Hall, Institute of Medical Research
B6.FVB-Tg( <i>Rorc</i> -cre)1Litt/J ( <i>Rorc</i> <sup>Cre</sup> x <i>ROSA26</i> <sup>mT/mG</sup> )	Tamoxifen inducible fate-mapping mouse model whereby mT is expressed ubiquitously in all tissues. Administration of tamoxifen causes recombination in ROR $\gamma$ t-expressing cells where a cre-recombinase is present. mT gene is excised and allows for the expression of mG through the action of the promoter.(122,125)	The Jackson Laboratory
B6.129- <i>Tbx21</i> <sup>tm2Srn/J</sup> ( <i>Id2</i> <sup>CreERT2</sup> <i>Tbx21</i> <sup>F/F</sup> x <i>ROSA26</i> <sup>RFP</sup> )	Exons 2-6 of the T-box 21 ( <i>Tbx21</i> ) gene, that encodes Tbet, are flanked due to <i>loxP</i> sites on either side.	The Jackson Laboratory

**Figure 2.1 Schematic of frequently used tamoxifen-inducible Cre mouse models in our investigations.**

A)  $Id2^{CreERT2} \times ROSA26^{RFP}$ . Administration of tamoxifen, by either oral gavage or in diet, induces to the expression of RFP in cells that express Cre under the action of the *Id2* promoter. Cells that express Cre during, or just before, the window period of tamoxifen administration can be identified using flow cytometry based on expression of RFP. B)  $Id2^{CreERT2} \times ROSA26^{mT/mG}$ . The membrane Tomato “mT” protein is ubiquitously expressed in all tissues. Administration of tamoxifen, by either oral gavage or in diet, induces site-specific deletion of “mT” and expression of membrane Green “mG” in cells that express Cre under the action of the *Id2* promoter. Cells that express Cre during, or just before, the window period of tamoxifen administration can be identified using flow cytometry based on expression of “mG”.(121–123)



**A**  $\text{Id2}^{\text{CreERT2}}$  x  $\text{ROSA26}^{\text{RFP}}$



**B**  $\text{Id2}^{\text{CreERT2}}$  x  $\text{ROSA26}^{\text{mT/mG}}$

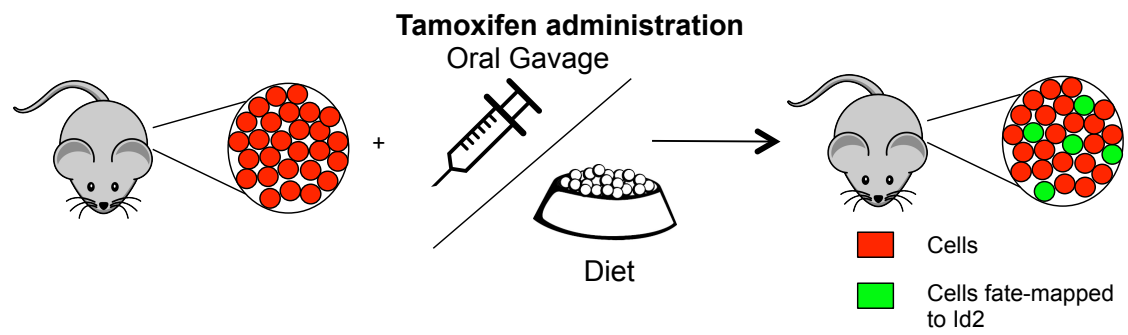
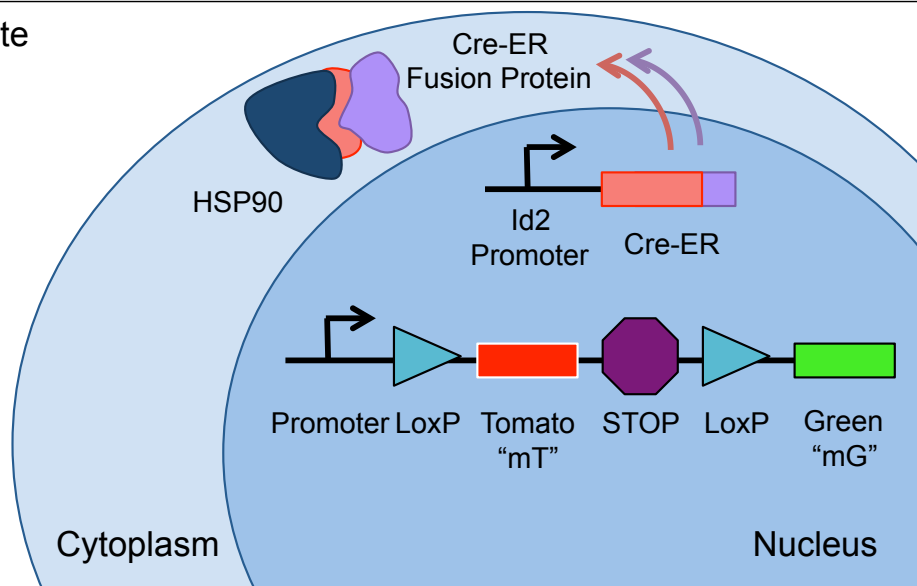


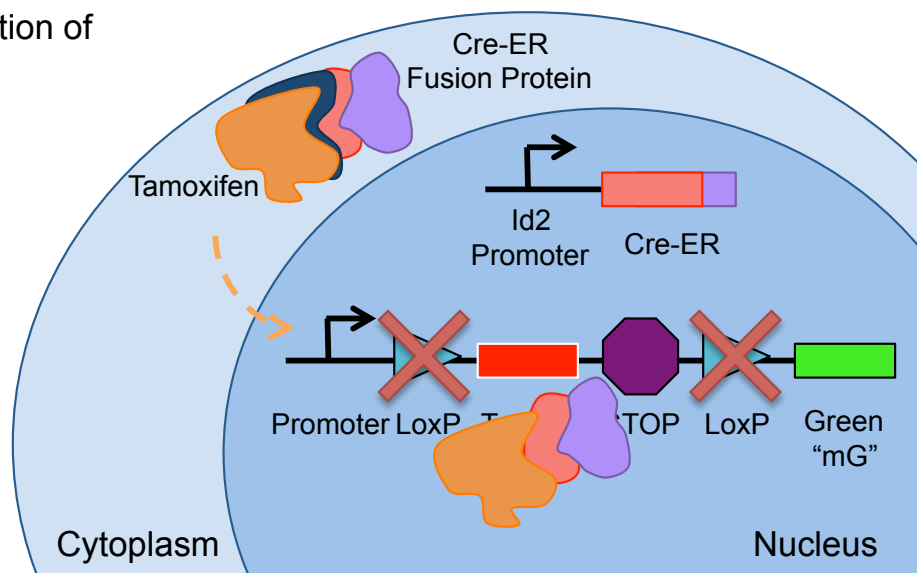
**Figure 2.2 Mechanism of Cre induction following administration of tamoxifen in  $Id2^{CreERT2} \times ROSA26^{mT/mG}$  mice.**

$Id2^{CreERT2} \times ROSA26^{mT/mG}$  is a tamoxifen-inducible fate-mapping model that enables specific labelling of cells that express Id2 during, and just before, the administration period when Cre is expressed. 1) “mT” is ubiquitously expressed in all tissues. In cells where Id2 is expressed, a transgene containing a mutated oestrogen receptor fused to a Cre-recombinase (Cre-ER) sits under the action of the Id2 promoter. When “switched on”, the transgene undergoes transcription and translation to create the Cre-ER protein that sits in the cytoplasm of these cells bound to Heat Shock Protein (HSP) 90. 2) Binding of the active tamoxifen metabolite, 4-hydroxytamoxifen (4-OHT), mutates the Cre-ER so that HSP90 is displaced and Cre-ER translocates to the nucleus where Cre recognises a specific DNA fragment, known as locus of x-over P1 (LoxP), and enables site specific deletion of the “mT” gene and stop codon. 3) This results in the expression of “mG” in these cells. Both “mT” and “mG” can be identified using flow cytometry without the need for additional antibodies.(122,126,127)

### 1. Steady state



### 2. Administration of tamoxifen



### 3. Expression of "mG"

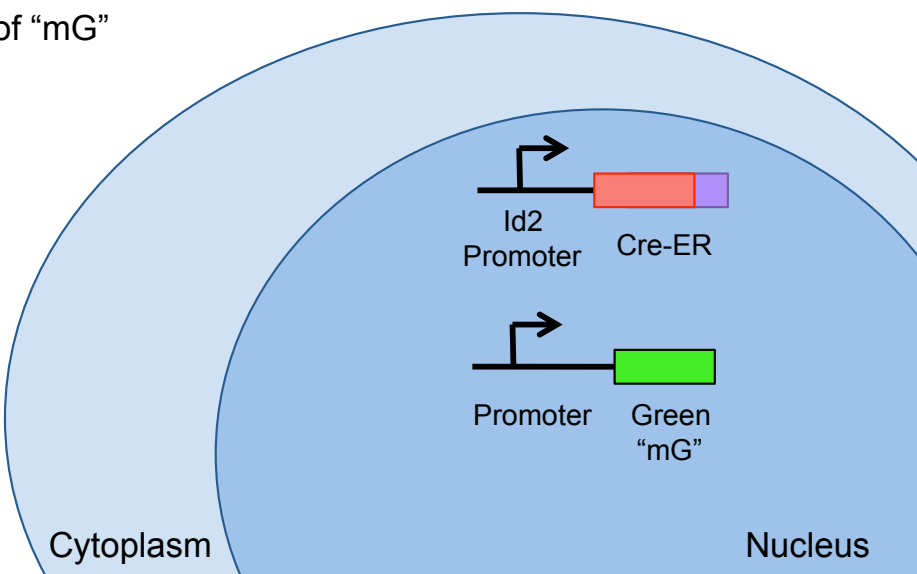
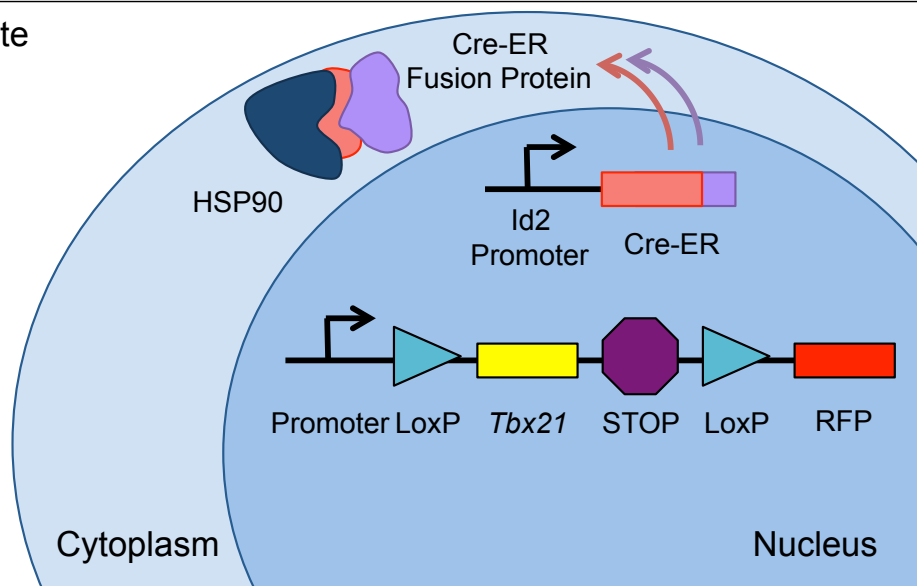


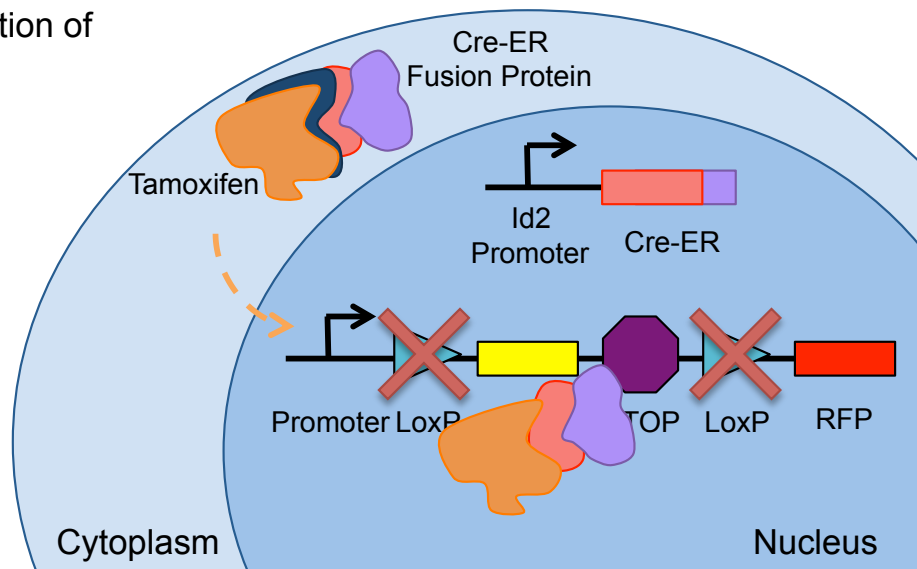
**Figure 2.3 Mechanism of Cre induction following administration of tamoxifen in  $Id2^{CreERT2} Tbx21^{F/F}$  x  $ROSA26^{RFP}$  mice.**

$Id2^{CreERT2} Tbx21^{F/F}$  x  $ROSA26^{RFP}$  is a tamoxifen-inducible fate-mapping model that enables specific deletion of *Tbx21* and expression of Red Fluorescent Protein (RFP) in cells that express *Id2* during, and just before, the administration period when Cre is expressed. 1) In cells where *Id2* is expressed, a transgene containing a mutated oestrogen receptor fused to a Cre-ER sits under the action of the *Id2* promoter. When “switched on”, the transgene undergoes transcription and translation to create the Cre-ER protein that sits in the cytoplasm of these cells bound to HSP90. 2) Binding of the active tamoxifen metabolite, 4-OHT, mutates the Cre-ER so that HSP90 is displaced and Cre-ER translocates to the nucleus where Cre recognises a specific DNA fragment, LoxP, and enables site specific deletion of the *Tbx21* gene and stop codon. 3) This results in the loss of Tbet and expression of RFP in these cells. RFP can be identified using flow cytometry without the need for additional antibodies.(123)

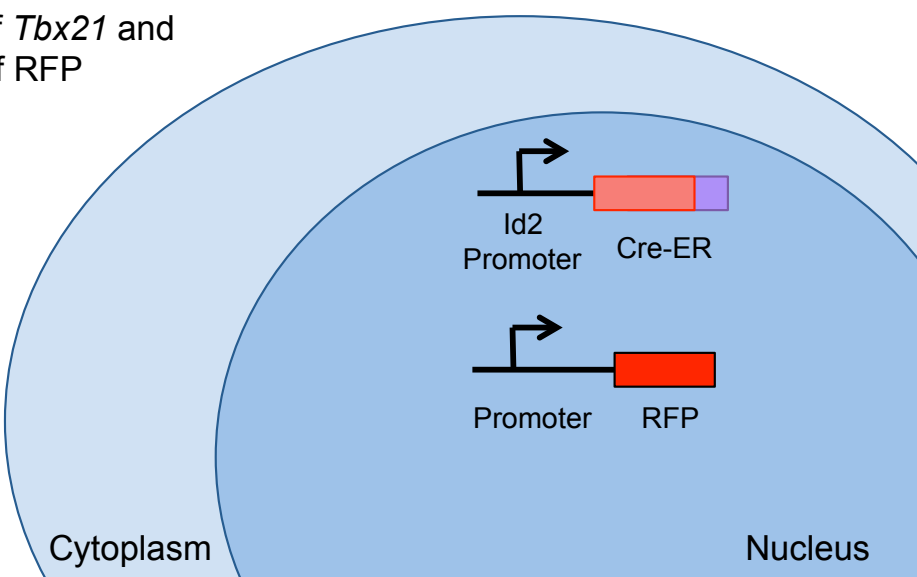
### 1. Steady state



### 2. Administration of tamoxifen



### 3. Deletion of *Tbx21* and expression of RFP



## 2.2 Medium and reagents

### 2.2.1 Medium

**Table 2.2 Components used in staining buffer**

Medium and reagents	Volume required	Final concentration	Supplier
D-PBS	500 ml	/	Sigma-Aldrich
Heat inactivated Foetal Calf Serum (FCS)	10 ml	2%	Sigma-Aldrich
EDTA	2.5 ml	2.5mM	Sigma-Aldrich

**Table 2.3 Components used in culture media**

Medium and reagents	Volume required	Final concentration	Supplier
RPML 1640 with L-glutamine	500 ml	/	Gibco
Penicillin/Streptomycin	5 ml	1%	Sigma-Aldrich
L-glutamine	5 ml	1%	Sigma-Aldrich
Heat inactivated FCS	50 ml	10%	Sigma-Aldrich

**Table 2.4 Components used in staining solution for immunofluorescence microscopy**

Medium and reagents	Volume required	Final concentration	Supplier
PBS	500 ml	/	Sigma-Aldrich
Bovine Serum Albumin (BSA)	5 ml	1%	Sigma-Aldrich

### 2.2.2 Gey's red blood cell lysis buffer

Gey's red blood cell lysis buffer was made within the laboratory by combining 10 ml of Solution A, and 2.5 ml of Solution B and C. The components of solutions A-C are shown in Table 2.5 with each solution being made to a final volume of 1 L with distilled water and autoclaved prior to mixing. The final solution was transferred to a Falcon tube (Corning®, Sigma-Aldrich) in 50 ml aliquots and stored at 4°C until required.

**Table 2.5 Components of Gey's red blood cell lysis buffer**

Solution	Component	Amount
A	1% Phenol red	1.5 ml
	Gelatin	25 g
	Glucose	5 g
	KCl	1.85 g
	$\text{KH}_2\text{PO}_4 \cdot 12\text{H}_2\text{O}$	1.5 g
	$\text{NH}_4\text{Cl}$	35 g
B	$\text{CaCl}_2$	3.4 g
	$\text{MgCl}_2 \cdot 6\text{H}_2\text{O}$	4.2 g
	$\text{MgSO}_4 \cdot 7\text{H}_2\text{O}$	1.4 g
C	$\text{NaHCO}_5$	22.5 g

## **2.3 Preparation of single cell suspensions**

Whole tissue for single cell suspensions was dissected within the BMSU and transported back to the laboratory in a 12-well plate (Thermo Scientific) with each well containing 1 ml of Roswell Park Memorial Institute (RPMI). Except for small intestine, this is described in 2.3.4. Efforts were maintained to keep tissue and cells on ice throughout all processes.

### **2.3.1 Lymph nodes**

Lymph nodes (LNs) were transferred to a small petri dish (Thermo Fisher Scientific) containing 3 ml of RPMI and cleaned of fat under a light microscope using fine forceps. Following the removal of fat, LNs were transferred to a new petri dish containing 3 ml of fresh RPMI. 0.025 mg/ml DNase I (Roche Diagnostics) and 0.25 mg/ml collagenase dispase (Roche Life Sciences) was added and samples were incubated for 20 minutes at 37°C/5% CO<sub>2</sub>. The reaction was stopped with the addition of 10 mM EDTA (Sigma-Aldrich). Samples were passed through a 70 µm nylon strainer (Falcon®, Fisher Scientific) and tissue was crushed through the membrane using the rubber end of a syringe plunger. Each petri dish was washed twice more with RPMI to maximise cell yield. Cells were pelleted by centrifugation and supernatant was removed prior to cell re-suspension in appropriate media. Samples were centrifuged for 5 minutes at 4°C and 394 rcf unless otherwise stated.

### **2.3.2 Spleen**

Fat was first removed from the spleen by eye using fine forceps and transferred to the top of a 70 µm nylon strainer where it was crushed using the rubber end of a



syringe plunger. Three washes using 5 ml of RPMI was performed to flush the cells into a Falcon tube. Following centrifugation and removal of the supernatant, cells were re-suspended in 5 ml of Gey's red blood cell lysis buffer and incubated on ice for 5 minutes. 30 ml of RPMI was added and cells were centrifuged once more and the supernatant was removed. Cells were re-suspended in appropriate media.

### **2.3.3 Thymus**

Care was taken during dissection to minimise the amount of fat attached to the thymus with any remaining fat removed by eye using fine forceps in the laboratory. Each thymus was transferred to a small petri dish containing 5 ml of RPMI and thymus tissue was mechanically disaggregated between two glass slides. Each side of the glass slides was washed with an additional 1 ml of RPMI prior to disposal. The sample solution was passed through a 70  $\mu$ m nylon strainer into a 50 ml Falcon tube. Any tissue caught on the strainer was crushed through using the rubber end of a syringe plunger and the petri dish was washed three more times using 5 ml of RPMI. Samples were centrifuged and the supernatant was removed prior to cell re-suspension in appropriate media.

### **2.3.4 Small intestine**

Preparation of single cells from small intestine required additional care from within the BMSU to preserve the viability of cells. The small intestine was removed by cutting from the bottom of the stomach down to the cecum and the tissue was placed in a large petri dish containing Hank's Balanced Salt Solution (HBSS) and 2% FCS. All HBSS used in small intestine preparation is calcium and magnesium free. The fat and Peyer's Patches (PP) were removed, and a longitudinal incision was performed to remove the contents of the small intestine. The tissue was washed once more in

HBSS containing 2% FCS and cut into 0.5 cm segments. These segments were transferred to a 50 ml Falcon tube containing 20 ml HBSS 2% FCS and shaken vigorously before transporting back to the laboratory on ice.

Pieces of small intestine were retrieved from solution by filtering through nylon mesh. Small intestine was transferred to a Falcon tube containing 20 ml pre-warmed HBSS 2 mM EDTA and shaken vigorously by hand for 20 seconds prior to incubation at 37°C/5% CO<sub>2</sub> in a shaking incubator. Sample was filtered as described above and added to 20 ml HBSS (no EDTA). This process was repeated twice. Pieces of small intestine were added to 15 ml pre-warmed culture media containing 1mg/ ml collagenase VIII (Sigma-Aldrich) and incubated for a total of 15 minutes at 37°C/5% CO<sub>2</sub> in a shaking incubator; removing intermittently to shake vigorously by hand. Following incubation, sample was placed on ice and filtered using a 100 µM nylon strainer Falcon®, Fisher Scientific). The sample was washed through the strainer twice with 5 ml staining buffer and filtered one final time through a 70 µM nylon strainer. Samples were centrifuged and the supernatant removed prior to re-suspension in staining buffer (Table 2.2).

### **2.3.5 Lung**

Additional care was required for dissection of the lung. Following exposure of the lung and heart by opening the chest cavity, a syringe was used to pierce the right atrium of the heart. The left ventricle was pierced using the same syringe and 10 ml of Phosphate Buffered Saline (PBS; Sigma-Aldrich) was flushed through the circulatory system to clear the lung tissue of red blood cells. The lung was dissected and transferred to a 12-well plate containing 1 ml of RPMI for transportation to the laboratory.

Lung was transferred to a small petri dish containing 1 ml culture media (Table 2.3) and broken into small pieces by pulling apart with fine forceps. Lung tissue along, with the culture media, was transferred to a 50 ml Falcon tube. The petri dish was washed with an additional 1 ml culture media that was also transferred to the Falcon tube. 3 ml culture media containing 424 µg/ml Liberase TM Research Grade (Sigma-Aldrich) and 0.025 mg/ml DNase I was added and samples were incubated for 45 minutes at 37°C/5% CO<sub>2</sub>, shaking intermittently. The sample was transferred into a new 50 ml Falcon by passing through a 70µM nylon strainer. The original Falcon tube was washed three times with 5 ml culture media and any tissue present on the strainer was crushed through using the rubber end of a syringe plunger. Sample was centrifuged and supernatant was removed prior to adding 3 ml Gey's red blood cell lysis buffer and incubating on ice for 2 minutes. 5 ml culture media was added and samples were centrifuged once more. The supernatant was removed and sample was re-suspended in an appropriate volume of staining buffer and filtered for a final time.

## **2.4 Flow cytometry**

A list of all antibodies and tetramers used throughout this investigation is shown in Table 2.6 and Table 2.7, respectively. Cells were stained in a 96-well plate (Thermo Scientific) unless otherwise stated. Cells from non-lymphoid tissue, such as the lung and small intestine, and those which have been used in cell culture, were incubated with APC efluor 780 (1:1000, eBioscience) in PBS for 20 minutes at 4°C to identify viable cells. Following incubation, 100 µl of PBS was added to each sample and centrifuged at 394 rcf for 3 minutes. All cells undergoing incubation with antibodies were washed under these conditions unless otherwise stated. The supernatant was

removed and cells were washed twice in 200 µl of staining buffer and centrifuged, removing the supernatant between each wash.

All samples were incubated with surface antibodies or tetramers in staining buffer on ice for 30 minutes. Except for CXCR5 and 2W1S:I-A<sup>b</sup> tetramer, where cells were incubated at room temperature for one hour, and CCR7 where cells were incubated for 30 minutes at 37°C. Antibodies used in a lineage gate were conjugated to the same fluorochrome to enable identification of multiple cells types in one flow cytometry channel. Following incubation, 100 µl staining buffer was added and cells were centrifuged. Cells were washed twice more and centrifuged in 200µl µl staining buffer to remove the unbound antibody prior to the next staining step. Where biotinylated antibodies were used, an additional staining step was incorporated before staining for all other surface antibodies; including a fluorochrome-conjugated streptavidin.

Intracellular staining was performed in experiments where transcription factor expression or cytokine production was assessed and required cell fixation and permeabilisation prior to antibody staining. Transcription factor analysis was performed using the FoxP3/Transcription Factor Fixation and Permeabilisation buffers (eBioscience). Evaluation of cytokine production was performed using the Cytofix/Cytoperm Plus Fixation and Permeabilisation buffers (BD Biosciences). Both kits were used in accordance with the manufacturer's instructions. Cells were fixed on ice for 30 minutes using 100µl µl fixative before 100µl µl permeabilisation buffer was added and cells were centrifuged. Cells were washed and centrifuged twice more using 200 µl permeabilisation buffer before incubation with antibodies against intracellular markers. Antibodies for analysis of intracellular markers were diluted

using permeabilisation buffer and 100 µl of antibody cocktail was incubated with cells for 45 minutes at room temperature. Following incubation, 100 µl permeabilisation buffer was added to each sample and cells were centrifuged. Cells were washed twice more and centrifuged in 200 µl staining buffer to remove the unbound antibody and cells were re-suspended in staining buffer for analysis by flow cytometry.

Where intracellular reporter dyes were present, such as GFP or RFP, cells were fixed using the FoxP3/Transcription Factor Fixation buffer (eBioscience) and permeabilised using the Cytofix/Cytoperm Plus (BD Biosciences) permeabilisation buffer. Antibodies against intracellular targets were diluted in Cytofix/Cytoperm Plus (BD Biosciences) permeabilisation buffer and incubation was extended to overnight at room temperature to enhance antibody signal strength.

Appropriate isotype, knockout (<sup>-/-</sup>) or fluorescence minus one (FMO) controls were used when necessary to identify negative populations. Splenocytes were typically used for single fluorochrome controls to adjust compensation values on the flow cytometer. Thymocytes were used for single fluorochrome controls where cells within the thymus were being assessed. The number of cells labelled with antibody varied depending on the tissue and cell-type under investigation. A greater number of cells were labelled in experiments where rare cell populations were being investigated.

Accucount blank particles (Spherotech) were added to samples to enable calculation of cell frequency and were acquired using the LSR Fortessa X-20 (BD Biosciences). Data was previewed and recorded using FACSDiva (BD Biosciences). Analysis of primary data from flow cytometry was performed using FlowJo (FlowJo, LLC) with GraphPad Prism version 6 (GraphPad) used for statistical analysis.

**Table 2.6 List of antibodies**

Specificity (anti-)	Clone	Conjugate	Working dilution	Manufacturer
B220	RA3-6B2	FITC	1:300	eBioscience
	RA3-6B2	PE-Cy7	1:200	eBioscience
	RA3-6B2	APC-Fire	1:100	eBioscience
CCR6	29-2L17	BV605	1:300	BioLegend
CCR7	4B12	PE	1:100	eBioscience
CD11b	M1/70	FITC	1:300	eBioscience
	M1/70	PE-Cy7	1:200	eBioscience
	M1/70	APC-Fire	1:100	BioLegend
CD11c	N418	FITC	1:300	eBioscience
	N418	PE-Cy7	1:200	eBioscience
	N418	APC-Fire	1:100	BioLegend
CD123	5B11	FITC	1:500	Invitrogen
CD19	eBio1D3	FITC	1:100	eBioscience
CD24	M1/69	PerCP/Cy5.5	1:1000	eBioscience
CD25	PC61	BV605	1:200	BioLegend
	PC61	BV650	1:200	
CD3ε	145-2C11	A700	1:50	eBioscience
	145-2C11	APC-Fire	1:100	BioLegend
	17A2	BV650	1:200	BioLegend
	145-2C11	FITC	1:100	BioLegend
	145-2C11	PE-Cy7		eBioscience
CD4	RM4-5	A700	1:100	BioLegend
	RM4-5	BV510	1:300	BioLegend
CD44	IM7	A700	1:200	eBioscience
	IM7	BV785	1:200	BioLegend
CD45	30-F11	BV785	1:200	BioLegend
CD49b	DX5	FITC	1:200	Invitrogen

CD5	5.3-7.3 5.3-7.3	FITC PE-Cy7	1:100	eBioscience BioLegend
CD62L	MEL-14	APC	1:1500	eBioscience
CD8 $\alpha$	53-6.7 53-6.7	BV510 BV711	1:200 1:200	BioLegend
CXCR5	2G8	PE-Cy7	1:50	BD Pharmingen
F4/80	BM8	FITC	1:200	eBioscience
Fc $\epsilon$ R1	MAR-1	FITC	1:200	Invitrogen
GATA3	TWAJ TWAJ	eFluor 660 PerCP-710	1:50 1:100	eBioscience eBioscience
Gr1	RB68C5	Alexa Fluor 488	1:2000	BioLegend
ICOS	C398.4A	PE-Cy7	1:200	BioLegend
IFN $\gamma$	XMG1.2	BV510	1:200	BioLegend
IL-13	eBio13A	PerCP-eFluor 710	1:100	eBioscience
IL-22	1H8PWSR	PerCP-eFluor 710	1:50	eBioscience
IL-5	TRFK5	BV421	1:200	BioLegend
IL-7R $\alpha$	A7R34 A7R34	BV421 BV711	1:50 1:50	BioLegend BioLegend
KLRG-1	2F1	BV421	1:200	BD Horizon
MHCII	M5/114.15.2	BV510	1:200	BioLegend
NK1.1	PK136	BV650	1:100	BD Horizon
NKp46	29A1.4	PE-Cy7	1:100	eBioscience
PD-1	29F.1A12	BV421	1:100	BioLegend
CD254 (RANK Ligand)	IK22/5	Biotin	1:50	eBioscience
ROR $\gamma$ t	AFKJS-9	APC PE	1:50 1:50	eBioscience
ST2	RMST2-2	PerCP-eFluor 710	1:50	eBioscience
Tbet	eBio4B10	eFluor 660	1:50	Invitrogen

	eBio4B10	PerCP/Cy-5.5	1:50	eBioscience
TCR $\beta$	H57-597	A700	1:100	BioLegend
TCR $\gamma\delta$	GL3	BV711	1:100	BD Horizon
Ter119	TER-199	FITC	1:100	Invitrogen
V $\gamma$ 1.1 TCR	2.11	BV421	1:200	BD Horizon
V $\gamma$ .2 TCR	UC3-10A6	PE-Cy7	1:200	eBioscience
CD45RB	C363-16A	PE	1:200	BioLegend

**Table 2.7 List of tetramers**

Tetramer	Conjugate	Working dilution	Source
2W1S	APC	1:200	NIH Tetramer Core Facility
	BV421	1:200	
CD1d	APC	1:200	NIH Tetramer Core Facility
	BV421	1:200	

## 2.5 Cell culture

### 2.5.1 *In vitro*

Cells were incubated for 4 hours or overnight in 1 ml culture media at 37°C/5% CO<sub>2</sub>. For analysis of IL-5 and IL-13 production, cells were incubated for a total of 4 hours in 1 ml culture media containing 20 ng/ml PMA and 1121 ng/ml ionomycin. 10 µg/ml Brefeldin A (BFA) was added after 1 hour to inhibit activity of the golgi apparatus and prevent export of cytokines outside of the cell. Where IL-22 production was being assessed, IL-1 $\beta$ , IL-2, IL-6 and IL-23, all at 20 ng/ml, were used in combination with PMA, Ionomycin and BFA, as described above. Thymocytes from neonatal thymus



were incubated overnight in 1 ml culture media only to assess RANKL expression. Typically, 1/3<sup>rd</sup> spleen, 1/2 mLN and  $\sim 6 \times 10^6$  thymocytes were set-up per 1 ml culture media. Samples investigating thymic ILC populations were set-up in duplicate and pooled following culture to ensure sufficient cell numbers were available for analysis.

### **2.5.2 Foetal Thymic Organ Culture (FTOC)**

The embryonic sack containing stage E16 mouse embryos was removed from a pregnant mouse following cervical dislocation. Each embryo was decapitated and cut along the breastbone to expose two thymic lobes, which were dissected under a light microscope in sterile conditions. Foetal thymic organ cultures were set up in optimal conditions as previously described by Jenkinson and Anderson (128). Thymic lobes were placed on an Isopore<sup>TM</sup> Membrane Filter (0.8  $\mu\text{m}$ , Millipore) and positioned on top of a 1cm<sup>2</sup> artwrap sponge within a small petri dish containing 2 ml DMEM (Sigma–Aldrich). Each petri dish was encapsulated within a sealed container containing 10 ml of H<sub>2</sub>O and incubated for 7 days at 37°C/5% CO<sub>2</sub>.

## **2.6 Immunofluorescence microscopy**

### **2.6.1 Preparation of frozen tissue**

Thymus tissue required for immunofluorescence microscopy was cleaned using forceps, mounted in optimal cutting temperature (OCT) and rapidly frozen using dry ice prior to freezing at -80°C until required. 6 $\mu\text{m}$  thymus sections were cut using a cryostat and mounted onto superfrost plus glass slides (Thermo Fisher Scientific) and were stored at -20°C before use in immunofluorescent labelling.

### **2.6.2 Immunolabelling of thymus sections**

Thymus sections were removed from storage at -20°C and rehydrated by placing in a

bath of PBS for 10 minutes. 1% bovine serum albumin (BSA) was used to prepare a staining solution, as detailed in Table 2.4. 75 µl 10% horse serum in 1% BSA was added to samples to prevent non-specific binding at protein binding sites and incubated for 15 minutes. Excess solution was aspirated from slides prior to incubation. Staining solution was used to prepare primary antibody mixes and 75 µl was added to each sample. Slides were incubated for 40 minutes in the dark inside a humidified chamber to prevent evaporation of staining solution and the drying out of tissue sections. Subsequent staining for all samples was performed using a 30-minute incubation time. A PBS bath was used to wash each slide for 10 minutes in between staining steps.

Multiple amplification steps were required for the detection of the transcription factor, GATA-3. Following incubation with a purified anti-rat antibody against GATA-3 (primary), tissue sections were incubated with donkey anti-rat-IgG conjugated to FITC (secondary), followed by rabbit anti-FITC conjugated to Alexa Fluor488 (tertiary), and finally donkey anti-rabbit-IgG conjugated to Alexa Fluor488. Details of the antibodies used for immunolabelling of thymus tissue sections are shown in Table 2.8 and Table 2.9.

With the exception of GATA-3, antibodies purified from rat were included after incubation with donkey anti-rat-IgG FITC to prevent non-specific binding of secondary anti-rat antibodies. This was aided by an additional step involving 15-minute incubation using 10% rat serum. Sections were incubated for 30 minutes in 100 µl 10% mouse serum, diluted in staining solution to achieve the desired concentration, to cross-absorb secondary, tertiary antibodies. Antibodies that were biotinylated were detected using fluorochromes conjugated to streptavidin. A final

step involved the counterstaining of sample sections with 4',6-diamidino-2-phenylindole (DAPI) and mounting each section with ProLong Gold (Invitrogen) was performed. Slides were sealed using clear nail varnish and were stored in the dark overnight to allow for drying. A Zeiss 780 Zen microscope (Zen) was used to analyse slides.

**Table 2.8 Primary antibodies used for immunofluorescence microscopy**

Specificity (anti-)	Clone	Conjugate	Working dilution	Manufacturer
CD3	eBio500A2	Biotin	1:100	eBioscience
GATA-3	TWAJ	/	1:20	eBioscience
ICOS	C398.4A	Alexa Fluor 647	1:25	BioLegend
IL-7R $\alpha$	A7R34	eFluor660	1:25	eBioscience

**Table 2.9 Additional antibodies and streptavidin for immunofluorescence microscopy**

Antibody	Conjugate	Type	Working dilution	Manufacturer
Donkey anti-rat-IgG	FITC	Secondary	1:150	Jackson ImmunoResearch
Rabbit anti-FITC	Alexa-Fluor488	Tertiary	1:200	Life Technologies
Donkey anti-rabbit-IgG	Alexa-Fluor488	Quaternary	1:200	Life Technologies
Streptavidin	Alexa-Fluor555	Quaternary	1:500	Life Technologies

## **2.7 *In vivo* experiments**

### **2.7.1 Sub-lethal irradiation**

Sub-lethal irradiations were required to investigate the radio-resistance of ILCs in the adult thymus. Mice were placed on Baytril 7 days prior to sub-lethal irradiation with 1x425 rad on day 1 of the protocol, and Baytril treatment continued for the first 7 days post-irradiation. Mice were culled at day 7 and 14 post-irradiation to investigate changes in thymic ILC populations at these time points.

### **2.7.2 Tamoxifen preparation and administration**

A 20 mg/ml stock solution of tamoxifen was prepared for administration by oral gavage. 200mg of tamoxifen was added to a 15 ml Universal tube containing 200µl µl absolute ethanol and made up to 10 ml with the addition of 9.8 ml of corn oil. The tube was wrapped in foil, vortexed and incubated in a 37°C water bath for approximately 4 hours until the tamoxifen was dissolved: identified by a translucent, yellow solution. The stock solution was stored at 4°C. When required, 200 µl of 20 mg/ml tamoxifen was given to mice by oral gavage for up to five consecutive days before analysis. Alternative experiments incorporated tamoxifen within the diet for a minimum of three weeks before analysis.

### **2.7.3 Immunisation with Lm-2W1S**

A model utilising *ActA-deficient Listeria monocytogenes-expressing* 2W1S peptide (Lm-2W1S) (sequence: EAWGALANWAVDSA) was used to investigate the role of Id2 in effector T cell function. Plates containing Lennox Luria-Bertani (LB) broth with agar (Sigma-Aldrich) and supplemented with 20 µg/ml chloramphenicol were used to culture Lm-2W1S overnight at 37°C. A single colony was selected and incubated at

37°C in LB broth supplemented with 20 µg/ml chloramphenicol overnight in a shaking incubator. Following overnight culture, bacteria were diluted 1/10, 1/20 and 1/50 in LB broth until an optical density (OD)<sup>600</sup> = 0.1 was obtained. A spectrophotometer (Jenway 6405) was used to measure OD and was calibrated using LB as a blank measurement. Bacteria was washed twice in sterile PBS and centrifuged at 394 rcf for 10 minutes in between washes to remove dead bacteria. A final dilution was performed to ensure 10<sup>7</sup> bacteria were present in 200µl µl sterile PBS. 10<sup>7</sup> Lm-2W1S in 200µl µl sterile PBS was administered to each mouse via intravenous injection of the tail vein on day 1 of the protocol.

## **2.8 Identification of 2W1S-specific T cells**

Mice were culled at day 4, 7 and 21 post immunisation and 2W1S-specific T cells within secondary lymphoid tissues were assessed. In order to identify T cells specific to 2W1S, 2W1S: I-Ab MHC class II tetramers conjugated to PE were incubated with cells, as described in 2.6. Tetramers were obtained from the National Health Institute (NIH) Tetramer Core Facility.

## **2.9 Tissue preparation for CD4<sup>+</sup> enrichment**

Enrichment of CD4<sup>+</sup> T cells was required for assessment of 2W1S<sup>+</sup> T cells 21 days after immunisation with Lm-2W1S, where 2W1S<sup>+</sup> numbers are reduced. Spleen and peripheral lymph nodes (axillary, brachial, inguinal and mesenteric) were excised from mouse and placed in 1 ml of RPMI for transportation to the laboratory. The spleen and lymph nodes from each mouse were transferred to a small petri-dish containing 5 ml of RPMI prior to cleaning of tissue. Additional fat attached to the spleen was removed by eye whereas lymph nodes were cleaned and teased apart using a light microscope. Fat removal for all tissues was performed using fine

forceps. Samples were crushed through a 70µM nylon strainer into a 50 ml Falcon tube using the rubber end of a syringe plunger. 5 ml of fresh RPMI was passed twice through the nylon strainer to wash through any remaining cells. Cells were pelleted by centrifugation at 394 rcf for 5 minutes. Supernatant was removed and 5 ml Gey's red lysis buffer was added to each sample and incubated on ice for 5 minutes. Following incubation, samples were washed with 30 ml RPMI, centrifuged and supernatant removed. Cells were re-suspended in 5 ml of RPMI and transferred to new 50 ml Falcon tube through a 70µM nylon strainer. 5 ml of fresh RPMI was passed twice through the nylon strainer and cells were centrifuged once again. The supernatant was removed and cells were re-suspended in staining buffer until required for antibody staining.

Following incubation with surface antibodies, including anti-CD4 conjugated to APC, and 2W1S: I-Ab (as described in 2.6), cells were re-suspended in 250µL staining buffer and 25µL of MACS anti-APC magnetic beads were added. Sample was vortexed and incubated on ice for 15 minutes. 2 ml staining buffer was added and the sample was centrifuged. Following removal of supernatant, the sample was re-suspended in 500 µL of staining buffer and positive selection of CD4<sup>+</sup> T cells was achieved using MACS LS-Columns (Miltenyi Biotech). Analysis of 2W1S-specific cells amongst the enriched CD4<sup>+</sup> T cell pool was performed using flow cytometry.

## **2.10 Statistical analysis**

Data from flow cytometry was analysed and enumerated using FlowJo (v10.2) and GraphPad Prism 6 (v6 Mac OS X). An unpaired, nonparametric Mann-Whitney *U* statistical test was used where applicable. Where more than 2 data sets were compared a Kruskal-Wallis one-way ANOVA with post hoc Dunn's test was used. For

each test, \* $p < 0.05$ , \*\* $p < 0.01$ , \*\*\* $p < 0.001$ , and \*\*\*\* $p < 0.0001$ . No bar present represents non-significant results.

## **CHAPTER 3: CHARACTERISING ILC POPULATIONS**

### **WITHIN THE THYMUS**



### **3.1 Introduction**

Much has been discovered about ILC since the recent emergence of this family of cells. While these cells are present at multiple sites, their exact phenotype and function is highly tissue specific.(129) Interestingly, the roles of ILC are diverse and vary across tissues where they can act to promote homeostasis or contribute to pathology.(129) In the lung, for example, ILC2 have involvement in tissue repair following acute viral infection but have also been implicated in inflammation in a model of allergic asthma.(130,131) Concerning ILC3, studies have demonstrated these cells to maintain intestinal homeostasis and limit the adaptive immune responses to commensal bacteria, demonstrating a role for these cells in peripheral immune tolerance.(6) While other research has demonstrated ILC3 to have a pathological role in a mouse model of inflammatory bowel disease where they mediate colitis. In addition to the specificity of ILC subsets within certain tissues, the precise composition of these cells at specific sites is regulated throughout development.

Encompassed within the ROR $\gamma$ t-dependent ILC3 family are LT $\alpha$ i cells that have reported roles in the development of primary and secondary lymphoid structures. In primary lymphoid tissue development, LT $\alpha$ i cells have been described in the embryonic thymus where they influence the establishment of the microenvironment through stromal interactions. Specifically, LT $\alpha$ i cells aid maturation of mTECs through the provision of RANKL signals.(98) At peripheral sites, LT $\alpha$ i cells orchestrate the development of secondary lymphoid tissues, such as lymph nodes and Peyer's patches.(129,132,133) The development of these tissues is a result of interactions between LT $\alpha$ i cells and the stroma, which initiates the recruitment of lymphocytes to

the site of the developing anlagen.(129,132,133) Therefore, ILC3 have an established role in the development of important primary and secondary lymphoid tissues that support the maturation of lymphocytes and subsequent immune responses. Moreover, ILC3 have been implicated in the recovery of tissue microenvironments following situations of tissue damage. In the spleen, for example, tissue recovery was impaired in *Rorc*<sup>-/-</sup> mice following viral infection.(134) However, in the thymus, LT $\alpha$ i cells are an endogenous source of IL-22 that promotes the recovery of thymic architecture following damage caused by radiation.

While ILC3 within the thymus has been the focal point of several studies over the last ten years, an interest in ILC2 within the thymus is only just gaining momentum. In fact, much of the progress concerning thymic ILC2 has been published in the last two years and provides evidence to support the idea of ILC2 with a thymic origin (Wang, 2017 and Qian, 2019). It is widely accepted that all ILC originate from a CLP in the bone marrow where Id2, an inhibitor of E protein transcription factors, is essential for the differentiation of all ILC subsets.(104) However, whether the development of ILC follow a single lineage or whether multi-potent progenitors outside of the bone marrow are able to produce ILC has yet to be elucidated.(104) It has been long established that CLP travel to the thymus where they have the potential to form early T cell progenitors (ETP).(104) Wang *et al.* (2017) hypothesised CLP within the thymus may also be a source of thymic ILC2. This idea is supported by the thymus being a rich source of IL-7 and Notch signals, which are essential for ILC2 differentiation.(104)

The authors demonstrated ILC2, defined as Lin<sup>-</sup> (Fc $\epsilon$ R<sup>-</sup> B220<sup>-</sup> CD19<sup>-</sup> Mac-1<sup>-</sup> Gr-1<sup>-</sup> CD11c<sup>-</sup> NK1.1<sup>-</sup> Ter-119<sup>-</sup> CD3<sup>-</sup> CD8 $\alpha$ <sup>-</sup> TCR $\beta$ <sup>-</sup> and  $\gamma\delta$ TCR<sup>-</sup>) ST2<sup>+</sup> Thy1<sup>+</sup>, to be present

in the thymus of a WT mouse. Furthermore, the deletion of H2A and HEB genes in the thymus resulted in an increase in ILC2 number. This was true for not only the thymus, but also ILC2 of the lung, mLN and spleen.(104) Later experiments demonstrated a similar outcome in transgenic mice with ectopic expression of Id1. While Id1 is not commonly expressed in lymphoid cells, T cell development is blocked at the DN stage in transgenic mice that are homozygous for Id1. Re-assessment of ILC2 in these mice identified, again, an increase in ILC2 number in the thymus, lung, mLN and spleen.(104) Collectively, the data presented within this study demonstrated the potential for ILC2 to be produced in the thymus following down regulation of the E proteins.

It was later discovered that DN1 and DN3 T cells were able to give rise to ILC2.(105) While this is unsurprising for DN1 cells given their multi-potent potential, cells other than T cells had not previously been shown to arise from DN3 cells. Moreover, previous *in vitro* studies have shown ILC2 were unable to develop from DN3 cells following culture with IL-7 and IL-33.(105) As such, this evidence postulates the idea that the ILC and T cell lineages are closer than first thought.(105)

While the ILC compartment in secondary lymphoid tissues has been extensively studied, a complete understanding of the composition of ILC within primary lymphoid structures, such as the thymus, is lacking. This is perhaps due to the phenotypic similarities between ILC and developing thymocytes that hinders the accurate identification of these cells. Furthermore, whether the ILC composition in the thymus changes across ontogeny has not been assessed. As such, we sought to undertake a detailed characterisation of ILC populations within the thymus, from the embryo through to adulthood, using a combination of robust *in vivo* models to aid the

accurate identification of these cells amongst developing thymocytes. An in depth understanding of the ILC composition in the thymus would support a function for these cells in supporting the thymic architecture. Based on the current literature, we hypothesise LT<sub>i</sub> cells to be the main ILC population in the thymus. This hypothesis will be addressed in 2 distinct aims:

1. Examine the ILC composition in the embryonic thymus
2. Characterise ILC populations from the neonatal thymus through to the adult thymus

## **3.2 Results**

### **3.2.1 Identification of ILCs within the developing thymus**

The presence of LT<sub>i</sub> cells within the embryonic thymus was first described more than 10 years ago, where their role in providing RANKL to immature mTEC progenitors was identified.(98,129) Much has changed since this early work by Rossi *et al.* (2007), including the discovery of a whole family of ILCs, of which LT<sub>i</sub> cells are encompassed. Furthermore, our knowledge and understanding of the thymus itself has changed. For example, recent studies have shown tuft cells, which were originally thought to reside only at peripheral locations, to be present within the thymus.(135,136) Amongst our understanding of ILC biology are clear definitions of both phenotype and function of ILCs, including LT<sub>i</sub> cells.(27) However, studies have predominantly focussed on descriptors of these cells within secondary lymphoid tissue while interest in primary lymphoid tissues, such as the thymus, has been lacking. Given the advances in our understanding of ILCs, including that of LT<sub>i</sub> cells,

we sought examine ILC populations within the embryonic thymus while incorporating the previously described LT<sub>i</sub> cells.

The early work by Rossi *et al.* (2007) identified LT<sub>i</sub> cells within the embryonic thymus using FTOCs that were cultured for a total of 7 days.(98) Small populations of cells expanded in these FTOCs and resulted in a greater number of cells available for analysis using flow cytometry. Within our investigation, this method was utilised to increase the number of ILCs, including the previously described LT<sub>i</sub> cells, within the embryonic thymus and aid their identification using flow cytometry.(98) To achieve this, thymic lobes from an E16 embryo were used to set up a FTOC and cultured for a total of 7 days. Cells isolated from 5 individual thymic lobes were pooled to ensure a sufficient number of cells for analysis by flow cytometry. Given that ILC1, ILC2 and ILC3, including LT<sub>i</sub> cells, have been described within the mLN of an adult mouse, cells isolated from this tissue were used as a positive control (Figure 3.1A).(88,89,137)

The phenotype of ILC and effector T cell populations is highly comparable due to their similar transcription factor usage.(27,74,138,139) Concerning the thymus, the ability to separate ILC and T cells populations has added complexity given the expression of GATA-3 and ROR $\gamma$ t at various stages of T cell development.(140,141) GATA-3, for example, is required for the development of early thymic progenitors (ETPs), the differentiation from double-negative (DN) stage 3 to DN4 T cells, and the development of T-helper 2 (Th2) cells. While ROR $\gamma$ t is expressed by immature CD4<sup>+</sup> CD8<sup>+</sup> double-positive (DP) thymocytes where it has a role in the maintenance of T cell survival.(142,143) As such, a robust method to discriminate between ILC and T cells is essential for accurate identification of ILC within the thymus, where vast

numbers of developing and mature T cells are present. This was achieved by adapting a well-defined gating strategy previously established within our laboratory for identification of ILC at peripheral sites.

Following identification of lymphocytes, cells lacking both CD8 $\alpha$  and CD3 $\epsilon$ -intracellular (CD3i) were selected (Figure 3.1A). The use of CD8 $\alpha$  and CD3i in combination eliminated a vast number of mature and developing T cells from subsequent FACS plots. Expression of CD8 $\alpha$  is specific to cytotoxic T cells and those at the double-positive stage of T cell development. All T cells, however, express CD3 $\epsilon$ , either intracellularly or surface bound, in association with the TCR, depending on their stage of maturation. Incorporation of CD3 $\epsilon$  into the intracellular panel of antibodies targets cytoplasmic CD3 $\epsilon$  and helps identify T cells with weak expression of surface CD3 $\epsilon$ . Furthermore, the introduction of CD3i was a simple addition to our flow cytometry panel considering there were already plans to permeabilise the cells for transcription factor staining. Importantly, CD8 $\alpha$  and CD3 $\epsilon$  are absent on ILC and therefore these cell markers are a suitable first step for the discrimination ILC from T cells in the thymus.

The use of CD8 $\alpha$  and CD3i removed approximately 60% of lymphocytes from analysis but further efforts were required to successfully identify ILC amongst the remaining cells (Figure 3.1A). ILC express IL-7R $\alpha$  but lack many cell surface receptors associated with other lineages, such as CD3 $\epsilon$ , CD5, B220, CD11b and CD11c. As such, antibodies against extracellular CD3 $\epsilon$ , CD5, B220, CD11b and CD11c, and conjugated to the same fluorochrome, were used. Within this analysis, the channel containing antibodies conjugated to the same fluorochrome is termed the “lineage” channel. This approach has been well defined within our laboratory and

seeks IL-7R $\alpha$ <sup>+</sup> Lineage<sup>-</sup> cells for the preliminary identification of total ILC (Figure 3.1A).

Finally, antibodies against transcription factors were used to identify individual subsets of ILC (27). GATA-3 and ROR $\gamma$ t are lineage defining transcription factors for ILC2 and ILC3, respectively, while ILC1 lack the expression of both transcription factors (27). Therefore, inclusion of antibodies against these transcription factors enables the identification of ILC2 and ILC3 amongst total ILC (Figure 3.1A). Unlike ILC2 and ILC3, ILC1 express the transcription factor Tbet, which can be used for discrimination of ILC1 from other subsets of ILC. However, due to restrictions in antibody availability, Tbet was not used in this analysis. Instead, cells lacking expression of GATA-3 and ROR $\gamma$ t were termed G<sup>-</sup>R<sup>-</sup> and require further analysis to confirm their identity (Figure 3.1A).

The gating strategy described above successfully identifies individual subsets of ILC amongst cells isolated from the adult mLN. As such, the gating strategy was applied to cells isolated from the E16 FTOC (Figure 3.1A). Consistent with populations observed in the adult mLN, this technique identified three distinct populations of ILC: GATA-3<sup>-</sup> ROR $\gamma$ t<sup>-</sup> (G<sup>-</sup>R<sup>-</sup> ILC), GATA-3<sup>+</sup> (ILC2) and ROR $\gamma$ t<sup>+</sup> (ILC3). Interestingly, in addition to ILC3, of which LT $\alpha$ i cells are incorporated, ILC2 and G<sup>-</sup>R<sup>-</sup> ILC were identified. It is possible for G<sup>-</sup>R<sup>-</sup> ILC to be ILC1, which express Tbet, or a subset of ILC that lack Tbet, GATA-3 and ROR $\gamma$ t, termed “Triple Negative” ILC that have been reported in other tissues.(88)

Enumeration of total thymic cellularity and total ILC, identified as CD8 $\alpha$ <sup>-</sup> CD3i<sup>-</sup> IL-7R $\alpha$ <sup>+</sup> Lineage<sup>-</sup>, demonstrated ILC populations make up almost 1% of total thymocytes at

E16 (Figure 3.1B-D). Analysis of ILC subsets by GATA-3 and ROR $\gamma$ t expression show ILC2 and ILC3 to be present in the E16 FTOC in similar proportions while G $\gamma$ R $\gamma$ <sup>-</sup> ILC were the least abundant, and was also true of the total cell numbers (Figure 3.1E). Reports of ILC3 at peripheral sites, such as the small intestine, have shown that ILC3 can be sub-divided into LTi cells, defined as CCR6<sup>+</sup> CD4<sup>+/+</sup>, and CCR6<sup>-</sup> CD4<sup>-</sup> NKp46<sup>+</sup> ILC3.(144) Therefore, we sought to define ILC3 subsets in the thymus where currently only LTi cells have been identified. Additional gating by flow cytometry demonstrated that approximately 70% of embryonic ILC3 were LTi cells (Figure 3.1F). However, enumeration of LTi cells and CCR6<sup>-</sup> CD4<sup>-</sup> ILC3 show a similar proportion and total number of these cells at E16 (Figure 3.1G). Overall, we have demonstrated ILC2 and ILC3, or at least their progenitors, account for the majority of ILC in the embryonic thymus under conditions of an *ex vivo* culture.(129) Other putative ILC are also present at this stage but further analysis including Tbet would be required to confirm the identity of these cells.

Owing to the advancement in knowledge and experimental tools available for ILC identification, we have added to our understanding of the ILC composition within the embryonic thymus. In addition to the role of LTi cells at this age, these cells have been described within the adult thymus where they provide an endogenous source of IL-22 for thymic regeneration.(98,100) As such, we sought to discover whether thymic ILC populations were maintained after birth. To address this question, ILC populations from the thymus at different stages post-birth were investigated using the gating strategy identified within the FTOCs.

Initial enumeration of the thymus was performed at day 1, 7 and 14 post-birth, and in adulthood; demonstrating a rapid increase in total thymic cellularity between day 1

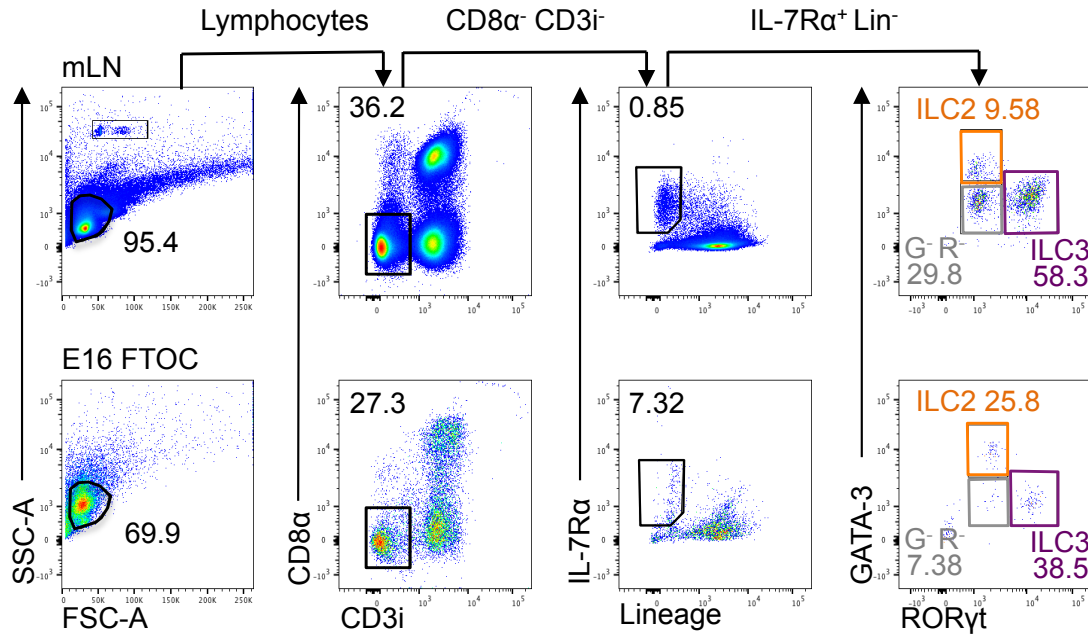
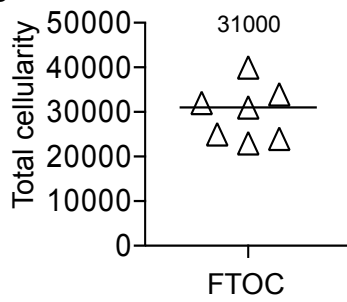
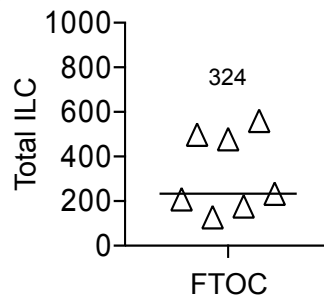
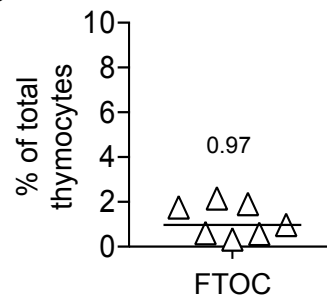
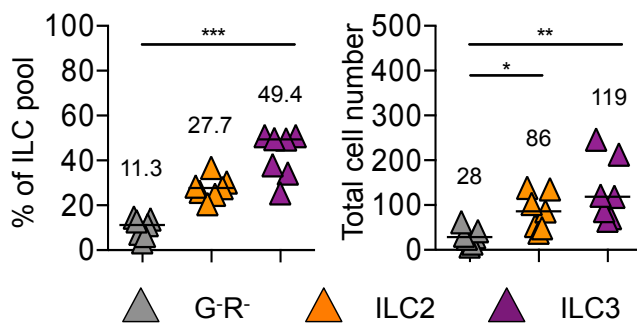
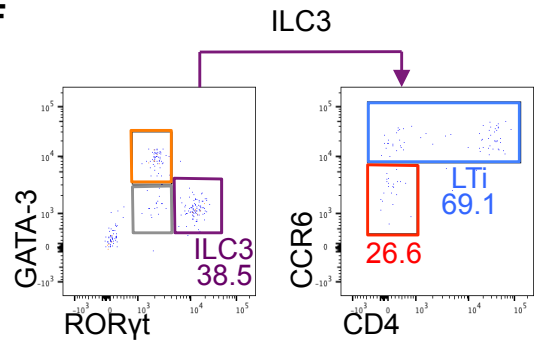
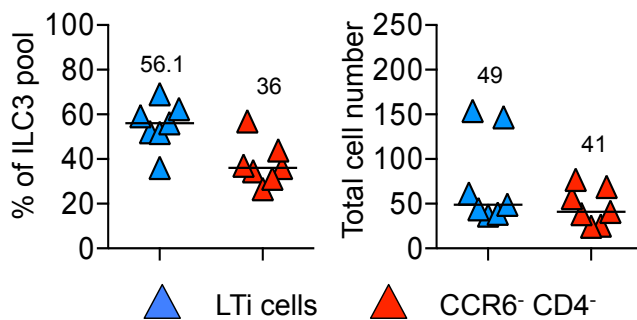


### Figure 3.1 Identification of ILC populations in foetal thymic organ cultures

Foetal thymic organ cultures (FTOC) using thymic lobes taken at embryonic day 16 (E16) were set up to investigate ILC populations in the embryonic thymus. Cells from an adult C57BL/6 mLN was used as a positive control for ILC staining. Cells from 5 E16 thymic lobes were combined to provide a sufficient number of cells for analysis by flow cytometry. Total numbers shown correspond to 5 E16 thymic lobes. Data in grey, orange and purple correspond to  $G\gamma R^-$  ILC, ILC2 and ILC3, respectively. Additional data in red and blue correspond to  $CCR6^-CD4^-$  ILC3 and LTi cells, respectively.

- A) Representative flow cytometry plots for the identification of ILC populations in the adult mLN and E16 FTOCs. ILCs are defined as  $CD8\alpha^-$  intracellular  $CD3^-(CD3i^-)$   $IL-7R\alpha^+$   $Lineage^-$   $GATA-3^-$   $ROR\gamma t^-$  ( $G\gamma R^-$ ),  $GATA-3^+$  (ILC2) and  $ROR\gamma t^+$  (ILC3). Lineage channel consists of antibodies against  $CD3$ ,  $CD5$ ,  $CD11b$ ,  $CD11c$  and  $B220$ .
- B) Total cellularity of 5 E16 thymic lobes following 7 days in culture.
- C) Total number of ILCs ( $CD8\alpha^-$   $CD3i^-$   $IL-7R\alpha^+$   $Lineage^-$ ) in 5 E16 thymic lobes following 7 days in culture.
- D) The percentage of ILC ( $CD8\alpha^-$   $CD3i^-$   $IL-7R\alpha^+$   $Lineage^-$ ) as a proportion of total thymic cellularity.
- E) The proportion and total number of  $G\gamma R^-$  ILC, ILC2 ( $GATA-3^+$ ) and ILC3 ( $ROR\gamma t^+$ ) within the ILC pool ( $CD8\alpha^-$   $CD3i^-$   $IL-7R\alpha^+$   $Lineage^-$ ) of 5 E16 thymic lobes.
- F) Representative flow cytometry plots for the identification of LTi-like ( $ROR\gamma t^+$   $CCR6^+$   $CD4^{+/-}$ ) and  $CCR6^-CD4^-$  ILC3 in the E16 thymus following 7 days in culture.
- G) Proportion and total number of LTi-like ( $ROR\gamma t^+$   $CCR6^+$   $CD4^{+/-}$ ) and  $CCR6^-CD4^-$  ILC3 cells in 5 E16 thymus following 7 days in culture.

Mann-Whitney U (non-parametric, two-tailed) test was used (comparing two data sets) and a Kruskal-Wallis one-way ANOVA with post hoc Dunn's test was used (comparing three or more data sets) for statistical analysis where  $*p<0.05$ ,  $**p<0.01$ ,  $***p<0.001$ , and  $****p<0.0001$ . In all graphs the bar represents the median,  $n=7$  from two independent experiments.

**A****B****C****D****E****F****G**

and 14, which plateaued into adulthood (Figure 3.2A). As described within our early investigations, total ILC were identified as  $CD8\alpha^- CD3i^- IL-7R\alpha^+ Lineage^-$  and were present at all ages investigated; with the greatest proportion of ILC observed by flow cytometry present at day 1 (Figure 3.2B). Enumeration of ILC as a proportion of total thymocytes indicated ILC at day 1 to be significantly higher than at day 14 and in adulthood (Figure 3.2C). However, analysis of total ILC number at all ages identified the number of these cells to be greatest at day 14 with no significant reduction into adulthood (Figure 3.2D). Overall, these data demonstrate that ILC number is increased between day 7 and 14 post-birth, and the number observed at day 14 is maintained in adulthood. However, the number of ILC as a proportion of total thymic cellularity is reduced due to the substantial increase in T cells during development.

$CD4^+ CD8^+$  (double-positive) thymocytes are the most abundant population of T cells during development and can be used as an indicator of thymic growth.<sup>(145)</sup> As such, we sought to strengthen our claims in Figure 3.2 and confirm the expansion of thymic cellularity at D14 is a result of  $CD4^+ CD8^+$  T cells. This was achieved through analysis of  $CD4^+ CD8^+$  DP thymocytes in the thymus at day 1, 7, and 14 post-birth, and in adulthood. Early observations by flow cytometry indicated no change in the proportion of  $CD4^+ CD8^+$  thymocytes throughout development, which was consistent across all experiments (Figure 3.3A-B). However, enumeration of  $CD4^+ CD8^+$  thymocytes demonstrated a significant increase between day 1 and day 14 post-birth and the maintenance of  $CD4^+ CD8^+$  cells from day 14 into adulthood (Figure 3.3C). The pattern of change observed in total  $CD4^+ CD8^+$  number (Figure 3.3C) is comparable to the change in total thymus cellularity (Figure 3.2A). Thus, confirming

### **Figure 3.2 The proportion of ILC in the thymus rapidly declines during neonatal development**

To understand whether ILC populations were maintained after birth, ILC populations in thymus at different ages were characterised. Cells were isolated from WT thymus at day 1, 7 and 14 post-birth, and in adulthood (6-12 weeks). All cells were analysed using flow cytometry and total numbers calculated per whole thymus.

- A) Total cellularity of WT thymus at day 1, 7 and 14 post-birth, and in adulthood (6-12 weeks).
- B) Representative flow cytometry plots of thymic ILCs ( $CD8\alpha^- CD3i^- IL-7R\alpha^+ Lineage^-$ ) in WT thymus at day 1, 7 and 14 post-birth, and in adulthood (6-12 weeks). Lineage channel consists of antibodies against CD3, CD5, CD11b, CD11c and B220.
- C) The proportion of ILC ( $CD8\alpha^- CD3i^- IL-7R\alpha^+ Lineage^-$ ) as a percentage of total thymic cellularity in WT thymus at day 1, 7 and 14 post-birth, and in adulthood (6-12 weeks).
- D) Total number of ILCs ( $CD8\alpha^- CD3i^- IL-7R\alpha^+ Lineage^-$ ) in WT thymus at day 1, 7 and 14 post-birth, and in adulthood (6-12 weeks).

Kruskal-Wallis one-way ANOVA with post hoc Dunn's test was used (comparing three or more data sets) for statistical analysis where  $*p<0.05$ ,  $**p<0.01$ ,  $***p<0.001$ , and  $****p<0.0001$ . In all graphs the bar represents the median,  $n=9$ ,  $9$ ,  $7$  and  $7$  for day 1, 7 and 14 post-birth, and adulthood (6-12 weeks), respectively (A) or  $n=9$ ,  $7$ ,  $7$  and  $7$  for day 1, 7 and 14 post-birth, and adulthood (6-12 weeks), respectively (B-D). Data shown from two independent experiments.

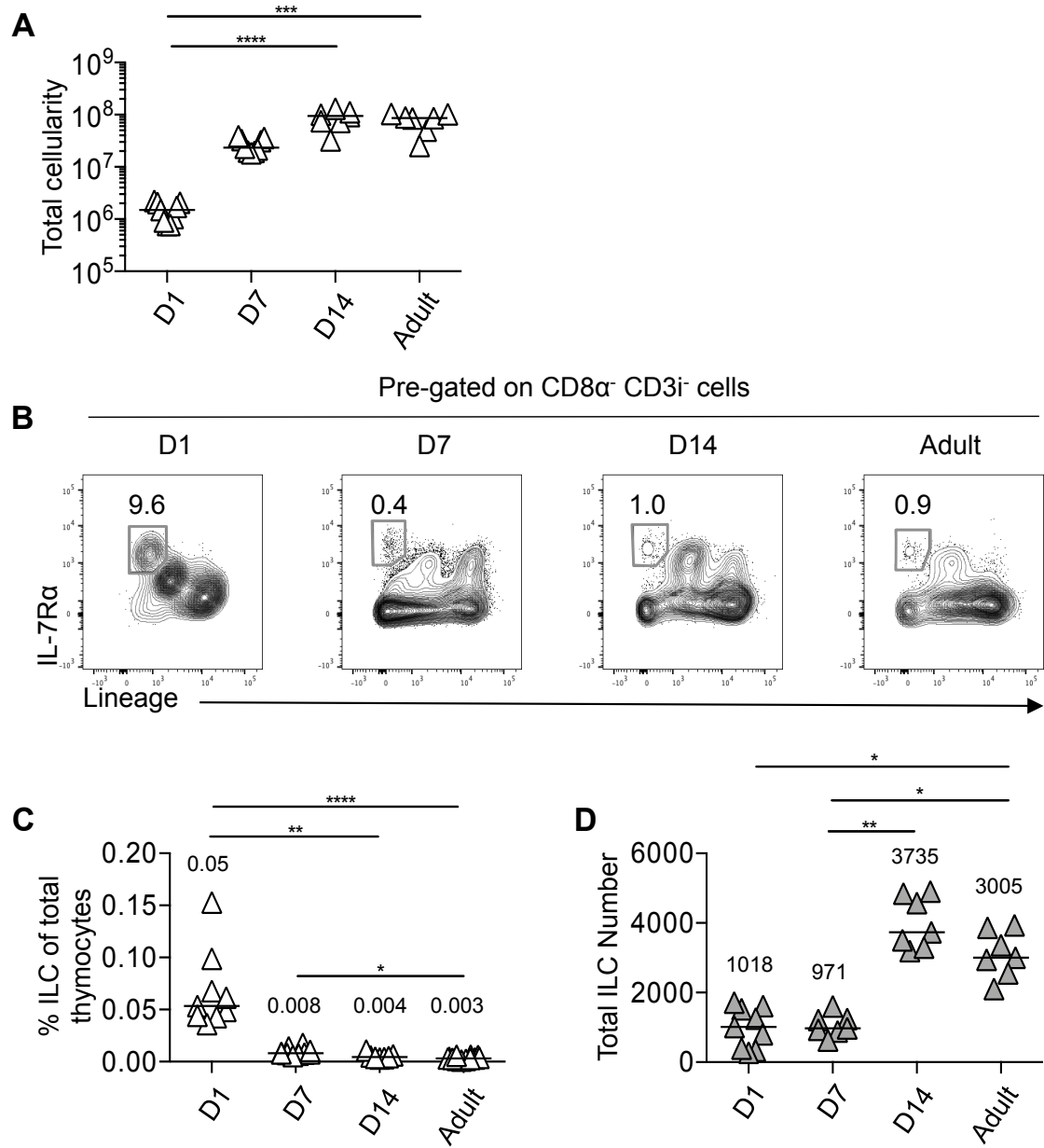


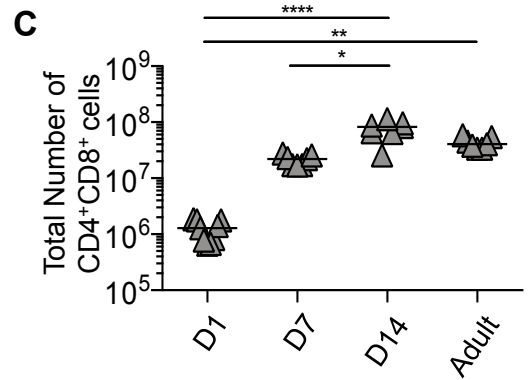
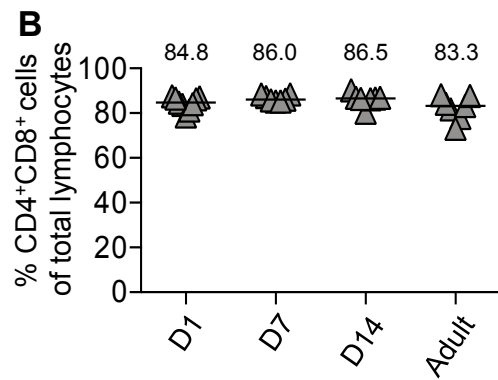
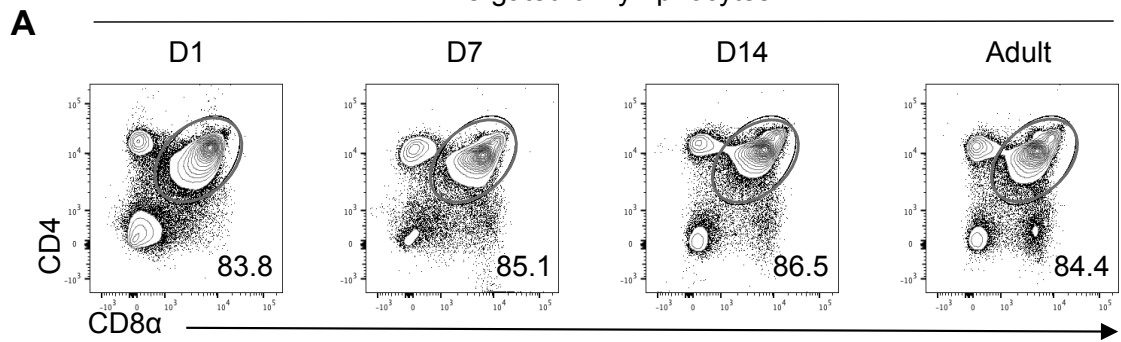
**Figure 3.3 The decline in the proportion of ILC coincides with an increase in T cell number**

To determine whether the decline in ILC number coincides with changes in T cell populations, double-positive ( $CD4^+CD8^+$ ) thymocytes at different ages were assessed. Cells were isolated from WT thymus at day 1, 7 and 14 post-birth, and in adulthood (6-12 weeks). All cells were analysed using flow cytometry and total numbers calculated per whole thymus.

- A) Representative flow cytometry plots of  $CD4^+ CD8^+$  thymocytes (pre-gated on lymphocytes) in WT thymus at day 1, 7 and 14 post-birth, and in adulthood (6-12 weeks).
- B) The proportion and of  $CD4^+ CD8^+$  thymocytes (pre-gated on lymphocytes) in WT thymus at day 1, 7 and 14 post-birth, and in adulthood (6-12 weeks).
- C) The total number of  $CD4^+ CD8^+$  thymocytes (pre-gated on lymphocytes) in WT thymus at day 1, 7 and 14 post-birth, and in adulthood (6-12 weeks).

Kruskal-Wallis one-way ANOVA with post hoc Dunn's test was used (comparing three or more data sets) for statistical analysis where  $*p<0.05$ ,  $**p<0.01$ ,  $***p<0.001$ , and  $****p<0.0001$ . In all graphs the bar represents the median,  $n=9$ , 7, 7 and 7 for day 1, 7 and 14 post-birth, and in adulthood, respectively. Data from two independent experiments (day 1, 7 and 14 post-birth) and four independent experiments (adulthood).

Pre-gated on lymphocytes



CD4<sup>+</sup> CD8<sup>+</sup> T cells to be responsible for the increase in thymic cellularity observed through development.

Thus far, these data have identified changes in total ILC numbers during neonatal development that are maintained into adulthood. However, changes in individual ILC subsets were yet to be determined. To address this, we enumerated ILC2 and ILC3 subsets in the thymus at day 1, 7, and 14 post-birth, and in adulthood. Cells isolated from the thymus at these time points were assessed by flow cytometry and ILC populations were defined according to their expression of GATA-3 (ILC2) and ROR $\gamma$ t (ILC3), as previously described (Figure 3.4A). Initial observations identified a similar proportion of ILC2 and ILC3 at day 1 and 7 post-birth (Figure 3.4A), consistent with the FTOC data shown in Figure 3.1. However, the proportion of ILC3 declined rapidly by day 14 and remained low into adulthood (Figure 3.4A). Upon enumeration, the proportion of ILC2 was maintained until day 14 but reduced into adulthood (Figure 3.4B). In comparison, the proportion of ILC3 was maintained only until day 7 and followed by a sudden decrease (Figure 3.4C). Interestingly, a similar number of ILC2 and ILC3 are observed up to day 7 (Figure 3.4D-E). However, from day 7 onwards the total numbers of ILC2 increase while the total number of ILC3 decline (Figure 3.4D-E).

Our early investigations identified a population of ILC within the thymus that lacked both GATA-3 and ROR $\gamma$ t, likely to be ILC1, which express Tbet.(27) To investigate whether ILC1 reside in the neonatal thymus, ILC populations from the thymus at day

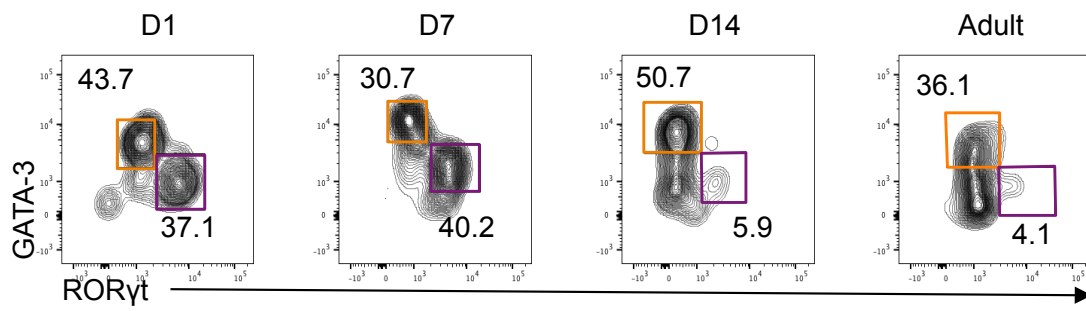
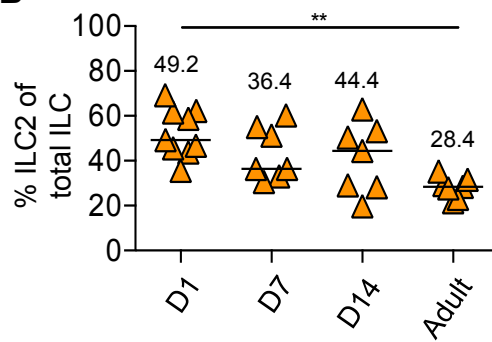
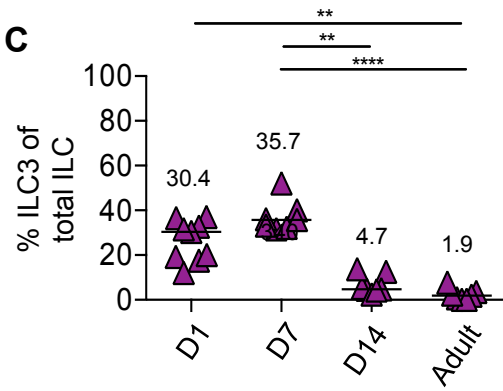
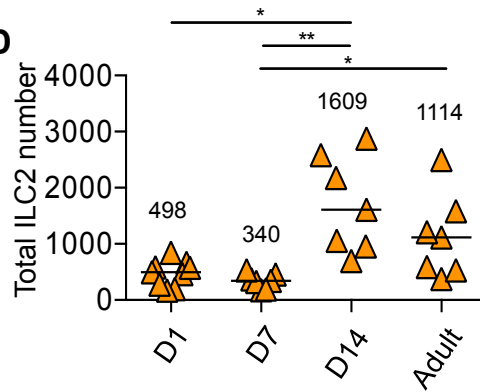
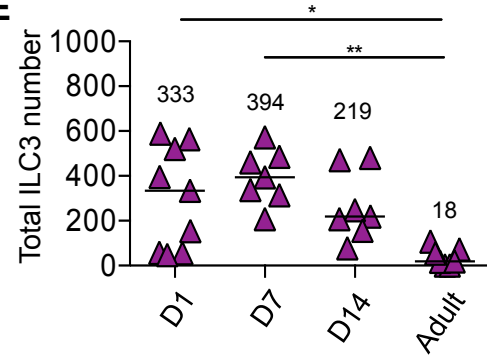


**Figure 3.4 Tracking of ILC2 and ILC3 populations through neonatal development reveals a dramatic decline in ILC3 over time**

To assess changes in ILC2 and ILC3 populations during development, ILC2 and ILC3 in the thymus at different ages were assessed. ILC2 and ILC3 were isolated from the thymus at day 1, 7 and 14 post-birth, and in adulthood (6-12 weeks). All cells were analysed using flow cytometry and total numbers calculated per whole thymus. Data corresponding to ILC2 and ILC3 is shown in orange and purple, respectively.

- A) Representative flow cytometry plots of thymic ILC2s (GATA-3<sup>+</sup>) and ILC3 (RORγt<sup>+</sup>) in WT thymus at day 1, 7 and 14 post-birth, and in adulthood (6-12 weeks). ILC2 and ILC3 pre-gated on CD8α<sup>-</sup> CD3i<sup>-</sup> IL-7Rα<sup>+</sup> Lineage<sup>-</sup> cells where the lineage channel consists of antibodies against CD3, CD5, CD11b, CD11c and B220.
- B) The proportion of thymic ILC2 (GATA-3<sup>+</sup>) at day 1, 7 and 14 post-birth, and in adulthood (6-12 weeks).
- C) The proportion of thymic ILC3 (RORγt<sup>+</sup>) at day 1, 7 and 14 post-birth, and in adulthood (6-12 weeks).
- D) The total number of thymic ILC2 (GATA-3<sup>+</sup>) at day 1, 7 and 14 post-birth, and in adulthood (6-12 weeks).
- E) The total number of thymic ILC3 (RORγt<sup>+</sup>) at day 1, 7 and 14 post-birth, and in adulthood (6-12 weeks).

Kruskal-Wallis one-way ANOVA with post hoc Dunn's test was used (comparing three or more data sets) for statistical analysis where \*p<0.05, \*\*p<0.01, \*\*\*p<0.001, and \*\*\*\*p<0.0001. In all graphs the bar represents the median, n=9, 7, 7 and 7 for day 1, 7 and 14 post-birth, and in adulthood, respectively. Data shown two independent experiments (day 1, 7 and 14) and three independent experiments (adulthood).

**A**Pre-gated on CD8<sup>-</sup> CD3<sup>-</sup> IL-7R $\alpha$ <sup>+</sup> Lin<sup>-</sup> cells**B****C****D****E**

7 and 14 post-birth were assessed with the addition of antibodies against Tbet in the flow cytometry panel. Representative flow cytometry plots demonstrate a distinct population of ILC1 in the thymus at day 7, identified as CD8 $\alpha$ <sup>-</sup> CD3<sup>-</sup> IL-7R $\alpha$ <sup>+</sup> extended Lineage<sup>-</sup> (Figure 3.5A). The inclusion of an antibody against CD49b within this extended lineage panel enabled the exclusion of NK cells that also express Tbet; preventing the misidentification of ILC1.(146) Interestingly, a population lacking Tbet, GATA-3 and ROR $\gamma$ t, which we have termed “Triple Negative” (TrN) ILC, was also observed (Figure 3.5A). TrN ILC has previously been reported in multiple other tissues where prolonged enzymatic digestion has been linked to their increase.(88,129) However, thymus tissue in this investigation is disaggregated by mechanical means.(129) Both ILC1 and TrN were observed in the thymus at day 7 and day 14 post-birth. The proportion and total number of TrN ILC was shown to increase between day 7 and day 14 while there was no significant change in the proportion or total number of ILC1 between day 7 and 14 post-birth (Figure 3.5B).

### **3.2.2 Using fate-mapping of Id2 to track bona fide ILC populations in the thymus**

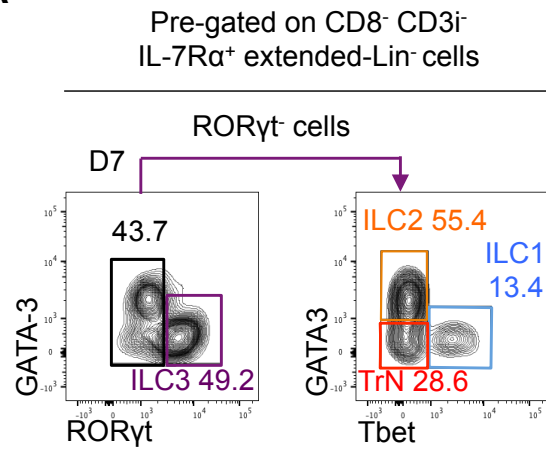
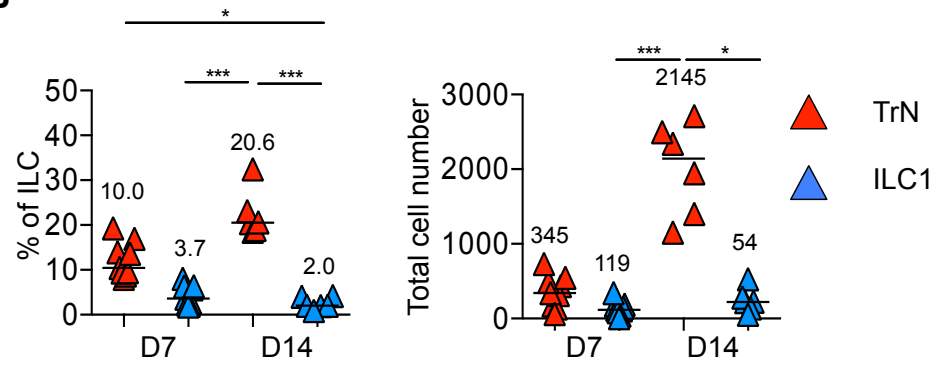
The surface phenotype of ILCs is highly comparable to T cells with the exclusion of its TCR and its associated signalling molecules.(74,138,139) Furthermore, the expression of the TCR varies throughout different stages of T cell development, increasing the difficulty of separating ILCs from T cells.(129) As a result, we anticipated correct identification of thymic ILC might prove difficult using surface markers alone and thus sought an additional model to help identify ILC populations within the thymus. Moreover, published data by Dudakov *et al.* (2012) described a substantial population of ILC3 present in the adult thymus. This population of ILC3

**Figure 3.5 ILC1 and ILCs lacking GATA-3, ROR $\gamma$ t and Tbet are found within the neonatal thymus**

Our previous data identified ILC2 and ILC3 in the thymus during development. Additional staining using Tbet was performed to expand our assessment of ILCs within the thymus to ILC1. Cells were isolated from WT thymus at day 7 and 14 post-birth. All cells were analysed using flow cytometry and total numbers calculated per whole thymus. Data in purple, red, orange and blue correspond to ILC3, TrN ILC, ILC2 and ILC1, respectively.

- A) Representative flow cytometry plots showing gating strategy for thymic ILCs identified as CD8 $\alpha$ <sup>-</sup>CD3i<sup>-</sup>IL-7R $\alpha$ <sup>+</sup>extended-Lin<sup>-</sup> cells with ILC1 (Tbet<sup>+</sup>), ILC2 (GATA-3<sup>+</sup>), ILC3 (ROR $\gamma$ t<sup>+</sup>), and “triple negative” ILC (‘TrN’; GATA-3<sup>-</sup>ROR $\gamma$ t<sup>-</sup>Tbet<sup>-</sup>) gated in the neonatal thymus at 7 days post-birth. Extended lineage channel consists of antibodies against B220, CD3, CD5, CD11b, CD11c, CD19, CD49b, CD123, F4/80, Fc $\epsilon$ R1, Gr-1, and Ter119.
- B) The proportion and total number of ‘TrN’ ILC and ILC1 in the neonatal thymus at 7 and 14 days post-birth.

Kruskal-Wallis one-way ANOVA with post hoc Dunn’s test was performed (comparing three or more data sets) for statistical analysis where \*p<0.05, \*\*p<0.01, \*\*\*p<0.001, and \*\*\*\*p<0.0001. In all graphs the bar represents the median, n=8 for day 7 and n=6 for day 14. Data shown from three independent experiments.

**A****B**

was not observed within our data and created a discrepancy between our data and that of Dudakov *et al.* (2012).(100) To strengthen the findings in our initial investigations, we anticipated that Id2 could be used as an aid for ILC identification using an *in vivo* model that enabled cell “fate-mapping” of Id2 expression. The Id2 transcription factor is a requirement of all ILC progenitors to enable differentiation from the common lymphoid progenitor (CLP) to the common helper ILC progenitor (CHILP), which is restricted to ILCs. Importantly, Id2 is largely absent, and not required, by developing thymocytes.(147–149)

To address this, ILC populations were first assessed in the mLN of Id2<sup>CreERT2</sup> x ROSA<sup>mT/mG</sup> mice after five consecutive days of tamoxifen administration by oral gavage with a three day gap between the last tamoxifen dose and mouse sacrifice. The administration of tamoxifen in these mice results in a switch from membrane tagged tomato-fluorescence (‘mT’) to expression of a membrane tagged green fluorescent protein (‘mG’ or ‘mGreen’ in Figures) in cells that express Id2 during, and just before, the window period of tamoxifen administration when Cre is expressed. Thus, providing a method to identify cells by their expression of Id2. Total cells (upper panel) were compared with cells that only expressed Id2 (lower panel) (Figure 3.6A).

Pre-gating on mGreen<sup>+</sup> cells indicated a substantial enrichment of ILC; demonstrated by an increase in the proportion IL-7R $\alpha$ <sup>+</sup> Lineage<sup>-</sup> cells compared to ILC amongst total lymphocytes (Figure 3.6A). Furthermore, the proportion of ILC2 and ILC3 subsets from enrichment was comparable to those arising from total lymphocytes (Figure 3.6A). Comparison of mGreen<sup>+</sup> ILCs with total ILCs highlighted a significant enrichment of ~30-fold when compared with total lymphocytes in the same tissue

### Figure 3.6 Analysis of thymic ILC populations through fate-mapping Id2 expression

To aid identification of thymic ILC populations, Id2<sup>creERT2</sup> x ROSA<sup>mT/mG</sup> mice were used to 'fate map' Id2 expression. Administration of tamoxifen by oral gavage on five consecutive days was performed and ILC populations in the thymus and mLN were analysed 3 days later. Samples were analysed using flow cytometry and total numbers calculated per whole thymus or mLN. Data shown in green, orange and purple correspond to mGreen, ILC2 and ILC3, respectively.

- A) Full gating strategy for flow cytometry data showing analysis of IL-7R $\alpha$ <sup>+</sup>Lin<sup>-</sup>CD3i<sup>-</sup>GATA-3<sup>+</sup> (ILC2) and IL-7R $\alpha$ <sup>+</sup>Lin<sup>-</sup>CD3i<sup>-</sup>ROR $\gamma$ t<sup>+</sup> (ILC3) cells gated on all lymphocytes (upper panels) versus pre-gating on mGreen<sup>+</sup> Id2 'fate-mapped' cells (lower panels) among mLN cells. Lineage channel consists of antibodies against CD3, CD5, CD11b, CD11c and B220.
- B) The proportion of 'fate mapped' ILC (IL-7R $\alpha$ <sup>+</sup>Lin<sup>-</sup>CD3i<sup>-</sup>mGreen<sup>+</sup>) and total ILC (IL-7R $\alpha$ <sup>+</sup>Lin<sup>-</sup>CD3i<sup>-</sup>) in the mLN of Id2<sup>creERT2</sup> x ROSA<sup>mT/mG</sup> mice.
- C) Full gating strategy for flow cytometry data showing analysis of IL-7R $\alpha$ <sup>+</sup>Lin<sup>-</sup>CD3i<sup>-</sup>GATA-3<sup>+</sup> (ILC2) and IL-7R $\alpha$ <sup>+</sup>Lin<sup>-</sup>CD3i<sup>-</sup>ROR $\gamma$ t<sup>+</sup> (ILC3) cells gated on all lymphocytes (upper panels) versus pre-gating on mGreen<sup>+</sup> Id2 'fate-mapped' cells (lower panels) among thymus cells. Lineage channel consists of antibodies against CD3, CD5, CD11b, CD11c and B220.
- D) The proportion of 'fate mapped' ILC (IL-7R $\alpha$ <sup>+</sup>Lin<sup>-</sup>CD3i<sup>-</sup>mGreen<sup>+</sup>) and total ILC (IL-7R $\alpha$ <sup>+</sup>Lin<sup>-</sup>CD3i<sup>-</sup>) in the thymus of Id2<sup>creERT2</sup> x ROSA<sup>mT/mG</sup> mice.
- E) The proportion and total number of mGreen<sup>+</sup> ILC2 (mGreen<sup>+</sup> IL-7R $\alpha$ <sup>+</sup> Lin<sup>-</sup> CD3i<sup>-</sup> GATA-3<sup>+</sup>) in the mLN and thymus of Id2<sup>creERT2</sup> x ROSA<sup>mT/mG</sup> mice.
- F) The total number of mGreen<sup>+</sup> ILC2 (IL-7R $\alpha$ <sup>+</sup>Lin<sup>-</sup>CD3i<sup>-</sup>GATA-3<sup>+</sup>) and ILC3 (and IL-7R $\alpha$ <sup>+</sup>Lin<sup>-</sup>CD3i<sup>-</sup>ROR $\gamma$ t<sup>+</sup>) in the mLN and thymus of Id2<sup>creERT2</sup> x ROSA<sup>mT/mG</sup> mice.

Mann-Whitney U (non-parametric, two-tailed) test was used for statistical analysis where \*p<0.05, \*\*p<0.01, \*\*\*p<0.001, and \*\*\*\*p<0.0001. In all graphs the bar represents the median, n=5. Data shown from two independent experiments.

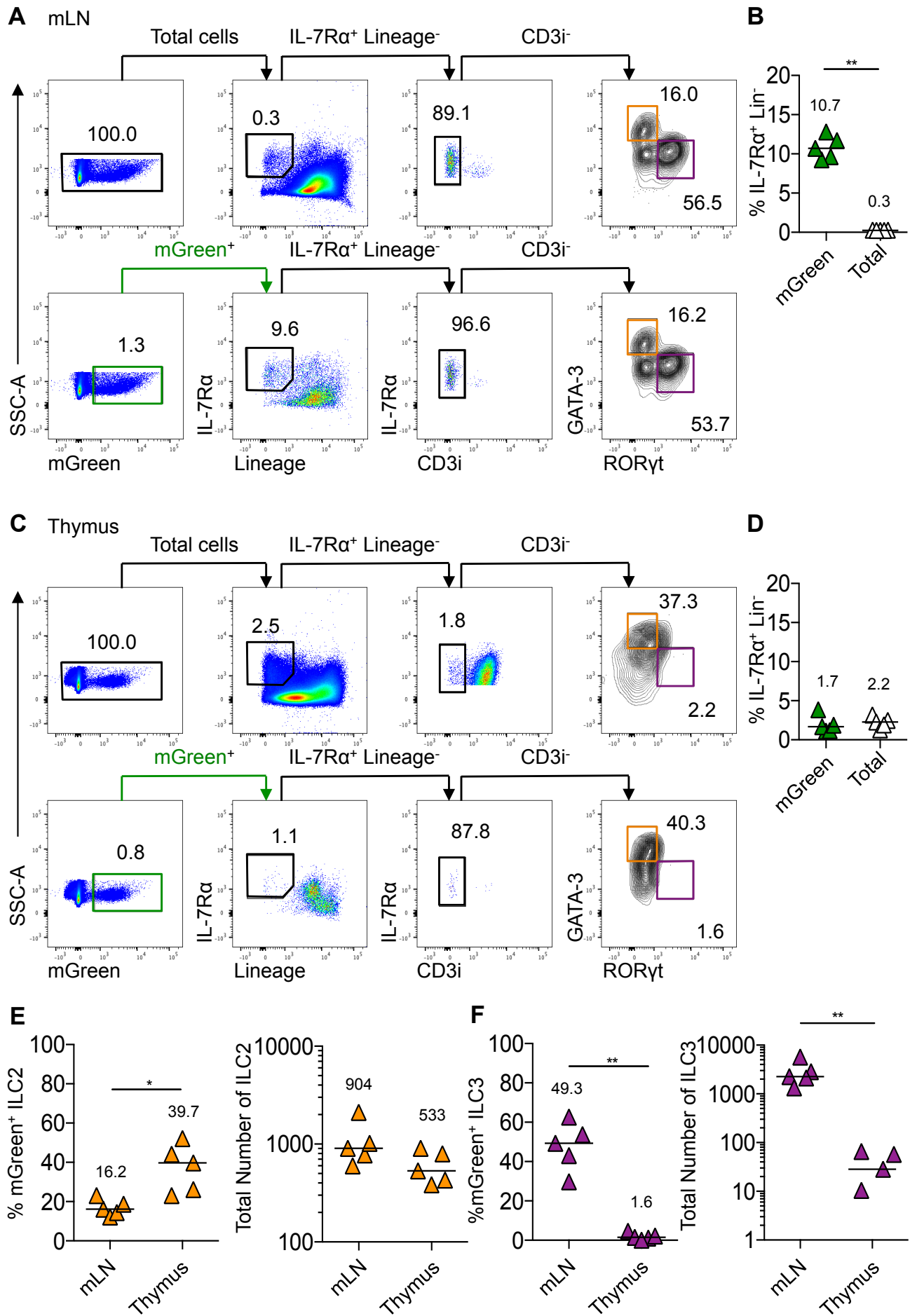




(Figure 3.6B). This approach was then applied to cells from the thymus to aid identification of ILCs (Figure 3.6C). Pre-gating on mGreen<sup>+</sup> cells compared to total thymocytes did not enrich for IL-7Rα<sup>+</sup> Lineage<sup>-</sup> but instead enabled more accurate gating on those cells for the identification of ILCs (Figure 3.6C-D). To enumerate ILC populations from the thymus, the efficiency of “fate-mapping” ILCs in the mLN was calculated and applied to data from the thymus; assuming a comparable induction of cre in both tissues. Comparison of % mGreen<sup>+</sup> ILC2 identified a greater proportion of ILC2 in the thymus than the mLN; however, when total ILC2 number within each tissue was calculated the final values were comparable (Figure 3.6E). Interestingly, a significant reduction in the proportion of mGreen<sup>+</sup> ILC3 and total ILC3 was observed in the thymus compared to the mLN (Figure 3.6F). These data is consistent with our earlier studies whereby very few ILC3 were detected in the adult thymus.(129)

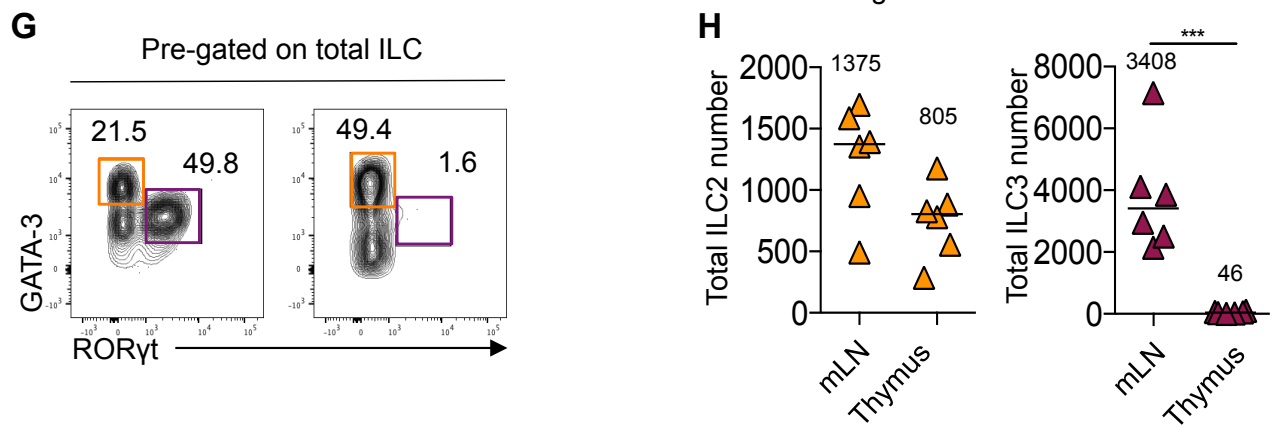
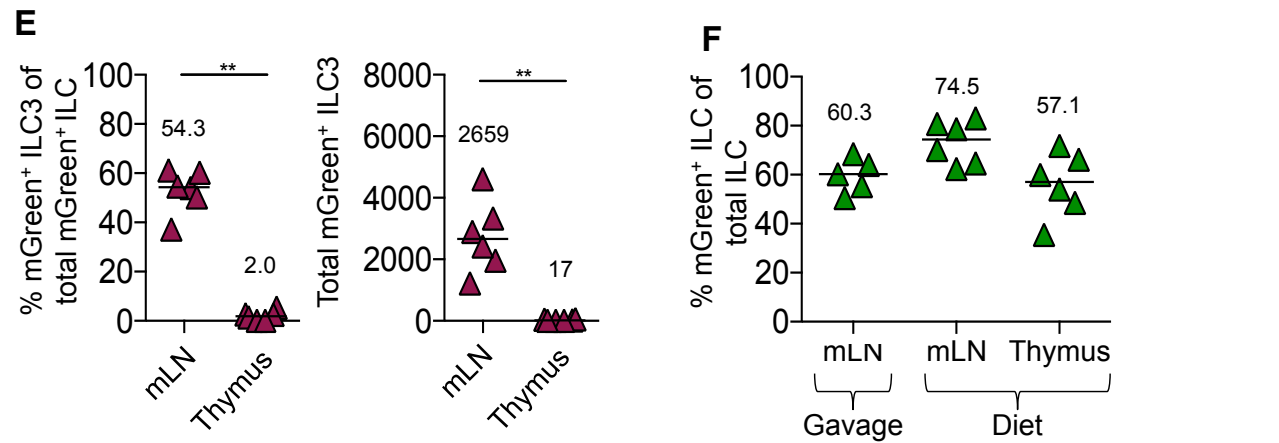
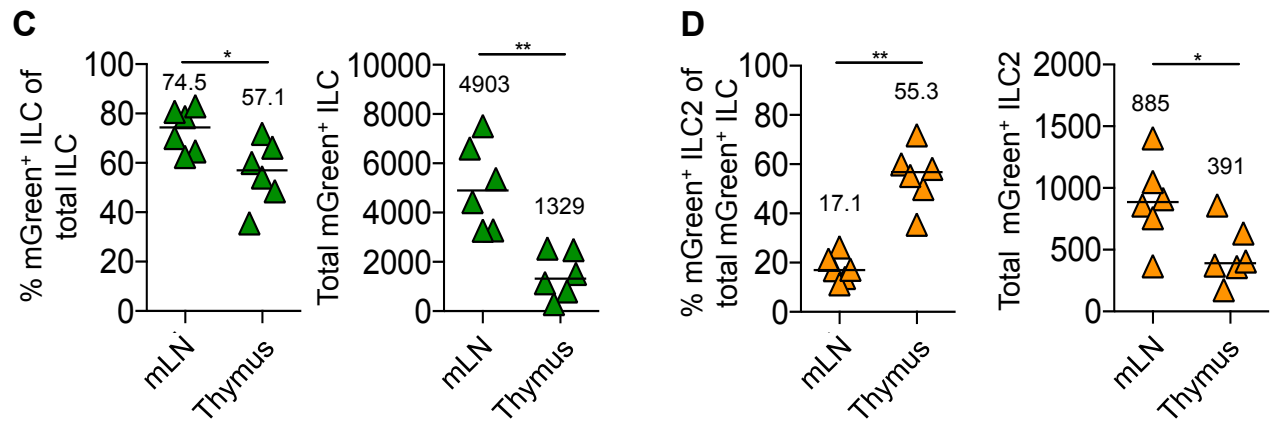
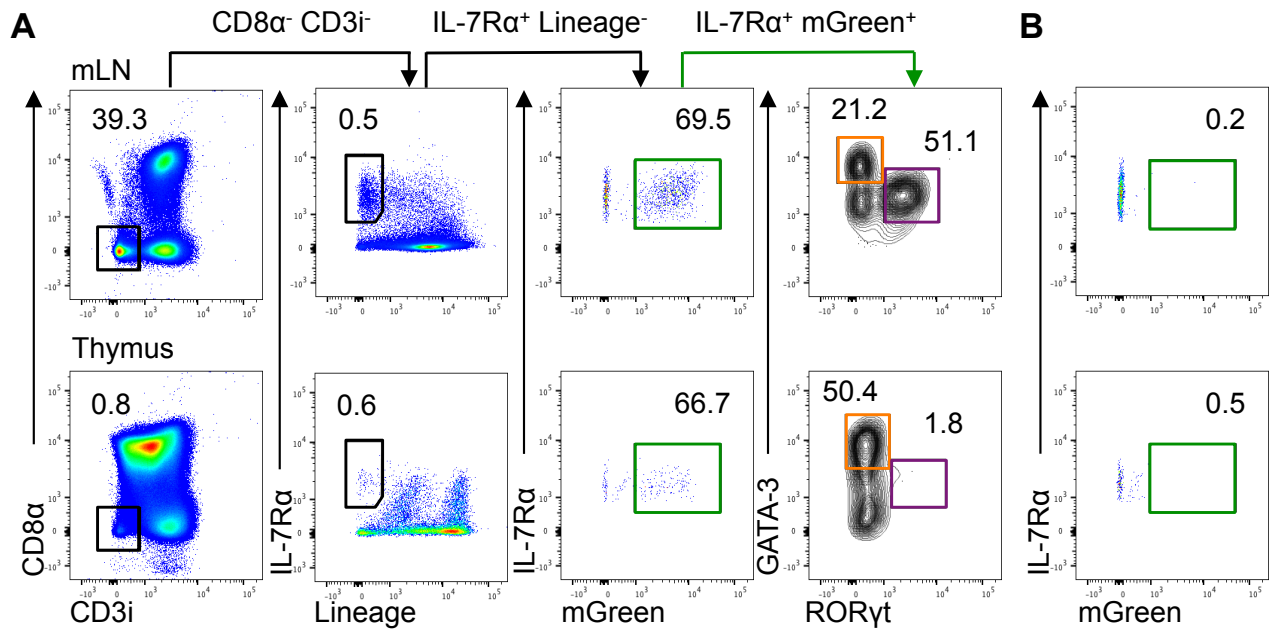
The frequency of mGreen<sup>+</sup> cells is influenced by the method and duration of tamoxifen administration. As such, we sought to determine whether prolonged exposure to tamoxifen altered the identification of mGreen<sup>+</sup> ILC. This involved assessment of thymic ILC populations in Id2<sup>CreERT2</sup> x ROSA<sup>mT/mG</sup> mice that have been exposed to a tamoxifen diet for five weeks. The mLN was used a positive control for the identification of mGreen<sup>+</sup> ILC populations, identified as CD8α<sup>-</sup> CD3i<sup>-</sup> IL-7Rα<sup>+</sup> Lineage<sup>-</sup> mGreen<sup>+</sup>, and the gating strategy applied to cells isolated from thymus tissue (Figure 3.7A). Unlike in earlier ‘fate-mapping’ experiments (Figure 3.6) whereby cells were initially identified as mGreen<sup>+</sup>, here the gating strategy has been optimised by first gating on CD8α<sup>+</sup> CD3i<sup>-</sup> populations and enabled identification of thymic ILC populations without the prior need of gating on mGreen<sup>+</sup> cells.

### Figure 3.7 Analysis of thymic ILC populations through fate-mapping Id2 expression induced by a tamoxifen diet

Administration of tamoxifen in the diet was used as an alternative approach to enable prolonged tamoxifen exposure in Id2<sup>creERT2</sup> x ROSA26<sup>mT/mG</sup> mice. Mice consumed a tamoxifen diet for 3 weeks before cells were isolated from the mLN and thymus for analysis. Cells were analysed using flow cytometry and total numbers were calculated per whole tissue. Data shown in green, orange and purple corresponds with mGreen, ILC2 and ILC3, respectively.

- A) Full gating strategy for flow cytometry used to identify mGreen<sup>+</sup> ILC2 (mGreen<sup>+</sup> GATA-3<sup>+</sup>) and ILC3 (mGreen<sup>+</sup> RORγt<sup>+</sup>) isolated from mLN (upper panel) and thymus (lower panel). Lineage channel consists of antibodies against CD3, CD5, CD11b, CD11c and B220.
- B) Gating controls for mGreen<sup>+</sup> cells were based upon cells from WT mLN (upper panel) and thymus (lower panel). Controls were pre-gated on CD8α<sup>-</sup>CD3i<sup>-</sup> Lin<sup>-</sup>IL-7Rα<sup>+</sup> cells.
- C) Proportion and total number of mGreen<sup>+</sup> ILC (CD8α<sup>-</sup> CD3i<sup>-</sup> Lin<sup>-</sup> IL-7Rα<sup>+</sup> mGreen<sup>+</sup>) in the mLN and thymus.
- D) Proportion and total number of mGreen<sup>+</sup> ILC2 (mGreen<sup>+</sup> GATA-3<sup>+</sup>) in the mLN and thymus.
- E) Proportion and total number of mGreen<sup>+</sup> ILC3 (mGreen<sup>+</sup> RORγt<sup>+</sup>) in the mLN and thymus.
- F) Proportion of mGreen expression by ILC (CD8α<sup>-</sup> CD3i<sup>-</sup> Lin<sup>-</sup> IL-7Rα<sup>+</sup> mGreen<sup>+</sup>) within the mLN of Id2<sup>creERT2</sup> x ROSA26<sup>mT/mG</sup> mice following administration of tamoxifen by oral gavage.
- G) Representative flow cytometry plots for the identification of total ILC2 (GATA-3<sup>+</sup>) and ILC3 (RORγt<sup>+</sup>) in the mLN (left FACS plot) and thymus (right FACS plot) of Id2<sup>creERT2</sup> x ROSA26<sup>mT/mG</sup> mice.
- H) Enumeration of total ILC2 (GATA-3<sup>+</sup>) and ILC3 (RORγt<sup>+</sup>) in the mLN and thymus of Id2<sup>creERT2</sup> x ROSA26<sup>mT/mG</sup> mice.

Mann-Whitney U (non-parametric, two-tailed) test was used (comparing two data sets) and a Kruskal-Wallis one-way ANOVA with post hoc Dunn's test was used (comparing three or more data sets) for statistical analysis where \*p<0.05, \*\*p<0.01, \*\*\*p<0.001, and \*\*\*\*p<0.0001. In all graphs the bar represents the median, n=6. Data shown from two independent experiments.



Observations from the FACS plots demonstrated a similar proportion of mGreen<sup>+</sup> ILCs in both mLN and thymus, with appropriate gating for mGreen expression set using cells from WT tissues (Figure 3.7A-B). Prior gating on CD8α<sup>-</sup> CD3i<sup>-</sup> in Figure 3.7 removes the enrichment effect of mGreen expression seen in Figure 3.6A-B. However, this approach builds on our earlier data that successfully identifies ILC populations in the thymus by first gating on CD8α<sup>-</sup> CD3i<sup>-</sup> cells whilst using mGreen to correctly identify ILC. Importantly, the proportions of ILC2 and ILC3 subsets arising from mGreen<sup>+</sup> ILC in Figure 3.7A were consistent with the proportion of ILCs fate-mapped to Id2 by oral gavage, despite alterations in the gating strategy and manner of dosing (Figure 3.6A and C).

Upon enumeration of these data, the proportion of mGreen<sup>+</sup> ILC was greater in the mLN than in the thymus, which was also true when comparing total mGreen<sup>+</sup> ILC number (Figure 3.7C). Additional gating of mGreen<sup>+</sup> ILC populations enabled characterisation of these cells based on their GATA-3 (ILC2) and RORγt<sup>+</sup> (ILC3) expression. While the proportion of mGreen<sup>+</sup> ILC2 was significantly lower in the mLN compared to the thymus, the total numbers of these cells were significantly greater in the mLN. In contrast, the proportion of mGreen<sup>+</sup> ILC3 was significantly higher in the mLN than the thymus, and proved consistent when comparing total mGreen<sup>+</sup> ILC3 between these tissues. Interestingly, fewer than 50 mGreen<sup>+</sup> ILC3 were identified, consistent with our earlier studies. Moreover, method of tamoxifen administration did not affect the proportion of mGreen<sup>+</sup> ILCs within these investigations (Figure 3.7F).

As previously mentioned, pre-gating on CD8α<sup>-</sup> CD3i<sup>-</sup> cells was used as an alternative approach to address the same aim of robustly identifying ILC populations within the thymus. First gating on CD8α<sup>-</sup> CD3i<sup>-</sup> cells enabled the identification of total ILC in the

thymus without pre-gating on mGreen<sup>+</sup> cells, again utilising cells from the mLN as a positive control (Figure 3.7G). Observations from these FACS plots identified proportions of ILC2 and ILC3 comparable to those when gating on mGreen<sup>+</sup> ILC only (Figure 3.7A). Enumeration of these populations discovered a similar number of total ILC2 between mLN and thymus. Total ILC3, however, was significantly lower in the thymus than in the mLN, whereby very few ILC3 were again detected in the adult thymus (Figure 3.7H). Thus far, a number of different experimental models have been used to identify ILC populations within the adult thymus, each with the same conclusion. Whilst ILC are present within the adult thymus their numbers are few and consist mainly of ILC2 rather than ILC3, as previously described.

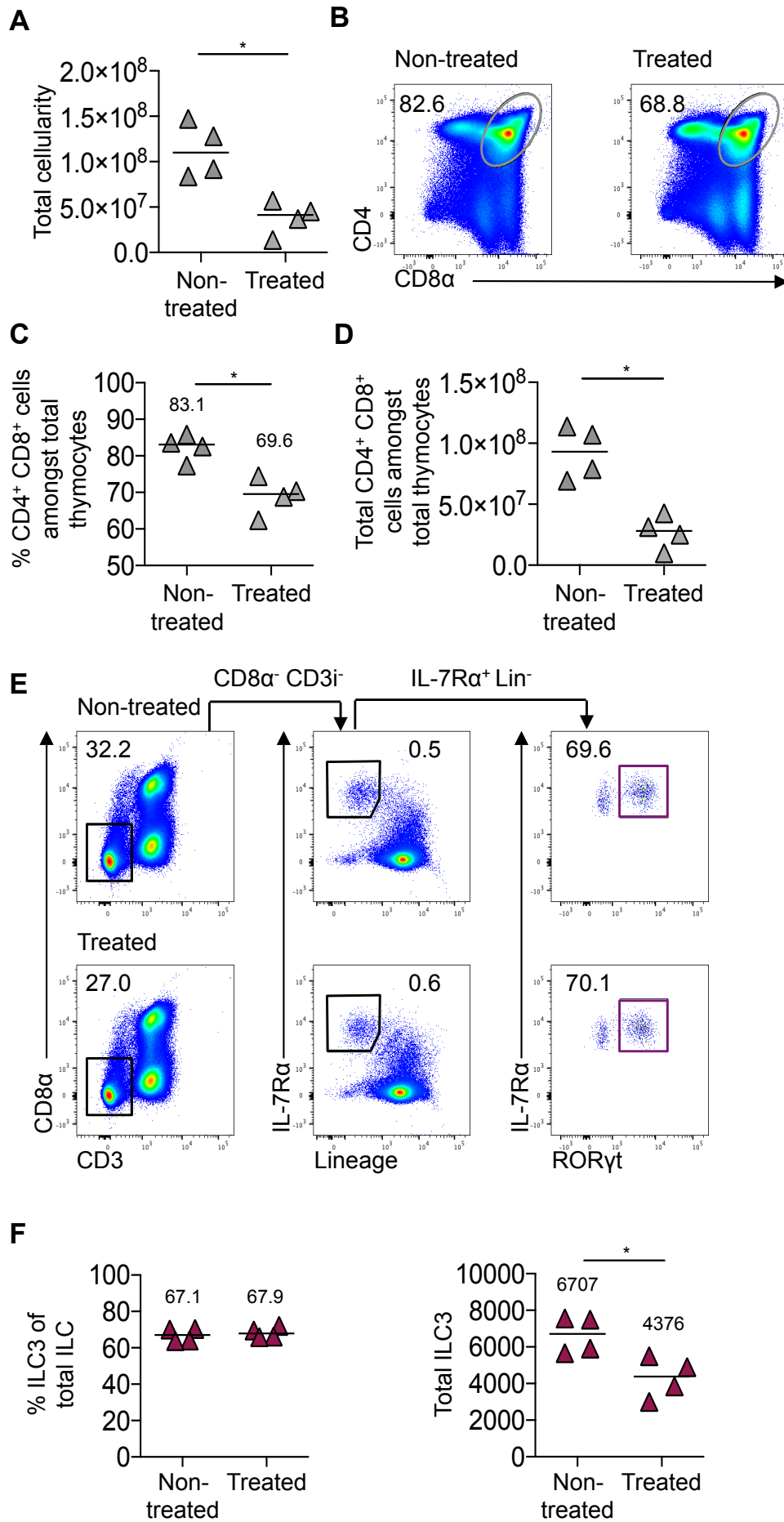
Early reports have indicated thymic cellularity is impacted by treatment with tamoxifen.<sup>(150)</sup> To assess the effect of acute tamoxifen administration on populations within the thymus, cells from the thymus of WT mice treated with tamoxifen were compared to non-treated mice. Comparison of total cellularity between these mice demonstrated a reduction in the number of cells in the thymus of mice that had received tamoxifen (Figure 3.8A). Analysis by flow cytometry indicated CD4<sup>+</sup> CD8<sup>+</sup> populations were largely accountable for this change (Figure 3.8B). Moreover, a significant reduction in the proportion and total number of CD8 $\alpha$ <sup>+</sup> CD4<sup>+</sup> was observed in mice that had received tamoxifen in this manner (Figure 3.8C-D). To determine whether ILC populations were sensitive to the effects of tamoxifen, ILC3 populations were compared in the mLN of treated and non-treated mice. The proportions of ILC3 identified by flow cytometry were comparable between these mice, while a significant, but modest reduction in ILC3 number was observed (Figure 3.8E-F). These data demonstrate a reduction in thymocyte populations within the

### **Figure 3.8 Administration of tamoxifen by oral gavage results in reduction of double positive thymocytes**

To assess the effect of acute tamoxifen administration on thymocyte populations, WT mice were gavaged for 5 consecutive days with tamoxifen and then analysed 3 days later alongside untreated age-matched litter mates. Cells were analysed using flow cytometry and total numbers calculated per whole tissue. Data shown in purple corresponds with ILC3.

- A) Enumeration of total thymic cellularity in non-treated and treated mice.
- B) Representative flow cytometry plots identifying CD4<sup>+</sup>CD8<sup>+</sup> cells amongst thymocytes in the thymus of non-treated and treated mice. Cells were pre-gated on lymphocytes.
- C) Proportion of CD4<sup>+</sup>CD8<sup>+</sup> cells amongst thymocytes in the thymus of non-treated and treated mice.
- D) Total number of CD4<sup>+</sup>CD8<sup>+</sup> cells amongst thymocytes in the thymus of non-treated and treated mice.
- E) Gating strategy used for the identification of ILC3 (CD8 $\alpha$ <sup>-</sup> CD3<sup>-</sup> IL-7R $\alpha$ <sup>+</sup> Lin<sup>-</sup> ROR $\gamma$ t<sup>+</sup>) in the mLN of non-treated (upper panel) and treated (lower panel) mice.
- F) The proportion and total number of ILC3 (CD8 $\alpha$ <sup>-</sup>CD3<sup>-</sup>IL-7R $\alpha$ <sup>+</sup>Lin<sup>-</sup>ROR $\gamma$ t<sup>+</sup>) in the mLN of non-treated and treated mice.

Mann-Whitney U (non-parametric, two-tailed) test was used for statistical analysis where \*p<0.05, \*\*p<0.01, \*\*\*p<0.001, and \*\*\*\*p<0.0001. In all graphs the bar represents the median, n=4. Data shown one independent experiments.



thymus that were largely accountable to CD4<sup>+</sup> CD8<sup>+</sup> cells in response to acute tamoxifen administration. Although administration of tamoxifen resulted in a modest reduction in total ILC3 number within the mLN, the effect was limited and it is very unlikely that the inability to detect ILC3 in the thymus of Id2 cre fate mapping mice reflected a tamoxifen-induced loss of these cells.(129)

So far within this chapter, investigations have used the fate mapping of Id2 to better identify ILC populations within the adult thymus. However, as observed in our earlier data, tamoxifen has a detrimental effect on T cell populations within the thymus and a modest impact on ILC3 number in secondary lymphoid tissue. To further assess the ILC compartment of the adult thymus, whilst continuing to use Id2-expression as a tool but in the absence of tamoxifen, ILC populations were investigated in the mLN and thymus of Id2-eGFP reporter mice. In comparison to Id2<sup>creERT2</sup> x ROSA<sup>mT/mG</sup> mice, where cells that express Id2 during, and just before, the window period of tamoxifen administration when Cre is present express mGreen, GFP is only expressed in Id2-eGFP mice by cells currently expressing Id2. Therefore, Id2-eGFP mice are useful in identifying cells by live expression of Id2 without the requirement of tamoxifen.

In the mLN, subsets of GFP<sup>+</sup> ILCs were defined by first gating on GFP<sup>+</sup> Lin<sup>-</sup> IL-7Rα<sup>+</sup> cells followed by GATA-3 and RORγt; identifying proportions of ILC subsets comparable to those previously reported in the mLN of WT mice (Figure 3.9A).(89) Application of this gating strategy to cells isolated from the thymus identified a very small population of GFP<sup>+</sup> Lin<sup>-</sup> cells that, upon subsequent gating on IL-7Rα<sup>+</sup> cells, were comparable to ILC2 and ILC3 populations observed in our earlier investigations (Figure 3.9A). Cells isolated from the mLN and thymus of a WT mouse, and thus



GFP<sup>-</sup>, were used as gating controls for GFP expression (Figure 3.9B). Unsurprisingly, comparison of total cellularity between the thymus and mLN identified a significantly higher number of cells within the thymus (Figure 3.9C). Characterisation of these cells by flow cytometry, as gated in Figure 3.9A, identified a population of GFP<sup>+</sup> Lin<sup>-</sup> cells that expressed IL-7R $\alpha$ , identifying GFP<sup>+</sup>, and thus Id2-expressing, ILC. The proportion of which was greater in the mLN when compared to the thymus. However, comparison of total number of these cells revealed no significant difference between tissues (Figure 3.9D). Total number of GFP<sup>+</sup> ILC was used to calculate the proportion of GFP<sup>+</sup> ILC as a percentage of total tissue cellularity (Figure 3.9E). This shows the proportion of ILC as a percentage of total cells to be greater in the mLN than the thymus (Figure 3.9E). Characterisation of GFP<sup>+</sup> ILC using antibodies against GATA-3 and ROR $\gamma$ t identified cells lacking both transcription factors in addition to ILC2 and ILC3. A greater proportion of GFP<sup>+</sup> G $\gamma$ R<sup>-</sup> cells were shown to be present in the thymus compared to the mLN, however no significant difference was observed between the total numbers of these cells (Figure 3.9F).

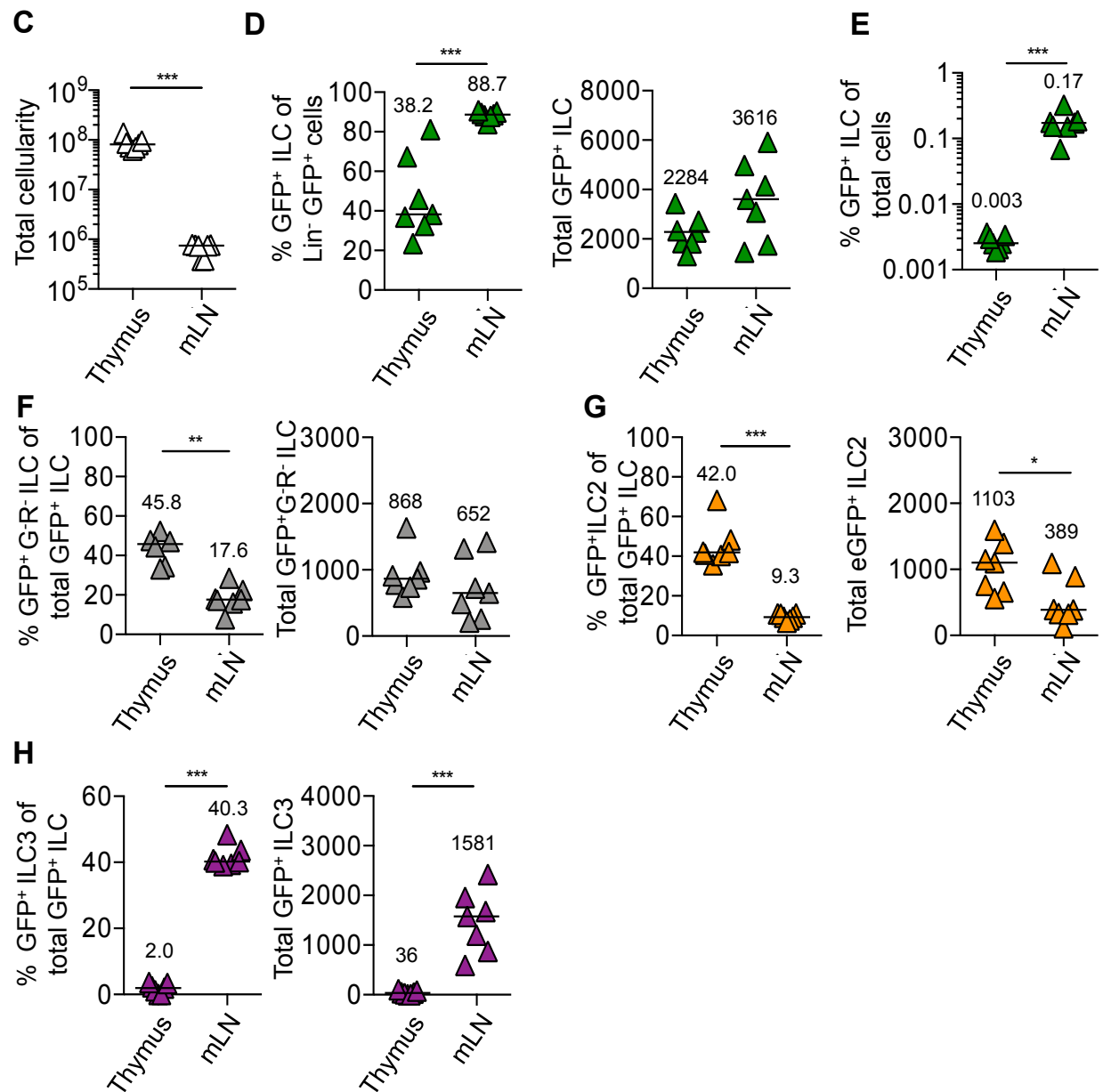
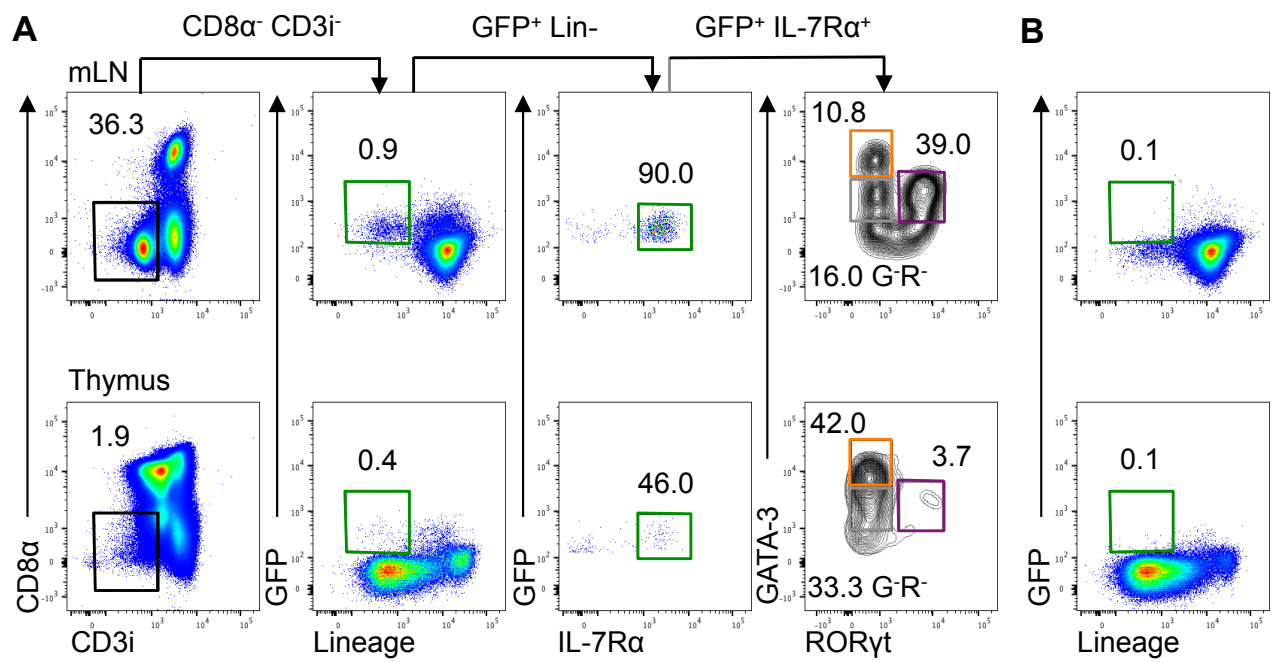
Our earlier data identified ILC2 to be the predominant population in the thymus of Id2<sup>creERT2</sup> x ROSA<sup>mT/mG</sup> mice following induction with tamoxifen. This was true of data in Id2-eGFP mice where GFP<sup>+</sup> ILC2 are accountable for ~40% of all GFP<sup>+</sup> ILC (Figure 3.9G). GFP<sup>+</sup> ILC2 are significantly greater in both proportion and total cell number in the thymus when compared to the mLN (Figure 3.9G). These data contrast that observed for GFP<sup>+</sup> ILC3, whereby the proportion and total number of these cells is much greater in the mLN when compared to the thymus (Figure 3.9H). Therefore, very few ILC3 are present within the adult thymus while clearly detectable within the mLN.

### Figure 3.9 Analysis of ILC populations in the thymus of adult Id2-eGFP reporter mice

To directly assess Id2-expressing ILC populations in the mLN and thymus in the absence of tamoxifen, cells from these tissues were isolated from Id2-eGFP reporter mice. Cells were analysed using flow cytometry and total numbers were calculated per whole tissue. Data shown in green, grey, orange and purple correspond to GFP, G<sup>-</sup>R<sup>-</sup> ILC, ILC2 and ILC3, respectively.

- A) Full gating strategy for flow cytometry used to identify GATA-3<sup>+</sup> (ILC2) and RORγt<sup>+</sup> (ILC3) amongst the GFP<sup>+</sup> ILC pool (identified as CD8α<sup>-</sup> CD3i<sup>-</sup> GFP<sup>+</sup> Lin<sup>-</sup> IL-7Rα<sup>+</sup>) in the mLN and thymus of Id2-eGFP reporter mice. Lineage channel consists of antibodies against CD3, CD5, CD11b, CD11c and B220.
- B) Gating controls for eGFP<sup>+</sup> cells were based upon eGFP<sup>-</sup> cells from WT mLN and thymus.
- C) Total cellularity of the mLN and thymus in Id2-eGFP reporter mice.
- D) Proportion and total number of GFP<sup>+</sup> cells amongst ILCs (CD8α<sup>+</sup> CD3i<sup>-</sup> Lin<sup>-</sup> IL-7Rα<sup>+</sup>) in the thymus and mLN of Id2-eGFP reporter mice.
- E) The percentage of eGFP<sup>+</sup> ILC (CD8α<sup>-</sup> CD3i<sup>-</sup> Lin<sup>-</sup> IL-7Rα<sup>+</sup>) as a proportion of total cells isolated from thymus and mLN.
- F) The proportion and total number of GATA-3<sup>-</sup> RORγt<sup>-</sup> (G<sup>-</sup>R<sup>-</sup> ILC) amongst the eGFP<sup>+</sup> ILC pool (CD8α<sup>-</sup> CD3i<sup>-</sup> eGFP<sup>+</sup> Lin<sup>-</sup> IL-7Rα<sup>+</sup>) in the mLN and thymus of Id2-eGFP reporter mice.
- G) The proportion and total number of GATA<sup>+</sup> (ILC2) amongst the eGFP<sup>+</sup> ILC pool (CD8α<sup>-</sup> CD3i<sup>-</sup> eGFP<sup>+</sup> Lin<sup>-</sup> IL-7Rα<sup>+</sup>) in the mLN and thymus of Id2-eGFP reporter mice.
- H) The proportion and total number of RORγt<sup>+</sup> (ILC3) amongst the eGFP<sup>+</sup> ILC pool (CD8α<sup>-</sup> CD3i<sup>-</sup> eGFP<sup>+</sup> Lin<sup>-</sup> IL-7Rα<sup>+</sup>) in the mLN and thymus of Id2-eGFP reporter mice.

Mann-Whitney U (non-parametric, two-tailed) test was used for statistical analysis where \*p<0.05, \*\*p<0.01, \*\*\*p<0.001, and \*\*\*\*p<0.0001. In all graphs the bar represents the median, n=7. Data shown from three independent experiments.



Observations surrounding ILC3 from Id2-eGFP mice are consistent with all our previous findings and describe very few ILC3 present in the thymus of an adult mouse. Importantly, these data argue that our descriptions of Id2-expressing thymic ILC populations are not an artefact of tamoxifen administration. Collectively, we can conclude that thymic ILC populations in mice change over time; altering in both proportion and total cell number through neonatal development into adulthood. Initially, ILC3, specifically LTi-cells, and ILC2 are present in similar capacities within the embryonic thymus. This is continued post-birth with little difference between the number of ILC2 and ILC3 observed up to day 7. By day 14, the number of ILC2 was shown to increase while the number of ILC3 demonstrated a decrease. Moreover, ILC2 are maintained into adulthood while ILC3 continue to decline with very few of these cells present in the adult thymus.

### **3.2.3 Assessing plasticity amongst thymic ILC populations**

Multiple reports have described plasticity amongst ILC populations.(80,81,151,152) In particular, ILC3 have been shown to down regulate expression of ROR $\gamma$ t and up regulate the expression of Tbet; adopting an ex-ILC3 phenotype similar to that of IFN $\gamma$ <sup>+</sup> Tbet<sup>+</sup> ILC1.(81,151) Therefore, we asked whether the loss of ILC3 observed in adulthood is a result of plasticity amongst ILC populations within the thymus. To test this, the expression of ROR $\gamma$ t was fate-mapped using *Rorc*<sup>cre</sup> x ROSA<sup>mT/mG</sup> mice, thus enabling the differentiation of ILC3 into another cell fate to be identified. mGreen expression within these mice identifies cells that are currently expressing or have previously expressed ROR $\gamma$ t. Therefore, GATA-3<sup>-</sup> ROR $\gamma$ t<sup>-</sup> ILC or ILC2 that have previously expressed ROR $\gamma$ t can be identified by mGreen expression in flow

cytometry. As with our earlier investigations,  $Id2^{CreERT2} \times ROSA^{mT/mG}$  mice were administered tamoxifen by oral gavage for five consecutive days and followed by analysis of mLN and thymus.

Data obtained from flow cytometry demonstrated the majority of ILC within the mLN were mGreen<sup>+</sup> (identified as CD8 $\alpha$ <sup>-</sup> CD3 $\beta$ <sup>-</sup> IL-7R $\alpha$ <sup>+</sup> Lin<sup>-</sup> mGreen<sup>+</sup>), reflecting the high number of ILC3 in this tissue (Figure 3.10A). In comparison, only a minority (~20%) of ILC in the thymus were mGreen<sup>+</sup> (Figure 3.10A-B). Furthermore, ROR $\gamma$ t expression at a protein level was assessed using intracellular flow cytometry and revealed a clear population of “ex-ILC3” (identified as CD8 $\alpha$ <sup>-</sup> CD3 $\beta$ <sup>-</sup> IL-7R $\alpha$ <sup>+</sup> Lin<sup>-</sup> mGreen<sup>+</sup> ROR $\gamma$ t<sup>-</sup>) in both the mLN and thymus (Figure 3.10A). Total ILC populations within the thymus, identified as G-R<sup>-</sup> ILC, ILC2 (GATA-3<sup>+</sup>) and ILC3 (ROR $\gamma$ t) amongst the total ILC pool (CD8 $\alpha$ <sup>-</sup> CD3 $\beta$ <sup>-</sup> IL-7R $\alpha$ <sup>+</sup> Lin<sup>-</sup>) were comparable to previous data (Figure 3.10D). Comparison of total and mGreen<sup>+</sup> ILC within the thymus allowed for identification ILC of an “ex-ILC3” phenotype (Figure 3.10E). Since the vast majority of thymic ILC show no evidence of previous ROR $\gamma$ t expression, these data argue against the loss of ILC3 during thymic development due to plasticity and differentiation to an alternative phenotype (Figure 3.10E).

#### **3.2.4 ILC2 increase in mice lacking ILC3**

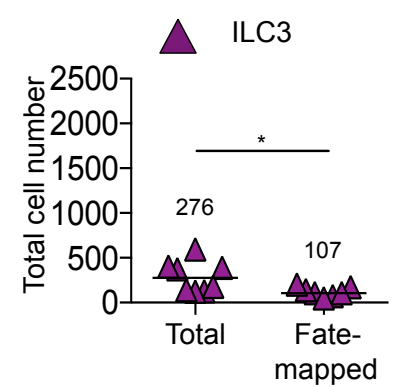
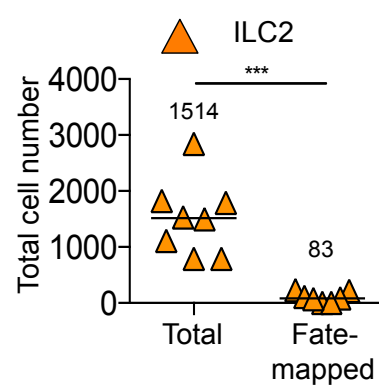
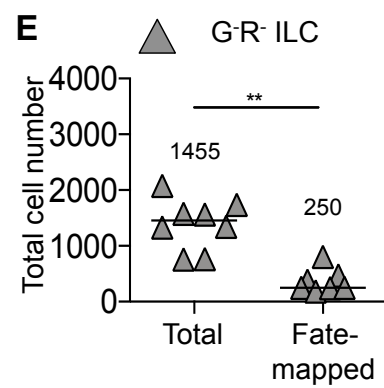
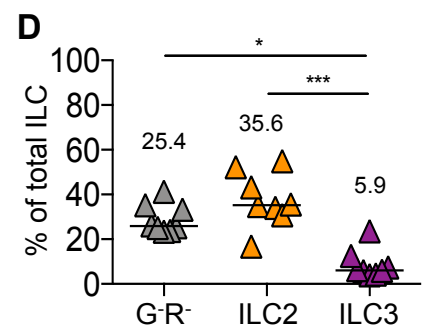
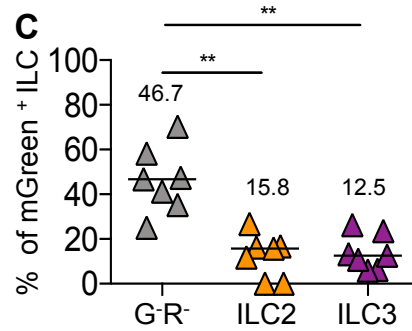
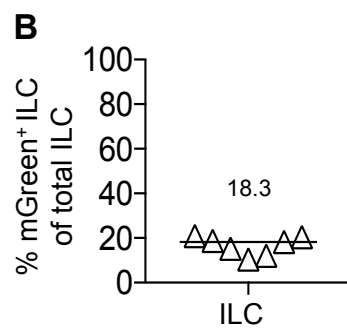
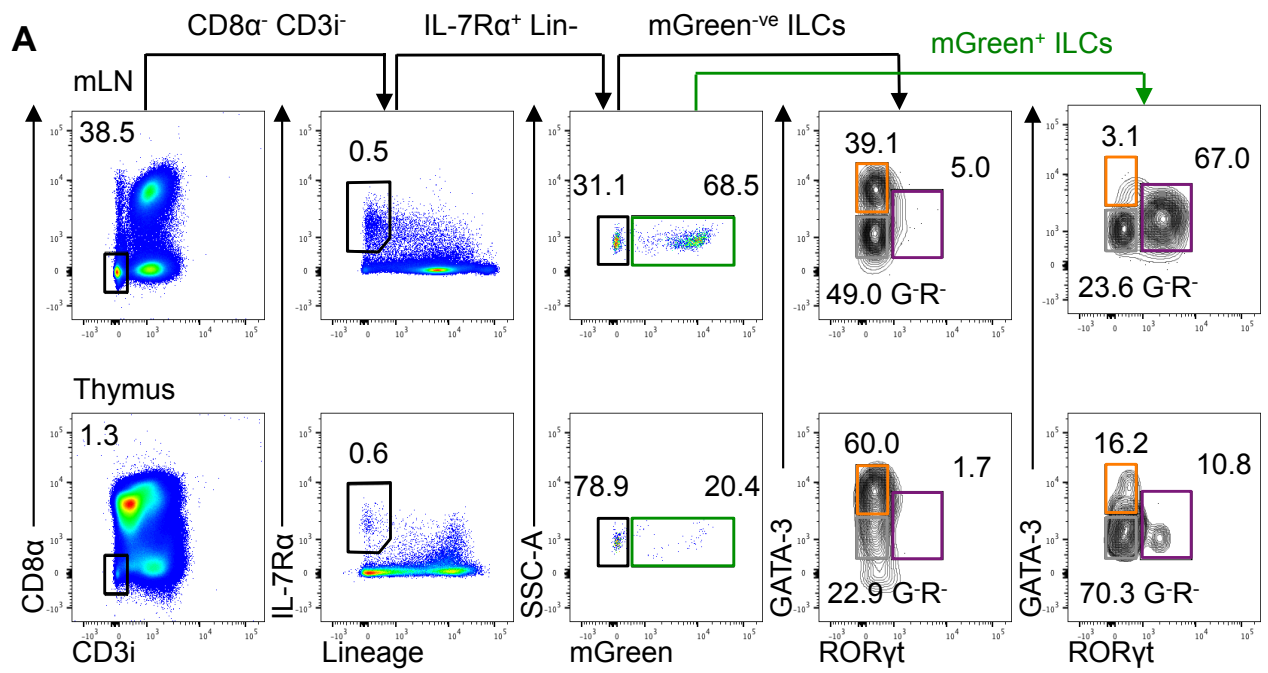
So far, we have shown the composition of ILCs in the adult thymus to be very different to an embryonic thymus. While the majority of ILC within the embryonic thymus are ILC3, this is superseded by ILC2 following birth where ILC2 outnumber ILC3 by day 14. Furthermore, the number of ILC2 is maintained into adulthood whereas the number of ILC3 continues to decline. Interestingly, earlier publications have described ILC3 in vast quantities in the adult thymus, which differs greatly from

**Figure 3.10 ILC3 plasticity does not account for the changes amongst ILC subsets post-birth**

To test whether the loss of thymic ILC3 after birth could be attributed to differentiation to another ILC type, ROR $\gamma$ t expression was fate-mapped using *Rorc*<sup>cre</sup> x ROSA<sup>mT/mG</sup> mice. Isolated cells were analysed using flow cytometry and total numbers calculated per whole thymus or mLN. Gates and triangles shown in green, grey, orange and purple correspond to mGreen, G $\gamma$ R $\gamma$  ILC, ILC2 and ILC3, respectively.

- A) Full gating strategy for flow cytometry data identifying mGreen<sup>+</sup> ('fate-mapped') and mGreen<sup>-</sup> populations among ILC (CD8 $\alpha$ <sup>-</sup>CD3 $\gamma$ <sup>-</sup>IL-7R $\alpha$ <sup>+</sup>Lin<sup>-</sup>) in the mLN (upper panel) and thymus (lower panel). Lineage channel consists of antibodies against CD3, CD5, CD11b, CD11c and B220.
- B) The proportion of mGreen expression by ILCs (CD8 $\alpha$ <sup>-</sup>CD3 $\gamma$ <sup>-</sup>IL-7R $\alpha$ <sup>+</sup>Lin<sup>-</sup>) in the thymus.
- C) The proportion of G $\gamma$ R $\gamma$  ILC, ILC2 (GATA-3<sup>+</sup>) and ILC3 (ROR $\gamma$ t<sup>+</sup>) amongst the mGreen<sup>+</sup> ILC (CD8 $\alpha$ <sup>-</sup>CD3 $\gamma$ <sup>-</sup>IL-7R $\alpha$ <sup>+</sup>Lin<sup>-</sup>mGreen<sup>+</sup>) pool in the thymus
- D) The proportion of G $\gamma$ R $\gamma$  ILC, ILC2 (GATA-3<sup>+</sup>) and ILC3 (ROR $\gamma$ t<sup>+</sup>) amongst the total ILC pool (CD8 $\alpha$ <sup>-</sup>CD3 $\gamma$ <sup>-</sup>IL-7R $\alpha$ <sup>+</sup>Lin<sup>-</sup>) in the thymus.
- E) Enumeration of thymic ILC showing G $\gamma$ R $\gamma$  ILC, ILC2 (GATA-3<sup>+</sup>) and ILC3 (ROR $\gamma$ t<sup>+</sup>) comparing numbers of each population among total ILC versus mGreen<sup>+</sup> ILC.

Mann-Whitney U (non-parametric, two-tailed) test was used for statistical analysis where \*p<0.05, \*\*p<0.01, \*\*\*p<0.001, and \*\*\*\*p<0.0001. In all graphs the bar represents the median, n=8 (total) and n=7 (fate-mapped). Data shown from three independent experiments.



our findings.(100) To verify our claims, we sought use of alternative mouse models where ILCs may be more numerous.

Collectively, we have described an increase in ILC2 number that coincided with the loss of ILC3 during neonatal development.(129) From this, we postulated that ILC2 number might be enhanced in a thymus lacking ILC3.(129) To test this, ILC2 and ILC3 populations from the thymus of a *Rorc*<sup>-/-</sup> mouse, where ILC3 are absent, were compared to cells within a WT thymus.(129) ILC2 and ILC3 populations were easily identifiable within the WT thymus in proportions comparable to those seen in previous experiments (figure 3.11A). Application of this gating strategy to the *Rorc*<sup>-/-</sup> thymus revealed a number of differences in comparison to the WT thymus (figure 3.11A). The proportion of ILC2 in the *Rorc*<sup>-/-</sup> thymus was slightly elevated compared to the WT thymus while the proportion of ILC3 dropped to below 1% (Figure 3.11A). *Rorc*<sup>-/-</sup> mice were genotyped prior to their use and lymph nodes were absent upon visual inspection. Therefore, the minor proportion of RORγt<sup>+</sup> cells observed in Figure 3.11A is a result of background fluorescence. Despite a rise in the proportion of total ILC within the *Rorc*<sup>-/-</sup> thymus, the total cellularity of this tissue was significantly reduced compared to the WT (figure 3.11B). Enumeration of total ILC identified an increase in *Rorc*<sup>-/-</sup> thymus compared to the WT and, owing to the reduced thymic cellularity in *Rorc*<sup>-/-</sup> mice, made up a greater proportion of total thymocytes (figure 3.11C-D). Subsequent gating on total ILC within these mice enabled comparison of the ILC2 and ILC3 subsets using GATA-3 and RORγt. Interestingly, ILC2 were significantly increased in both proportion and total number in *Rorc*<sup>-/-</sup> thymus compared to the WT (figure 3.11E). Analysis of the proportion and total number of ILC3 between WT and *Rorc*<sup>-/-</sup> mice compared very few ILC3 in the WT thymus with a

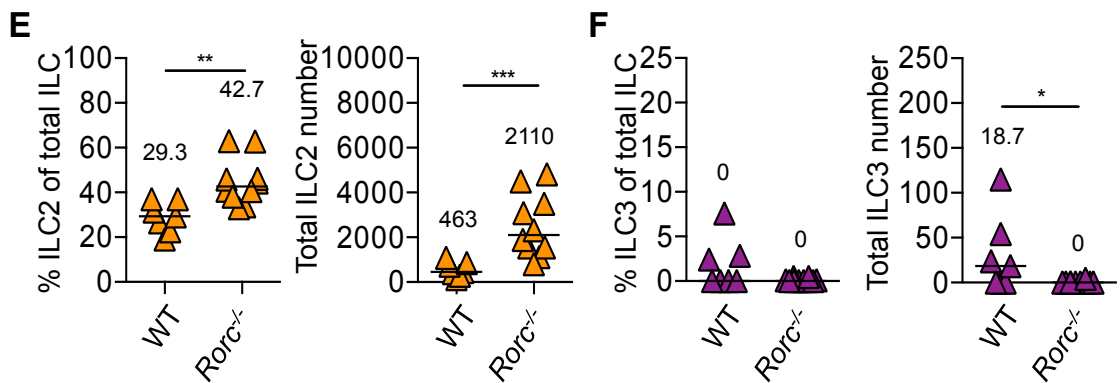
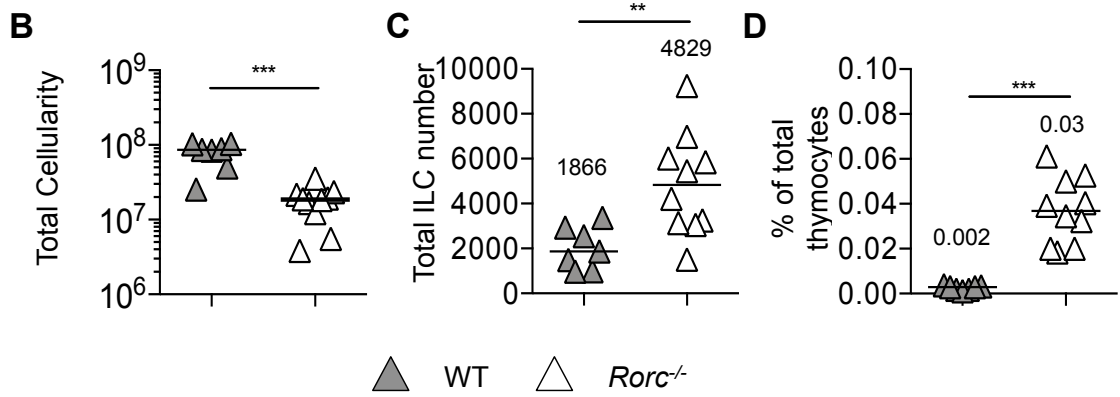
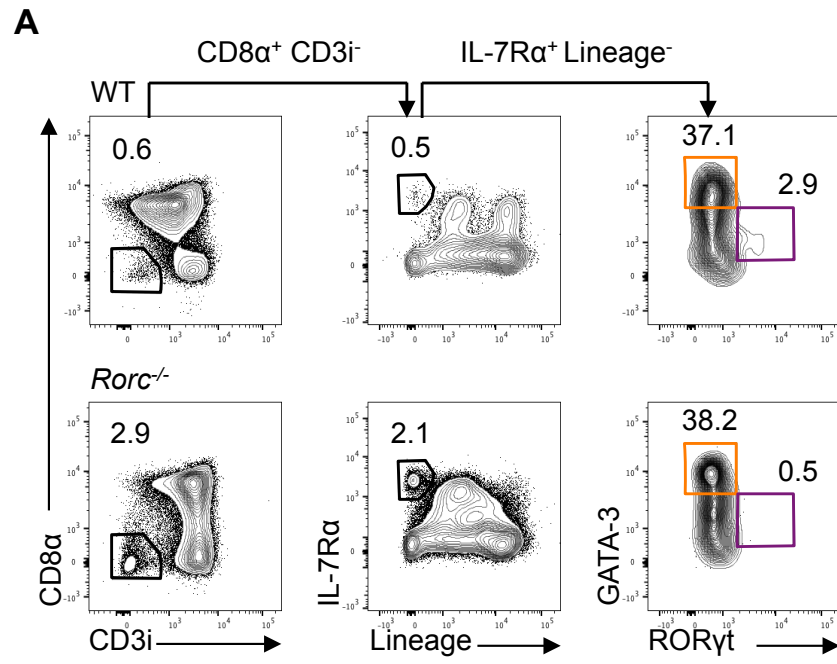


**Figure 3.11 Analysis of ILC populations in the thymus of adult mice deficient in ROR $\gamma$ t reveal an increase in ILC2**

To determine the effect of ILC3 loss on ILC2 number, ILC populations were assessed in the thymus of WT and *Rorc*<sup>-/-</sup> mice, where ILC3 are absent. Total numbers were calculated per whole thymus. Data shown in orange and purple identify ILC2 and ILC3, respectively.

- A) Gating strategy for the identification of total ILC (CD8 $\alpha$ <sup>-</sup> CD3 $\gamma$ <sup>-</sup> IL-7R $\alpha$ <sup>+</sup> Lin<sup>-</sup>), ILC2 (GATA-3<sup>+</sup>) and ILC3 (ROR $\gamma$ t<sup>+</sup>) in WT (upper panel) and *Rorc*<sup>-/-</sup> (lower panel) mice. Lineage channel consists of antibodies against CD3, CD5, CD11b, CD11c and B220.
- B) Total thymic cellularity in WT and *Rorc*<sup>-/-</sup> mice.
- C) Enumeration of total ILC in the thymus of in WT and *Rorc*<sup>-/-</sup> mice.
- D) Total number of ILC as a proportion of total cellularity in the thymus of WT and *Rorc*<sup>-/-</sup> mice.
- E) Proportion and total number of ILC2 (GATA-3<sup>+</sup>) amongst the ILC pool (CD8 $\alpha$ <sup>-</sup> CD3 $\gamma$ <sup>-</sup> IL-7R $\alpha$ <sup>+</sup> Lin<sup>-</sup>) in the thymus of WT and *Rorc*<sup>-/-</sup> mice.
- F) Proportion and total number of ILC3 (ROR $\gamma$ t<sup>+</sup>) amongst the ILC pool (CD8 $\alpha$ <sup>-</sup>CD3 $\gamma$ <sup>-</sup> IL-7R $\alpha$ <sup>+</sup> Lin<sup>-</sup>) in the thymus of WT and *Rorc*<sup>-/-</sup> mice.

Mann-Whitney U (non-parametric, two-tailed) test was used for statistical analysis where \*p<0.05, \*\*p<0.01, \*\*\*p<0.001, and \*\*\*\*p<0.0001. In all graphs the bar represents the median, n=7 for WT and n=10 for *Rorc*<sup>-/-</sup>. Data shown from two or four independent experiments for WT and *Rorc*<sup>-/-</sup> mice, respectively.



tissue that lacks ILC3. As such, no difference was observed between the proportions of ILC3 in these mice while the total number of these cells was reduced in the *Rorc*<sup>-/-</sup> thymus (figure 3.11F).

Given ILC2 were shown to increase in the absence of ILC3 in the adult thymus (figure 3.11), we sought to determine the impact of no ILC3 within the neonatal thymus, where ILC3 dominate. To test this, a comparison of ILC2 and ILC3 in the thymus of WT and *Rorc*<sup>-/-</sup> was performed. While putative ILC were observed in both mouse strains, identified as IL-7Rα<sup>+</sup> Lineage<sup>-</sup> cells, this population was enriched in *Rorc*<sup>-/-</sup> thymus (figure 3.12A). Populations of ILC2 and ILC3 were identified in WT thymus in proportions similar to those reported in earlier experiments (figure 3.12A). Of ILC2 and ILC3, only ILC2 were identified within the *Rorc*<sup>-/-</sup>, as expected. Consistent with our reports in their adult counterparts, initial observations from the FACS plots revealed the proportion of ILC2 to be greater in the *Rorc*<sup>-/-</sup> thymus compared to the WT (figure 3.12A).

While the total cellularity of the thymus across tissues is similar, there appears to be an increase in the number of total ILC in the *Rorc*<sup>-/-</sup> thymus compared to the WT (figure 3.12B-C). This is demonstrated by the rise in median total ILC in the WT thymus compared to the *Rorc*<sup>-/-</sup> thymus (figure 3.12C). As such, the proportion of ILC as a percentage of total thymocytes was greater in the *Rorc*<sup>-/-</sup> thymus (figure 3.12D). Subsequent analysis identified an upward trend in the proportion and total number of ILC2 in the *Rorc*<sup>-/-</sup> thymus (figure 3.12E). As expected, the proportion and total number of ILC3 was greater in the WT thymus compared to the *Rorc*<sup>-/-</sup> (figure 3.12F). A very small number of ILC3 were calculated to be present in this thymus, however,

this is also a result of background fluorescence given these mice lack ILC3 (figure 3.12F).

The presence of ILC2 within the neonatal thymus is a recent discovery from our laboratory.(129) Prior to our work, ILC2 within this context had not been described. Therefore, little is known about the function of ILC2 of in the neonatal thymus and warrants further investigation. In order to find out more about these cells, we sought to characterise the phenotype of these cells using known markers of ILC2, based on our knowledge of these cells at peripheral sites. Previous work from within our group has shown KLRG-1, ST2 and ICOS to be expressed by ILC2 isolated from the lung and mLN.(88) While ILC in the small and large intestine, and mLN, can be divided by their expression of c-Kit, termed c-Kit<sup>lo</sup> or c-kit<sup>+</sup>.(153) This work identified c-kit<sup>lo</sup> cells to be Lin<sup>-</sup> IL-7R $\alpha$ <sup>+</sup> CD25<sup>+</sup> CCR6<sup>-</sup> ROR $\gamma$ t<sup>-</sup>; fitting with the ILC2 profile.(153) The expression of these markers is closely linked to the function of these cells at various sites but their expression in the neonatal thymus has not yet been determined. As such, identifying the expression of these markers by ILC2 from the neonatal thymus would provide insight into the function of these cells.

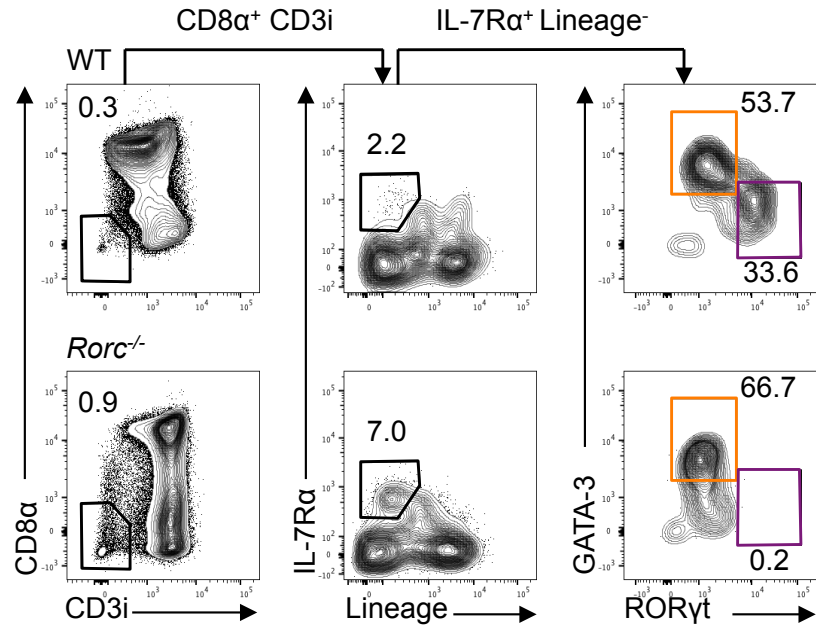
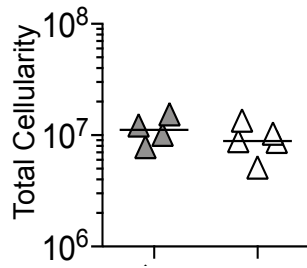
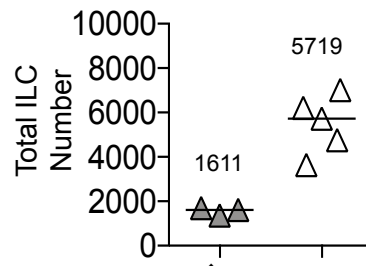
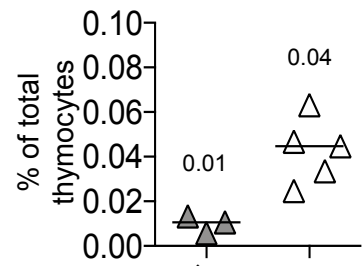
In the periphery, ST2, also termed IL-33 receptor (IL-33R), has been shown to bind IL-33 and stimulate the production of the type 2 cytokines IL-5, IL-13 and amphiregulin .(154) In addition, IL-33/IL-33R binding promotes upregulation of killer cell lectin-like receptor G1 (KLRG-1), where it acts as an inhibitory receptor. For example, the binding of E-cadherin by KLRG-1 inhibits the expression of ILC2-mediated type 2 cytokines in the inflammatory response. However, when tissue expression of E-cadherin is reduced, such as in atopic dermatitis (AD), there is uncontrolled production of type 2 cytokines by ILC2. Concerning ICOS, the binding of

**Figure 3.12 The absence of ILC3 in neonatal mice leads to an increase in thymic ILC2 number**

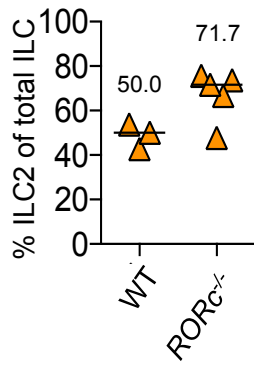
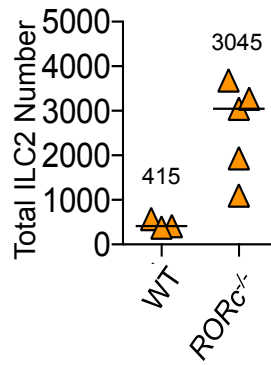
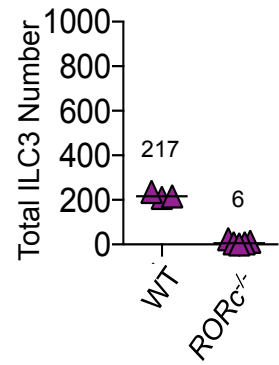
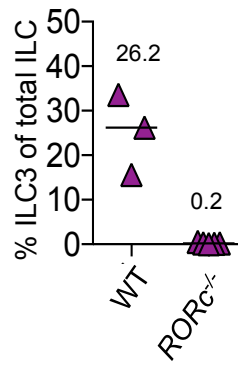
To determine the effect of ILC3 loss on ILC2 populations in the neonate, ILC2 and ILC3 populations in the thymus of WT and *Rorc*<sup>-/-</sup> mice 7 days post-birth were compared. Isolated cells were analysed using flow cytometry and total numbers calculated per thymus. Data shown in orange and purple correspond to ILC2 and ILC3, respectively.

- A) Gating strategy for the identification of total ILC (CD8 $\alpha$ <sup>-</sup> CD3i<sup>-</sup> IL-7R $\alpha$ <sup>+</sup> Lin<sup>-</sup>), ILC2 (GATA-3<sup>+</sup>) and ILC3 (ROR $\gamma$ t<sup>+</sup>) in WT (upper panel) and *Rorc*<sup>-/-</sup> (lower panel) mice. Lineage channel consists of antibodies against CD3, CD5, CD11b, CD11c and B220.
- B) Total thymic cellularity in WT and *Rorc*<sup>-/-</sup> mice 7 days post-birth.
- C) Enumeration of total ILC in the thymus of WT and *Rorc*<sup>-/-</sup> mice 7 days post-birth.
- D) Total number of ILC as a proportion of total cellularity in the thymus of WT and *Rorc*<sup>-/-</sup> mice 7 days post-birth.
- E) Proportion and total number of ILC2 (GATA-3<sup>+</sup>) in the thymus of WT and *Rorc*<sup>-/-</sup> mice 7 days post-birth.
- F) Proportion and total number of ILC3 (ROR $\gamma$ t<sup>+</sup>) in the thymus of WT and *Rorc*<sup>-/-</sup> mice 7 days post-birth.

Mann-Whitney U (non-parametric, two-tailed) test was used for statistical analysis where \*p<0.05, \*\*p<0.01, \*\*\*p<0.001, and \*\*\*\*p<0.0001. In all graphs the bar represents the median, n=4 for WT (B), n=3 for WT (C-F) and n=10 for *RORC*<sup>-/-</sup>. Data shown from one independent experiments.

**A****B****C****D**

▲ WT    △ *Rorc*<sup>-/-</sup>

**E****F****F**

IL-33 to IL-33R (ST2) has been shown to promote the expression of ICOS on ILC2 and is implicated in ILC2 proliferation in the lungs.(154) As such, evidence of ST2 expression by ILC2 in the neonatal thymus would indicate their capability of responding to IL-33 and stimulating the production type 2 cytokines, or up regulating the expression of KLRG-1 and ICOS. Therefore, our gating strategy for identifying ILC within the thymus was adapted to include these ILC2-associated markers.

As aforementioned, the abundance of ILC2 in the lung, as well as the expression of ST2, KLRG-1 and ICOS, has previously been published from members of our research group.(88) As such, the lung was identified as an appropriate positive control for identifying ILC2 in the neonatal thymus (Figure 3.13A). However, the composition of the lung differs from that of the thymus and consists of cells of both hematopoietic and non-hematopoietic origin. Further to this, the preparation of a single cell suspension from lung tissue requires both mechanical dissociation and enzymatic digestion while the thymus requires mechanical disaggregation only. As such, our gating strategy was adapted to optimise the identification of ILC2 in this tissue. This included the addition of a viability dye to identify live cells to identify live cells and the inclusion of CD45 to identify cells of the lymphoid lineage.

Live lymphocytes were identified amongst cells isolated from both lung and neonatal thymus, and further gating found distinct populations of ILC2 to be present in comparable proportions (Figure 3.13A). Assessment of ILC2-associated markers by thymic ILC2 in the neonate showed that these cells did not express KLRG-1 (Figure 3.13B). Interestingly, two distinct populations of ICOS<sup>+</sup> and ICOS<sup>-</sup> ILC2 were identified while the expression of ST2 by these cells was variable (Figure 3.13B). The expression of these markers was further assessed by comparison of the MFI

between the neonatal thymus and the adult lung. Consistent with observations in the histograms, very little expression of KLRG-1 was expressed by neonatal ILC2 in the thymus and was significantly lower than the MFI of KLRG-1 in the adult lung (Figure 3.13C). Assessment of MFI identified all ILC2 in the thymus to express ICOS (Figure 3.13C). However, two clusters of ICOS<sup>+</sup> cells were observed and reflect the two peaks shown in the histogram (Figure 3.13B-C). All ICOS<sup>+</sup> ILC2 in the thymus had greater expression than ILC2 in the lung (Figure 3.13C). Furthermore, the expression of ST2 by ILC2 was greater in the neonatal thymus compared to the adult lung. A significantly higher MFI of ST2 by ILC2 was demonstrated in the neonatal thymus (Figure 3.13C).

To aid identification of c-kit expression amongst thymic ILC2 in the neonate, cells isolated from the mLN of an adult mouse were used. In the mLN, ILC3 demonstrate a high level of c-kit expression while ILC2 are c-Kit<sup>lo</sup> and, therefore, these cells make for appropriate controls (Figure 3.13D). These populations were used to set the gate to assess c-kit expression by ILC2 within the neonatal thymus; identifying greater than three quarters of these cells positive for c-kit (Figure 3.13D). Enumeration of ILC2 in the neonatal thymus was consistent with observations in the histogram (Figure 3.13E). This equated to greater than 1000 c-kit<sup>+</sup> ILC2 within the neonatal thymus (Figure 3.13E).

Data from our initial experiments revisited the work described by Rossi *et al.* (2007) and confirmed the presence of LT<sub>i</sub> cells within the embryonic thymus (Figure 3.1).(98) Our early investigations built upon this data and discovered ILC3, of which LT<sub>i</sub> cells are part of, in the neonatal thymus prior to their rapid decline 14 days post-birth (Figure 3.4). As such, we aimed to determine whether the ILC3 present in the

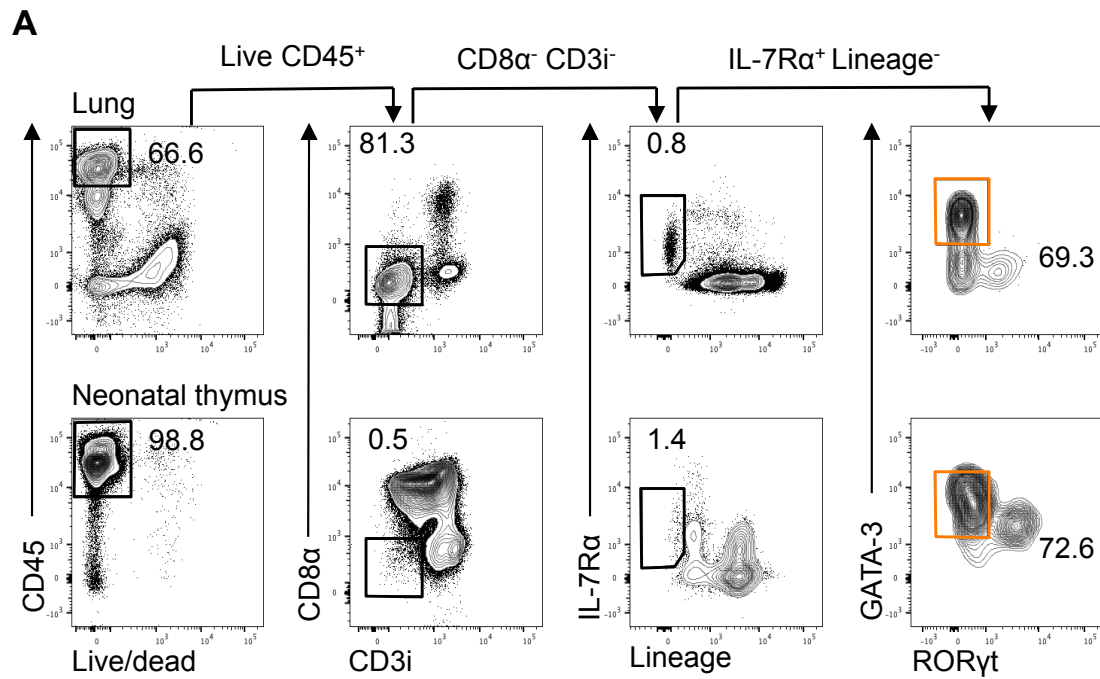


### Figure 3.13 Phenotyping ILC2 populations within the neonatal thymus

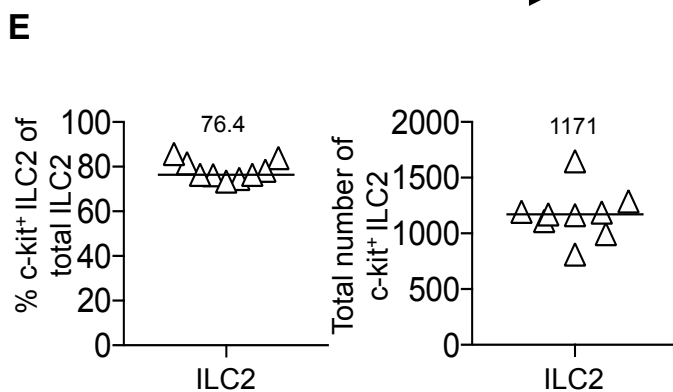
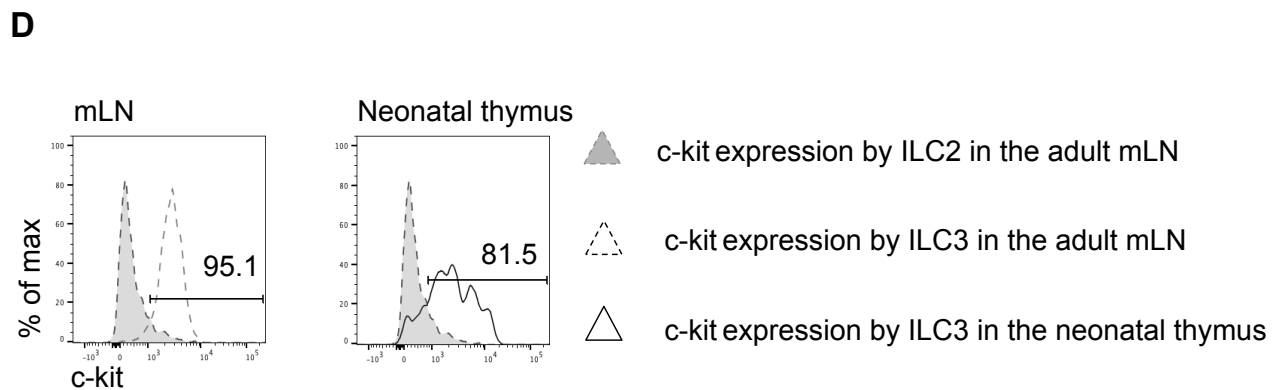
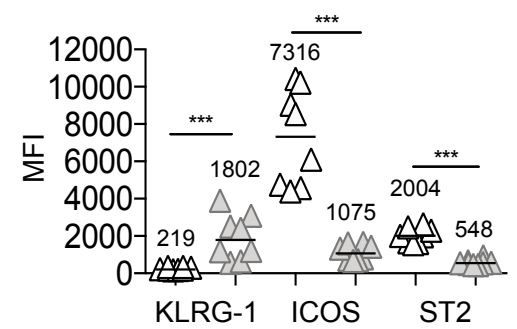
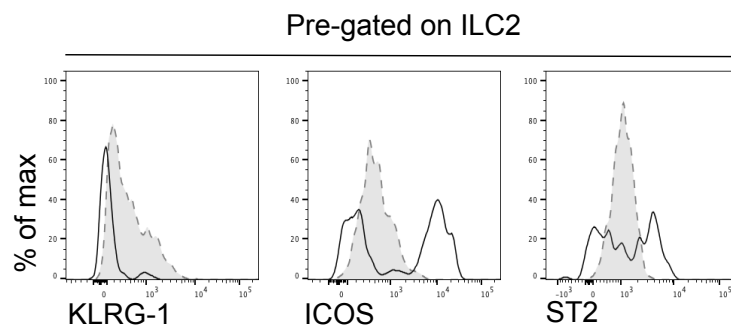
In order to determine the phenotype of thymic ILC2 within the neonate, cells isolated from the thymus of a WT neonate 7 days post-birth were incubated with antibodies specific for markers of ILC2. Cells isolated adult TCR $\alpha^{-/-}$  lung were used as a positive control for ILC staining. Cells from both tissues were analysed using flow cytometry and total numbers calculated per thymus or lung.

- A) Gating strategy for the identification of ILC2 (CD45<sup>+</sup> Live/dead<sup>-</sup> CD8 $\alpha^{-}$  CD3i<sup>-</sup> IL-7R $\alpha^{+}$  Lineage<sup>-</sup> GATA-3<sup>+</sup>) in the lung (upper panel) and neonatal thymus (lower panel). Lineage channel consists of antibodies against CD3, CD5, CD11b, CD11c, B220, CD19, Ter119, Fc $\epsilon$ R1, F4/80, CD49b, CD123 and Gr-1 Gata in orange corresponds to ILC2.
- B) Representative histograms comparing the expression of KLRG-1, ICOS and ST2 in the adult lung and neonatal thymus.
- C) Comparison of the MFI of KLRG-1, ICOS and ST2 by ILC2 in the TCR $\alpha^{-/-}$  lung and neonatal thymus.
- D) Representative histograms showing the expression of c-kit by ILC2 in the neonatal thymus (solid black line). ILC2 and ILC3 isolated from the mLN of TCR $\alpha^{-/-}$  mice were used as positive (black dashed line) and negative (grey dashed line) controls for the detection of c-kit expression.
- E) Proportion and total number of c-kit<sup>+</sup> ILC2 in the neonatal thymus.

Mann-Whitney U (non-parametric, two-tailed) test was used for statistical analysis where \*p<0.05, \*\*p<0.01, \*\*\*p<0.001, and \*\*\*\*p<0.0001. In all graphs the bar represents the median, n=8 (B-C) and n=9 (D-E). Data shown from two independent experiments.



**B** Neonatal thymus Adult TCRα<sup>-/-</sup> lung



neonate were phenotypically similar to those within the embryonic thymus and consisted of LTi cells. Returning to our methods that were previously established to identify ILC populations within the neonatal thymus, we utilised cells isolated from an adult mLN to provide a positive control for our analysis. Additional markers, such as CCR6 and CD4, were incorporated within the analysis so that LTi cells could be clearly identified.

ILC3 were first identified within the mLN control by gating on  $CD8\alpha^- CD3i^- IL-7R\alpha^+$  Extended Lineage $^- ROR\gamma t^+$  cells (Figure 3.14A). As demonstrated in our earlier investigations, LTi cells were identified amongst the ILC3 pool by expression of CCR6, and presence or absence of CD4. Using this approach, LTi cells were successfully identified within these experiments where two distinct populations of LTi cells, identified as  $CCR6^+ CD4^+$  and  $CCR6^+ CD4^-$ , were identified (Figure 3.14A). A third, small proportion of cells, identified as  $CCR6^- CD4^-$ , are also present within this plot and are expected to be  $NKp46^+$  ILC3 that are known to lack CCR6 (Figure 3.14A). This gating strategy was applied to cells isolated from the neonatal thymus and identified ILC3 and LTi cells present in similar proportions to those seen in the mLN (Figure 3.14A). The proportion of ILC3 observed from the FACS plots appeared consistent across experiments and enumeration of these cells identified ~700 ILC3 to be present (Figure 3.14B). As demonstrated within the FACS plots, the number of ILC3 present in the neonatal thymus was sufficient for identification of LTi cells within this tissue (Figure 3.14A). From enumeration of these cells, it was clear LTi cells dominated the ILC3 compartment within the neonatal thymus and were significantly higher in both proportion and number than  $CCR6^-$  ILC3 (Figure 3.14C). It

could be speculated that this may be attributed to their function in lymphoid tissue development at this early stage.

Mounting evidence has described the expression of MHCII by ILC3 in multiple tissues, including the small and large intestine, lymph nodes and spleen.(6) In particular, descriptions within the literature have reported the expression of MHCII to be by LT<sub>i</sub> cells.(6,139) Therefore, we sought to determine whether ILC3 in the neonatal thymus, where the majority of these cells are LT<sub>i</sub> cells, expressed MHCII.

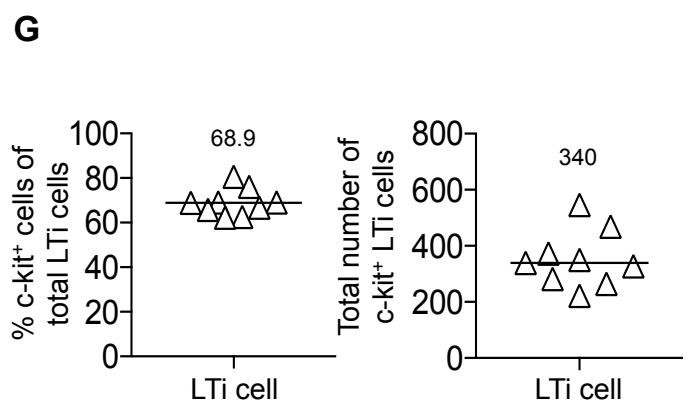
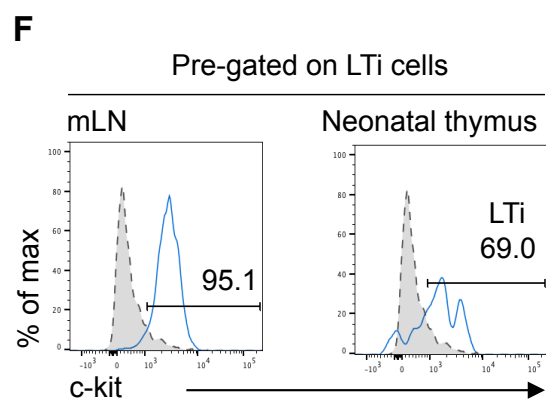
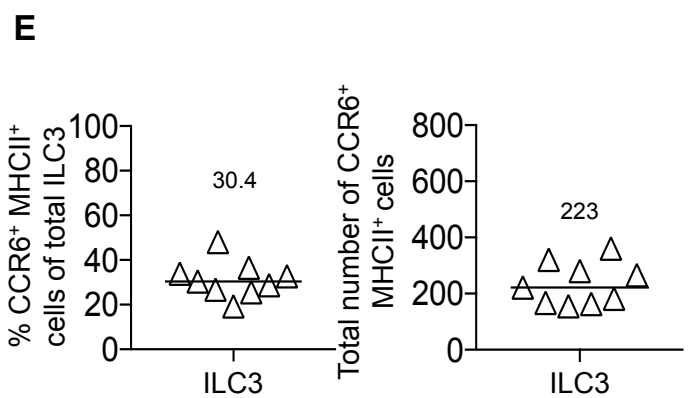
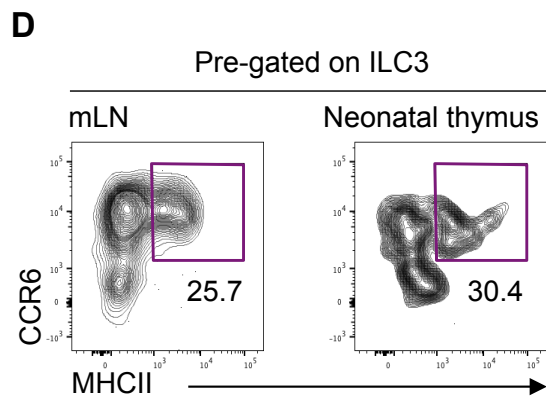
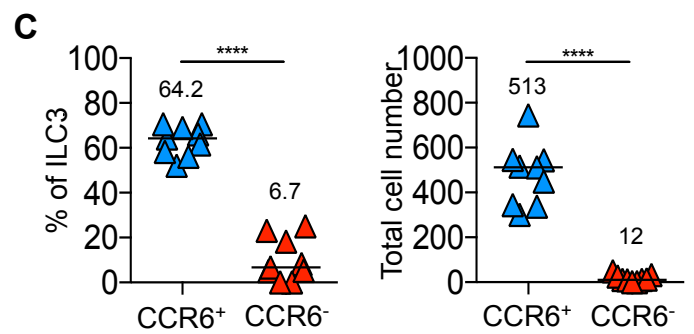
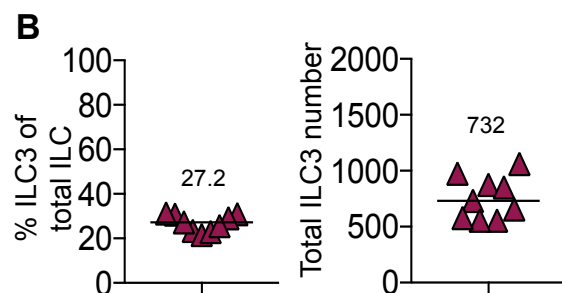
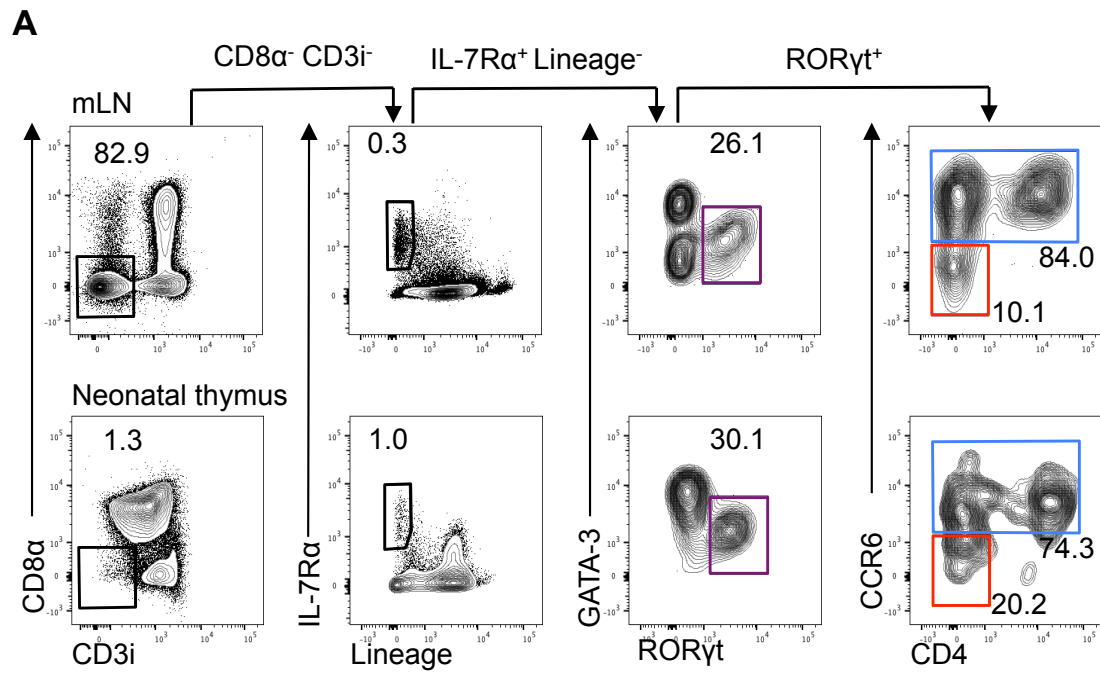
First gating on ILC3, MHCII was plotted against CCR6 so that both CD4<sup>+</sup> and CD4<sup>-</sup> LT<sub>i</sub> cells could be accounted for (Figure 3.14D). ILC3 from the mLN were first used as a positive control and initial assessment from the FACS plot demonstrated approximately one quarter of ILC3 to express MHCII (Figure 3.14D). Interestingly, all MHCII<sup>+</sup> ILC3 in this tissue were LT<sub>i</sub> cells. This gating strategy was applied to ILC3 isolated from the neonatal thymus and revealed a proportion of MHCII<sup>+</sup> similar to that observed in the mLN, albeit slightly elevated (Figure 3.14D). Again, all MHCII<sup>+</sup> ILC3 cells present in the neonatal thymus are LT<sub>i</sub> cells. Enumeration of MHCII<sup>+</sup> LT<sub>i</sub> cells in the neonatal thymus demonstrate the proportion of these cells observed in the FACS plot were consistent across all mice and accounted for a third of LT<sub>i</sub> cells; ~200 cells (Figure 3.14E). In addition to investigating MHCII expression by ILC3, we extended our assessment to include c-kit, which reports have described to be present on LT<sub>i</sub> cells (155). As shown in figure 3.17, LT<sub>i</sub> cells isolated from the mLN were utilised for positive and negative controls of c-kit; with positive expression demonstrated by ILC3 and negative expression demonstrated by ILC2 (Figure 3.14F). This gating could be applied to LT<sub>i</sub> cells isolated from the neonatal thymus and identified more than half these cells to express c-kit. Enumeration of c-kit<sup>+</sup> LT<sub>i</sub> cells in the neonatal thymus

### Figure 3.14 Phenotyping ILC3 populations within the neonatal thymus

In order to determine the phenotype of thymic ILC3 within the neonate, cells isolated from the thymus of a WT neonate 7 days post-birth were incubated with antibodies specific for markers of ILC3. Cells isolated from adult TCR $\alpha^{-/-}$  mLN were used as a positive control for ILC staining. Cells from both tissues were analysed by flow cytometry and total numbers calculated per whole thymus. Gates, triangles and histograms in purple, blue and red represent ILC3, LTi cells and CCR6 $^{-}$  CD4 $^{-}$  ILC3, respectively.

- A) Gating strategy used for the identification of LTi cells (CCR6 $^{+}$  CD4 $^{+/-}$ ) and CCR6 $^{-}$  CD4 $^{-}$  ILC3 amongst the ILC3 pool (CD8 $\alpha^{-}$  CD3i $^{-}$  IL-7R $\alpha^{+}$  Lin $^{-}$  ROR $\gamma$ t $^{+}$ ) in the mLN (upper panel) and neonatal thymus (lower panel). Lineage channel consists of antibodies against CD3, CD5, CD11b, CD11c, B220, CD19, Ter119, Fc $\epsilon$ R1, F4/80, CD49b, CD123 and Gr-1.
- B) Proportion and total number of ILC3 (ROR $\gamma$ t $^{+}$ ) amongst the ILC pool (CD8 $\alpha^{-}$  CD3i $^{-}$  IL-7R $\alpha^{+}$  Lin $^{-}$ ) in the neonatal thymus.
- C) Proportion and total number of LTi cells (CCR6 $^{+}$  CD4 $^{+/-}$ ) and CCR6 $^{-}$  CD4 $^{-}$  ILC3 amongst the ILC3 pool (CD8 $\alpha^{-}$  CD3i $^{-}$  IL-7R $\alpha^{+}$  Lin $^{-}$  ROR $\gamma$ t $^{+}$ ) in the neonatal thymus.
- D) Representative flow cytometry plots showing MHCII expression by ILC3 in the mLN and neonatal thymus. Pre-gated on ILC3 as identified in A.
- E) Proportion and total number of CCR6 $^{+}$  MHCII $^{+}$  ILC3 in the neonatal thymus.
- F) Representative flow cytometry plots showing the expression of c-kit by LTi cells (CD8 $\alpha^{-}$  CD3i $^{-}$  IL-7R $\alpha^{+}$  Lin $^{-}$  ROR $\gamma$ t $^{+}$  CCR6 $^{+}$  CD4 $^{+/-}$ ) in the mLN and neonatal thymus. Expression of c-kit by ILC2 in the TCR $\alpha^{-/-}$  mLN used as a negative control.
- G) Proportion and total number of c-kit $^{+}$  LTi-like cells (CD8 $\alpha^{-}$  CD3i $^{-}$  IL-7R $\alpha^{+}$  Lin $^{-}$  ROR $\gamma$ t $^{+}$  CCR6 $^{+}$  CD4 $^{+/-}$ ) in the neonatal thymus.

Mann-Whitney U (non-parametric, two-tailed) test was used for statistical analysis where \*p<0.05, \*\*p<0.01, \*\*\*p<0.001, and \*\*\*\*p<0.0001. In all graphs the bar represents the median, n=9. Data shown from two independent experiments.



identified the proportion of these cells to be consistent to that observed in the FACS across all mice and accounted for two third of LT<sub>i</sub> cells, ~300 cells (Figure 3.14G).

### **3.2.5 Characterisation of ILC populations in alternative transgenic mouse models**

Our ability to identify ILC populations within the adult thymus is made difficult by the vast number of T cells that are phenotypically similar to ILC. To address this, we sought to utilise alternative mouse strains that would aid identification of ILC populations either through a reduction in T cells or an increase in ILCs, such as TCR $\alpha^{-/-}$  and BALB/c mice, respectively. BALB/c mice have an enhanced response in type 2 immunity, of which ILC2 are involved.(156,157) As such, we hypothesised ILC2 would be more numerous in these mice and provide a sufficient number of cells to assess their phenotype.

To address this, ILC populations were compared in the thymus of C57BL/6 and BALB/c background. ILC2 and ILC3 populations were first identified in the C57BL/6 thymus as CD8 $\alpha^{-}$  CD3 $i^{-}$ , IL-7R $\alpha^{+}$  Lineage $^{-}$ , GATA-3 $^{+}$  and ROR $\gamma^{t+}$ , respectively (figure 3.15A). This gating strategy was applied to cells isolated from the thymus of BALB/c mice and a similar proportion of ILC2 and ILC3 were observed in these mice (Figure 3.15A). Enumeration in these mice demonstrated the total cellularity of the thymus to be reduced in BALB/c mice when compared to a C57BL/6 (Figure 3.15B). However, total ILC were increased in BALB/c mice compared to C57BL/6 (Figure 3.15C). As a result of a lower total thymic cellularity but greater number of total ILC, ILC make up a greater proportion of total thymocytes in the BALB/c thymus compared to C57BL/6 (Figure 3.15D).

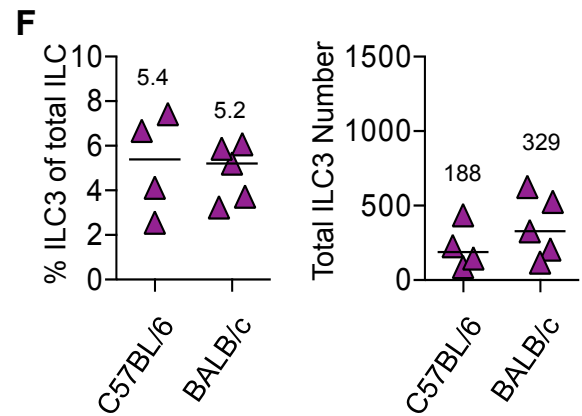
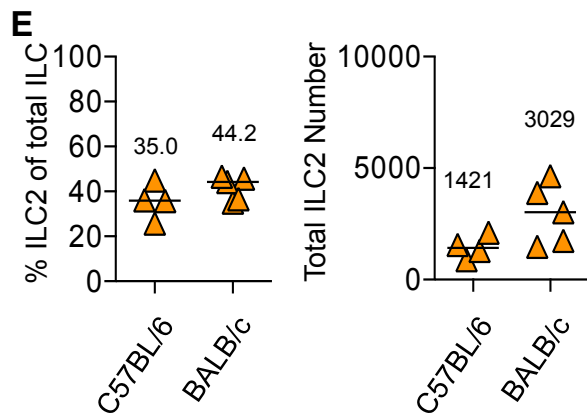
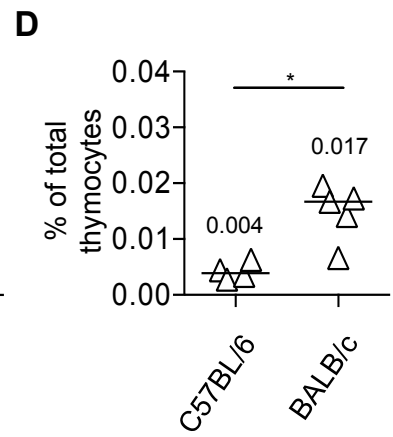
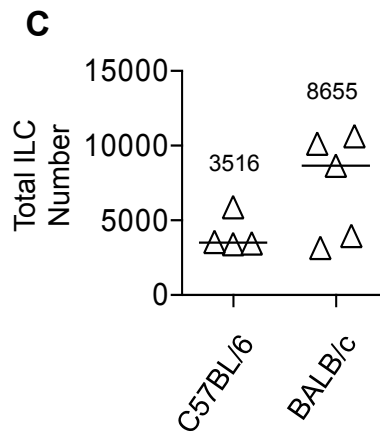
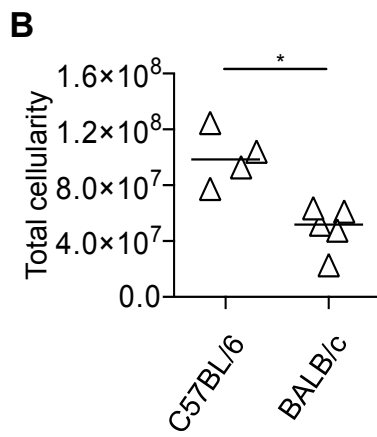
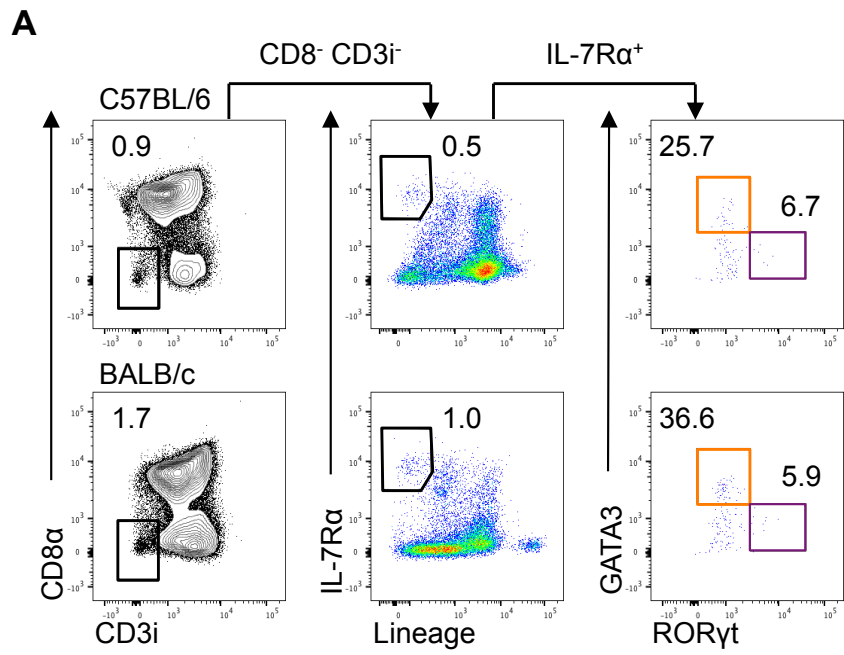
**Figure 3.15 Assessment of ILC2 and ILC3 in the thymus of C57BL/6 and BALB/c mice identified a similar number of these cells in both mouse strains**

To determine whether ILC populations are altered in mice of different genetic backgrounds, ILC2 and ILC3 populations were compared in the thymus of C57BL/6 and BALB/c mice. Cells were analysed by flow cytometry and total numbers calculated per whole thymus. Data shown in orange and purple correspond to ILC2 and ILC3, respectively.

- A) Gating strategy for the identification of total ILC ( $CD8\alpha^- CD3i^- IL-7R\alpha^+ Lin^-$ ), ILC2 ( $GATA-3^+$ ) and ILC3 ( $ROR\gamma t^+$ ) in the thymus of C57BL/6 and BALB/c mice.
- B) Enumeration of total thymic cellularity in C57BL/6 and BALB/c mice.
- C) Enumeration of total ILC ( $CD8\alpha^- CD3i^- IL-7R\alpha^+ Lin^-$ ) in the thymus of C57BL/6 and BALB/c mice.
- D) Total number of ILC ( $CD8\alpha^- CD3i^- IL-7R\alpha^+ Lin^-$ ) as a proportion of total thymic cellularity in C57BL/6 and BALB/c mice.
- E) Proportion and total number of ILC2 ( $GATA-3^+$ ) amongst the ILC pool ( $CD8\alpha^- CD3i^- IL-7R\alpha^+ Lin^-$ ) in  $TCR\alpha^{-/-}$ , C57BL/6 and BALB/c mice.
- F) Proportion and total number of ILC3 ( $ROR\gamma t^+$ ) amongst the ILC pool ( $CD8\alpha^- CD3i^- IL-7R\alpha^+ Lin^-$ ) in  $TCR\alpha^{-/-}$ , C57BL/6 and BALB/c mice.

Mann-Whitney U (non-parametric, two-tailed) test was used for statistical analysis where \* $p < 0.05$ , \*\* $p < 0.01$ , \*\*\* $p < 0.001$ , and \*\*\*\* $p < 0.0001$ . In all graphs the bar represents the median,  $n=4$  for C57BL/6 and  $n=5$  for BALB/c. Data shown from two independent experiments.





Despite our early hypothesis, no difference in the proportion and total number of ILC2 was observed in the thymus of BALB/c mice compared to C57BL/6 (Figure 3.15E). Furthermore, no difference in the proportion and total number of ILC3 was identified between these mice (Figure 3.15F). The absence of the  $\alpha\beta$  T cell receptor (TCR) in  $\text{TCR}\alpha^{-/-}$  mice is a result of a targeted mutation and has a direct impact on the development of T cells within these mice. Under normal conditions, the generation of a complete  $\alpha\beta$ -TCR requires re-arrangement of the  $\alpha$ -chain at the double-positive stage. This enables the subsequent process of positive selection, which is required for  $\text{CD4}^+$  or  $\text{CD8}^+$  single-positive T cell development, to occur through interactions with cTEC.(158–160) As a result,  $\text{TCR}\alpha^{-/-}$  mice display normal numbers of  $\text{CD4}^- \text{CD8}^-$  double-negative (DN) and  $\text{CD4}^+ \text{CD8}^+$  double-positive (DP) thymocytes, however subsequent development of SP thymocytes is halted.(161) Therefore, we anticipated ILC populations in these mice would be more easily identified given the absence of single positive thymocytes in these mice that are phenotypically similar to ILC.

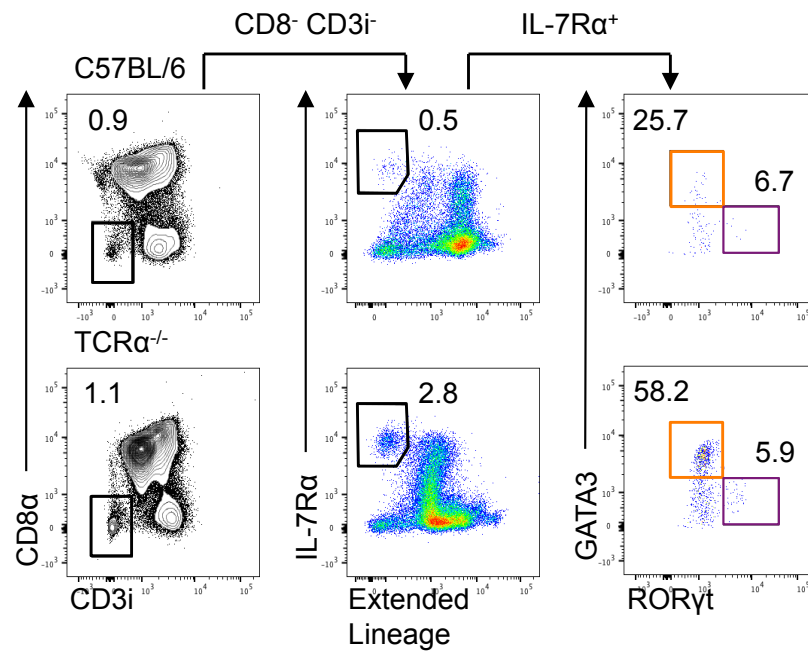
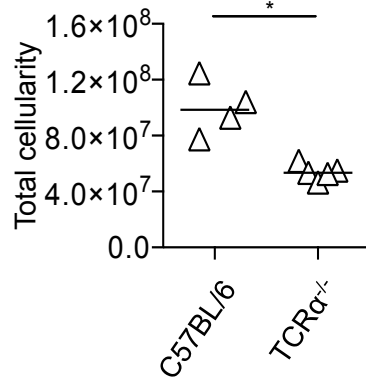
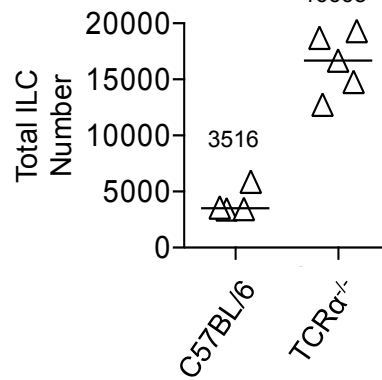
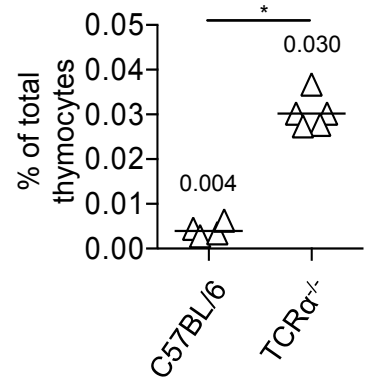
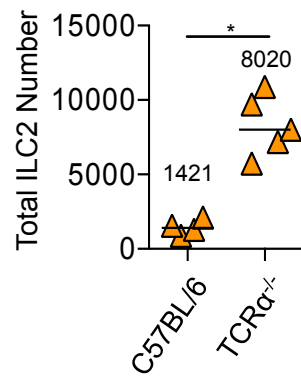
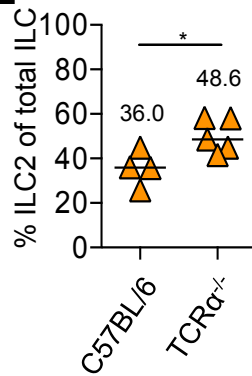
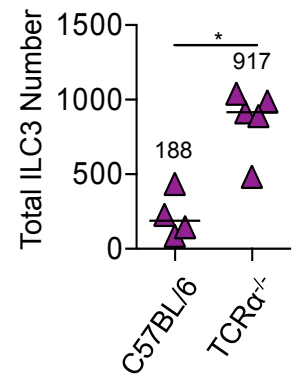
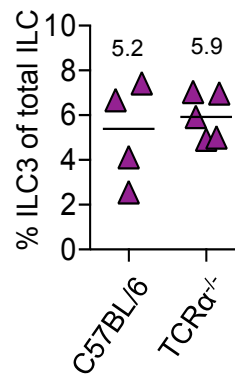
This was determined by comparing ILC2 and ILC3 populations in the thymus of WT mice to the thymus of  $\text{TCR}\alpha^{-/-}$  mice (Figure 3.16). ILC2 and ILC3 populations were first identified in the WT thymus as  $\text{CD8}\alpha^- \text{CD3i}^- \text{IL-7R}\alpha^+ \text{Lin}^- \text{GATA-3}^+$  or  $\text{ROR}\gamma^t^+$ , respectively. This gating strategy was applied to cells isolated from the  $\text{TCR}\alpha^{-/-}$  thymus where total ILC, defined as  $\text{CD8}\alpha^- \text{CD3i}^- \text{IL-7R}\alpha^+ \text{Lin}^-$ , and ILC2 appeared enriched (Figure 3.16A). While the total cellularity of the thymus was reduced in  $\text{TCR}\alpha^{-/-}$  mice, the total number of ILC appeared increased (Figure 3.16B-C). This resulted in a 10-fold increase in the proportion of ILC as a percentage of total cellularity in the thymus of  $\text{TCR}\alpha^{-/-}$  mice when compared to the WT thymus (Figure 3.16D). ILC2 were identified amongst total ILC by their expression of GATA-3 and an

**Figure 3.16 Comparison of ILC2 and ILC3 in thymus of C57BL/6 and TCR $\alpha^{-/-}$  identified an increase in these cells in TCR $\alpha^{-/-}$  mice**

It was anticipated the abundance of T cells within the adult thymus may hinder the identification of ILC given the phenotypic similarities between these cells. To test this, ILC2 and ILC3 populations were compared in the thymus of TCR $\alpha^{-/-}$  and WT mice. Cells were analysed by flow cytometry and total numbers calculated per whole thymus. Data shown in orange and purple correspond to ILC2 and ILC3, respectively.

- A) Gating strategy for the identification of total ILC (CD8 $\alpha^{-}$  CD3 $i^{-}$  IL-7R $\alpha^{+}$  extended-Lin $^{-}$ ), ILC2 (GATA-3 $^{+}$ ) and ILC3 (ROR $\gamma^{t+}$ ) in the thymus of C57BL/6 and TCR $\alpha^{-/-}$  mice. Extended lineage channel consists of antibodies against B220, CD3, CD5, CD11b, CD11c, CD19, CD49b, CD123, F4/80, Fc $\epsilon$ R1, Gr-1, and Ter119.
- B) Enumeration of total thymic cellularity in C57BL/6 and TCR $\alpha^{-/-}$  mice.
- C) Enumeration of total ILC (CD8 $\alpha^{-}$  CD3 $i^{-}$  IL-7R $\alpha^{+}$  Lin $^{-}$ ) the thymus of C57BL/6 and TCR $\alpha^{-/-}$  mice.
- D) Total number of ILC (CD8 $\alpha^{-}$  CD3 $i^{-}$  IL-7R $\alpha^{+}$  Lin $^{-}$ ) as a proportion of total thymic cellularity in C57BL/6 and TCR $\alpha^{-/-}$  mice.
- E) Proportion and total number of ILC2 (GATA-3 $^{+}$ ) amongst the ILC pool (CD8 $\alpha^{-}$ CD3 $i^{-}$ IL-7R $\alpha^{+}$ Lin $^{-}$ ) in the thymus of C57BL/6 and TCR $\alpha^{-/-}$  mice.
- F) Proportion and total number of ILC3 (ROR $\gamma^{t+}$ ) amongst the ILC pool (CD8 $\alpha^{-}$ CD3 $i^{-}$ IL-7R $\alpha^{+}$ Lin $^{-}$ ) in the thymus of C57BL/6 and TCR $\alpha^{-/-}$  mice.

Mann-Whitney U (non-parametric, two-tailed) test was used for statistical analysis where \*p<0.05, \*\*p<0.01, \*\*\*p<0.001, and \*\*\*\*p<0.0001. In all graphs the bar represents the median, n=4 for C57BL/6 and n=5 for TCR $\alpha^{-/-}$ . Data shown from two independent experiments.

**A****B****C****D****E****F**

increase in both the proportion and total number of these cells was observed in the  $\text{TCR}\alpha^{-/-}$  thymus (Figure 3.16E). ILC3, however, were identified according to their expression of  $\text{ROR}\gamma^+$ . While there was no difference in the proportion of ILC3 in the thymus between these mice, there was an increase in total ILC3 number in the  $\text{TCR}\alpha^{-/-}$  thymus (Figure 3.16F). Overall, these demonstrate total ILC, and ILC2 and ILC3 subsets, to be increased in the thymus of  $\text{TCR}\alpha^{-/-}$  mice.

As described above, total ILC, including ILC2 and ILC3 subsets, were shown to be present in greater numbers in the thymus of  $\text{TCR}\alpha^{-/-}$  mice compared to a WT. As such, we sought to better understand the phenotype of ILC2 and ILC3 in the adult thymus of  $\text{TCR}\alpha^{-/-}$  mice where these cells are more numerous. We have previously shown ILC2 within the neonatal thymus to express ICOS and ST2, while KLRG-1 is absent. In order to determine whether ILC2 of the adult thymus share this phenotype, cells isolated from the thymus of  $\text{TCR}\alpha^{-/-}$  mice were compared with cells isolated from the mLN and lung of the same strain. As detailed in 3.12, the expression of ILC2-associated markers varies depending on their location and the use of tissue from the lung and mLN would control for differences in KLRG-1, ICOS and ST2 expression across these tissues. In addition, recently emerged evidence has shown that prolonged enzymatic digestion of lung tissue using enzymes at a higher concentration results in a reduction in  $\text{GATA-3}^+$  and an increase in cells lacking Tbet,  $\text{GATA-3}$  and  $\text{ROR}\gamma$ .(88) While our methods also use enzymes to isolate ILC populations from the mLN, this is only a mild procedure and TrN ILCs have not been described as a result.

ILC2, identified as live  $\text{CD45}^+ \text{CD8}\alpha^- \text{CD3i}^- \text{IL-7R}\alpha^+ \text{Lin}^- \text{GATA-3}^+$ , were identified in all three tissues (Figure 3.17A). As with our investigations into ILC2 phenotype within

the neonatal thymus, CD45 and a viability dye were included to separate live cells of the lymphoid lineage from cells of non-hematopoietic origin. Adaptation of our established gating strategy to include CD45 and a viability dye enabled successful identification of ILC2 in all three tissues; defined as live CD45<sup>+</sup> CD8α<sup>-</sup> CD3i<sup>-</sup> IL-7Rα<sup>+</sup> Lineage<sup>-</sup> GATA-3<sup>+</sup> cells (figure 3.17A). While there appears to be contamination in the CD8α versus CD3i FACS plot in the lung, this does not hinder our identification of ILC2 in this tissue. Through this strategy, ILC2 were shown to be the main ILC subset within these tissues, making up >50% of all ILCs in each tissue (figure 3.17A).

KLRG-1, ST2 and ICOS are expressed by the majority of ILC2 within the lung; however, the median fluorescence intensity (MFI) of these surface markers is variable depending on the tissue investigated.(88) Here, the MFI of KLRG-1, ICOS and ST2 are compared amongst TCRα<sup>-/-</sup> lung, mLN and thymus. From these data, KLRG-1, ICOS and ST2 expression varies across tissues (figure 3.17B). In particular, ILC2 of the thymus have a unique pattern of expression that does not match that of the other tissues investigated (figure 3.17B). Within the thymus, very little expression of KLRG-1 is expressed by ILC2 (figure 3.17B). This contrasts the expression of ICOS and ST2 by ILC2 within the thymus, which is expressed at a level higher than in the lung and mLN (figure 3.17B).

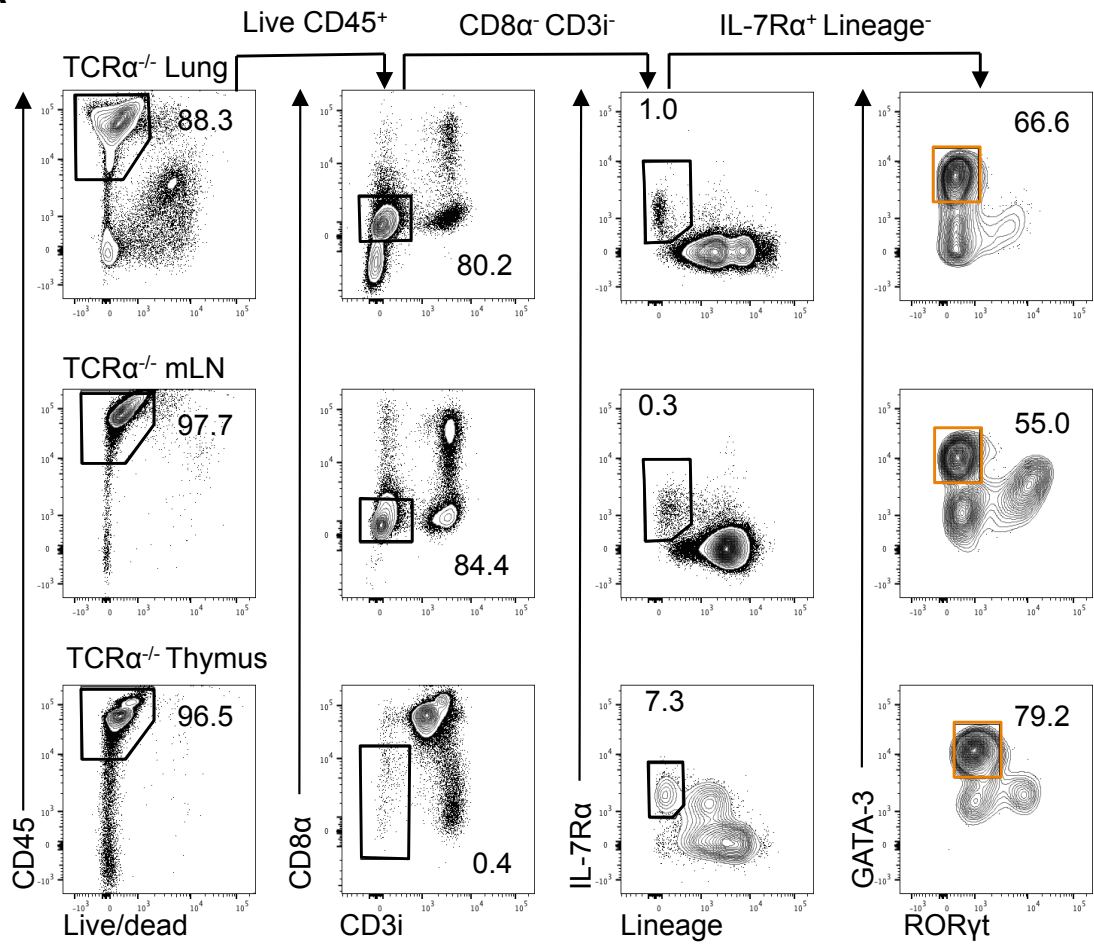
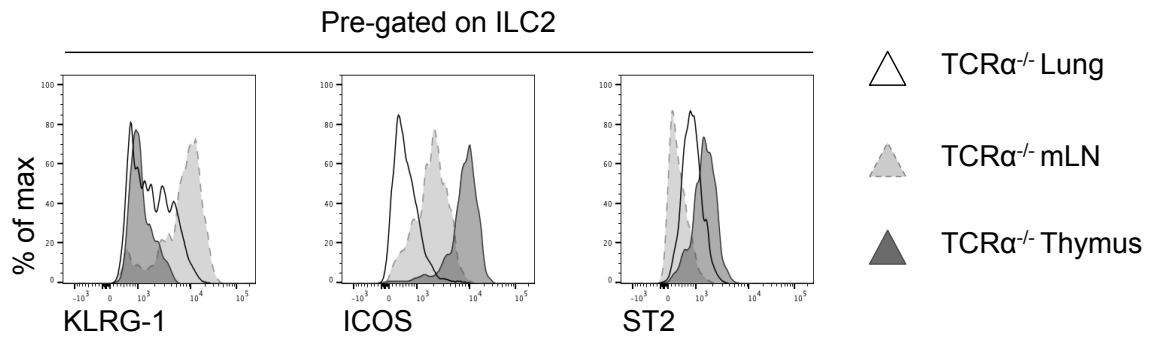
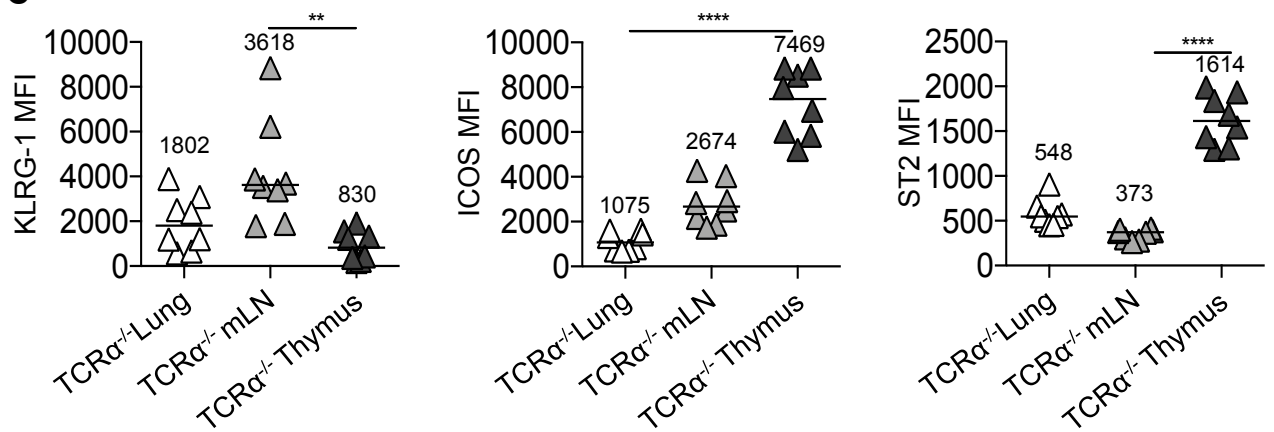
THE MFI of these markers was used to assess their expression across tissues (figure 3.17C). Consistent with the histogram shown in 3.17B, the lowest level of KLRG-1 expression is by ILC2 of the thymus, and is significantly lower than KLRG-1 expression by ILC2 of the mLN (figure 3.17C). Interestingly, thymic ILC2 demonstrate the highest level of expression of both ICOS and ST2 across all tissues assessed

**Figure 3.17 Phenotyping ILC2 in non-lymphoid and lymphoid tissues in TCR $\alpha^{-/-}$  mice.**

The phenotype of ILC2 is well defined in both non-lymphoid and lymphoid tissues within the periphery but the phenotype of thymic ILC2 has yet to be established. To investigate the phenotype of ILC2 in the thymus, cells were isolated from the thymus of TCR $\alpha^{-/-}$  mice, where we have shown ILC2 number is increased, and compared with ILC2-associated markers in the lung and mLN. Cells were analysed using flow cytometry and total numbers were calculated per whole tissue. The gate shown in orange corresponds to ILC2.

- A) Gating strategy for the identification of ILC2 (CD45<sup>+</sup> Live/dead<sup>-</sup> CD8 $\alpha^{-}$  CD3 $\gamma^{-}$  IL-7R $\alpha^{+}$  Lin<sup>-</sup> GATA-3<sup>+</sup>) in the lung (upper panel), mLN (middle panel) and thymus (lower panel) of TCR $\alpha^{-/-}$  mice. Lineage channel consists of antibodies against CD3, CD5, CD11b, CD11c and B220.
- B) Representative histograms comparing the expression of KLRG-1, ICOS and ST2 by ILC2 in the lung, mLN and thymus of TCR $\alpha^{-/-}$  mice. Histograms pre-gated on ILC2 (as defined in 3.14A).
- C) Comparison of the MFI of KLRG-1, ICOS and ST2 by ILC2 in the lung, mLN and thymus of TCR $\alpha^{-/-}$  mice.

Kruskal-Wallis one-way ANOVA with post hoc Dunn's test was used (comparing three or more data sets) for statistical analysis where \*p<0.05, \*\*p<0.01, \*\*\*p<0.001, and \*\*\*\*p<0.0001. In all graphs the bar represents the median, n=8. Data shown from two independent experiments.

**A****B****C**



(figure 3.17C). Furthermore, the expression of ICOS and ST2 by thymic ILC2 is significantly greater than ILC2 originating from the lung (figure 3.17C). Our earlier investigations revealed a third of LT<sub>i</sub> cells within the neonatal thymus expressed MHCII. This evidence demonstrates the capability of LT<sub>i</sub> cells in the thymus to express MHCII and, as such, we wanted to explore whether this was also true in the adult thymus.

As shown in Figure 3.16, the total numbers of ILC3 were increased in the TCR $\alpha^{-/-}$  thymus. This is much greater than the number of ILC3 present in the thymus of a WT mouse, where our earlier investigations have identified few ILC3 to be present within this tissue. Therefore, we identified TCR $\alpha^{-/-}$  mice as an appropriate model for further phenotyping ILC3 in the adult thymus, where a sufficient number of cells are required. Furthermore, data in Figure 3.17 has shown these mice to be useful in phenotyping ILC2. As in previous experiments, cells isolated from the thymus were compared to those from the mLN, which acts as an appropriate positive control.

As with our earlier investigations, cells isolated from the mLN were used as a positive control for ILC3, including LT<sub>i</sub> cells. Although ILC3 are increased in the thymus of TCR $\alpha^{-/-}$  mice, ILC3 are still a rare population in comparison to other cell types. As such, a viability dye was included to reduce the presence of dead cells that may interfere with our identification of ILC3. Firstly, ILC3, defined as live CD8 $\alpha^{-}$  CD3 $i^{-}$  IL-7R $\alpha^{+}$  Lin $^{-}$  ROR $\gamma^{t+}$ , were identified in the mLN of TCR $\alpha^{-/-}$  mice (Figure 3.18A). Subsequent gating identified clear populations of total ILC and ILC3 within this tissue (figure 3.18A). Further analysis based on the expression of CCR6 and CD4 identified LT<sub>i</sub> cells (CCR6 $^{+}$  CD4 $^{+/-}$ ) and non-LT<sub>i</sub> cells (CCR6 $^{-}$  CD4 $^{-}$ ) amongst total ILC3 in the mLN (Figure 3.18A). This gating strategy was applied to cells isolated from the

thymus of  $\text{TCR}\alpha^{-/-}$  mice where ILC3, LTi cells and non-LTi cells could also be identified (Figure 3.18A).

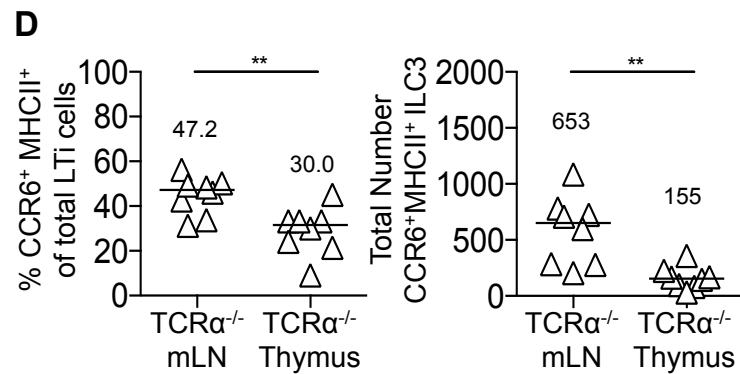
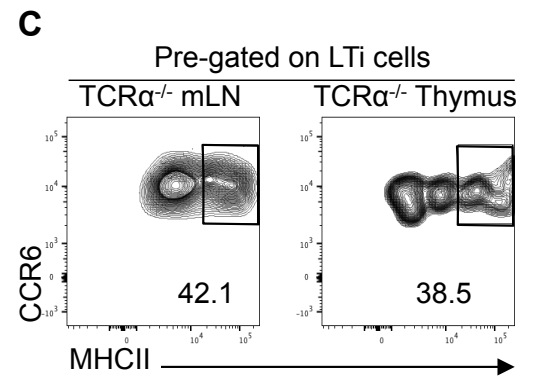
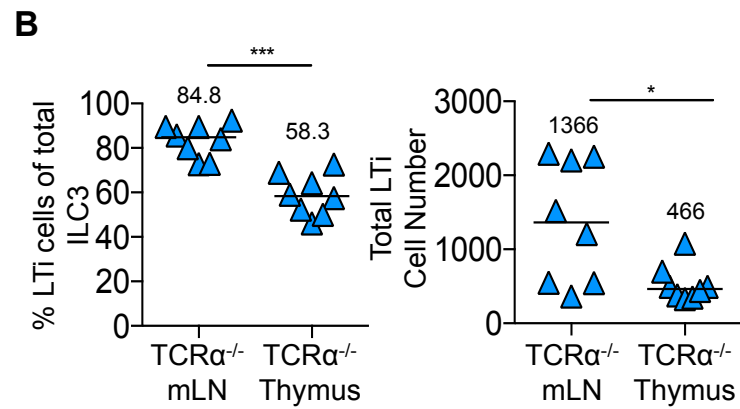
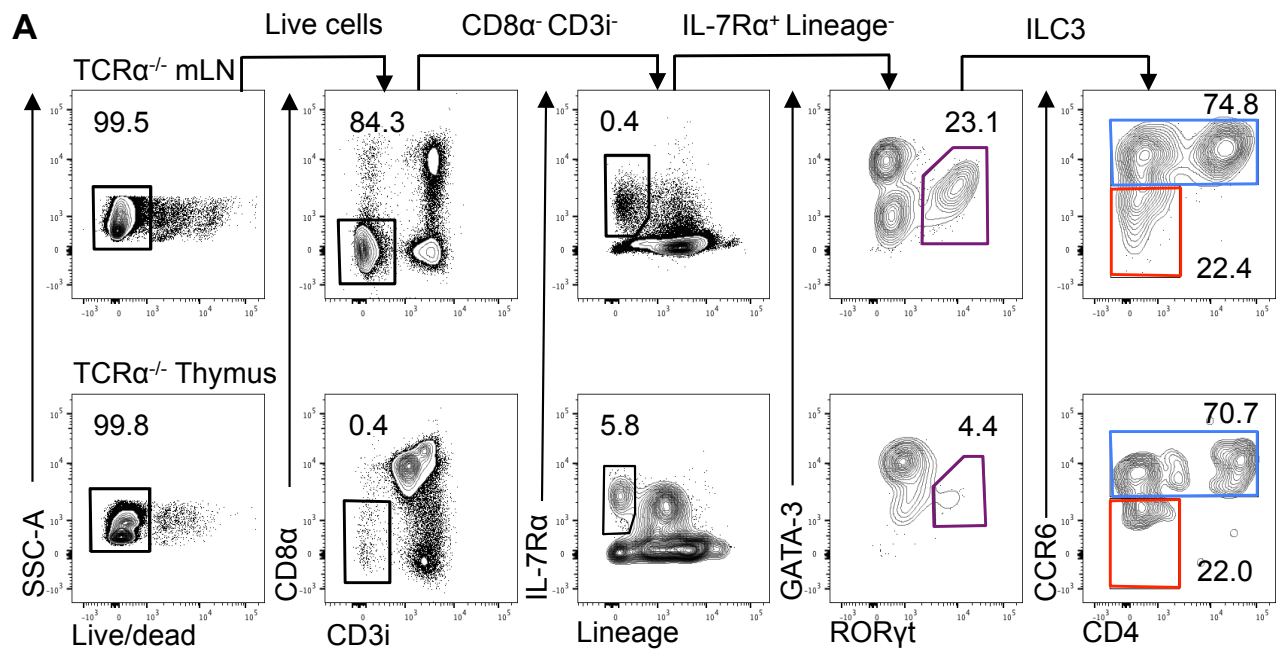
Enumeration of these cells identified a significantly lower proportion and total number of LTi cells present in the  $\text{TCR}\alpha^{-/-}$  thymus compared to the mLN (figure 3.18B). However, LTi cells compose greater than half of all ILC3 in both tissues (figure 3.18B). Further gating on LTi cells was performed to assess their expression of MHCII. Gating on thymic LTi cells alone proved difficult given the few LTi cells present in this tissue to allow for accurate gating. As such, MHCII expression was applied to LTi cells of the mLN and subsequently applied to LTi cells of the thymus, where similar proportions of MHCII expression were observed (figure 3.18C). Further analysis of  $\text{MHCII}^+$  LTi cells across tissues identified a significantly lower proportion and number of these cells in the thymus compared to the mLN (figure 3.18D). Although low in number, the expression of MHCII by thymic LTi cells indicates a role for MHCII in their function.

### Figure 3.18 Phenotyping of ILC3 in the mLN and thymus of $\text{TCR}\alpha^{-/-}$ mice

The presence of ILC3 within the thymus is a recent discovery and their phenotype has yet to be fully elucidated. To investigate the phenotype of thymic ILC3, cells were isolated from the thymus of  $\text{TCR}\alpha^{-/-}$  mice, where we have shown ILC3 number to be increased, and compared with ILC3-associated markers in the mLN from the same mouse. Cells were analysed using flow cytometry and total numbers were calculated per whole tissue. Data shown in purple, blue and red correspond to ILC3, LTi cells and  $\text{CCR6}^{-}$  ILC3.

- A) Gating strategy for the identification of LTi cells ( $\text{CCR6}^{+} \text{CD4}^{+/-}$ ) and  $\text{CCR6}^{-} \text{CD4}^{-}$  ILC3 amongst the ILC3 pool (Live/dead $^{-}$   $\text{CD8}\alpha^{-} \text{CD3i}^{-} \text{IL-7R}\alpha^{+} \text{Lin}^{-} \text{ROR}\gamma\text{t}^{+}$ ) in the mLN (upper panel) and thymus (lower panel) of  $\text{TCR}\alpha^{-/-}$  mice. Lineage channel consists of antibodies against CD3, CD5, CD11b, CD11c and B220.
- B) Proportion and total number of LTi cells ( $\text{ROR}\gamma\text{t}^{+} \text{CCR6}^{+} \text{CD4}^{+/-}$ ) amongst the ILC pool (Live/dead $^{-}$   $\text{CD8}\alpha^{-} \text{CD3i}^{-} \text{IL-7R}\alpha^{+} \text{Lin}^{-}$ ) in the mLN and thymus of  $\text{TCR}\alpha^{-/-}$  mice.
- C) Representative flow cytometry plots showing  $\text{MHCII}^{+}$  LTi cells in the mLN (left) and thymus (right) of  $\text{TCR}\alpha^{-/-}$  mice. Cells pre-gated on LTi cells (identified as Live/dead $^{-}$   $\text{CD8}\alpha^{-} \text{CD3i}^{-} \text{IL-7R}\alpha^{+} \text{Lin}^{-} \text{ROR}\gamma\text{t}^{+} \text{CCR6}^{+} \text{CD4}^{+/-}$ ).
- D) Proportion and total number of  $\text{MHCII}^{+}$  LTi cells in the mLN and thymus of  $\text{TCR}\alpha^{-/-}$  mice. Cells pre-gated on LTi cells (identified as Live/dead $^{-}$   $\text{CD8}\alpha^{-} \text{CD3i}^{-} \text{IL-7R}\alpha^{+} \text{Lin}^{-} \text{ROR}\gamma\text{t}^{+} \text{CCR6}^{+} \text{CD4}^{+/-}$ ).

Mann-Whitney U (non-parametric, two-tailed) test was used for statistical analysis where \* $p < 0.05$ , \*\* $p < 0.01$ , \*\*\* $p < 0.001$ , and \*\*\*\* $p < 0.0001$ . In all graphs the bar represents the median,  $n=8$ . Data shown from two independent experiments.



### 3.3 Discussion

Overall, these data provide a detailed characterisation of ILC populations within the thymus across ontogeny. The evidence presented within this body of research demonstrates ILC3 to be the most abundant ILC subset in the embryonic thymus and numbers of these cells persist in the neonate. Interestingly, similar numbers of ILC2 and ILC3 were present in the neonatal thymus at one week post-birth. However, the number of ILC3 were shown to decline at two weeks post-birth and continued to decline into adulthood where very few ILC3 were observed, while we demonstrate the number of ILC2 to increase by two weeks post-birth and maintained into adulthood.

ILC are often described as innate counterparts to T-helper subsets due to their phenotypic similarities. This makes their identification within the thymus, where there are vast numbers of developing thymocytes with varying levels of TCR expression, incredibly challenging. This was overcome within our investigations using a combination of *ex vivo* and *in vivo* approaches. For example, FTOC were used to enrich ILC populations within the embryonic thymus and enabled their identification using flow cytometry. Using this approach, we not only identified ILC3, or at least their progenitors, that had previously been observed by Rossi *et al.* (2007), but also ILC2.(98)

Following birth, the identification of ILC within the thymus becomes increasingly difficult as the number of T cells within this tissue rapidly expands with development. Id2 was used as a tool to resolve this issue where it is known to be indispensable in ILC differentiation yet redundant in  $\alpha\beta$  T cell development.(149) Using this approach, Id2 expression was assessed in both fate-mapping and reporting approaches and

clearly identified thymic ILC. However, these cells account for less than 0.05% of the haematopoietic compartment of the thymus following birth and less than 0.001% in the adult thymus.(129)

These findings differ to those previously published by Dudakov *et al.* (2012) where LT $\alpha$ i cells were described in their abundance within the adult thymus.(100) Moreover, the authors describe LT $\alpha$ i cells as a key source of IL-22 and promote regeneration of the thymic microenvironment that was triggered by the depletion of CD4 $^{+}$  CD8 $^{+}$  DP thymocytes.(100) While the differences between our observations and that of Dudakov *et al.* (2012) are not entirely clear, our investigations used a range of robust *in vivo* models; each demonstrating very few ILC3 to be present within the adult thymus.(100) Whether these few ILC3 are capable of producing IL-22 or rapidly expand in response to thymic damage will be answered in the proceeding chapter.

The increase in ILC2 and substantial decline in ILC3 populations post-birth was a striking find in our investigations. As such, we sought to determine a reason for the loss in ILC3 in neonatal development. It has been demonstrated in recent fate-mapping studies that some ILC3 lose the expression of ROR $\gamma$ t and adopt an “ex-ILC3” phenotype that is similar to Tbet $^{+}$  IFN $\gamma$  $^{+}$ .(81) Therefore, it was not unreasonable to propose that the loss in ILC3 within the thymus could be accounted for by plasticity amongst these cells. However, our studies revealed that the majority of ILC within the thymus had no previous expression of the *Rorc* locus, indicating that the plasticity of ILC3 did not account for the rise in ILC2 and loss of ILC3 in this tissue.

Amongst the data presented within this chapter, we had sought to quantify the true number of ILC within the adult thymus. This was investigated using a variety of

mouse models, each with their own strengths and weaknesses that were taken into consideration when interpreting the data. It was evident through our findings that the total number of ILC recovered from the adult thymus was variable amongst these different mouse models. For example, our earlier experiments characterised ILC in the adult thymus of a WT mouse where approximately 3000 of these cells were discovered. This value was higher than our proceeding investigations, which used both  $Id2^{CreERT2} \times ROSA26^{mT/mG}$  and  $Id2-eGFP$  mice, where approximately 1300 and 2000 ILC were identified, respectively.

First concerning the use of WT mouse in characterising ILC in the adult thymus (Figure 3.2), which has suitable advantages. These mice represent a natural model and it is expected that the results obtained in this model reflect the true numbers of ILC in the wild. However, in the context of our investigations, the nature of the thymus in WT mice added difficulty in isolating ILC from the large of numbers of thymocytes, given the phenotypic similarities between ILC and T cells, as commonly discussed within this thesis. Although best efforts were made in our investigations to separate ILC from T cells using a intricate gating strategy, the very nature of our analysis meant that overestimation of ILC number may be possible.

This caveat was not overlooked within our studies and therefore we used other *in vivo* tools to aid identification ILC in the thymus. Figure 3.7 characterised the number of ILC in the adult thymus of  $Id2^{CreERT2} \times ROSA26^{mT/mG}$  mice following administration of tamoxifen within the diet. This model enabled the identification of  $mGreen^+$  ILC, and therefore ILC that expressed  $Id2$  during, or just before tamoxifen administration, when Cre was expressed. However, as aforementioned, approximately 1300 ILC were identified in this model, which relates to  $mGreen^+$  ILC only. We understand that

the induction of Cre using tamoxifen is not 100%, and is influenced by the method, duration and dose of tamoxifen administration. Therefore, it is unlikely that the mGreen<sup>+</sup> ILC that we have identified account for all ILC in this tissue and thus underestimating the true number of these cells. As stated above, the method of tamoxifen administration can also have an affect. Administration of tamoxifen within the diet, as discussed here, has greater variability than administration by oral gavage due to mice having greater control over tamoxifen intake.

Future analysis could look to quantify mGreen<sup>+</sup> ILC and total ILC in the mLN where ILC are easily identifiable without the need of a reporter strain. This would enable us to calculate the efficiency of Cre induction in our mouse model. However this is not without its disadvantages, as induction of Cre with tamoxifen is not always consistent across tissues and may well vary between the mLN and thymus.(162) Furthermore, our own data demonstrated a modest reduction in ILC3 number in secondary lymphoid tissue as a result of tamoxifen administration. Although we were unable to determine the effect of tamoxifen administration on ILC in the thymus, it is possible that tamoxifen may have resulted in a further reduction in total ILC number. We have previously shown that the thymus is affected by the administration of thymus where a reduction in the number of DP thymocytes was observed.

To overcome the challenges of using a tamoxifen-inducible Cre, we pursued investigations using Id2-eGFP reporter mice.(124) One of the main advantages of using Id2-eGFP reporter mice is that they do not require the administration of an exogenous substance in order to activate the fluorescent molecule.(163) In comparison, this mouse reports live expression of Id2 and does not require administration of tamoxifen. As such, these mice are not subject to the variability that



would be introduced by tamoxifen and it is possible to suggest that the number of ILC identified in these mice is closer to the true number of cells. However, during our analysis of these cells using flow cytometry, it was discovered that the brightness of GFP on GFP<sup>+</sup> cells was often difficult to pull apart from GFP<sup>-</sup> cells, hindering our interpretation of these cells. Although we used suitable GFP<sup>-</sup> controls in these investigations, it is still possible that the low brightness of GFP may have impacted on our identification of GFP<sup>+</sup> cells and subsequent quantification of ILC.

While it may not be possible to fully elucidate the true number of ILC in the thymus, our investigations have used a variety of mouse models to provide evidence to support an approximate value of these cells. Moreover, in the context of the thymus, a difference of 2000 cells, if we compare data obtained from the WT thymus and mice administered tamoxifen, is only minor in comparison to the millions of thymocytes that are present. Ultimately highlighting ILC as a rare population of immune cells that exist in the thymus.

Although our investigations used a variety of *in vivo* models to study the ILC composition of the thymus, this was, in part, limited by the availability of certain mice within the university. The *RAG* genes, for example, have a fundamental role in T cell development and exert their function in two distinct waves. The absence of either *RAG-1* or *RAG-2* genes result in mice lacking mature B and T lymphocytes due to blockages in cell development. As such, RAG-deficient mice would have been an appropriate model of choice given the main challenge of identifying ILC in a tissue that is heavily dominated by T cells. However, the thymic microenvironment is perturbed in RAG-deficient and effect of this on ILC populations is largely unknown. Given the reduced competition for ILC stimulating cytokines, such as IL-7, in the

thymus of RAG-deficient mice, it is not unreasonable to suggest ILC numbers may also increase within these mice compared to WT tissues.(164)

Our data demonstrated the decline in ILC3 post-birth to coincide with the increase in ILC2. Given that ILC3 have previously been described within the thymic medulla, we hypothesised that ILC2 might be elevated in the absence of ILC3. Indeed, a rise in the number of ILC2 was observed in the thymus of both adult and neonatal ROR $\gamma$ t-deficient mice, consistent with the idea of a competitive niche within the thymic medulla. Whether the changes in ILC composition observed within these mice are a result of the intrinsic effects of ILC or the abnormal T-cell development is yet to be determined.

It is well established that ILC require signalling through IL-7R $\alpha$  for their development and maintenance.(27) Given that the thymus is a rich source of IL-7 where it is required for several stages of T cell development, it not unreasonable to suggest that ILC2 and ILC3 may compete for these signals. Furthermore, this idea is supported by the variations in ILC number observed in TCR $\alpha$ -deficient and ROR $\gamma$ t-deficient mice. In addition to our observations in the ROR $\gamma$ t-deficient thymus, described above, we also demonstrate an increase in total ILC number in the thymus of TCR $\alpha$ -deficient mice. In the context of these perturbed environments, the competition for IL-7 is reduced, which may account for ILC expansion.

It was clear through our investigations that ILC account for only a small percentage of total cells within the thymus where they were heavily outnumbered by the expansion of thymocytes during postnatal development.(129,165) However, the absolute number of ILC2 continued to increase by 2 weeks post-birth where numbers were

maintained into adulthood. Our current understanding of ILC development states that all ILC arise from the CLP in the bone marrow that also gives rise to T and B lymphocytes.(104,138) Id2 is indispensable in ILC differentiation where it is required for the differentiation of CLP to ILCP that is no longer able to differentiate into other cells of the adaptive immune system.(138) Therefore, these data suggest that ILC2 are recruited to the thymus following birth and do not appear to increase relative to the decline in ILC3.(129,165) However, it is currently unclear to whether ILC differentiation follows a single route or if ILC can arise from multipotent progenitors that are found outside of the bone marrow.(104) This is not unreasonable to suggest given that progenitors that lie upstream of the CLP in the haematopoietic lineage have been shown to migrate to the thymus where they exhibit potential to differentiate into the earliest T cell progenitors.(166–168) Whether these progenitors can also give rise to ILC2 is yet to be fully determined.

It is quite possible that ILC2 have the potential to develop in the thymus from these ETP given that the microenvironment is rich in IL-7 and Notch signals that are required for ILC2 differentiation.(102,104) Moreover, progenitors of the T cell lineage also possess the transcription factors required for ILC2 differentiation, such as B cell leukaemia 11b (*bcl11b*), GATA-3 and T cell Factor-1 (TCF-1).(169) Furthermore, *in vitro* studies demonstrated ILC2 to arise from DN1 and DN2 cells when cultured with IL-33 and IL-7.(104)

Recently, evidence has emerged to support a thymic origin of ILC2 using *in vivo* models.(104) The E proteins, E2A and HEB, have redundant roles within the thymus whereby the absence of one is compensated by the action of the other. Meanwhile deletion of both E proteins results in blocking T cell development at the DN3

stage.(104) Researchers have manipulated the expression of inhibitor of DNA-binding 1 (Id1), which is not usually expressed in lymphocytes, to inhibit the action of E proteins and investigate ILC2 development in the thymus.(104) In this study, mice that were homozygous for the ectopic expression of Id1 off the proximal promoter of the *lck* gene (*plck*) had T cell development blocked at the DN stage and were absent of any T cell lineage committed cells.(104) Interestingly, analysis of the ILC2 compartment in these mice revealed a substantial number of these cells in the thymus and at peripheral sites, such as the lung, mLN and spleen.(104) Furthermore, the use of a *plck*-Cre transgene to delete the genes for E2A and HEB resulted in a similar phenotype to the mice utilising ectopic expression of Id1.(104,170) Collectively, these data highlight the potential for ILC2 to arise in the thymus following downregulation of the E proteins required for T cell development. However, further work is required to determine whether downregulation of E proteins in the postnatal thymus is responsible for the increase in ILC2 number post-birth.

Throughout our investigations we sought to determine the phenotype of thymic ILC to provide some indication of the function of these cells. Amongst our data, we demonstrated approximately 30% of LT<sub>i</sub> cells within the thymus of WT neonatal and TCR $\alpha^{-/-}$  adult mice to express MHCII. Our current understanding of MHCII expression by ILC3 is predominantly focussed on the action of these cells at peripheral sites. But, the impact of MHCII expression in the context of the thymus has yet to be fully understood.

At peripheral sites, MHCII expression by ILC3 has been shown to regulate CD4<sup>+</sup> T cell responses to commensal bacteria by MHCII-mediated antigen presentation.(6) This was illustrated through the conditional deletion of MHCII on ILC3 and resulted in

moderate colitis in mice due to the inability to control T cell responses to the commensal bacteria.(6) This highlights a role for ILC3 in maintaining tissue homeostasis in the gastrointestinal tract where they regulate CD4<sup>+</sup> T cell activity.(6) The effects of which were, in part, due to ILC3 outcompeting T cells for IL-2 and therefore limiting the growth factors required for T cell differentiation and survival, leading to the induction of apoptosis in these cells.(94,171) Additionally, it is anticipated that ILC3 are capable of regulating the T cell pool by limiting other key cytokines, such as IL-7.(171) Whether ILC3 have a similar role within the thymus requires further investigation. Interestingly, interactions between ILC3 and other immune populations is not limited to CD4<sup>+</sup> T cells. Other studies have demonstrated that LT<sub>i</sub> cells are capable of presenting lipid antigens to iNKT cells mediated by CD1d.(171) Taken together, these data highlight a role for ILC in regulating other immune populations through the presentation of surface antigens, either in the context of MHCII or CD1d. Given that the primary role of the thymus is to generate a vast repertoire of immunocompetent T cells and the ability of LT<sub>i</sub> cells to express MHCII in this tissue, it is not unreasonable to propose a role for LT<sub>i</sub> cells in regulating thymocyte development through antigen presentation. However, further work is required to provide evidence for this role.

Earlier in this chapter we sought to characterise the phenotype of ILC2 in the neonatal thymus to aid our understanding about the function of these cells. To approach this, we compared the expression of markers associated with ILC2, particularly KLRG-1, ICOS and ST2, in the neonatal thymus with those isolated from the lung. The lung was an appropriate control for this investigation given that our laboratory had previously published findings on the phenotype of lung ILC2 and we

already knew much about their expression by these cells.(88) During our analysis, it was first considered appropriate for these markers to be compared to ILC2 in the lung by comparing MFI. However, the resulting data highlighted bimodal distribution of ICOS by ILC2 in the neonatal thymus prompting us to consider whether MFI is an appropriate method of analysis for this marker.

In the context of our investigation, MFI was used to compare the intensity of fluorescence of KLRG-1, ICOS and ST2 on the surface of ILC2 in the neonatal thymus with those found in the lung. In principal, the greater the expression of these markers on the cell surface, then the amount of antibody binding, and thus fluorescence, will be greater. Therefore, observing the shift in MFI could provide insight on the positive expression by ILC2 in the lung and neonatal thymus. However, this method of analysis is only appropriate when analysing normally distributed data. This is not true of ICOS expression by ILC2 in the neonatal thymus where two distinct populations are identified, adding limited value to our interpretation. Future analysis of this data would seek to present this data as a dot plot where the proportions and total number of the two populations could be quantified.

While there were some limitations to our method of analysis, it was still possible to identify ICOS and ST2 expression amongst the ILC2 population. ILC2 are frequently associated with ICOS, which belongs to the CD28 superfamily, where it has been shown to regulate effector T cell function and also influence humoral immunity.(172) Furthermore, it has been demonstrated in the lung and intestine that ICOS signalling in mice regulates homeostasis independently of T and B cells in a manner that promotes proliferation and accumulation of mature ILC2.(172) Additionally, ICOS has been implicated in ILC2 activation and eosinophil infiltration in the lung in a model of

IL-33 airway inflammation.(172) Together, this evidence highlights a role for ICOS in controlling the ILC2 pool. Unlike secondary lymphoid sites in the periphery, the thymus does not have a role in the initiation of the adaptive immune response and ILC2 in this tissue are not required to control effector CD4<sup>+</sup> T cell populations. However, it is quite possible that ILC2 have a function in maintaining tissue homeostasis in this tissue. Finally, our data demonstrated thymic ILC2 to express some level of ST2. Given that ST2 is a receptor for IL-33, a cytokine of the IL-1 superfamily, it is plausible to suggest that these cells respond to IL-33, which initiates the signalling cascade for IL-5 and IL-13 production.(172) This will be investigated further in the proceeding chapter.

Collectively, these data strengthen our knowledge of ILC composition within the thymus across ontogeny. Whilst previous studies have supported the role of ILC3 within the embryonic and adult thymus, our work was the first to demonstrate the composition of ILC to alter from the embryonic stages through to adult. Furthermore, little work had been performed previously to characterise ILC2 within this tissue. Using a range of *in vivo* models, we describe an increase in ILC2 during development that is maintained in the adult thymus. Continuing with the use of robust *in vivo* models, the subsequent body of work will focus on exploring the function of these cells in the neonatal and adult thymus. Furthermore, thymus tissue will be used to investigate the location of these cells using immunofluorescence microscopy.

## **CHAPTER 4: INVESTIGATING THE FUNCTION OF**

### **THYMIC ILC**



## 4.1 Introduction

Our findings within Chapter 3 add significant knowledge to the field of ILC biology with regard to their presence within the thymus. While the function of these cells has been well defined at peripheral sites, our understanding of the role of these cells within the thymus is limited. As such, the overall aim of this chapter sought to identify the function of ILCs within the thymus.

Current research surrounding the role of ILCs within the thymus has predominantly focussed on the presence of ILC3 and their associated function while the function of other ILC subsets within this tissue are less well known. LT<sub>i</sub> cells, of the ILC3 family, are of particular interest and have been described within both embryonic and adult thymus.(98,100) While the age of the thymus may differ within these studies, the role of LT<sub>i</sub> cells within this tissue is somewhat similar where they have been implicated in the establishment of the thymic microenvironment.(98,100)

Beginning with the adult thymus, work published by Dudakov *et al.* (2012) suggested a role for LT<sub>i</sub> cells, defined as ROR $\gamma$ <sup>+</sup> CCR6<sup>+</sup> NKp46<sup>+</sup> ILC3, in regeneration of the thymus following injury. It was shown that the depletion of CD4<sup>+</sup> CD8<sup>+</sup> double-positive (DP) thymocytes initiated the production of IL-23 by thymic dendritic cells (tDCs).(100) Subsequent binding of IL-23 to the IL-23 receptor (IL-23R) present on LT<sub>i</sub> cells stimulated the upregulation of IL-22 from these cells which had beneficial effects on the thymic microenvironment.(100) Thymic epithelial cells (TECs) responded to IL-22, which promoted their proliferation and enhanced their survival. Furthermore, LT<sub>i</sub> cells were shown to up regulate their expression of the IL-23R in response to injury and thus strengthen their ability to act within this signalling cascade.(100) Overall, the endogenous production of IL-22 by LT<sub>i</sub> cells was defined

as fundamental in the recovery of thymopoiesis and ultimate restoration of the thymic tissue.(100)

The conclusions founded by Dudakov *et al.* (2012) were summative of a number of key investigations performed within their research group.(100) While similar quantities of IL-22 were produced within the thymus of untreated WT and *Rorc*<sup>-/-</sup> mice, the production of IL-22 in the WT thymus significantly increased compared with the *Rorc*<sup>-/-</sup> thymus 3 days post sub-lethal irradiation (SLI). Moreover, an increase in the proportion of IL-22<sup>+</sup> ILC within the WT thymus was observed following lethal total body irradiation (L-TBI). Interestingly, Dudakov *et al.* (2012) identified near 80 000 LTi cells within the WT thymus in the steady state, with half of these cells still present following three days recovery post-irradiation. These numbers differ from our findings presented within Chapter 3, however an alternative gating strategy was used within this study compared to that established within our research group.

Additional investigations by Dudakov *et al.* (2012) sought to determine the trigger for IL-22 production. These investigations identified an increase in IL-22 production by LTi cells as a result of blocking T cell development at the DP thymocyte stage using Dexamethasone.(100) Furthermore, the addition of exogenous murine IL-22 was shown to enhance thymopoiesis by improving the viability of TECs and promoting their proliferation.(100) More recently, the depletion of thymic ILC3 in a model of Graft versus Host Disease (GvHD) resulted in impaired recovery of the thymus due to a deficiency in intrathymic IL-22.(100,101) As such, it was inferred that endogenous IL-22 production by LTi cells influenced thymic regeneration in a similar manner. While the data presented in these investigations provide logical evidence for the presence of ILC3 within the adult thymus, discrepancies remain between this

work and that described in Chapter 3. Therefore, this chapter looked to characterise ILC populations within the adult thymus in response to thymic injury.

In addition to the presence of LT<sub>i</sub> cells within the adult thymus, these cells are described within the embryonic thymus where they have been implicated in the development of a functional thymic medulla. Early investigations by Rossi *et al.* (2007) utilised FTOCs at embryonic stages E14 and E16 and identified CD4<sup>+</sup> CD3<sup>-</sup> LT<sub>i</sub> cells by flow cytometry. Moreover, these cells were present at a time that correlates with the appearance of Aire<sup>+</sup> CD80<sup>+</sup> mTECs, suggesting LT<sub>i</sub> cells may have a role in their maturation from Aire<sup>-</sup> CD80<sup>-</sup> mTECs. These findings were consistent with confocal imaging, which identified LT<sub>i</sub> cells to be in close association to Aire<sup>+</sup> mTECs.(98)

Strikingly, Rossi *et al.* (2007) identified LT<sub>i</sub> cells within the adult thymus of Rag1<sup>-/-</sup> where they were phenotypically identical to LT<sub>i</sub> cells found at peripheral sites. Furthermore, assessment by flow cytometry of LT<sub>i</sub> cells isolated from the adult thymus revealed the expression of the TNF ligands OX40L and CD30L, as well as RANKL and IL-7R $\alpha$ . RANK, along with CD40 and lymphotoxin- $\beta$  receptor, regulate the development and function of mTECs through NF- $\kappa$ B signalling as demonstrated in mice deficient in RelB, Traf6 and NF- $\kappa$ B inducing kinase (Nik) which exhibited abnormalities within the medulla.(99)

Given the capability of LT<sub>i</sub> cells to express RANKL, it was anticipated that RANK-RANKL interactions in the embryonic thymus were responsible for mTEC development and this was later confirmed using *in vitro* and *in vivo* methods.(98) However, more recent studies have demonstrated normal medullary formation occurs

in *Rorc*<sup>-/-</sup> mice, which lack LTi cells. Moreover, Aire<sup>+</sup> mTECs were shown to exist in the thymus of these mice, albeit reduced in number.(173)  $\alpha\beta$ <sup>+</sup> T cells did not account for the emergence of of Aire<sup>+</sup> mTECs in the thymus of *Rorc*<sup>-/-</sup> given the existence of mature mTECs prior to  $\alpha\beta$  T cell selection.(99) It was later discovered that V $\gamma$ 5<sup>+</sup> dendritic epidermal T cells (DETC) were a source of RANKL within the embryonic thymus. As such, it was concluded that the development of the first cohort of Aire<sup>+</sup> mTECs at E16 was a result of RANK-RANKL interactions where RANKL was jointly provided by LTi cells and DETCs.(99)

The evidence reviewed so far has focussed solely on the role of ILC3 within the thymus. This is due, in part, to limited discussion in the literature of other ILC subsets within this thymus. Recently published data from our laboratory characterised other ILC subsets within the thymus and identified ILC2 to be present within the neonatal and adult thymus.(129) Other studies have also described ILC2 within the adult thymus where they are thought to have a thymic origin. However, the function of cells in this context is yet to be understood.(103,104)

Collectively, this chapter sought to review the functions of ILC3 and investigate the potential roles of ILC2 within the thymus. While T cells are considered to be the likely source of RANKL post birth, we hypothesised that ILC3 are capable of expressing RANKL in neonatal thymus prior to their decline. Furthermore, ILC3 have been reported to be a key provider of IL-22 in the thymus following injury. Together, these data implicate ILC3 in the maintenance of microenvironments that support central tolerance in the embryonic thymus and repair of this tissue in the adult, however the role of other ILC subsets following birth is largely unknown. As such, we wanted to better understand the function of ILC populations in the thymus in the context of

homeostasis, and as a way of testing this, their involvement in thymic repair following damage. Therefore, we hypothesise that ILC have a role in tissue repair following damage to the thymic microenvironment.

To address this hypothesis, we had 2 distinct aims:

1. Examine the effects of sub-lethal irradiation on ILC populations within the thymus
2. Investigate the potential functions of ILC within the thymus

## **4.2 Results**

### **4.2.1 Early evidence suggests recovery of the thymus is impaired in the absence of ROR $\gamma$ t following injury**

As previously stated, published data has predominantly focused on the function of LT $\alpha$ i cells within the thymus, while other subsets have been overlooked (98,100,101). Concerning the adult thymus, one study describes a model of thymic regeneration driven by endogenous effects of IL-22 following thymic injury.(100) Within this proposal, LT $\alpha$ i cells, defined as ROR $\gamma$ t<sup>+</sup> CCR6<sup>+</sup> NKp46<sup>+</sup> ILC3, were identified as a key provider of IL-22 in response to depletion of CD4<sup>+</sup> CD8<sup>+</sup> DP thymocytes.(100) This data contradicts our findings within chapter 3 where very few ILC3 were identified within the thymus. Moreover, the very few ILC3 that do exist are lost following a short period of neonatal development.(129) One possibility is the expansion of ILC3 in response to damage leading to the increased production of IL-22 by these cells. As such, we sought to investigate these claims within our laboratory and test the requirement for ILC3 in the regeneration of the thymus following damage.

To investigate this, adult WT and *Rorc*<sup>-/-</sup> mice were sub-lethally irradiated and the total cellularity of the thymus was assessed following 7 or 14 days recovery. The thymus of non-irradiated WT and *Rorc*<sup>-/-</sup> mice was used for controls (Figure 4.1A). It was anticipated that thymic recovery would be impaired in *Rorc*<sup>-/-</sup> mice given the requirement of ROR $\gamma$ t in LT $\alpha$ i cell development.(143,153) Within the literature, the production of IL-22 within the thymus has been shown to be significantly reduced in thymus of *Rorc*<sup>-/-</sup> mice compared to a WT thymus following sub-lethal irradiation.(100) However, this data did not attribute IL-22 production directly to LT $\alpha$ i cells. Therefore, it is possible the reduction in IL-22 observed here is due to the absence of other ROR $\gamma$ t-dependent lymphocytes that are also capable of producing IL-22, such as T-helper 17 (Th17) cells.(100,174)

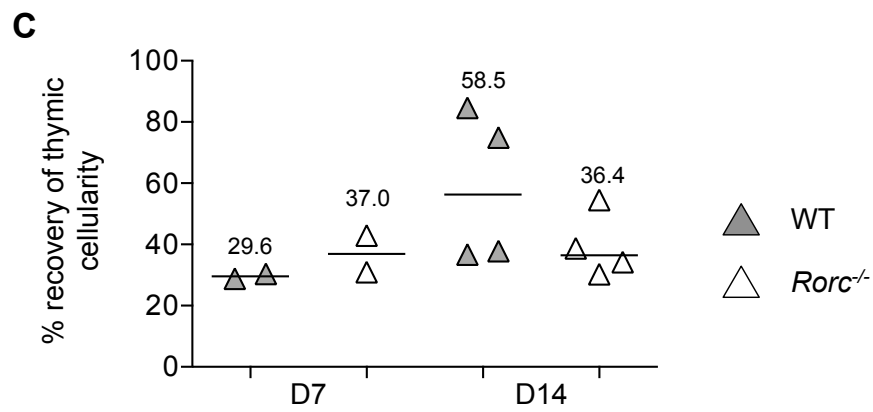
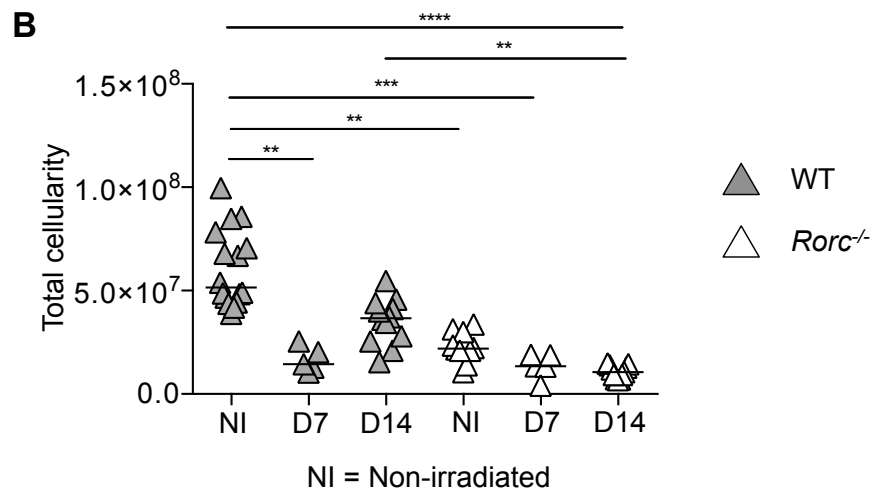
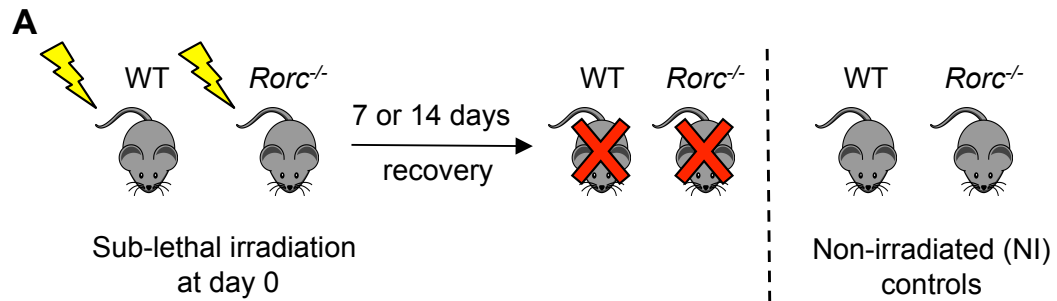
To confirm the impact of irradiation on the thymus, the depletion of thymocytes was assessed by comparing the total cellularity of the thymus of non-irradiated WT and *Rorc*<sup>-/-</sup> mice with the thymus of sub-lethally irradiated WT and *Rorc*<sup>-/-</sup> mice following either 7 or 14 days recovery (Figure 4.1B). In non-irradiated mice, the total thymic cellularity in WT mice was significantly greater than the total thymic cellularity of *Rorc*<sup>-/-</sup> mice (Figure 4.1B). Comparison across WT mice demonstrated a reduction in cellularity 7 days after sub-lethal irradiation, which recovered by day 14 (Figure 4.1B). While no significant changes were observed across *Rorc*<sup>-/-</sup> mice, there was a reduction in the median cellularity at day 7 and 14 after sub-lethal irradiation compared to non-irradiated mice (Figure 4.1B). While this early evidence suggests the recovery of the thymus in *Rorc*<sup>-/-</sup> may be impaired, further investigations following longer periods of recovery are required.

#### Figure 4.1 Recovery of thymus tissue following sub-lethal irradiation is impaired in mice lacking ILC3

To determine whether recovery of total thymic cellularity would be impaired in mice lacking *Rorc*<sup>-/-</sup>, adult WT and *Rorc*<sup>-/-</sup> mice were sub-lethally irradiated and total cellularity of the thymus was assessed following 7 or 14 days recovery. Where possible, WT littermates were matched with *Rorc*<sup>-/-</sup> littermates for age and sex. All cells were analysed using flow cytometry and total numbers calculated per whole thymus. Data shown in grey and white corresponds to WT and *Rorc*<sup>-/-</sup> mice, respectively.

- A) Illustration of the experimental model used. WT and *Rorc*<sup>-/-</sup> mice were sub-lethally irradiated at baseline (day 0) and allowed to recover for either 7 (D7) or 14 (D14) days. Sub-lethally irradiated mice were culled at either day 7 or day 14 and cells isolated from the thymus were used for analysis. Thymus tissue from sub-lethally irradiated mice was compared to the thymus of non-irradiated controls.
- B) Enumeration of total thymic cellularity in non-irradiated, and sub-lethally irradiated WT and *Rorc*<sup>-/-</sup> mice following 7 or 14 days recovery.
- C) Percentage thymic recovery at day 7 and 14 following sub-lethal irradiation. Thymic recovery determined by comparing the mean thymic cellularity of sub-lethally irradiated mice as a proportion of the mean thymic cellularity of non-irradiated mice of the same strain within the same experiment.

Kruskal-Wallis one-way ANOVA with post hoc Dunn's test was used (comparing three or more data sets) for statistical analysis where \*p<0.05, \*\*p<0.01, \*\*\*p<0.001, and \*\*\*\*p<0.0001. In all graphs the bar represents the median. For experiments involving 7 days recovery, n=6 (non-irradiated) and n=5 (irradiated) for WT and n= 4 (non-irradiated) and n=5 (irradiated) for *Rorc*<sup>-/-</sup> with data shown from two independent experiments. For experiments involving 14 days recovery, n=10 (non-irradiated) and n=12 (irradiated) for WT and n= 6 (non-irradiated) and n=11 (irradiated) for *Rorc*<sup>-/-</sup> with data shown from four independent experiments.





Our ability to repeat these experiments with later time points was hindered by the reduced survival rates amongst *Rorc*<sup>-/-</sup> as a result of increased incidence of thymoma and reduced immune competence. Therefore, we sought an additional method to analyse our existing data to determine whether recovery of the thymus was impaired in mice lacking *Rorc*. To achieve this, the percentage thymic recovery was defined by calculating the mean thymic cellularity of the sub-lethally irradiated mice as a proportion of the mean thymic cellularity of non-irradiated mice within each experiment (Figure 4.1C). This was calculated across both WT and *Rorc*<sup>-/-</sup> mice at day 7 and day 14 following sub-lethal irradiation. From these data, the median percentage recovery of thymic cellularity 7 days after sub-lethal irradiation is lower in WT mice compared to *Rorc*<sup>-/-</sup> (Figure 4.1C). However, fewer cells are present in the thymus of non-irradiated *Rorc*<sup>-/-</sup> mice compared to the thymus of non-irradiated WT mice. Therefore, the expansion of cells in a *Rorc*<sup>-/-</sup> mouse would lead to a greater percentage recovery than would be observed if there were an increase in the same number of cells within the WT thymus. Analysis of thymic recovery 14 days after sub-lethal irradiation shows the median percentage recovery for WT mice is greater than the value shown for *Rorc*<sup>-/-</sup> mice at this time (Figure 4.1C). Moreover, the median percentage recovery of thymic cellularity for *Rorc*<sup>-/-</sup> mice is similar at day 14 to the value shown at day 7; indicating there may be some impairment in the recovery of the thymus of *Rorc*<sup>-/-</sup> mice.

Overall, these data suggest the recovery of thymus may be impaired in *Rorc*<sup>-/-</sup> mice compared to WT mice following sub-lethal irradiation. While statistical analysis in Figure 4.1C identified no significant differences across results, this may be due to the limited data points in this data comparison. Furthermore, only a short period of

recovery was investigated. While longer periods of recovery were attempted, these were halted due to the reduced survival amongst *Rorc*<sup>-/-</sup> mice as a result of increased thymoma incidence.

#### **4.2.2 ILC3 are not involved in thymic regeneration following thymic damage**

Data described within the literature pre-empted DP thymocyte depletion as trigger for IL-22 production by LT<sub>i</sub> cells.(100) Dudakov *et al.* (2012) proposed the production of IL-23 by thymic dendritic cells (DCs) was triggered by the depletion or absence of DP thymocytes. Furthermore, the binding of this IL-23 to the IL-23 receptor (IL-23R) on the surface of LT<sub>i</sub> cells stimulated their production of IL-22, which acted upon medullary thymic epithelial cells (mTEC). This proposal indicated the up regulation of IL-23R by LT<sub>i</sub> cells in response to thymic injury would enhance the binding capacity of these cells for IL-23 and, ultimately, increase the production of IL-22 in response. In turn, IL-22 acts on mTECs and leads to their enhanced proliferation and survival. It is hypothesised that it is this series of events which leads to restoration of the thymic microenvironment and recovery of the DP thymocyte pool.(100)

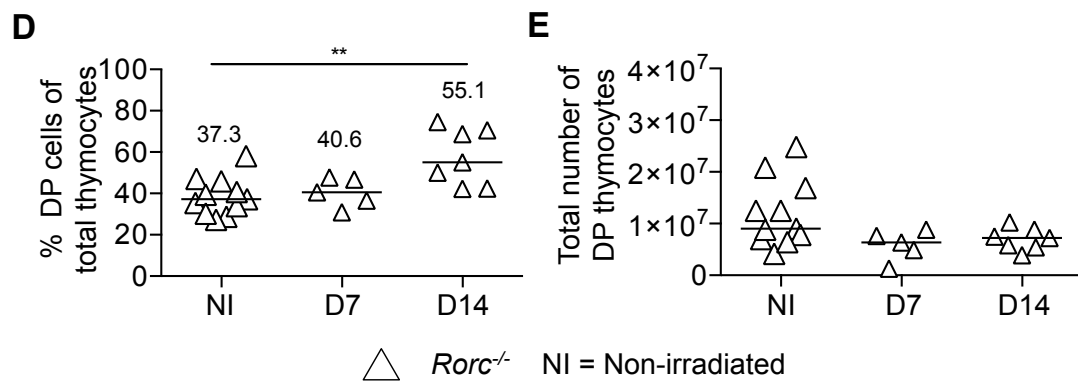
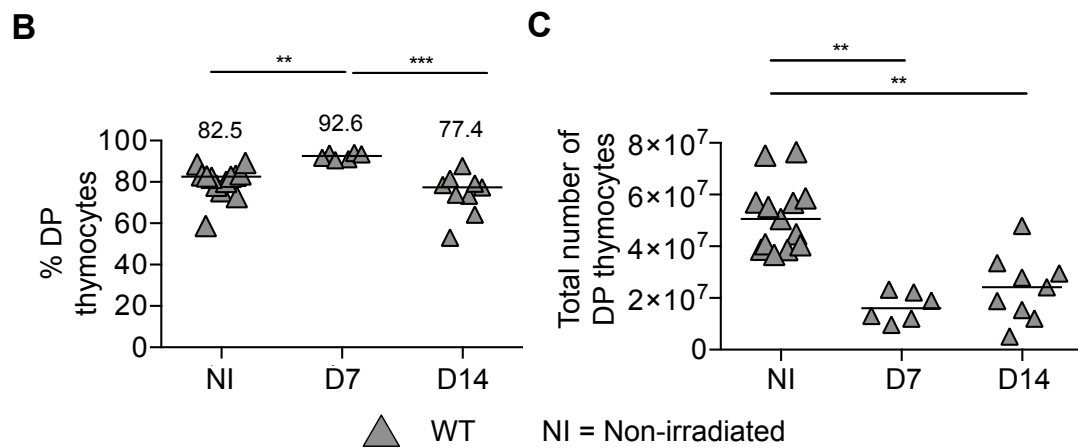
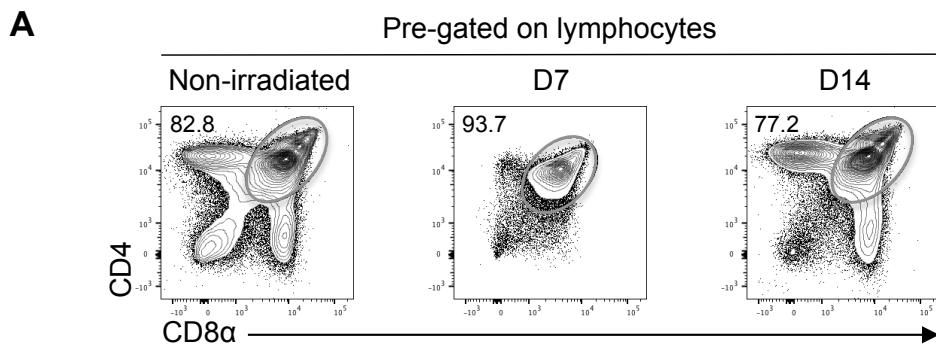
Given that DP thymocytes are described as the trigger for thymic regeneration, it was important to determine the effect of sub-lethal irradiation on DP thymocytes in our experimental model. This required investigation of the proportion and total number of DP thymocyte populations in the thymus of non-irradiated WT and *Rorc*<sup>-/-</sup> mice with sub-lethally irradiated mice following 7 or 14 days recovery (Figure 4.2). Representative flow cytometry plots displaying DP thymocyte populations, defined as CD4<sup>+</sup> CD8<sup>+</sup>, demonstrate a distinct population of these cells in both non-irradiated and sub-lethally irradiated WT mice (Figure 4.2A). Comparison of DP thymocytes in

#### Figure 4.2 Double-positive thymocytes are depleted following sub-lethal irradiation

To determine whether sub-lethal irradiation affected DP thymocytes, these cells were quantified in the thymus of non-irradiated WT and *Rorc*<sup>-/-</sup> mice and to mice that have been sub-lethally irradiated followed by 7 or 14 days recovery. All cells were analysed using flow cytometry and total numbers calculated per whole thymus. Data shown in grey and white corresponds to WT and *Rorc*<sup>-/-</sup> mice, respectively.

- A) Representative flow cytometry plots of CD4<sup>+</sup> CD8<sup>+</sup> (double-positive) thymocytes in non-irradiated, and sub-lethally irradiated WT mice following 7 (D7) or 14 (D14) days recovery.
- B) Proportion of double-positive (DP) thymocytes amongst total cells in the thymus of non-irradiated, and sub-lethally irradiated WT mice following 7 or 14 days recovery.
- C) Enumeration of DP thymocytes amongst total cells in the thymus of non-irradiated, and sub-lethally WT irradiated mice following 7 or 14 days recovery.
- D) Proportion of DP thymocytes amongst total cells in the thymus of non-irradiated, and sub-lethally irradiated *Rorc*<sup>-/-</sup> mice following 7 or 14 days recovery.
- E) Enumeration of DP thymocytes amongst total cells in the thymus of non-irradiated, and sub-lethally *Rorc*<sup>-/-</sup> irradiated mice following 7 or 14 days recovery.

Kruskal-Wallis one-way ANOVA with post hoc Dunn's test was used (comparing three or more data sets) for statistical analysis where \*p<0.05, \*\*p<0.01, \*\*\*p<0.001, and \*\*\*\*p<0.0001. In all graphs the bar represents the median. For experiments involving 7 days recovery, n=6 (non-irradiated) and n=6 (irradiated) for WT and n= 4 (non-irradiated) and n=5 (irradiated) for *Rorc*<sup>-/-</sup> with data shown from two independent experiments. For experiments involving 14 days recovery, n=7 (non-irradiated) and n=9 (irradiated) for WT and n= 4 (non-irradiated) and n=7 (irradiated) for *Rorc*<sup>-/-</sup> with data shown from three independent experiments.



the WT thymus across independent experiments demonstrated the proportion of CD4<sup>+</sup> CD8<sup>+</sup> cells to be greater at day 7 following sub-lethal irradiation compared to both non-irradiated mice and sub-lethally irradiated mice following 14 days recovery (Figure 4.2B). However, subsequent analysis of total DP thymocyte number identified a significant reduction in the number of these cells at both 7 and 14 days following sub-lethal irradiation when compared to a non-irradiated thymus in WT mice (Figure 4.2C). Thus, confirming DP thymocytes are successfully depleted in our model of sub-lethal irradiation in WT mice.

Our initial investigations aimed to determine whether thymic recovery in *Rorc*<sup>-/-</sup> mice was impaired compared to WT mice. In addition to ILC3, ROR $\gamma$ t is critical for the development of the Th17 effector T cell lineage, which are also a source of IL-22.(175,176) As such, it was appropriate to also assess DP thymocyte populations in the thymus of *Rorc*<sup>-/-</sup> mice and investigate the effect of sub-lethal irradiation on these cells. However, this is met with additional challenges given the critical involvement of ROR $\gamma$ t in thymocyte development and enhanced survival.(176) Furthermore, severe immunodeficiency is associated in mice due to mutations in their *Rorc* gene.(120,175,176)

Comparison of the proportion of DP thymocytes in both non-irradiated and sub-lethally irradiated *Rorc*<sup>-/-</sup> mice following 7 or 14 days recovery identified a significant increase in the proportion of these cells after 14 days recovery compared to the non-irradiated thymus, suggesting the expansion of these cells or loss of other cells during this time (Figure 4.2D). Comparison of total DP thymus, however, demonstrated no significant difference in the number of cells following sub-lethal irradiation at either day 7 or 14 recovery compared to the non-irradiated thymus

(Figure 4.2E). Furthermore, both the proportion and total number of DP thymocytes is lower in cells isolated from the thymus of *Rorc*<sup>-/-</sup> mice compared to those from the thymus of WT mice in both non-irradiated and sub-lethally irradiated following both 7 and 14 days recovery (Figure 4.2B-E). Therefore the effect of irradiation on DP thymocytes is less clear given that there are fewer of these cells to start with in the *Rorc*<sup>-/-</sup> thymus.

Based on previous findings, the depletion of DP thymocytes within our model of thymic injury is thought to trigger the production of IL-22 by LT $\alpha$ i cells.(100) However, we have not yet characterised ILC3 within the thymus of mice following sub-lethal irradiation. To overcome this, we characterised ILC3 populations within the adult thymus using our functional model of sub-lethal irradiation whilst incorporating markers of ILC2, which we have previously demonstrated to be the most abundant ILC population within the adult thymus.

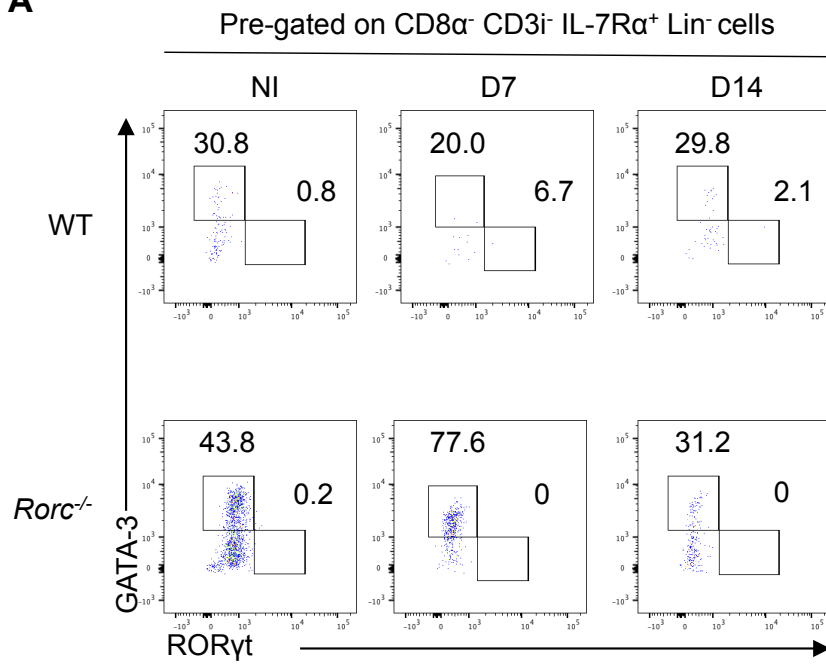
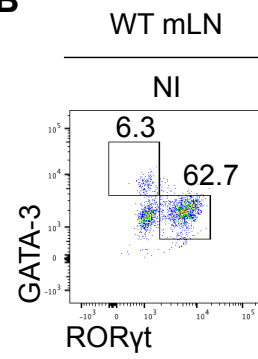
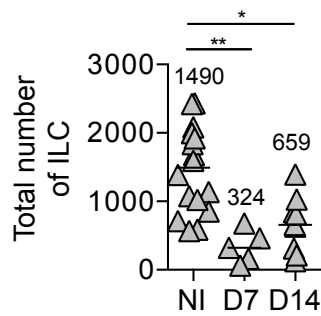
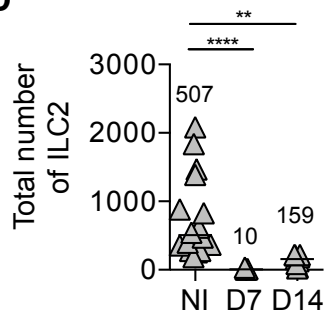
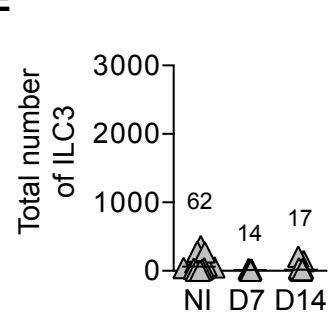
The total number of ILC, and indeed ILC2, are greater in the thymus of *Rorc*<sup>-/-</sup> mice, as described previously in Figure 3.11. As such, the flow cytometry gate for ILC2 was set using cells from the non-irradiated *Rorc*<sup>-/-</sup> thymus where these cells are easily identified (Figure 4.3A). Furthermore, ILC3 are absent in the thymus of *Rorc*<sup>-/-</sup> mice and cells isolated from this tissue were used to set the flow cytometry gate for ILC3 (Figure 4.3A). These gates were applied to all other samples for consistent analysis (Figure 4.3A). Representative flow cytometry plots for cells isolated from the thymus of non-irradiated and sub-lethally irradiated mice following 7 or 14 days recovery is shown in the upper panel (Figure 4.3A). Representative flow cytometry plots for the corresponding time points in *Rorc*<sup>-/-</sup> mice is shown in the lower panel (Figure 4.3A).

**Figure 4.3 ILC populations within the thymus of WT and *Rorc*<sup>-/-</sup> mice are depleted following sub-lethal irradiation**

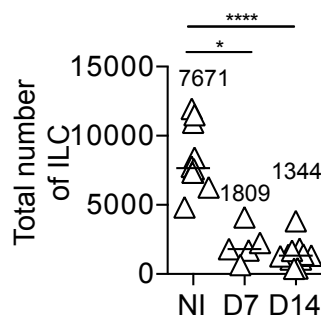
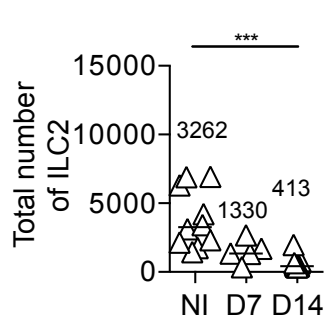
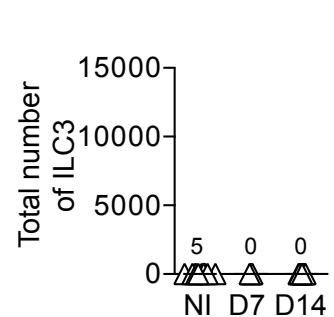
To determine the effect of sub-lethal irradiation on ILCs within the adult thymus, ILC3 were characterised following sub-lethal irradiation whilst incorporating markers of ILC2, which we have previously demonstrated to be the main ILC population within the adult thymus. All cells were analysed using flow cytometry and total numbers calculated per whole thymus. Data shown in grey and white corresponds to WT and *Rorc*<sup>-/-</sup> mice, respectively.

- A) Representative FACS plots of ILC2 (GATA-3<sup>+</sup>) and ILC3 (RORγt<sup>+</sup>) in the adult thymus of non-irradiated (NI), and irradiated mice following 7 (D7) or 14 (D14) days recovery in WT (upper panel) and *Rorc*<sup>-/-</sup> (lower panel) mice. Cells were pre-gated on CD8α<sup>-</sup> CD3i<sup>-</sup> IL-7Rα<sup>+</sup> Lineage<sup>-</sup> (Lin<sup>-</sup>) cells. Lineage channel consists of antibodies against CD3, CD5, CD11b, CD11c and B220.
- B) Representative FACS plot for the identification of cells isolated from the non-irradiated mLN of a WT mouse. Cells were pre-gated on CD8α<sup>-</sup> CD3i<sup>-</sup> IL-7Rα<sup>+</sup> Lineage<sup>-</sup> (Lin<sup>-</sup>) cells. Lineage channel consists of antibodies against CD3, CD5, CD11b, CD11c and B220.
- C) Enumeration of total ILC (identified as CD8<sup>-</sup> CD3i<sup>-</sup> IL-7Rα<sup>+</sup> Lin<sup>-</sup> cells) in the WT thymus of non-irradiated (NI), and irradiated mice following 7 or 14 days recovery.
- D) Enumeration of ILC2 (identified as CD8<sup>-</sup> CD3i<sup>-</sup> IL-7Rα<sup>+</sup> Lin<sup>-</sup> GATA-3<sup>+</sup> cells) in the WT thymus of non-irradiated (NI), and irradiated mice following 7 or 14 days recovery.
- E) Enumeration of ILC3 (identified as CD8<sup>-</sup> CD3i<sup>-</sup> IL-7Rα<sup>+</sup> Lin<sup>-</sup> RORγt<sup>+</sup> cells) in the WT thymus of non-irradiated (NI), and irradiated mice following 7 or 14 days recovery.
- F) Enumeration of total ILC (identified as CD8<sup>-</sup> CD3i<sup>-</sup> IL-7Rα<sup>+</sup> Lin<sup>-</sup> cells) in the *Rorc*<sup>-/-</sup> thymus of non-irradiated (NI), and irradiated mice following 7 or 14 days recovery.
- G) Enumeration of ILC2 (identified as CD8<sup>-</sup> CD3i<sup>-</sup> IL-7Rα<sup>+</sup> Lin<sup>-</sup> GATA-3<sup>+</sup> cells) in the *Rorc*<sup>-/-</sup> thymus of non-irradiated (NI), and irradiated mice following 7 or 14 days recovery.
- H) Enumeration of ILC3 (identified as CD8<sup>-</sup> CD3i<sup>-</sup> IL-7Rα<sup>+</sup> Lin<sup>-</sup> RORγt<sup>+</sup> cells) in the *Rorc*<sup>-/-</sup> thymus of non-irradiated (NI), and irradiated mice following 7 or 14 days recovery.

Kruskal-Wallis one-way ANOVA with post hoc Dunn's test was used (comparing three or more data sets) for statistical analysis where \*p<0.05, \*\*p<0.01, \*\*\*p<0.001, and \*\*\*\*p<0.0001. In all graphs the bar represents the median. For experiments involving 7 days recovery, n=6 (non-irradiated) and n=5 (irradiated) for WT and n= 4 (non-irradiated) and n=5 (irradiated) for *Rorc*<sup>-/-</sup> with data shown from two independent experiments. For experiments involving 14 days recovery, n=10 (non-irradiated) and n=9 (irradiated) for WT and n= 6 (non-irradiated) and n=11 (irradiated) for *Rorc*<sup>-/-</sup> with data shown from four independent experiments.

**A****B****C****D****E**

▲ WT NI = Non-irradiated

**F****G****H**

△ *Rorc*<sup>-/-</sup> NI = Non-irradiated



Much like our earlier work, cells isolated from the mLN of a non-irradiated WT mouse were used as a positive control for the identification of ILC3 (Figure 4.3B).

Enumeration of total ILC (identified as CD8 $\alpha$ <sup>-</sup> CD3 $\gamma$ <sup>-</sup> IL-7R $\alpha$ <sup>+</sup> Lin<sup>-</sup>) demonstrated a depletion in these cells at day 7 following sub-lethal irradiation. Furthermore, the number of total ILC was not fully recovered at day 14 (Figure 4.3C). ILC2 and ILC3 were identified amongst total ILC by their expression of GATA-3 and ROR $\gamma$ t, respectively, and the total number of these cells was calculated (Figure 4.3D-E). A significant reduction in the total number of ILC2 in the WT thymus at day 7 and 14 following sub-lethal irradiation was observed (Figure 4.3D). No significant reduction in ILC3 was identified within the thymus of non-irradiated and sub-lethally irradiated. However, this is due to very few ILC3 to be present within the non-irradiated thymus and these low numbers persist after sub-lethal irradiation. Previously, a population of ~80 000 LT $\alpha$ i cells were described within the adult thymus of WT mice in the steady state. Despite a reduction following irradiation, ~40 000 of radio-resistant cells have been thought to persist.(100) Overall, our data argues against these findings, demonstrating very few ILC3 are present within the thymus of an adult WT mouse with the low numbers of these cells persisting following sub-lethal irradiation.

Consistent with our earlier experiments, the number of total ILC and ILC2 within the non-irradiated *Rorc*<sup>-/-</sup> is raised in comparison to a WT thymus (Figure 4.3C, D, F and G). Moreover, a significant reduction in total ILC is observed at day 7 following sub-lethal irradiation in the *Rorc*<sup>-/-</sup> thymus (Figure 4.3F). Much like our observations in the WT thymus, the number of total ILC in the *Rorc*<sup>-/-</sup> was not recovered at day 14 (Figure 4.3F). These findings are also true when comparing the number of ILC2

where a reduction in the number of these cells is observed at day 7 and 14 following sub-lethal irradiation in comparison to non-irradiated mice (Figure 4.3G). ILC3 were expected to be non-existent in the thymus of non-irradiated and sub-lethally irradiated *Rorc*<sup>-/-</sup> mice, given the requirement for ROR $\gamma$ t in their development.(143) However, a median of 5 for total ILC3 was observed in the non-irradiated thymus of *Rorc*<sup>-/-</sup> mice (Figure 4.3H). Given that the *Rorc*<sup>-/-</sup> mice are genotyped prior to their use, it is unlikely for these cells to be true. Instead, the presence of background noise within the flow cytometer could be one explanation for their presence. Overall, these data demonstrate ILC populations within the thymus to be depleted within our model of sub-lethal irradiation. Interestingly, the depletion of ILC3 demonstrated these cells not to be radio-resistant as previously described.

The data described in Figure 4.2 demonstrates the depletion of DP thymocytes in the WT thymus as a result of sub-lethal irradiation. Previously published work has reported the production of IL-22 by LTi cells as a result of DP depletion. Within this proposed mechanism, depletion of DP thymocytes initiates the release of IL-23 from thymic DCs and binds to the IL-23R on LTi cells and stimulates the production of IL-22 from these cells (100). However, data shown in Figure 4.3 demonstrates very few LTi cells to be present in the non-irradiated thymus of WT mice and maintained following sub-lethal irradiation. As such, there is no evidence of the enrichment or expansion of these cells following sub-lethal irradiation. Therefore arguing against a role for LTi cells in regeneration of the thymus following damage.

Despite these findings, we sought to determine whether LTi cells were capable of producing IL-22 in the thymus of non-irradiated and sub-lethally irradiated mice. Given the differences observed between our work and the data of that previously

published, we looked back at the primary article to aid direct comparison of the data. Within the literature, cells were identified as CD45<sup>+</sup> IL-7R $\alpha$ <sup>+</sup> CD3<sup>-</sup> CD8<sup>-</sup> IL-22<sup>+</sup> ROR $\gamma$ t<sup>+</sup>, which varies from the strategy established within our laboratory. Furthermore, radio-resistant LT<sub>i</sub> cells were identified following 3 days recovery after irradiation. Whilst total thymic cellularity was shown to be at its lowest at this time point, the frequency of LT<sub>i</sub> cells per 10<sup>7</sup> cells was shown to increase. Thus, we anticipated that LT<sub>i</sub> cells, if present, would be easier to identify under these conditions.

The sparsity of ILC3 in the thymus, inclusive of LT<sub>i</sub> cells, is evident throughout our studies. Therefore, cells isolated from the mLN of WT mice were included as a positive control to provide confidence in our flow cytometry gating. Overall, this model assessed tissue from WT mice three days after sub-lethal irradiation. As with our earlier investigations, cells isolated from sub-lethally irradiated mice were compared to cells isolated from non-irradiated controls. All cells underwent *ex vivo* culture with for a total of 4 hours to stimulate the production of IL-22. IL-1 $\beta$ , IL-2, IL-6, IL-23, PMA and Ionomycin were added at 0 hours while BFA was added after 1 hour.

At this point in our investigations, methods established within our laboratory were limited by the ability to identify cells by their cytokine expression or transcription factor expression only, but not a combination of both. Therefore, we identified LT<sub>i</sub> cells within the thymus based on their expression of CCR6 in the absence of ROR $\gamma$ t<sup>+</sup>. ILC3 can be subdivided into two main subsets based on their expression of the natural cytotoxicity receptor (NCR), NKp46. While it is acknowledged that both NKp46<sup>+</sup> and NKp46<sup>-</sup> ILC3 are capable of providing IL-22, only LT<sub>i</sub> cells express

CCR6<sup>+</sup> IL-22<sup>+</sup> LTi cells using CCR6 is appropriate strategy in the absence of RORγt<sup>+</sup> cells.

This method enabled the identification of IL-22<sup>-</sup> and IL-22<sup>+</sup> LTi cells within the non-irradiated mLN and was defined as live IL-7Rα<sup>+</sup> CD45<sup>+</sup> CD3<sup>-</sup> CD8α<sup>-</sup> CCR6<sup>+</sup> IL-22<sup>+/-</sup> cells (Figure 4.4A; upper panel). While LTi cells could be identified using this gating strategy, demonstrated by their expression of CCR6, only a small proportion of these cells were shown to produce IL-22 (Figure 4.4A; upper panel). This gating strategy was applied to cells isolated from the mLN of sub-lethally irradiated mice following 3 days recovery (Figure 4.4A; lower panel). Whilst it was still possible to identify CCR6<sup>+</sup> LTi cells in these mice, the proportion of CCR6<sup>+</sup> IL-22<sup>-</sup> cells was greatly reduced with CCR6<sup>+</sup> IL-22<sup>+</sup> near absent (Figure 4.3A; lower panel).

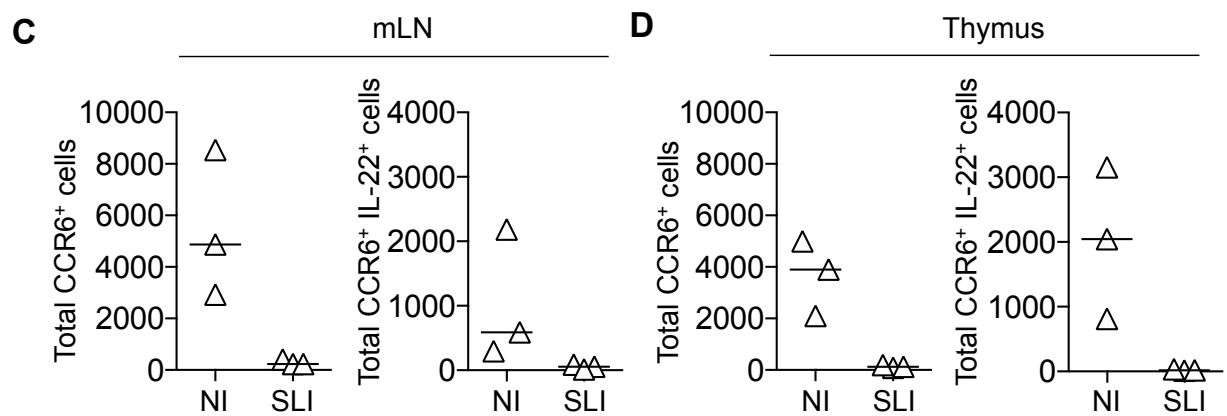
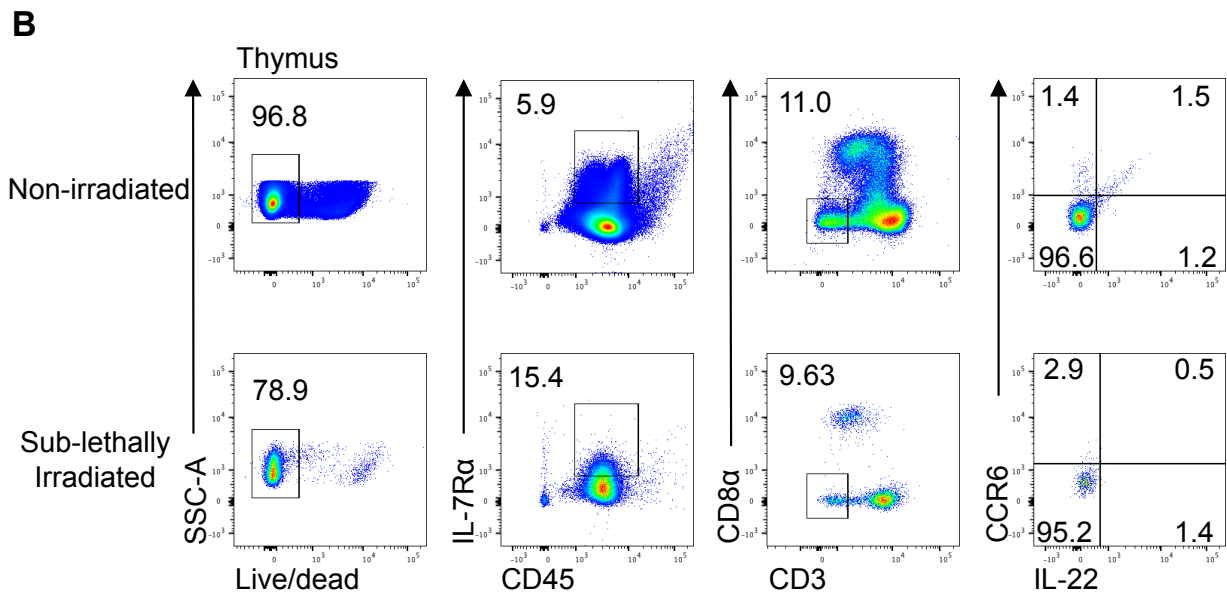
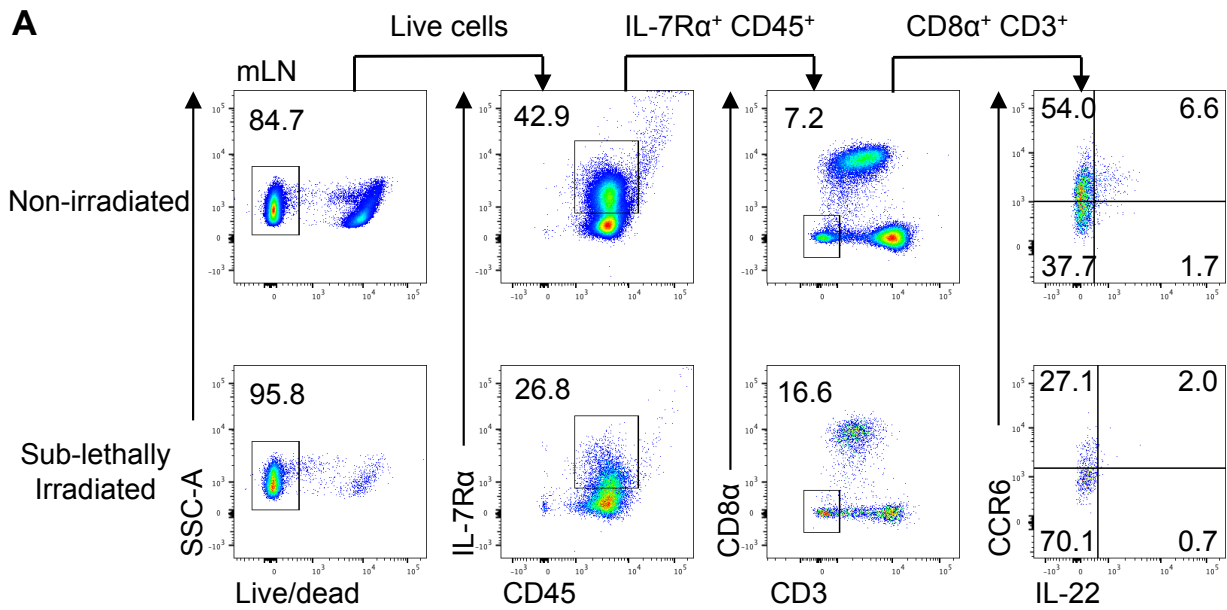
The gating strategy in Figure 4.4A was applied to cells isolated from the thymus of non-irradiated and sub-lethally irradiated WT mice following 3 days recovery to characterise IL-22-producing LTi cells in this tissue (Figure 4.4B). Whilst live IL-7Rα<sup>+</sup> CD45<sup>+</sup> CD3<sup>-</sup> CD8<sup>-</sup> cells could be identified in the non-irradiated thymus, the staining of CCR6 and IL-22 is less convincing and representative of all samples (Figure 4.4B; upper panel). Furthermore, application of this gating strategy to cells isolated from sub-lethally irradiated mice following 3 days recovery demonstrated few CCR6<sup>+</sup> cells to be present (Figure 4.4B). Enumeration of CCR6<sup>+</sup> and CCR6<sup>+</sup> IL-22<sup>+</sup> cells identified their presence in the mLN of a non-irradiated mouse but numbers of these were depleted following sub-lethal irradiation (Figure 4.4C). The total number of CCR6<sup>+</sup> cells present in the thymus of non-irradiated mice was comparable to those present in the mLN. Although approximately half of CCR6<sup>+</sup> cells were shown to express IL-22

**Figure 4.4 Assessment of IL-22 production by ILC3 in the adult thymus following sub-lethal irradiation using an alternative gating strategy**

To assess the production of IL-22 by LT $\alpha$ i cells in the thymus, cells isolated from the adult WT thymus were assessed for IL-22 production following *ex-vivo* culture while adapting our gating strategy to match that of previously published work. All cells were analysed using flow cytometry and total numbers calculated per whole thymus.

- A) Representative flow cytometry plots for the identification of IL-22-producing ILC3, defined as live CD45<sup>+</sup> IL-7R $\alpha$ <sup>+</sup> CD8 $\alpha$ <sup>+</sup> CD3<sup>i</sup> CCR6<sup>+</sup> IL-22<sup>+</sup> cells, in the mLN of a non-irradiated (upper panel), and sub-lethally irradiated (lower panel) WT mice following 3 days recovery.
- B) Representative flow cytometry plots for the identification of IL-22-producing ILC3, defined as live CD45<sup>+</sup> IL-7R $\alpha$ <sup>+</sup> CD8 $\alpha$ <sup>+</sup> CD3<sup>i</sup> CCR6<sup>+</sup> IL-22<sup>+</sup> cells, in the thymus of a non-irradiated (upper panel), and sub-lethally irradiated (lower panel) WT mice following 3 days recovery.
- C) Enumeration of CCR6<sup>+</sup> and CCR6<sup>+</sup> IL-22<sup>+</sup> amongst total ILC, defined as as live CD45<sup>+</sup> IL-7R $\alpha$ <sup>+</sup> CD8 $\alpha$ <sup>+</sup> CD3<sup>i</sup> cells, in the mLN of non-irradiated, and sub-lethally irradiated WT mice following 3 days recovery.
- D) Enumeration of CCR6<sup>+</sup> and CCR6<sup>+</sup> IL-22<sup>+</sup> amongst total ILC, defined as as live CD45<sup>+</sup> IL-7R $\alpha$ <sup>+</sup> CD8 $\alpha$ <sup>+</sup> CD3<sup>i</sup> cells, in the thymus of non-irradiated, and sub-lethally irradiated WT mice following 3 days recovery.

Mann-Whitney U (non-parametric, two-tailed) test was used for statistical analysis where \*p<0.05, \*\*p<0.01, \*\*\*p<0.001, and \*\*\*\*p<0.0001. In all graphs the bar represents the median, n=3. Data shown from one independent experiment.



NI = Non-irradiated

SLI = Sub-lethally irradiated

in the non-irradiated thymus, the primary data, shown in the flow cytometry plots, was unconvincing (Figure 4.4D).

In summary, the data described within this section of work is consistent with our observations in chapter 3. Very few ILC3 were detected within the adult thymus of both non-irradiated and sub-lethally irradiated mice following various lengths of recovery. Our model of sub-lethal irradiation successfully depleted DP thymocytes but additionally depleted the few ILC3 that were also present, arguing against the radio-resistance of these cells. Interestingly, IL-22 production by LT<sub>i</sub> in the mLN was not increased in response to sub-lethal irradiation. However, it was not possible to comment on the effect of sub-lethal irradiation on IL-22 production by LT<sub>i</sub> cells in the thymus given the unconvincing antibody staining shown in our data. Nonetheless, it is not unreasonable to suggest a similar effect in the thymus given the reduction in LT<sub>i</sub> cells following sub-lethal irradiation; however, repeat analysis is required to provide evidence of this.

#### **4.2.3 LT<sub>i</sub> cells of the neonatal thymus are capable of producing IL-22**

The data described thus far argues against the production of IL-22 by LT<sub>i</sub> cells being critical for thymic recovery since very few of these cells exist and the total number of LT<sub>i</sub> cells does not increase in response to sub-lethal irradiation. Our previous findings have demonstrated ILC3 to be present in greater numbers within the embryonic and neonatal thymus until numbers of these cells decline at two weeks post-birth onwards. Moreover, earlier research by others has demonstrated LT<sub>i</sub> cells have the capability of producing important signals within the thymic microenvironment while more recent studies have demonstrated their role in providing IL-22 in the periphery (98,177,178). Combining these findings, we sought to determine whether neonatal

ILC3, which were detectable within the neonatal thymus, to be capable of producing IL-22.

To approach this, cells were isolated from the thymus of WT neonatal mice at day 7 and day 14 post-birth and stimulated with IL-1 $\beta$ , IL-2, IL-6, IL-23, PMA, Ionomycin and BFA in an *ex vivo* culture. Given our understanding of the few ILC3 present in this tissue compared to the periphery, cells isolated from the mLN of an adult WT mouse were used to provide confidence when positioning the flow cytometry gates. Using the cells isolated from the adult mLN, a population of IL-22 producing ILC3, defined as live CD45<sup>+</sup> CD8 $\alpha$ <sup>-</sup> CD3<sup>-</sup> IL-7R $\alpha$ <sup>+</sup> ROR $\gamma$ t<sup>+</sup> IL-22<sup>+</sup> cells, were identified (Figure 4.5A; upper panel). This gating strategy was applied to cells isolated from the neonatal thymus at day 7 post-birth (Figure 4.5A; lower panel). This strategy was successful in identifying IL-22-producing ILC3 in the thymus at this stage of neonatal development and is representative of all samples.

Further analysis applied this gating strategy to cells isolated from the neonatal thymus at day 14 to determine whether ILC3 at stage in development demonstrated the same capability (Figure 4.5B). In comparison to cells at day 7, flow cytometry identified fewer IL-22<sup>+</sup> ILC3 were present at day 14 (Figure 4.5B). For all samples, the position of the IL-22<sup>+</sup> ROR $\gamma$ t<sup>+</sup> gate was confirmed using an unstimulated control using cells isolated from the neonatal thymus (Figure 4.5C). In this sample, cells were cultured in an *ex vivo* culture for the same duration as all other samples but excluded the addition of IL-1 $\beta$ , IL-2, IL-6, IL-23, PMA and Ionomycin. Enumeration of proportion and total number of IL-22<sup>+</sup> ILC3 at day 7 and 14 of neonatal development revealed a reduction in these cells by day 14 (Figure 4.5D). However, given the limited availability of neonatal mice at these ages there are an insufficient number of

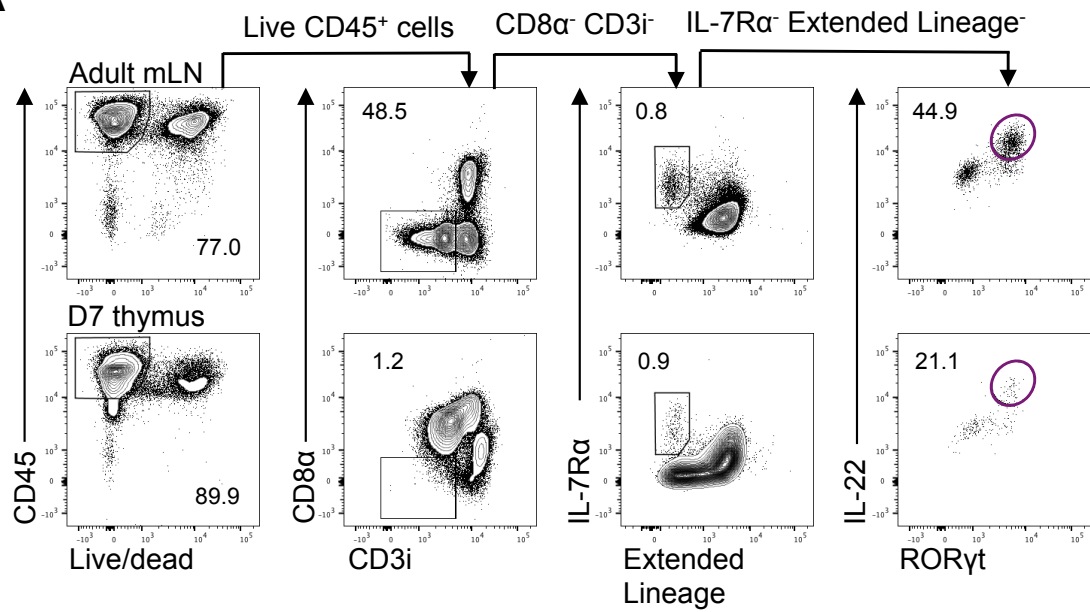
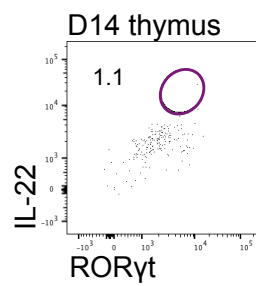
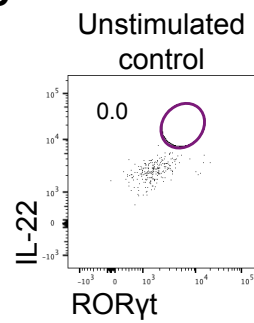
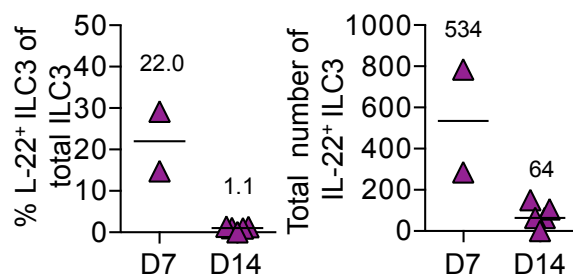


**Figure 4.5 ILC3 isolated from the neonatal thymus are capable of producing IL-22 following *ex vivo* stimulation at 7 days post-birth**

The ability of ILC3 within the neonatal thymus to provide IL-22 was assessed following *ex vivo* culture. Data shown in purple corresponds to ILC3. Cells isolated from the mLN of an adult WT mouse were used as a positive control. All cells were analysed using flow cytometry and total numbers calculated per whole thymus.

- A) Representative flow cytometry plots for the identification of IL-22 producing ILC3, defined as live CD45<sup>+</sup> CD8α<sup>-</sup> CD3i<sup>-</sup> IL-7Rα<sup>+</sup> Extended Lineage<sup>-</sup> IL-22<sup>+</sup> RORγt<sup>+</sup> cells, in the adult mLN (upper panel) and neonatal thymus (lower panel) at day 7 post-birth following *ex vivo* stimulation. Cells isolated from the adult mLN were used as a positive control. Extended lineage channel consisted of antibodies against B220, CD3, CD5, CD11b, CD11c, CD19, CD49b, CD123, F4/80, FcεR1, Gr-1, and Ter119.
- B) Representative flow cytometry plot for the identification of IL-22 producing ILC3 in the neonatal thymus at day 14 post-birth following *ex vivo* stimulation.
- C) Representative flow cytometry plot for the identification of IL-22 producing ILC3 in an unstimulated control using cells isolated from a neonatal thymus at day 14 post-birth following *ex vivo* culture with BFA only.
- D) Proportion and total number of ILC3, defined as live CD45<sup>+</sup> CD8α<sup>-</sup> CD3i<sup>-</sup> IL-7Rα<sup>+</sup> Extended Lineage<sup>-</sup> RORγt<sup>+</sup>, expressing IL-22 in the neonatal thymus at day 7 and 14 post-birth.

Mann-Whitney U (non-parametric, two-tailed) test was used for statistical analysis where \*p<0.05, \*\*p<0.01, \*\*\*p<0.001, and \*\*\*\*p<0.0001. In all graphs the bar represents the median, n=2 and n=5 for day 7 and day 14 post-birth, respectively. Data shown from one independent experiment.

**A****B****C****D**

samples for statistical analysis. In addition, these results are representative of one independent experiment and would require repeating before valid conclusions could be made.

#### **4.2.4 ILC3 is a source of RANKL within the neonatal thymus**

The development and maturation of the thymic epithelial compartment is modulated by several factors that act by regulating the NF- $\kappa$ B pathway.(35,179,180) Signalling through this pathway is mediated by four receptors of the Tumour Necrosis Factor (TNF) family, of which Receptor activator of NF- $\kappa$ B (RANK) is one, along with osteoprotegerin (OPG), CD40 and lymphotoxin- $\beta$  receptor.(35,179,180) Action through these receptors, along with cross talk between thymocytes and TECs, modulates the development of the thymic microenvironment.(35,179,180) There are multiple sources of RANKL within the thymus that has been shown to alter throughout ontogeny. Within the embryonic thymus this signal is provided by LT $\alpha$ i cells and V $\alpha$ 5<sup>+</sup> invariant dendritic epidermal T cell (DETC) progenitors, which contributes to the establishment of central tolerance through maturation of Aire<sup>-</sup> mTECs to Aire<sup>+</sup> mTECs.(98,179) Moreover, LT $\alpha$ i cells of the adult thymus have been shown to increase RANKL expression in response to total body irradiation.(100) While T cells are considered to be the likely source of RANKL post birth, we wanted to identify whether ILC3 are able to express RANKL in neonatal thymus prior to their decline.

To determine whether ILC3 are able to express RANKL in the neonatal thymus, cells were isolated from the thymus of neonatal mice 14 days post-birth and cultured overnight under *ex vivo* conditions with no additional stimulants. Cells isolated from the adult mLN were used as a positive control and were subject to the same conditions as those isolated from the thymus. Representative flow cytometry plots for

cells isolated from the adult mLN are shown in Figure 4.6A (upper panel) and populations of ILC2 and ILC3 were identified as live CD8 $\alpha$ <sup>-</sup> CD3<sup>-</sup> IL-7R $\alpha$ <sup>+</sup> Lin<sup>-</sup> GATA-3<sup>+</sup> (ILC2) and ROR $\gamma$ t<sup>+</sup> (ILC3). This gating strategy was applied to cells isolated from the neonatal thymus and proportions of ILC2 and ILC3 consistent with previous data were identified by their expression of GATA-3 and ROR $\gamma$ t<sup>+</sup>, respectively (Figure 4.6A; lower panel).

Subsequent analysis investigated the expression of RANKL by ILC3 in the adult mLN (Figure 4.6B). As shown, ILC3 in the adult mLN were used as a positive control and demonstrated expression of RANKL by these cells (Figure 4.6B). Moreover, an additional control using a streptavidin-conjugate in the absence of biotin was used as a negative control (Figure 4.6C). The absence of RANKL expression in Figure 4.6C argues the expression of RANKL by ILC3 in Figure 4.6 B is true and not reflective of the secondary reagent binding to cells. The RANKL<sup>+</sup> gate shown in Figure 4.6B and C was applied to cells isolated from the neonatal thymus and demonstrated little expression of RANKL by ILC2 (Figure 4.6D) but clear expression of RANKL by ILC3 (Figure 4.6E). Enumeration of the proportion and total number of RANKL<sup>+</sup> ILC2 and ILC3 demonstrates more than half of ILC3 in the neonatal thymus were capable of providing RANKL (Figure 4.6F). Furthermore, the total number of ILC3 expressing RANKL was significantly higher than that of ILC2, where little RANKL expression was observed (Figure 4.6F). Thus, RANKL expression by ILC persists after birth but it is restricted to the ILC3 subset.

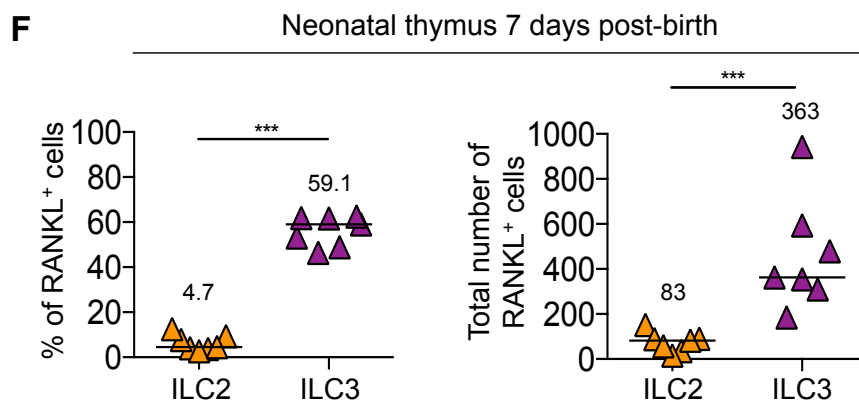
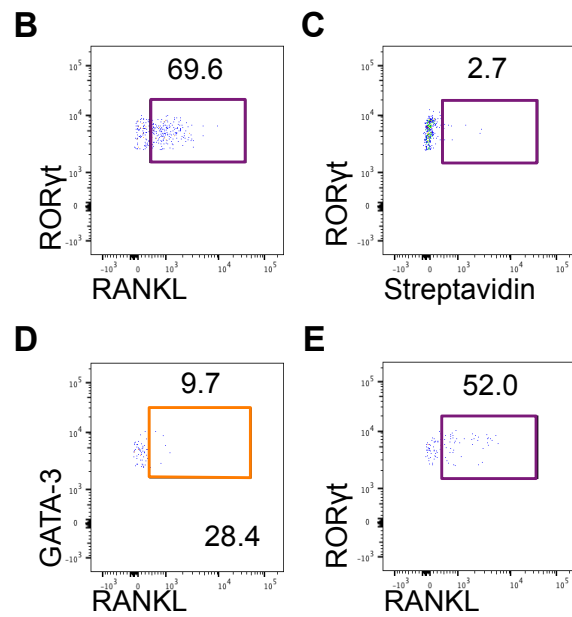
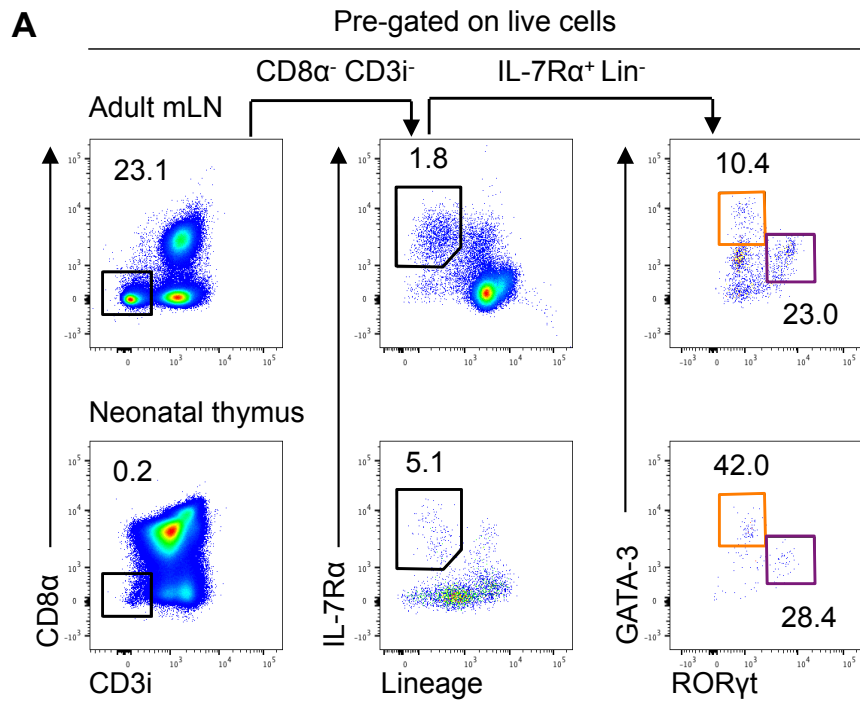
Our earlier data demonstrated expansion of ILC2 in the thymus of *Rorc*<sup>-/-</sup> mice, which lack ILC3. We next investigated whether absence of ILC3 would alter the function of ILC2. To investigate this, we compared the expression of RANKL by ILC2 in the

#### Figure 4.6 ILC3 are a source of RANKL in the neonatal thymus

To add to our knowledge of the function of ILC post-birth, cells isolated from the thymus of WT neonatal mice 7 days post-birth were cultured ex vivo and assessed for their expression of RANKL. Samples were cultured in duplicate wells and pooled for analysis. All cells were analysed using flow cytometry and total numbers calculated per whole thymus. Data shown in orange and purple corresponds to ILC2 and ILC3, respectively.

- A) Gating strategy used for the identification of ILC2, defined as  $CD8^- CD3i^- IL-7R\alpha^+ Lin^- GATA-3^+$  cells, and ILC3, defined as  $CD8^- CD3i^- IL-7R\alpha^+ Lin^- ROR\gamma t^+$  cells, in the mLN (upper panel) and neonatal thymus (lower panel) of WT mice. Lineage channel consists of antibodies against CD3, CD5, CD11b, CD11c and B220.
- B) Representative FACS plot showing RANKL expression by ILC3 ( $ROR\gamma t^+$ ) in the adult mLN.
- C) Representative FACS plot showing RANKL expression by ILC3 in the adult mLN in a streptavidin only control in the absence of biotin.
- D) Representative FACS plot showing RANKL expression by ILC2 ( $GATA-3^+$ ) in the neonatal thymus.
- E) Representative FACS plot showing RANKL expression by ILC3 ( $ROR\gamma t^+$ ) in the neonatal thymus.
- F) Proportion and total number of ILC2 and ILC3 expressing RANKL in the neonatal thymus.

Mann-Whitney U (non-parametric, two-tailed) test was used for statistical analysis where  $*p<0.05$ ,  $**p<0.01$ ,  $***p<0.001$ , and  $****p<0.0001$ . In all graphs the bar represents the median,  $n=7$ . Data shown from two independent experiments.



neonatal thymus of WT and *Rorc*<sup>-/-</sup> mice following an overnight *ex vivo* culture in the absence of additional stimulants. As with earlier investigations, cells isolated from the mLN of a WT adult mouse were used for positive and streptavidin only controls. Representative flow cytometry plots displaying the identification of RANKL by ILC2 in the neonatal thymus of WT (upper panel) mice and *Rorc*<sup>-/-</sup> (lower panel) mice are shown in Figure 4.7A. ILC2 populations were pre-gated on CD8α<sup>-</sup> CD3i<sup>-</sup> IL-7Rα<sup>+</sup> Lin<sup>-</sup> cells, as demonstrated in Figure 4.5A. RANKL expression was successfully identified in cells isolated from the mLN of a WT mouse (Figure 4.7B) while no RANKL expression was observed in the streptavidin only control (Figure 4.7C). Enumeration of the proportion and total number of RANKL<sup>+</sup> ILC2 demonstrated a significant increase in RANKL expression in *Rorc*<sup>-/-</sup> mice, demonstrating the provision of RANKL by ILC2 when the thymic microenvironment is perturbed.(129)

#### **4.2.5 ILC2 are capable of producing IL-5 following *ex vivo* culture**

The abundance of ILC2 within the adult thymus is a consistent finding and is demonstrated by data both throughout chapter 3 and chapter 4 so far. However, little is known about the function of these cells within the thymus. To determine whether ILC2 within the adult thymus were capable of producing cytokines associated with ILC2 function, ILC2 isolated from the thymus of TCRα<sup>-/-</sup> mice were cultured *ex vivo* and the expression of IL-5 and IL-13 was assessed. Characterisation of ILC populations by flow cytometry in chapter 3 (Figure 3.16) confirmed the majority of ILC in the TCRα<sup>-/-</sup> to be ILC2. Thus, normal development of the thymic medulla, which is impaired in the absence of CD4 single-positive (SP) T cells, is not required for the predominance of ILC2 amongst ILC populations within the thymus.(129) Moreover, a greater number of ILC2 are present in the thymus of TCRα<sup>-/-</sup> mice when compared to

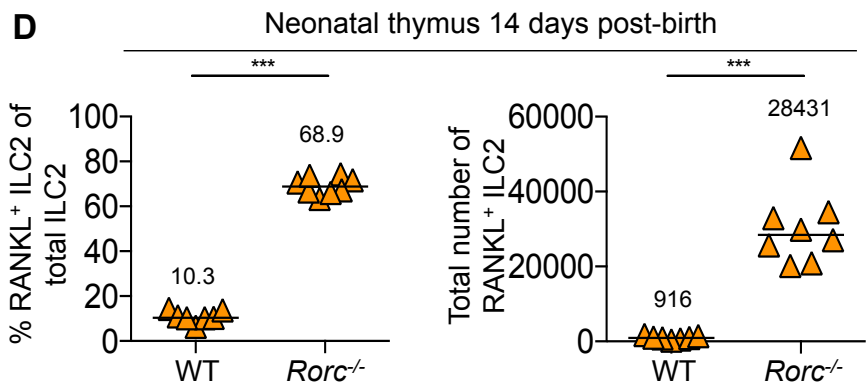
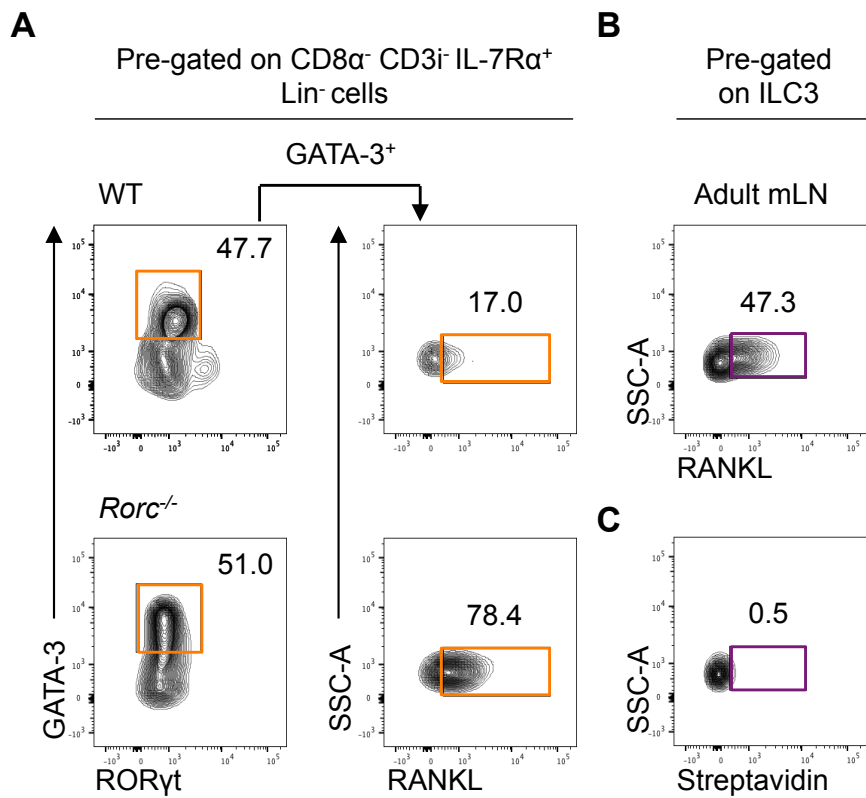
#### **Figure 4.7 RANKL expression by ILC2 is elevated in the thymus of *Rorc*<sup>-/-</sup> mice**

To investigate whether RANKL production by ILC2 changes in the absence of ILC3, cells isolated from thymus of neonatal WT and *Rorc*<sup>-/-</sup> 14 days post-birth were cultured *ex vivo* and their expression of RANKL was assessed. Samples were cultured in duplicate wells and pooled for analysis. All cells were analysed using flow cytometry and total numbers calculated per whole thymus. Data shown in orange and purple corresponds to ILC2 and ILC3, respectively.

- A) Representative flow cytometry plots for the identification RANKL expression by ILC2 (identified as CD8<sup>-</sup> CD3<sup>-</sup> IL-7R $\alpha$ <sup>+</sup> Lin<sup>-</sup> GATA-3<sup>+</sup> RANKL<sup>+</sup> cells) in the neonatal thymus of WT (upper panel) and *Rorc*<sup>-/-</sup> (lower panel) mice. Lineage channel consists of antibodies against CD3, CD5, CD11b, CD11c and B220.
- B) Representative flow cytometry plot for the identification of RANKL expression by ILC3 in the adult mLN.
- C) Representative flow cytometry plot for the identification of RANKL by ILC3 in the adult mLN of a streptavidin only control in the absence of biotin.
- D) Proportion and total number of ILC2 (GATA-3<sup>+</sup>) expressing RANKL in the neonatal thymus of WT and *Rorc*<sup>-/-</sup> mice.

Mann-Whitney U (non-parametric, two-tailed) test was used for statistical analysis where \*p<0.05, \*\*p<0.01, \*\*\*p<0.001, and \*\*\*\*p<0.0001. In all graphs the bar represents the median, n=8. Data shown from one independent experiment.





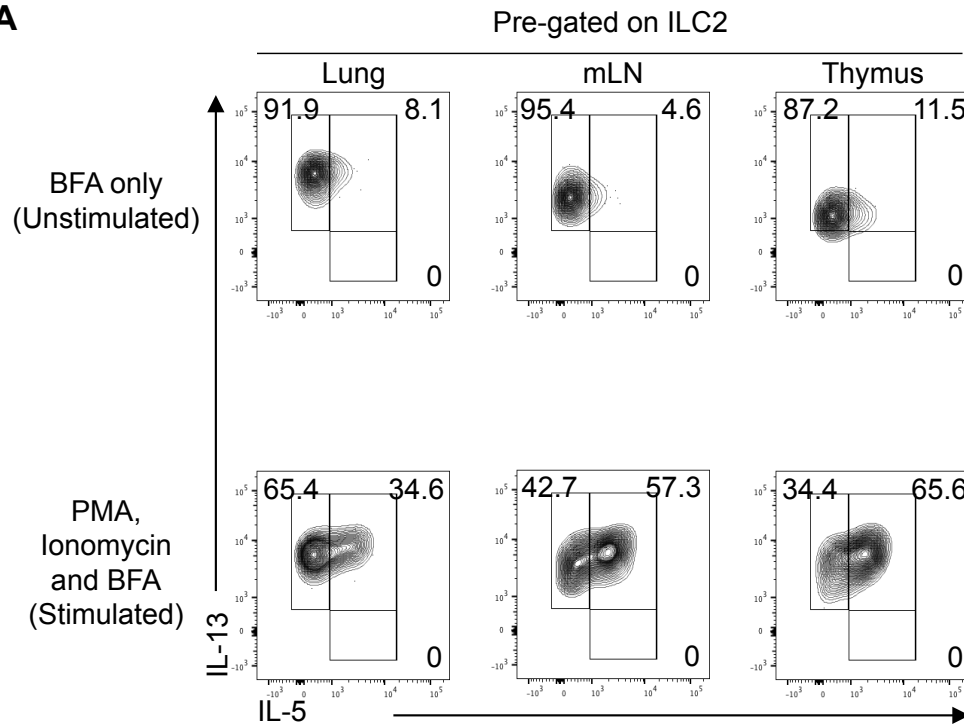
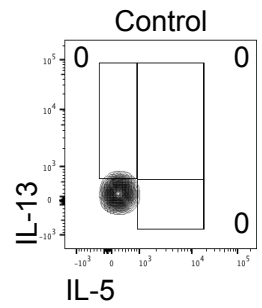
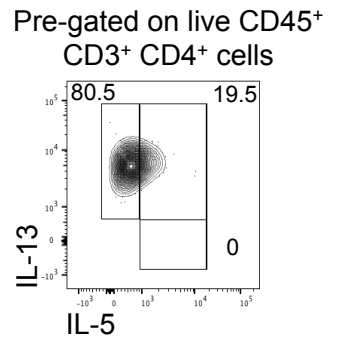
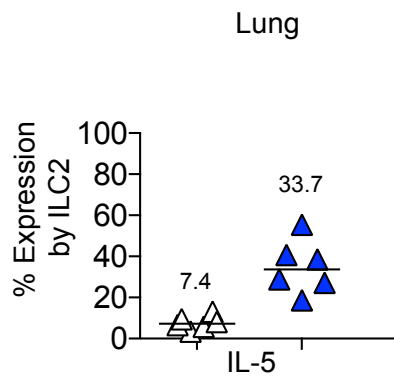
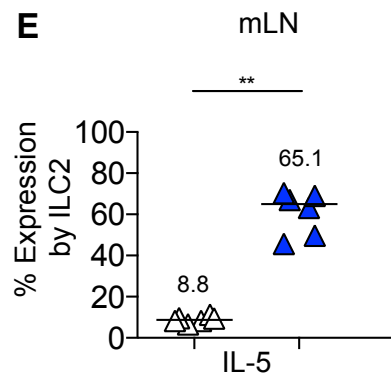
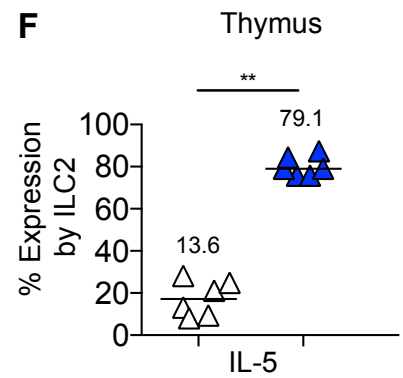
the WT. Furthermore, experience within the laboratory has shown the number of viable cells to be reduced following cell culture. As such, analysis of ILC2 in the thymus of  $\text{TCR}\alpha^{-/-}$  mice would provide a sufficient number of cells for characterisation and enhance the sensitivity of our experiment. The variation in the expression of ILC2-associated cytokines across peripheral sites are well documented within the literature.(181–185) Therefore, cells isolated from the lung and mLN of  $\text{TCR}\alpha^{-/-}$  mice were included to control for the expression of IL-5 and IL-13. Furthermore, comparison of cytokine production following *ex vivo* culture with BFA only (unstimulated) was compared with cytokine production by cells following *ex vivo* culture with PMA, Ionomycin and BFA (stimulated). Representative flow cytometry plots cells for the expression of IL-5 and IL-13 by unstimulated (upper panel) and stimulated (lower panel) ILC2 isolated from the lung, mLN and thymus is shown in Figure 4.8A. While the majority of ILC2 in all three tissues expressed IL-13 following culture with BFA only, only a small proportion of these cells were shown to express IL-5 under these conditions (Figure 4.8A; upper panel). The expression of IL-5 by ILC2 appeared vastly increased following *ex vivo* stimulation (Figure 4.8A; lower panel). The position of flow cytometry gates for IL-5 and IL-13 were positioned using ILC2 of the  $\text{TCR}\alpha^{-/-}$  thymus in the absence of antibodies against IL-5 and IL-13 (Figure 4.8B). The discovery that ILC2 in all 3 tissues demonstrated constitutive expression of IL-13 was a surprising find. As such, we examined the expression of IL-5 and IL-13 by  $\text{CD45}^+ \text{CD3}^+ \text{CD4}^+$  cells to determine whether our IL-13 staining was true or an artefact of our experiment (Figure 4.8C). These data demonstrated 100% of  $\text{CD45}^+ \text{CD3}^+ \text{CD4}^+$  cells to express IL-13; indicating that this staining was an

**Figure 4.8 ILC2 from the thymus of TCR $\alpha$ <sup>-/-</sup> mice are capable of producing IL-5 following ex-vivo stimulation**

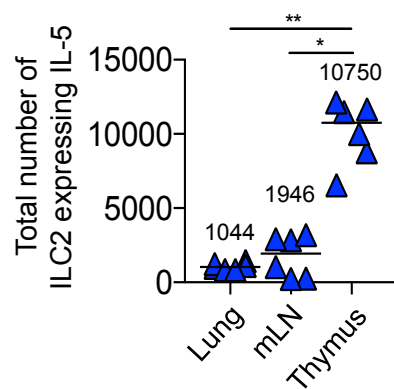
To determine whether ILC2 within the thymus were capable of producing cytokines associated with ILC2 function, ILC2 from the thymus of TCR $\alpha$ <sup>-/-</sup> mice were cultured *ex-vivo* and the expression of IL-5 and IL-13 was assessed. ILC2 isolated from the TCR $\alpha$ <sup>-/-</sup> lung and mLN are capable of producing IL-5 and IL-13 and were used as positive controls. ILC2 isolated from the TCR $\alpha$ <sup>-/-</sup> thymus, stimulated *ex-vivo* and analysed by flow cytometry in the absence of anti-IL-5 and anti-IL-13 antibodies were used as negative controls. All cells were analysed using flow cytometry and total numbers calculated per whole tissue. Data shown in white and blue corresponds to unstimulated and stimulated samples, respectively.

- A) Representative flow cytometry plots for IL-5 and IL-13 production by ILC2 in the lung, mLN and thymus of TCR $\alpha$ <sup>-/-</sup> mice following an *ex-vivo* culture with BFA only (unstimulated; upper panel) or BFA, PMA and Ionomycin (stimulated; lower panel).
- B) Flow cytometry plot demonstrating IL-5 and IL-13 expression in the thymus of a TCR $\alpha$ <sup>-/-</sup> mouse with anti-IL-5 and anti-IL-13 antibodies absent from the flow cytometry panel. The position of the IL-5 and IL-13 gates were set using the position of the negative population in this control.
- C) Representative flow cytometry plot for IL-5 and IL-13 production by live CD45<sup>+</sup> CD3<sup>+</sup> CD4<sup>+</sup> T cells in the mLN following *ex-vivo* culture with BFA only (unstimulated).
- D) Proportion of ILC2 in the lung of TCR $\alpha$ <sup>-/-</sup> mice expressing IL-5 following *ex-vivo* culture in unstimulated and stimulated samples. White and blue triangles correspond with unstimulated and stimulated samples, respectively.
- E) Proportion of ILC2 in the mLN of TCR $\alpha$ <sup>-/-</sup> mice expressing IL-5 following *ex-vivo* culture in unstimulated and stimulated samples. White and blue triangles correspond with unstimulated and stimulated samples, respectively.
- F) Proportion of ILC2 in the thymus of TCR $\alpha$ <sup>-/-</sup> mice expressing IL-5 following *ex-vivo* culture in unstimulated and stimulated samples. White and blue triangles correspond with unstimulated and stimulated samples, respectively.
- G) Enumeration of ILC2 capable of expressing IL-5 in the lung, mLN and thymus of TCR $\alpha$ <sup>-/-</sup> mice following *ex-vivo* stimulation.

Mann-Whitney U (non-parametric, two-tailed) test was used (comparing two data sets) and Kruskal-Wallis one-way ANOVA with post hoc Dunn's test was used (comparing three or more data sets) for statistical analysis where \*p<0.05, \*\*p<0.01, \*\*\*p<0.001, and \*\*\*\*p<0.0001. In all graphs the bar represents the median, n=6. Data shown from three independent experiments.

**A****B****C****D****E****F**

△ Unstimulated    ▲ Stimulated

**G**

artefact of our experiment. Therefore, quantification of IL-13 was excluded from subsequent analysis.

Comparison of the proportion of ILC2 expressing IL-5 in unstimulated and stimulated samples demonstrated no significant difference in the expression of IL-5 in the lung (Figure 4.8D). However, the proportion of ILC2 from the mLN and thymus expressing IL-5 was significantly increased following *ex vivo* stimulation (Figure 4.8E-F). Further analysis of the total number of ILC2 expressing IL-5 and following *ex vivo* stimulation revealed a greater number of these cells to be present within the thymus compared to the lung and mLN (Figure 4.8G).

Overall, these data demonstrate ILC2 isolated from the thymus of  $\text{TCR}\alpha^{-/-}$  mice to be capable of producing cytokines associated with the function of ILC2 at peripheral sites. However, further investigations are required to verify IL-13 production in this context.

#### **4.2.6 ILC2 reside in the thymic medulla**

So far, our data has predominantly focussed on the characterisation of ILC within the thymus and the signals they produce. As such, we sought to better understand the function of these cells by investigating their location within the thymus. The analysis of ILC in lymphoid tissue sections is challenging given the presence of T cells, which dominate the tissue and hinder the identification of other cell types (129). Therefore, we hypothesised ILC identification within the thymus would be easier in a  $\text{TCR}\alpha^{-/-}$  thymus where fewer T cells are present (129).

Given the abundance of ILC2 within the adult thymus, we aimed to determine the location of these cells by immunofluorescence. Using this technique, putative ILC2

(identified as CD3<sup>-</sup> IL-7Rα<sup>+</sup> GATA-3<sup>+</sup>) were found scattered within the medulla of the thymus (Figure 4.9A). Additional frozen sections of TCRα<sup>-/-</sup> thymus was assessed for the expression of ICOS; confirming these cells to be ILC2 (identified as CD3<sup>-</sup> IL-7Rα<sup>+</sup> ICOS<sup>+</sup>) (Figure 4.9B). Overall, the data shown in Figure 4.8 and Figure 4.9 demonstrate thymic ILC to be capable of producing signature cytokines associated with ILC2 while residing in the medulla of the thymus.

#### **4.2.7 ILC2 within the neonatal thymus share functional similarities to those isolated from adult tissue**

Our previous work assessed ILC2 cytokine production and the location of these cells in the thymus of TCRα<sup>-/-</sup>. Therefore, we wanted to confirm these observations in a WT thymus. To make this challenge technically easier, we chose to assess the neonatal thymus. While the number of ILC2 in the thymus of neonatal mice at day 14 is similar to the number present in the thymus of a WT adult, the total cellularity of the thymus within the neonate is much less. Therefore, the frequency of ILC amongst T cells is greater in the neonatal thymus and may be easier to identify.

From our earlier investigations, we demonstrated ILC2 isolated from the thymus of adult TCRα<sup>-/-</sup> mice to be capable of producing IL-5 following *ex vivo* stimulation. While our data concerning the production of IL-13 in these mice requires further validation in the adult thymus, we sought to determine whether ILC2 in the neonatal thymus of WT mice were capable of producing type-2 cytokines. To address this, cells isolated from the thymus of neonatal WT mice were stimulated *ex vivo* with PMA and Ionomycin in the presence of BFA. Cells isolated from the lung of an adult WT were used as a positive control for IL-5 and IL-13 expression by ILC2. Representative flow cytometry plots for the identification of IL-5 and IL-13 expression

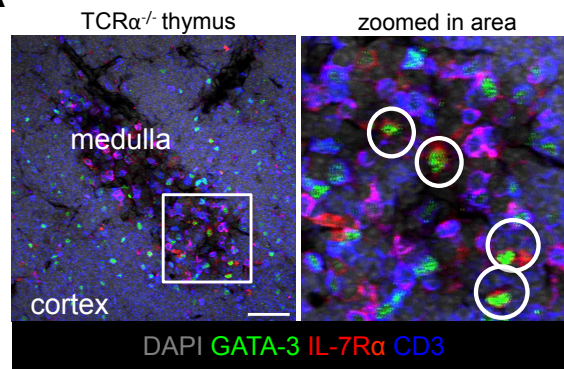
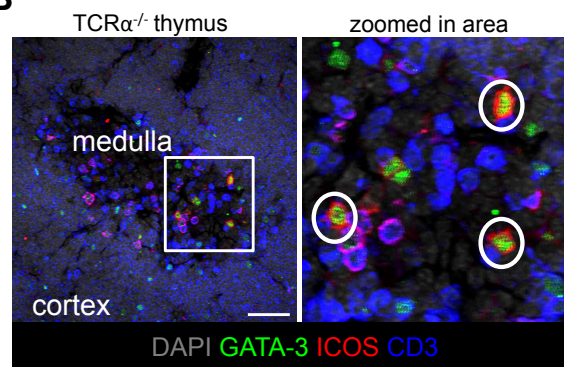
#### **Figure 4.9 ILC2 are located in the thymic medulla of TCR $\alpha$ <sup>-/-</sup> mice**

To better understand the location of thymic ILC2, frozen tissue sections from the thymus of adult TCR $\alpha$ <sup>-/-</sup> mice were assessed for the presence of ILC2 using confocal microscopy.

Data representative of 3 mice. Scale bar represents 100 $\mu$ m. Sections were counterstained using 4',6-diamidino-2-phenylindole (DAPI). Regions of interest are shown within a white square.

A) Tile scanned image (left) showing areas of the thymic medulla and cortex in the thymus of an adult TCR $\alpha$ <sup>-/-</sup> mice. Frozen tissue sections were stained for the expression of CD3, IL-7R $\alpha$  and GATA-3. Zoomed in image (right) showing region of interest manually zoomed in post-capture. Putative ILC2 are surrounded by a white circle.

B) Tile scanned image (left) showing areas of the thymic medulla and cortex in the thymus of an adult TCR $\alpha$ <sup>-/-</sup> mice. Frozen tissue sections were stained for the expression of CD3, GATA-3 and ICOS. Zoomed in image (right) showing region of interest manually zoomed in post-capture. Putative ILC2 are surrounded by a white circle.

**A****B**



by ILC2 (identified as CD45<sup>+</sup> CD8 $\alpha$ <sup>-</sup> CD3<sup>-</sup> IL-7R $\alpha$ <sup>+</sup> GATA-3<sup>+</sup> IL-5<sup>+</sup>/IL-13<sup>+</sup> in the lung (upper panel) and neonatal thymus (lower panel) is shown in Figure 4.10A. Fluorescent Minus One (FMO) controls for IL-5 (upper panel) and IL-13 (lower panel) expression using cells isolated from the neonatal thymus following *ex vivo* stimulation is shown in Figure 4.10B.

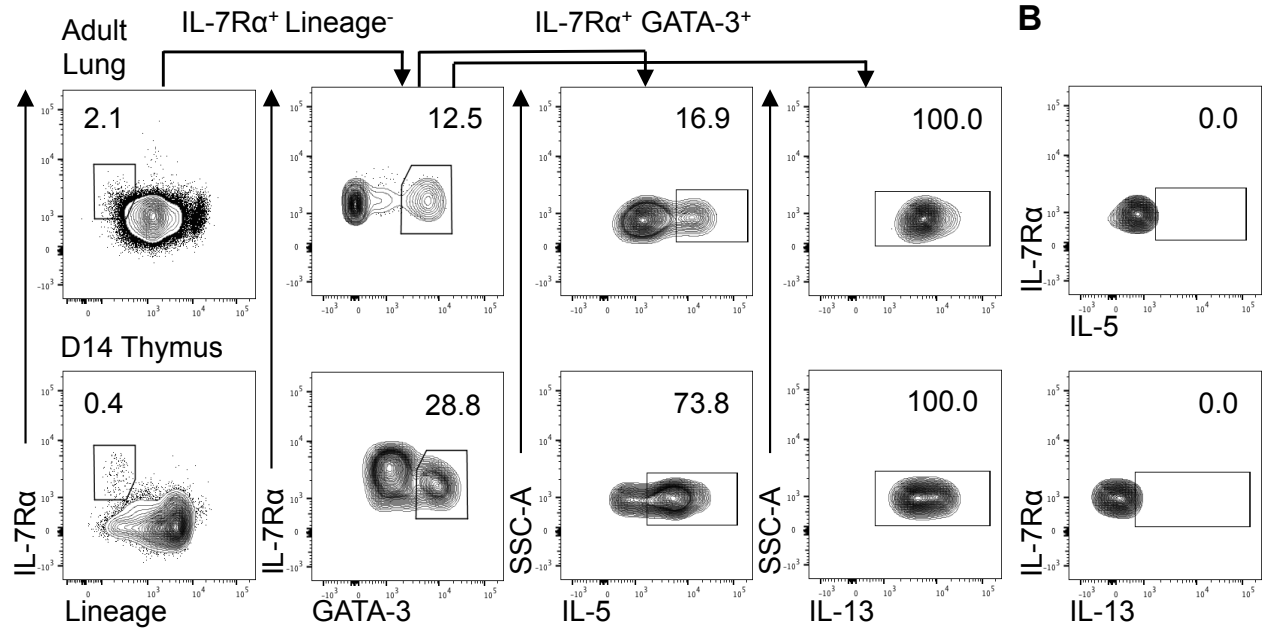
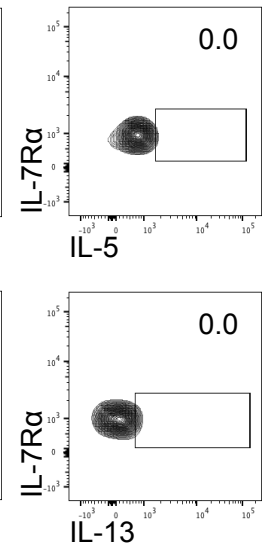
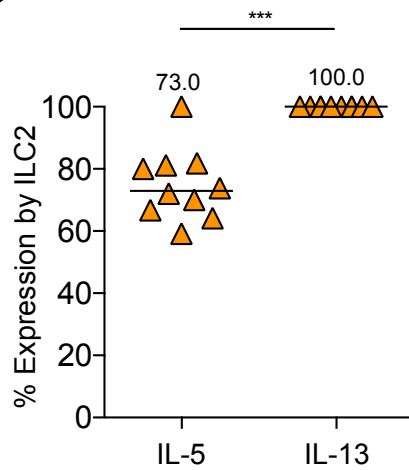
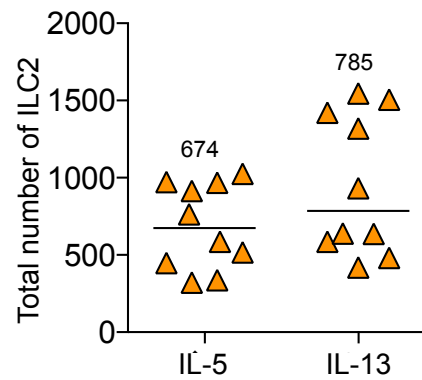
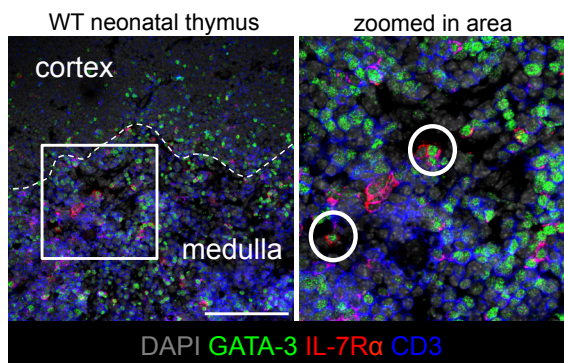
Initial observations from these flow cytometry plots show clear expression of IL-5 and IL-13 expression by ILC2 in both tissues (Figure 4.10A). Enumeration of the proportion of cytokine-expressing cells in the neonatal cells demonstrates a greater proportion of ILC2 expressing IL-13 compared to IL-5 (figure 4.10C). However, comparison of total numbers of these cells reveals no significant difference (Figure 4.10D). These findings are consistent with the functionality of cells isolated from the thymus of adult TCR $\alpha$ <sup>-/-</sup> mice. Furthermore, previous immunofluorescent analysis of the TCR<sup>-/-</sup> thymus demonstrated ILC2 to be present within the medulla. We anticipated ILC2 in the neonatal thymus to also be present within this location. To investigate the location of ILC2 within the neonatal thymus, frozen tissue sections from WT mice at day 14 post-birth were assessed by immunofluorescence. These data revealed putative ILC2, identified as CD3<sup>-</sup> IL-7R $\alpha$ <sup>+</sup> GATA-3<sup>+</sup> cells, were present in the medullary area.

**Figure 4.10 ILC2 isolated from the neonatal thymus are capable of producing IL-5 and IL-13 following ex vivo stimulation**

Our previous data has shown ILC2 to reside in the thymic medulla of TCR $\alpha^{-/-}$  mice where they are capable of producing IL-5 and IL-13. To better understand the function of ILC2 in the thymus of WT mice, cells isolated from the thymus of WT neonatal mice, where many ILC2 are present, and the capability of ILC2 to produce IL-5 and IL-13 was assessed following stimulation *ex vivo*. In addition, frozen tissue sections from the WT thymus 14 days post-birth were assessed for the presence of ILC2 using confocal microscopy. Data shown in orange corresponds to ILC2.

- A) Representative flow cytometry plots for the identification of IL-5 and IL-13 producing ILC2, defined as live CD45<sup>+</sup> CD8 $\alpha^{-}$  CD3 $\beta^{-}$  IL-7R $\alpha^{+}$  GATA-3<sup>+</sup> cells, in the adult lung (upper panel) and neonatal thymus (lower panel) at day 14 post-birth. The cells isolated from the adult lung were used as a positive control.
- B) Representative flow cytometry plots for FMO controls for IL-5 (upper panel) and IL-13 (lower panel) using cells isolated from the neonatal thymus at day 14 post-birth. The gates for IL-5 and IL-13 in A) were positioned using these controls.
- C) Proportion of ILC2 expressing IL-5 and IL-13 in the neonatal thymus at day 14 post-birth.
- D) Enumeration of ILC2 expressing IL-5 and IL-13 in the neonatal thymus at day 14 post-birth.
- E) Tile scanned image (left) showing areas of the thymic medulla and cortex in the thymus of a neonatal WT mouse at 14 days post-birth. Frozen tissue sections were stained for the expression of CD3, IL-7R $\alpha$  and GATA-3. Zoomed in image (right) showing region of interest (white square) manually zoomed in post-capture. Putative ILC2 are surrounded by a white circle. Data representative of 3 mice. Scale bar represents 100 $\mu$ m. Sections were counterstained using DAPI.

Mann-Whitney U (non-parametric, two-tailed) test was used for statistical analysis where \* $p < 0.05$ , \*\* $p < 0.01$ , \*\*\* $p < 0.001$ , and \*\*\*\* $p < 0.0001$ . In all graphs the bar represents the median,  $n = 10$ . Data shown from two independent experiments.

**A**Pre-gated on live CD45<sup>+</sup> CD8α<sup>-</sup> CD3i<sup>-</sup> cells**B****C****D****E**

### 4.3 Discussion

Overall, this study aimed to investigate the function of ILCs within the thymus. Firstly, we investigated the role of ILC3 in the regeneration of the thymus following injury, which was addressed using an *in vivo* approach of sub-lethal irradiation. However, contrary to previously published findings, we did not discover a role for ILC3. While our evidence suggested the recovery of the thymus might be impaired in mice lacking ROR $\gamma$ t when compared to a WT, very few ILC3 were detected in the thymus of non-irradiated WT mice. Furthermore, the numbers of ILC3 were further depleted following sub-lethal irradiation; arguing against the radio-resistant nature of these cells. As such, it is unlikely these cells are a main source of IL-22 given the very few ILC3 that exist within the thymus at steady state and following injury.

Given the stark differences in the conclusions within the literature compared to our own findings, we returned to dissect the approach of Dudakov *et al.* (2012).(100) However, the gating strategy was not included within the primary data and was inferred from their description of cell markers used. Nonetheless, our observations were not consistent with those published. While LT $\alpha$ i cells, including IL-22-producing LT $\alpha$ i cells, were observed in the mLN, very few of these cells were identified in the adult thymus. Furthermore, these results were observed 3 days after sub-lethal irradiation where thymic cellularity is described at its lowest following injury. Therefore, the presence of LT $\alpha$ i cells within this tissue should be easily identifiable at this time. Whereas, T cells vastly outnumber ILC in the steady-state and complicate ILC identification due to the phenotypic similarities between T cells and ILC.(138)

Of note, there were some differences between the methods used within our investigations compared to evidence in the literature. Firstly, Dudakov *et al.* (2012) digested the thymus using enzymes prior to analysis whereas we used mechanical means to disaggregate the thymus tissue.(100) In addition, an increase in the proportion of IL-22<sup>+</sup> ILC was observed in the thymus of L-TBI mice and cells isolated from this tissue were cultured *ex vivo* in BFA only. Experience within our laboratory has shown the production of IL-22 by T cells and ILC3 to require additional signals. Finally, the gating strategy described by Dudakov *et al.* (2012) is not as extensive as the strategy established within our laboratory.(100) Therefore, it is not unreasonable to suggest some level of misidentification within the published literature. As our findings demonstrate within Chapter 3, the identification of ILC3 within the adult thymus requires a well-defined gating strategy, which was confirmed using a series of robust *in vivo* models.

These data argue that, while LT<sub>i</sub> cells do not have a role in the recovery of the thymus following injury, there is still a requirement for an endogenous source of IL-22. Th17 are amongst other cells within the thymus with the capability of producing IL-22. Moreover, CD4<sup>+</sup> T cells differentiate into IL-22-producing Th17 cells as a result of signals from IL-23. This Th17 axis of IL-23 and IL-22 is comparable to that suggested for IL-22 production by LT<sub>i</sub> cells. Furthermore, CD4<sup>+</sup> SP T cells were present in the adult thymus following depletion of DP thymocytes with Dexamethasone.(100) As such, it is possible the production of IL-23 by thymic dendritic cells in response to depletion of DP thymocytes could act on pre-existing CD4<sup>+</sup> T cells and promote their differentiation into IL-22-producing Th17 cells. Moreover, IL-22 production is driven by the expression of ROR $\gamma$ t. Therefore, the loss

of IL-22 production in *Rorc*<sup>-/-</sup> mice following irradiation could be explained by the reduction in IL-22-producing T cells and not LT $\alpha$ i cells, which exist in very few numbers.

Until recently, thymic populations of ILC subsets other than ILC3 have been neglected. In Chapter 3 we demonstrate ILC2 to be a prominent population within the adult thymus where its function is largely unknown. As such, we also assessed the effect of thymic damage on ILC2. The idea that ILC2 may have a role in the repair of thymus tissue is not unreasonable given that ILC2 has been implicated in tissue repair at peripheral sites.(186–188) However, much like ILC3, the numbers of ILC2 in the WT thymus were depleted by day 7 following sub-lethal irradiation. Arguing against a role for either subset in the re-establishment of thymus tissue following damage.

However, there are challenges associated with irradiation experiments, including what determines recovery. This is evident in Figure 4.1B whereby there is a statistically significant difference in total cellularity between the NI control and day 7 in WT mice, however, there is no significant difference between the NI control and D14 even though the median total cellularity at day 14 is lower than in the NI control. We tried to overcome this within our investigations by calculating the percentage recovery of thymic cellularity in each experiment, as shown in Figure 4.1C. To achieve this, the median cellularity of the thymus from NI controls and irradiated mice were calculated. The median total cellularity of the irradiated thymus was then calculated as a percentage of median total cellularity of the NI control. This method

accounts for only 2 data points for day 7 in Figure 4.1C as the data point represents the median for the experiment and not individual mice.

Following our characterisation of ILC populations within the thymus, we sought to better understand the location of these cells to provide insight into what their function might be. However, analysis of ILC populations in thymus tissue is challenging given the vast number of T cells that likely surround ILC. This was addressed within our investigations by analysing thymus tissue from  $\text{TCR}\alpha^{-/-}$  mice and identified putative ILC2, defined as  $\text{GATA-3}^+ \text{CD3}^- \text{IL-7R}\alpha^+$ , which was present in the medullary region. Analysis of ICOS expression in this tissue identified a similar population of  $\text{GATA-3}^+ \text{CD3}^- \text{IL-7R}\alpha^+$ . Given that our earlier data identified ICOS expression amongst thymic ILC2 this provided further evidence to support the identification of these cells. Although the separation of the cortex and medulla is clear by the densely packed CD3 staining which is apparent in the cortex, these images could be strengthened with the addition of appropriate controls. One example of this is the use of keratin staining to clearly identify the separate regions of the cortex and medulla. For example, keratin-5 is exclusively expressed by medullary subsets and has been used by other groups to identify the medullary region.(173,189)

The prominence of ILC2 throughout neonatal development and adulthood prompted further investigation into the signals these cells can produce. It has been well established that ILC2 act as a source of type 2 cytokines at peripheral sites.(27) As such, it was not unreasonable to hypothesise that ILC2 are a local source of these cytokines within the thymus. While we sought to determine the expression of IL-13 by ILC2 in the adult  $\text{TCR}\alpha^{-/-}$  thymus, we identified an artefact in our experiment that

limited the value of our interpretation. However, ILC2 isolated from the neonatal thymus were later demonstrated to produce IL-5 and IL-13 upon *ex vivo* stimulation.

In addition to our own studies, there has been a growing appreciation for ILC2 within the thymus. Much of the recent work has focussed on the effect of E protein deletion on ILC2 development in the thymus.(104) However, much like our own investigations, other groups have also sought to assess the potential of ILC2 to produce type 2 cytokines *in vitro*. Studies *in vitro* have previously identified the requirement of IL-2, IL-7 and IL-33 for thymic ILC2 differentiation, survival and expansion.(105) Recently, Qian *et al.* (2019) demonstrated cytokine production by ILC2 in response to known ILC activators. The authors first assessed cytokine production in the presence of IL-2 and IL-7 only, and demonstrated little IL-5 and IL-13 to be produced by these cells.(105) However, culturing ILC2 in the presence of IL-2, IL-7 and IL-33 demonstrated the capability of ILC2 to produce IL-5 and IL-13.(105) While a similar effect was observed in the presence of IL-2, IL-7 and IL-25, the level of IL-5 and IL-13 production was to a lesser extent.(105) Although our own data requires further work to provide firm conclusions on the production of IL-13, the data shown in this study supports the idea that ILC2 from the thymus can produce these cytokines if provided with the correct signals, namely IL-25 or IL-33. Interestingly, single-cell mapping of the thymic stroma has identified a mTEC IV population with characteristics similar to epithelial tuft cells that are known to the gut.(136) This is of relevance here given that we have identified ILC2 to be present within the medulla and where others have shown ILC2 capable of responding to IL-25. The relevance of this in the wider context of thymic function has yet to be determined. However, it is



possible to hypothesise the role of ILC2 in the thymus given our current understanding of the thymic microenvironment.

The production of type 2 cytokines, such as these, have been implicated in T cell development within the thymus (129,165). In particular, signalling through the IL-4/IL-13 receptor complex on developing haematopoietic progenitors directly influence early decisions of cell fate; favouring myeloid differentiation over T cell differentiation.(190) Furthermore, IL-4 and IL-13 have been shown to have an influential effect on thymic epithelial cells. Within these studies, IL-4 and IL-13 signals from iNKT cells regulated mature T cell egression.(191) Given that we have identified ILC2 to be present in the thymic medulla, it is not unreasonable to suggest that ILC2-derived IL-13 supports the migration of mature T cells out of the thymus. However, whether these signals are redundant to iNKT cells requires further study.

Overall, evidence described within this thesis supports a role for ILC2 in providing a local source of type 2 cytokines within the thymus. Whether the functions of ILC2 are unique or redundant to other innate populations, such as iNKT cells, would require an *in vivo* model with specific deletion of ILC2, which is not an easy feat.(129,165) The phenotypic similarity between T cell and ILC populations has been repeatedly discussed within this thesis. Amongst the ILC population, ILC2 are distinguished by their expression of GATA-3 and ability to produce type-2 cytokines. However, ILC2 share components of the developmental pathway with ILC1 and ILC3 subsets, and mature ILC express many of the same surface antigens, such as IL-7R $\alpha$ .(147) While specific deletion of ILC2 in mice would aid our understanding of these cells, both the developmental and phenotypic similarities between ILC2 and other cell types make this objective difficult to achieve.

Over recent years, progress has been made in the field ILC biology owing thanks to the development of multiple mouse models. Of interest here, it is possible to use of conditional knock out mice to gain a greater understanding of ILC2 in the thymus. Using this method, researchers have developed IL-7R $\alpha$ <sup>Cre</sup> Rora<sup>flox</sup> mice that conditionally delete ROR $\alpha$ , a key regulator of ILC2 differentiation and function, from IL-7R $\alpha$ <sup>+</sup> cells.(192,193) The role of this transcriptional regulator in ILC2 development has been reaffirmed using “*staggerer*” mice that have a spontaneous deletion in the *Rora* gene and thus limiting their development.(153,194) However, such mice are not without their caveats. Studies at the mRNA level have shown *Rora* to be broadly expressed by all ILC subsets.(193) While the greatest expression is amongst ILC2, this identifies an issue whereby other ILC subsets may be affected.(195) Moreover, a similar issue may be encountered in mice where GATA3 is the subject of conditional targeting, given the early role of GATA3 in restricting the CLP to NKP or ChILP subsets prior to their commitment to NK cell, ILC1, ILC2 and ILC3 lineages.(75) While there is no perfect model to study the function of ILC2, or indeed other ILC subsets, in isolation, the availability of different strains may be used in combination to enhance our understanding of these cells. Together, these types of experiments are important in understanding the role of ILC2 cells and, subsequently, whether ILC2 are redundant against cells with parallel functions.

Since completion of my investigations, researchers at the University of Birmingham have obtained a unique mouse model that changes the way in which ILC2 can be studied. The novel mouse strain, known as Red5 x RAG<sup>GFP</sup>, combines the expression of tdTomato under the IL-5 promoter with GFP under the *RAG* genes. This mouse is particularly useful when investigating ILC2 in the thymus as it enables

discrimination of T cells using GFP; aiding identification of ILCs, from which ILC2 can be isolated and the expression of IL-5 by these cells determined. This has the additional advantage of assessing IL-5 production *in vivo*, which is advantageous over our *ex vivo* techniques.

Concerning the embryonic thymus, ILC3 have been implicated in the provision of RANKL where they aid the maturation of the first cohort of mTECs at E16. It was later discovered that this signal was jointly provided with V $\gamma$ 5<sup>+</sup> DETCs.(99) While CD4<sup>+</sup> T cells are the likely source of RANKL post-birth, we investigated whether ILC3 were able to produce RANKL in the neonatal thymus prior to their decline. Moreover, we assessed the provision of ILC2 to express RANKL in this tissue. Results from this investigation demonstrated that ILC3 were capable of expressing RANKL in the neonatal thymus but little RANKL was expressed by ILC2. Thus demonstrating the expanding population of ILC2 within the neonatal thymus do not take over the provision of RANKL from ILC3 following their decline. While we have identified ILC2 to reside within the thymic medulla, these data would argue ILC2 and ILC3 within the thymus to be functionally distinct.(129,165) Strikingly, ILC2 within the neonatal thymus of *Rorc*<sup>-/-</sup> mice express RANKL. This suggests ILC2 are capable of expressing RANKL when the thymic microenvironment is perturbed.(129)

To conclude, the data described within this chapter is consistent with our earlier characterisation of thymic ILC subsets. Despite published findings indicating a role for ILC3 in the regeneration of the adult thymus following injury, very few ILC3 were observed within this tissue. Importantly, numbers of ILC3, along with ILC2, were depleted following sub-lethal irradiation, demonstrating these cells not to be radio-resistant as first thought. While further research is required concerning the role of

ILC3 within the adult thymus, the role of these cells within the embryonic and neonatal thymus is much clearer, where they act to provide RANKL and aid mTEC maturation. Unless in otherwise perturbed environments, ILC2 are unable to provide RANKL signals and instead have a distinct function. Evidence supports a role for ILC2 in providing a local source of type 2 cytokines within this tissue. However, whether these signals are redundant to less rare populations within this tissue requires the specific deletion of ILC2.

**CHAPTER 5: ASSESSMENT OF ID2 EXPRESSION**  
**AMONGST INNATE AND EFFECTOR POPULATIONS**

## 5.1 Introduction

Thus far, this thesis has used several *in vivo* tools in an attempt to better identify and characterise ILC populations within the thymus. The expression of Id2 was used in a number of these models to definitively identify ILC populations within this tissue. From these investigations, it was evident that a surprising number of other cells expressed, or had previously expressed, Id2. Therefore, these data indicated that the Id2 transcription factor was much broader than we had anticipated amongst T cells populations, including  $\alpha\beta$  T cells and their innate-like counterparts. This chapter follows on from this interesting observation and aimed to characterise lymphocytes expressing Id2.

Recently, publications have started to identify roles for Id2 in  $\alpha\beta$  T cell populations. Shaw *et al.* (2016) reports a clear role for Id2 in the differentiation of CD4<sup>+</sup> T cells into effector T cell populations while its expression is largely absent in follicular helper T cells.(196) Previous studies in CD8<sup>+</sup> T cells have highlighted a similar function for this transcription factor where Id2 was up regulated during the effector response. Further to this, the loss of Id2 resulted in uncontrolled E protein activity and subsequent loss of effector CD8<sup>+</sup> T cells.(197,198) More recently, the authors have developed our understanding of Id2 in CD8<sup>+</sup> T cells using a murine model of lymphocytic choriomeningitis virus infection.(199) Here, Omilusik *et al.* (2018) showed that distinct CD8<sup>+</sup> T cell subsets require regulation of Id2 for their maintenance.(199) Novel discoveries have also identified a tissue-specific association between Id2 and adipose regulatory Tregs (aTregs). Expression of Id2 mRNA was 4-fold greater in aTregs in Visceral Adipose Tissue (VAT) compared to splenic aTregs. Moreover, the loss of Id2 resulted in a substantial decline in aTreg number in VAT while these cells

were unaffected in the lymphoid tissue.(200) The studies highlighted above demonstrate some advancement in our understanding of Id2 in lymphocyte populations over the last few years. However, it is important to note that much of this work was published following completion of our own work that will be described within this chapter.

Whilst Id2 has attracted a surge of interest towards investigating its functional role in  $\alpha\beta$  T cells, the role of Id2 in the development of these cells is not well understood. This can also be said for innate-like populations, such as iNKT cells and  $\gamma\delta$  T cells, which also arise from the thymus. This is perhaps owing to the lethality of Id2 knockout models that would otherwise be useful for deciphering the role of this transcription factor during development and the immune response. Furthermore, Id2-deficient mice that do make it to term are poorly developed with a host of defects; again arguing against these mice as an ideal model for such investigations.

D'Cruz *et al.* (2014) investigated Id2 and Id3 expression at the mRNA level in iNKT cells as they entered different stages of maturation in the thymus.(77) This study found Id3 mRNA to be most prominently expressed at stages 1 and 2 (identified as CD24<sup>lo</sup> CD44<sup>lo</sup> NK1.1<sup>lo</sup> and CD24<sup>lo</sup> CD44<sup>hi</sup> NK1.1<sup>lo</sup> cells, respectively) while Id2 was expressed amongst stage 3, representing mature iNKT cells. These investigations were continued using flow cytometry whereby CD1d-tetramer<sup>+</sup> TCR $\beta$ <sup>+</sup> cells were sorted from the thymus of Id2-YFP reporter mice based on their expression of Tbet, PLZF and ROR $\gamma$ t to identify iNKT1, iNKT2 and iNKT17 subsets, respectively. Of these, all three subsets were shown to express Id2 with iNKT1 cells demonstrating the highest level of expression defined by Median Fluorescence Intensity (MFI).

Until recently, our understanding of Id2 expression amongst  $\alpha\beta$  T cells was predominantly focussed on CD8<sup>+</sup> T cells where Id2 has been shown to promote effector T cell differentiation. This is mediated by inhibition of the E2A transcription factor that would otherwise activate several genes involved in the development and function of CD8<sup>+</sup> memory T cells.(201) This was identified using a conditional knockout model that enabled the specific deletion of Id2 in T cells to assess its function in CD8<sup>+</sup> T cells.(201) However, there has been growing interest in Id2 as an important regulator of CD4 T cell differentiation. This has led to a greater understanding the role of Id2 in these cells where it has been implicated in the differentiation of specific effector subsets; much like its action in CD8 T cells.

Effective host protection requires the differentiation of T cells into effector subsets that are able to mount a suitable response.(196) Shaw *et al.* (2016) investigated the role of the Id family of inhibitors in the differentiation of CD4 T cells into type 1 T-helper cell (Th1) and T follicular helper cell (Tfh) subsets, which had not previously been defined.(196) This study demonstrated Id2 to be expressed in Th1 cells while Id2 expression in Tfh cells was largely absent. Using RNA-interference to deplete Id2 in CD4 T cells, the authors demonstrated an increase the frequency of Tfh cells. Moreover, the generation of Th1 cells was impaired in Id2-deficient mice following infection with *Toxoplasma gondii*, which is known for polarizing CD4 T cells towards a Th1 response.(196,202) Overall, these investigations demonstrated Id2 to be a key regulator of Th1 cell differentiation in the context of this response.

In addition, Id2 has been implicated in the effector function of Th17 cells. One study demonstrated a role for Id2 in the development of Th17 driven Experimental Autoimmune Encephalomyelitis (EAE) using an Id2 knockout mouse model. The



absence of Id2 highlighted a decrease in CD4 T cell numbers at peripheral sites, owing to reduced proliferation and increased cell death.(203) More recently, Id2 has been further implicated in exacerbating the Th17 response required to drive EAE by influencing regulatory T cell ( $T_{reg}$ ) plasticity. In these studies, the authors demonstrated an increase in Id2 expression in response to pro-inflammatory cytokines, IL-1 $\beta$  and IL-6. This, in turn, reduced Forkhead box P3 (FoxP3) expression in  $T_{regs}$  whereby these cells were converted to an “ex-FoxP3” Th17 phenotype capable of producing the Th17-associated cytokine, IL-17A.(204)

While there appear to be a number of factors that influence the development of  $\gamma\delta$  T cells in the thymus, our understanding of E proteins and their transcriptional regulators, the Id proteins, is less well documented. One publication demonstrated Id2 and Id3 act together to regulate the development and population size of innate-like  $\gamma\delta$  T cells that express the V $\gamma$ 1.1 and V $\gamma$ 6.3 segments.(66) Concerning Id2 only, this paper demonstrated Id2 to be absent in developing cells and Id2 expression to be restricted to mature  $\gamma\delta$  T cells (TCR $\gamma\delta^+$  CD24 $^-$  CD44 $^{high}$ ). (66) Moreover, Id2 expression is higher in V $\gamma$ 1.1 $^+$  and V $\gamma$ 6.3 $^+$  subsets compared to cells negative for V $\gamma$ 1.1 V $\gamma$ 1.1 and V $\gamma$ 6.3 segments. Furthermore, Id2 was deleted using a conditional knock out model and this enabled the moderate expansion of  $\gamma\delta$  T cells, demonstrating a role for Id2 in restricting expansion of these cells. Much like our investigations, the authors understood the value of Id2-eGFP reporter mice for investigating cellular expression of Id2. GFP $^-$   $\gamma\delta$  T cells were sorted from these mice and cultured with OP9-DL1 cells, which is known to support differentiation of progenitors to T-lymphocytes, and IL-7. Interestingly, GFP expression was up

regulated following stimulation with an anti- $\gamma\delta$ TCR antibody, proposing Id2 expression may be controlled by stimulation of the TCR.(66)

Together, the evidence discussed here suggests a role for Id2 in multiple lymphocyte populations. However, much of this work, including that published after our own investigations, describes the expression of Id2 at peripheral locations. Therefore neglecting the expression of Id2 expression during lymphocyte development. There has been some attempt to characterise Id2 expression amongst iNKT cells, and to some extent,  $\gamma\delta$  T cells, in the thymus. However, little is known about the influence of Id2 throughout development on the effector fates of these cells. As such, we sought to exploit our Id2 reporter and fate-mapping models to address 3 distinct aims:

1. Characterise the expression of Id2 amongst iNKT1, iNKT2 and iNKT17 subsets in the thymus and peripheral lymphoid tissues
2. Examine the expression of Id2 in  $\gamma\delta$  T cells associated with different effector fates in the thymus and peripheral lymphoid tissues of adult and neonatal mice
3. Investigate the expression of Id2 in CD4<sup>+</sup> T cells following initiation of a type-1 immune response

## **5.2 Results**

### **5.2.1 Characterisation of Id2 expression amongst iNKT cells, $\alpha\beta$ T cells and $\gamma\delta$ T cells**

To examine the expression of Id2 amongst innate and effector populations, Id2<sup>creERT2</sup> x ROSA26<sup>RFP</sup> mice were administered tamoxifen by oral gavage for 5 consecutive days and cells isolated from the mLN and thymus were assessed. As with our earlier investigations, this model enables the identification of cells that are expressing Id2

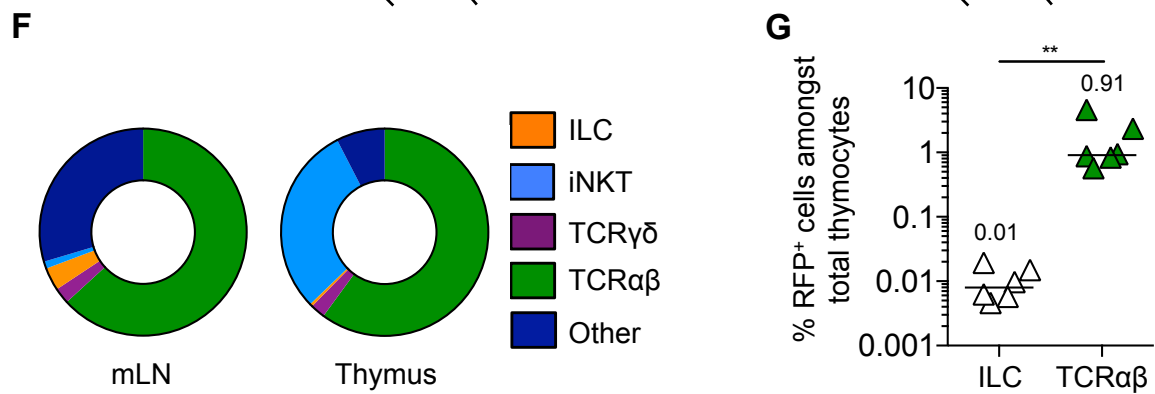
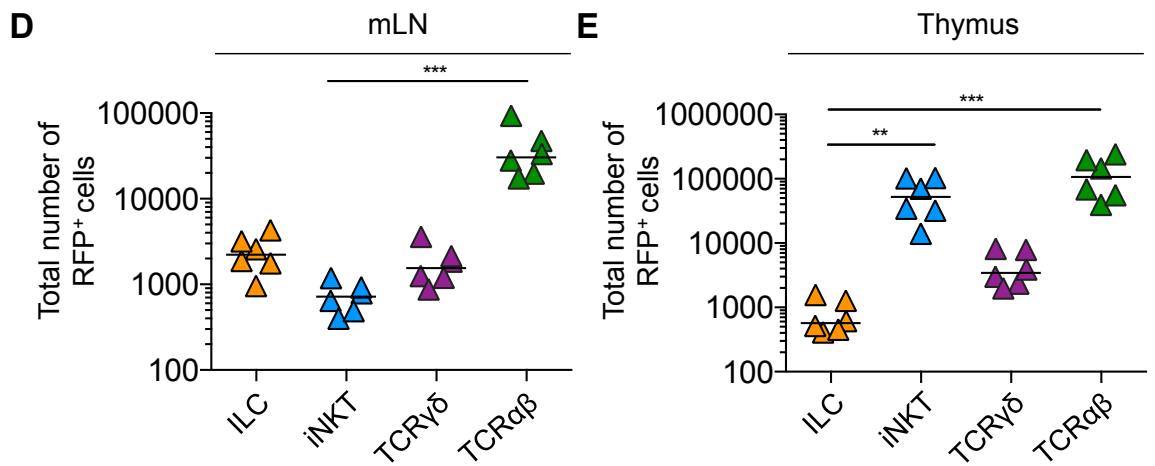
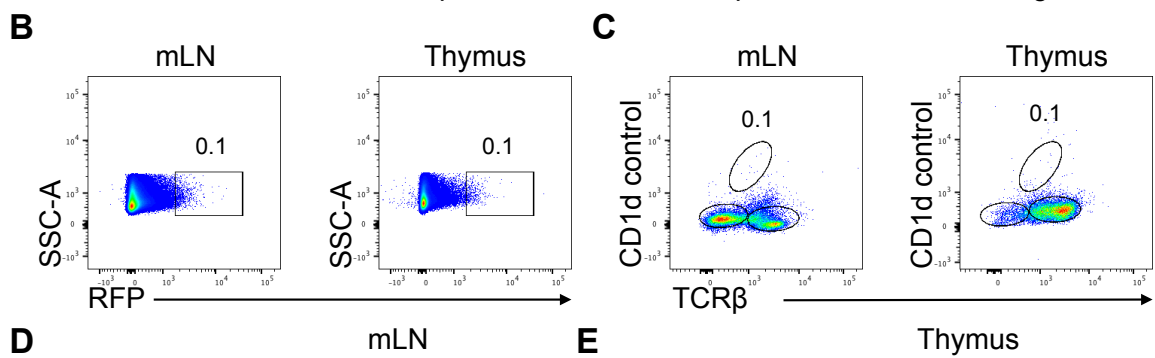
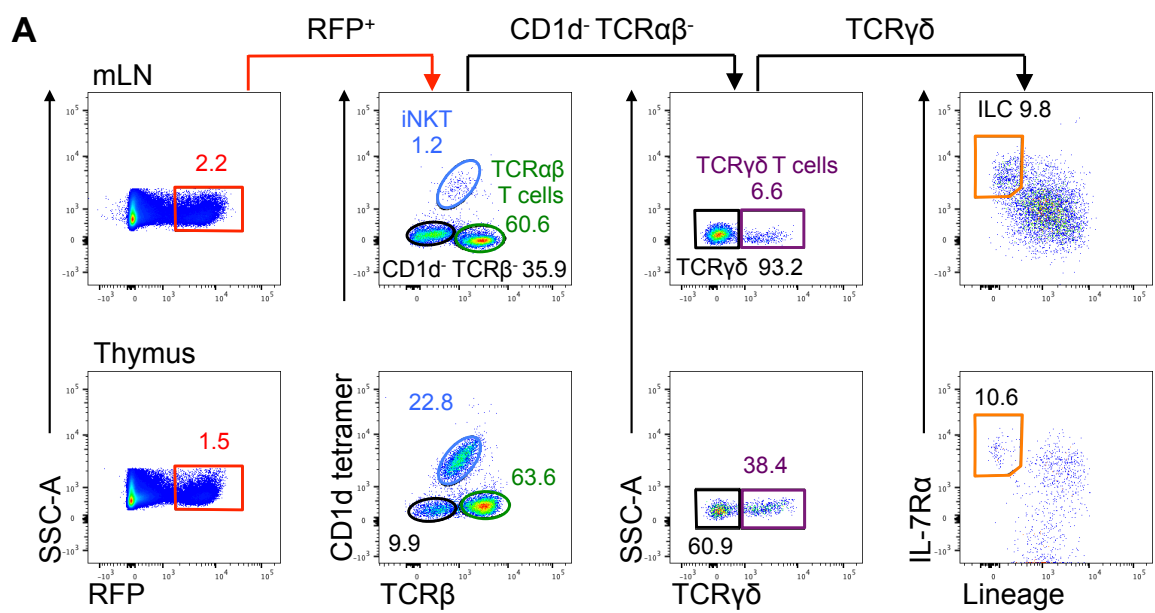
during the window of tamoxifen administration, and just before. The extent of fate-mapping cells to Id2 in this manner is dependent on the efficiency of Cre induction following tamoxifen administration. Using a combination of markers specific for iNKT cells,  $\alpha\beta$  T cells,  $\gamma\delta$  T cells and ILCs, these cells were characterised amongst cells fate-mapped to Id2 (RFP<sup>+</sup>) using flow cytometry. First gating on cells isolated from the mLN, RFP<sup>+</sup> iNKT cells (CD1d-tetramer<sup>+</sup> TCR $\beta$ <sup>+</sup>),  $\alpha\beta$  T cells (CD1d-tetramer<sup>-</sup> TCR $\beta$ <sup>+</sup>),  $\gamma\delta$  T cells (CD1d-tetramer<sup>-</sup> TCR $\beta$ <sup>-</sup> TCR $\gamma\delta$ <sup>+</sup>) and ILCs (CD1d-tetramer<sup>-</sup> TCR $\beta$ <sup>-</sup> TCR $\gamma\delta$ <sup>-</sup> IL-7R $\alpha$ <sup>+</sup> Lineage<sup>-</sup>) were identified (Figure 5.1A; upper panels). Subsequent analysis applied this gating strategy to cells isolated from the thymus and, once again, each of these subsets could be observed (Figure 5.1A; lower panels). Gating controls used cells isolated from the mLN (left) and thymus (right) of WT mice (Figure 5.1B) while gating controls for CD1d-tetramer were based on CD1d-tetramer in the absence of  $\alpha$ -GalCer in the mLN (left) and thymus (right) of Id2<sup>creERT2</sup> x ROSA26<sup>RFP</sup> mice (Figure 5.1C). Enumeration of these subsets in the mLN identified the majority of cells fate-mapped to Id2 to be  $\alpha\beta$  T cells (Figure 5.1D). While this was also true of cells isolated from the thymus, the number of iNKT cells fate-mapped to Id2 was comparable to  $\alpha\beta$  T cells. The fact  $\alpha\beta$  T cells are the most abundant cells arising from cells that fate-map to Id2 is unsurprising given the thymus is home to many developing  $\alpha\beta$  T cells. This was illustrated using a graphical representation of iNKT cells,  $\alpha\beta$  T cells,  $\gamma\delta$  T cells and ILCs amongst RFP<sup>+</sup> cells whereby  $\alpha\beta$  T cells (shown in green) are the most abundant population in both tissues (Figure 5.1F). Furthermore, comparison of the number of  $\alpha\beta$  T cells that fate-map to Id2 as a proportion of total thymocytes with the number of ILCs that fate-map to Id2 as a proportion of total thymocytes revealed the proportion of  $\alpha\beta$  T cells to be significantly

### Figure 5.1 $\alpha\beta$ T cells are the most abundant cells fate-mapped to Id2 in the thymus and mLN

To identify other Id2 expressing populations within the thymus and mLN, Id2<sup>creERT2</sup> x ROSA26<sup>RFP</sup> mice were used to 'fate map' Id2 expression. Administration of tamoxifen by oral gavage on five consecutive days was performed and cells isolated from the thymus and mLN were analysed 3 days later. Samples were analysed using flow cytometry and total numbers calculated per whole thymus or mLN. Data shown in red identifies RFP<sup>+</sup> cells while data for individual populations is shown in orange, blue, purple and green correspond with ILCs, iNKT cells,  $\gamma\delta$  T cells and  $\alpha\beta$  T cells, respectively.

- A) Full gating strategy for flow cytometry data showing identification of fate-mapped iNKT cells (RFP<sup>+</sup> CD1d-tetramer<sup>+</sup> TCR $\beta$ <sup>+</sup>),  $\alpha\beta$  T cells (RFP<sup>+</sup> CD1d-tetramer<sup>-</sup> TCR $\beta$ <sup>+</sup>),  $\gamma\delta$  T cells (RFP<sup>+</sup> CD1d-tetramer<sup>-</sup> TCR $\beta$ <sup>-</sup> TCR $\gamma\delta$ <sup>+</sup>) and ILC (RFP<sup>+</sup> CD1d-tetramer<sup>-</sup> TCR $\beta$ <sup>-</sup> TCR $\gamma\delta$ <sup>-</sup> IL-7R $\alpha$ <sup>+</sup> Lineage<sup>-</sup>) in the mLN (upper panel) and thymus (lower panel). Lineage channel consists of antibodies against CD3, CD5, Gr-1, CD11c and B220.
- B) Gating controls for RFP<sup>+</sup> cells were based on RFP expression in mLN (left) and thymus (right) of Id2<sup>ERT2</sup> x ROSA26<sup>RFP</sup> mice that were absent of cre.
- C) Gating controls for CD1d-tetramer<sup>+</sup> cells were based on CD1d-tetramer in the absence of  $\alpha$ -GalCer (unloaded control) in the mLN (left) and thymus (right) of Id2<sup>creERT2</sup> x ROSA26<sup>RFP</sup> mice.
- D) Total number of ILC, iNKT cells,  $\alpha\beta$  T cells, and  $\gamma\delta$  T cells amongst RFP<sup>+</sup> cells in the mLN. Each population was identified using the strategy described in A).
- E) Total number of ILC, iNKT cells,  $\alpha\beta$  T cells, and  $\gamma\delta$  T cells amongst RFP<sup>+</sup> cells in the thymus. Each population was identified using the strategy described in A).
- F) The percentage of RFP<sup>+</sup> ILC and  $\alpha\beta$  T cells as a proportion of the total number of cells in the thymus.
- G) Graphical representation of the mean proportion of ILC, iNKT cells,  $\alpha\beta$  T cells, and  $\gamma\delta$  T cells amongst RFP<sup>+</sup> cells in the mLN (left) and thymus (right). Cells outside of these phenotypes are defined as "other" and are shown in dark blue.

Mann-Whitney U (nonparametric, two-tailed) test (comparing two data sets) and Kruskal-Wallis one-way ANOVA with post hoc Dunn's test was used (comparing three or more data sets) for statistical analysis where \*p<0.05, \*\*p<0.01, \*\*\*p<0.001, and \*\*\*\*p<0.0001. In all graphs the bar represents the median, n=6. Data shown from two independent experiments.



greater (Figure 5.1G). Collectively, these data demonstrate  $\alpha\beta$  T cells to be the most abundant lymphocyte that fate-map to Id2 in both the mLN and thymus.

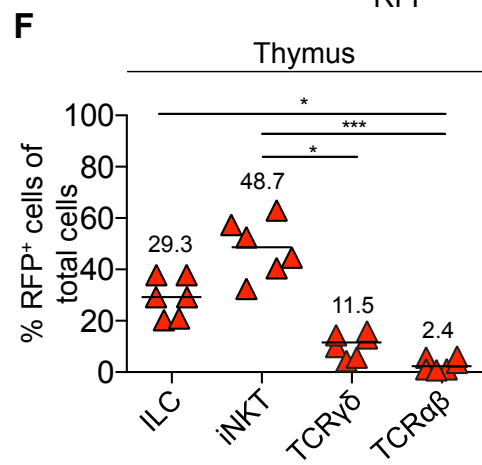
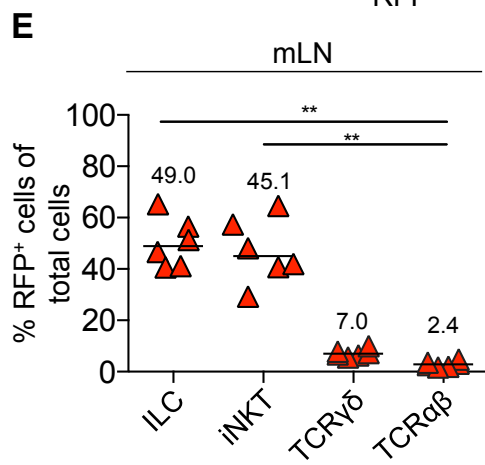
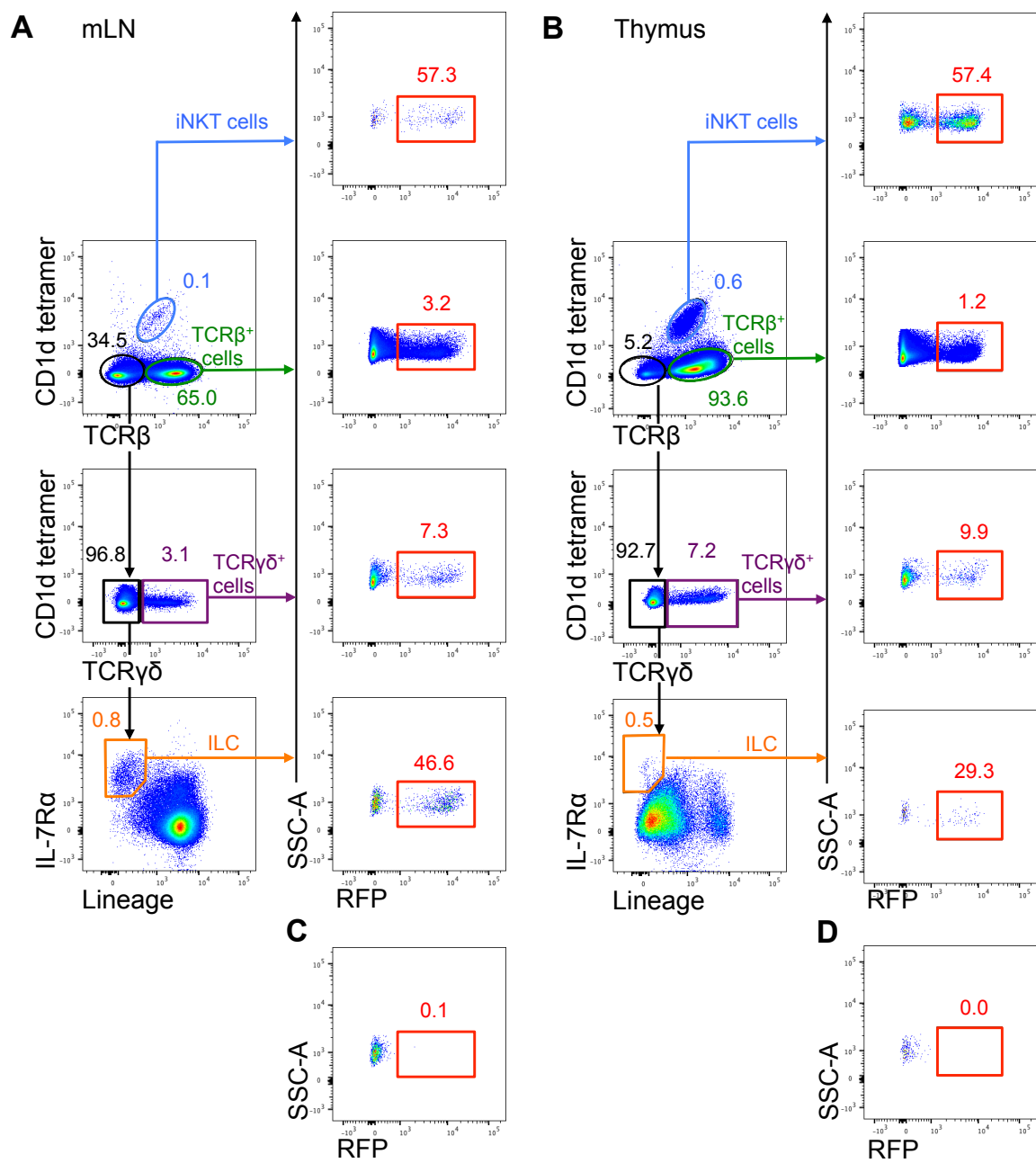
While Figure 5.1 clearly indicates  $\alpha\beta$  T cells to be the most abundant lymphocyte amongst RFP<sup>+</sup> cells, we sought to determine the proportion of RFP expressed by iNKT cells,  $\alpha\beta$  T cells,  $\gamma\delta$  T cells and ILCs (Figure 5.2). This approach would help us better understand the proportion of cells that fate-map to Id2. To achieve this, the gating strategy in Figure 5.1 was adapted so that each population was identified prior to gating on RFP<sup>+</sup> cells. This was first illustrated using cells isolated from the mLN where iNKT cells (CD1d-tetramer<sup>+</sup> TCR $\beta$ <sup>+</sup>),  $\alpha\beta$  T cells (CD1d-tetramer<sup>-</sup> TCR $\beta$ <sup>+</sup>),  $\gamma\delta$  T cells (CD1d-tetramer<sup>-</sup> TCR $\beta$ <sup>-</sup> TCR $\gamma\delta$ <sup>+</sup>) and ILCs (CD1d-tetramer<sup>-</sup> TCR $\beta$ <sup>-</sup> TCR $\gamma\delta$ <sup>-</sup> IL-7R $\alpha$ <sup>+</sup> Lineage<sup>-</sup>) were shown and expression of RFP amongst these cells was identified (Figure 5.2A). This gating strategy was applied to cells isolated from the thymus where RFP expression amongst each of the corresponding subsets was easily identified (Figure 5.2B). Gating controls for RFP expression used cells isolated from the mLN (Figure 5.2C) and thymus (Figure 5.2D) of a WT mouse. Enumeration of the proportion of cells expressing RFP demonstrated this to be greatest amongst ILC and iNKT cells where RFP expression amongst these subsets was significantly greater than the proportion of RFP expressed by  $\alpha\beta$  T cells in the mLN (Figure 5.2E). Moreover, these findings were consistent when assessing RFP expression amongst cells isolated from the thymus with both iNKT cells and ILC expressing the greatest proportion of RFP (Figure 5.2F). In addition, the expression of RFP amongst iNKT cells and ILC in the thymus was greater than that expressed by  $\alpha\beta$  T cells (Figure 5.2F).

## Figure 5.2 The proportion of iNKT cells fate-mapped to Id2 is comparable to that of ILC

To compare the proportion of ILCs, iNKT cells,  $\gamma\delta$  T cells and  $\alpha\beta$  T cells that fate-map to Id2, tamoxifen was administered to Id2<sup>creERT2</sup> x ROSA26<sup>RFP</sup> mice by oral gavage for five consecutive days and cells isolated from the thymus and mLN were assessed 3 days later. Samples were analysed using flow cytometry and total numbers calculated per whole thymus or mLN. Flow cytometry gates shown in blue, green, purple and orange correspond with iNKT cells,  $\alpha\beta$  T cells,  $\gamma\delta$  T cells and ILCs, respectively. Data shown in red corresponds with RFP<sup>+</sup> cells.

- A) Representative flow cytometry plots for the identification of RFP<sup>+</sup> cells amongst iNKT cells (CD1d-tetramer<sup>+</sup> TCR $\beta$ <sup>+</sup>),  $\alpha\beta$  T cells (CD1d-tetramer<sup>-</sup> TCR $\beta$ <sup>+</sup>),  $\gamma\delta$  T cells (CD1d-tetramer<sup>-</sup> TCR $\beta$ <sup>-</sup> TCR $\gamma\delta$ <sup>+</sup>) and ILCs (CD1d-tetramer<sup>-</sup> TCR $\beta$ <sup>-</sup> TCR $\gamma\delta$ <sup>-</sup> IL-7R $\alpha$ <sup>+</sup> Lineage<sup>-</sup>) in the mLN. Lineage channel consists of antibodies against CD3, CD5, Gr-1, CD11c and B220.
- B) Representative flow cytometry plots for the identification of RFP<sup>+</sup> cells amongst iNKT cells,  $\alpha\beta$  T cells,  $\gamma\delta$  T cells and ILCs in the thymus. Lineage channel consists of antibodies against CD3, CD5, Gr-1, CD11c and B220.
- C) Gating controls for RFP<sup>+</sup> cells in the mLN were based on RFP expression in mLN of Id2<sup>ERT2</sup> x ROSA26<sup>RFP</sup> mice that are absent of cre.
- D) Gating controls for RFP<sup>+</sup> cells in the thymus were based on RFP expression in thymus of Id2<sup>ERT2</sup> x ROSA26<sup>RFP</sup> mice that are absent of cre.
- E) Proportion of RFP<sup>+</sup> cells amongst iNKT cells,  $\alpha\beta$  T cells,  $\gamma\delta$  T cells and ILCs in the mLN.
- F) Proportion of RFP<sup>+</sup> cells amongst iNKT cells,  $\alpha\beta$  T cells,  $\gamma\delta$  T cells and ILCs in the thymus.

Kruskal-Wallis one-way ANOVA with post hoc Dunn's test was used (comparing three or more data sets) for statistical analysis where \*p<0.05, \*\*p<0.01, \*\*\*p<0.001, In all graphs the bar represents the median, n=6. Data shown from two independent experiments.





In order to interpret these findings it is important to appreciate the efficiency of cre induction in these cells. While the proportion of iNKT cells that fate-map to Id2 is ~50% in both the mLN and thymus, this is comparable to the proportion of ILC that fate-map to Id2 in the mLN. Given that all ILC require Id2, it is possible to suggest the labelling efficiency within our model to be ~50%; indicating all iNKT cells also express Id2 and not just the proportion that were shown to fate-map to Id2. Together, these data demonstrate the proportion of cells that fate-map to Id2 varies in different lymphocyte populations. The greatest proportion of cells that fate-map to Id2 is shown amongst iNKT cells and ILC, while only a small percentage of  $\alpha\beta$  T cells and  $\gamma\delta$  T cells were shown to fate-map to this transcription factor. The reason for these differences is poorly understood and our subsequent investigation will explore the expression of Id2 in iNKT cell,  $\alpha\beta$  T cell and  $\gamma\delta$  T cell populations. However, no further investigation of ILC will be made given these cells are the focus of Chapter 3 and Chapter 4.

### **5.2.2 Id2 is expressed by iNKT1, iNKT2 and iNKT17 cells in the thymus and is maintained in the periphery**

The developing thymus encompasses a subpopulation of innate lymphocytes known as iNKT cells and, while NKT cells in their entirety can be subdivided into several classes, iNKT cells are the most commonly studied.(58) This is owing to the highly restricted TCR $\alpha\beta$  chains amongst iNKT cells. In mice, these are V $\alpha$ 14, J $\alpha$ 18, V $\beta$ 2 V $\beta$ 7 and V $\beta$ 8, and are easily detected using CD1d-tetramers loaded with  $\alpha$ -GalCer, such as that used within our investigations.(58)

Whilst iNKT cells share some functional similarities to NK cells and conventional, naïve T cells, they also have immune functions distinct of both these cells. These

include the ability to activate naïve NK cells and B cells, and influence the bias of T cell responses and activity of DCs.(58–61,205) Moreover, these actions have been implicated in multiple disease states, such as bacterial and viral infections, cancer, autoimmune disease and allergy syndromes.(58) As aforementioned, the TCR repertoire of iNKT is highly restricted, differing greatly from that of naïve T cells. Furthermore, iNKT cells demonstrate an immediate TCR-mediated or cytokine stimulated immune reaction compared to a much slower response demonstrated by naïve T cells following initial T cell priming.(58) Most interestingly, immature iNKT cells are able to migrate into the periphery where they complete their final steps of maturation.(58)

As mentioned within the chapter introduction, the developmental stage of iNKT cells can be defined based on the expression of the cell surface markers CD44, CD24 and NK1.1. In addition, mature iNKT cells can be sub-divided into iNKT1, iNKT2 and iNKT17 cells defined by the expression of Tbet, PLZF and ROR $\gamma$ t. Previously published research has demonstrated Id2 expression to be greater in mature iNKT1 cells, which are Tbet<sup>+</sup>.(77) As such, we sought to confirm these findings using our *in vivo* models and question whether Id2 influences the function of these cells. Given that mature iNKT cells are present within the thymus and at peripheral sites, cells isolated from the thymus and peripheral sites will be investigated.

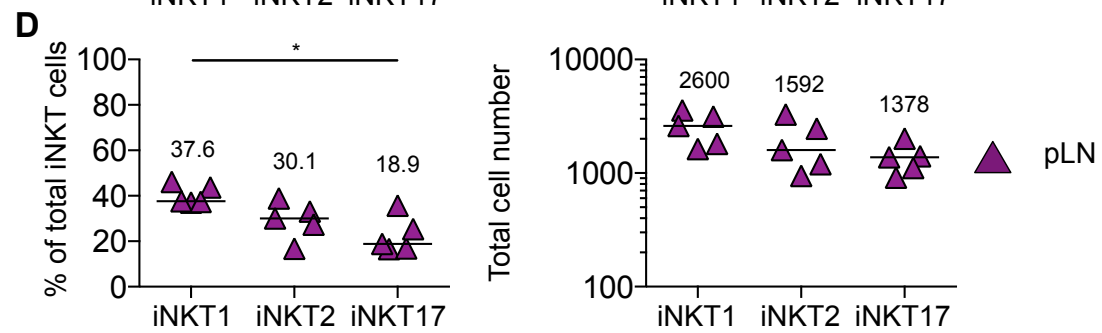
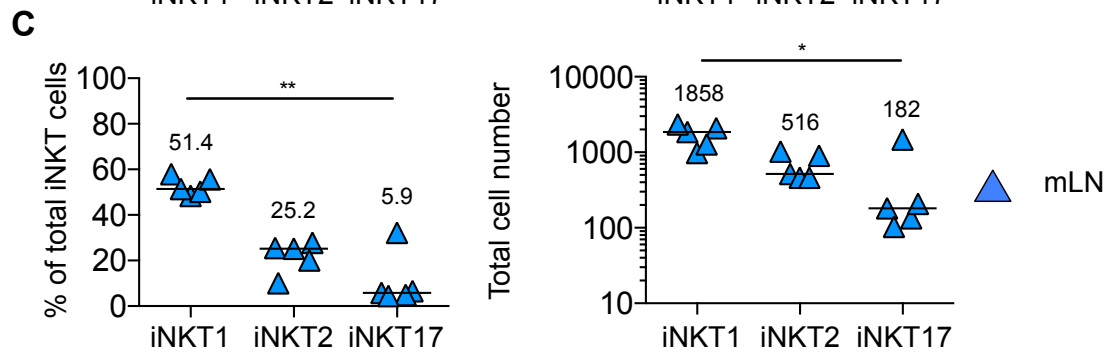
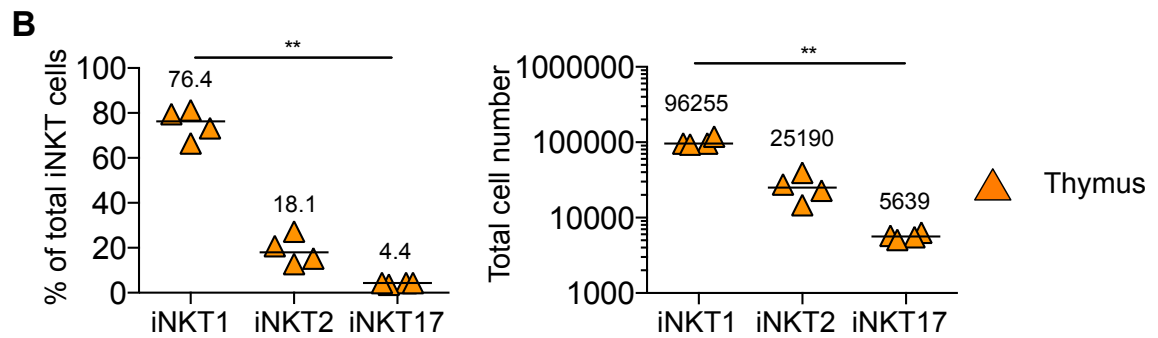
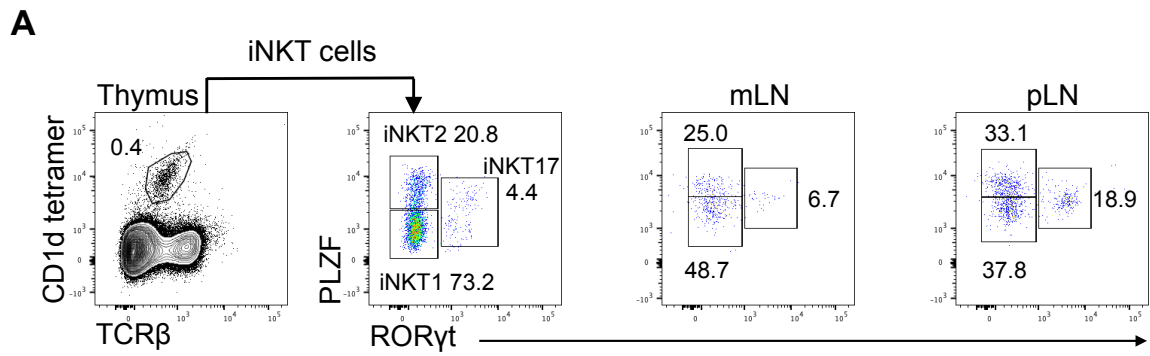
Although iNKT1, iNKT2 and iNKT17 cells have previously been defined in the thymus and at peripheral sites, we wanted to demonstrate that we were capable of identifying these populations in our investigations (Figure 5.3). To achieve this, cells were isolated from the thymus, mLN and pLN of WT mice, and total iNKT cells were identified using a CD1d-tetramer (CD1d<sup>+</sup> TCR $\beta$ <sup>+</sup>). Total iNKT cells were first shown in

### **Figure 5.3 Identification of iNKT1, iNKT2 and iNKT17 cells in the thymus and peripheral lymph nodes**

iNKT1, iNKT2 and iNKT17 cells were identified in the thymus, mLN and pooled peripheral lymph nodes (pLN) of WT mice. Samples were analysed using flow cytometry and total numbers calculated per whole tissue. Pooled peripheral lymph nodes consisted of cells isolated from the axillary, cervical and inguinal lymph nodes to provide a sufficient number of cells for analysis. Data shown in orange, blue and purple corresponds with cells isolated from the thymus, mLN and pLN, respectively.

- A) Representative flow cytometry plots showing the identification of iNKT1 (PLZF<sup>-</sup> RORγt<sup>+</sup>), iNKT2 (PLZF<sup>+</sup> RORγt<sup>+</sup>) and iNKT17 (PLZF<sup>-</sup> RORγt<sup>+</sup>) subsets amongst total iNKT (CD1d-tetramer<sup>+</sup> TCRβ<sup>+</sup>) cells in the thymus, mLN and pLN.
- B) Comparison of the proportion and total number of iNKT1 amongst total iNKT in the thymus, mLN and pLN.
- C) Comparison of the proportion and total number of iNKT2 amongst total iNKT in the thymus, mLN and pLN.
- D) Comparison of the proportion and total number of iNKT17 amongst total iNKT in the thymus, mLN and pLN.

Kruskal-Wallis one-way ANOVA with post hoc Dunn's test was used (comparing three or more data sets) for statistical analysis where \*p<0.05, \*\*p<0.01, \*\*\*p<0.001, and \*\*\*\*p<0.0001. In all graphs the bar represents the median, n=4 (thymus) and 5 (mLN and pLN). Data shown from two independent experiments.



cells isolated from the thymus, where a greater number of cells aid their identification (Figure 5.3A). iNKT1, iNKT2 and iNKT17 subsets were identified amongst total iNKT cells using antibodies against PLZF and ROR $\gamma$ t (Figure 5.3A). As aforementioned, these transcription factors are commonly used to pull apart iNKT1 (PLZF<sup>lo</sup> ROR $\gamma$ t<sup>-</sup>), iNKT2 (PLZF<sup>hi</sup> ROR $\gamma$ t<sup>-</sup>) and iNKT17 (PLZF<sup>lo</sup> ROR $\gamma$ t<sup>+</sup>). This gating strategy was applied to cells isolated from the mLN and pLN. Interestingly, a cluster PLZF<sup>hi</sup> ROR $\gamma$ t<sup>+</sup> and PLZF<sup>lo</sup> ROR $\gamma$ t<sup>+</sup> cells were observed amongst iNKT17 cells isolated from the thymus that was not observed in the mLN or pLN.

iNKT1, iNKT2 and iNKT17 subsets were enumerated and compared within each tissue (Figure 5.3B-D). Comparison of these subsets within the thymus demonstrated iNKT1 to be the most abundant subset as demonstrated by the greatest proportion and total number of these cells when compared iNKT2 and iNKT17. These findings were also true of cells from the mLN where the greatest proportion and total number of cells was demonstrated by iNKT1 (Figure 5.3C). While the proportion of iNKT1 cells was significantly higher in the pLN than iNKT2 and iNKT 17, this was not true when comparing total numbers of iNKT1, iNKT2 and iNKT 17 where total numbers of these subsets were comparable (Figure 5.3D).

Figures 5.1 and 5.2 demonstrated almost half of all iNKT cells in the thymus and mLN expressed RFP; indicating the current or previous expression of Id2 amongst these cells. This is consistent with previously published data from other research groups that have described a role for both Id2 and Id3 in the development of iNKT subsets. While our data is not entirely novel, the consistency of our findings with published data provides further confidence in our experimental model in identifying cells that fate-map to Id2. Within the literature, Id2 is expressed in the greatest extent

by stage 3, mature iNKT cells (defined by CD24<sup>lo</sup> CD44<sup>hi</sup> NK1.1<sup>hi</sup> cells). Amongst these, the expression of Id2 in the thymus is significantly elevated in iNKT1 cells but expression was observed in all three subsets.(77) While these data described the influence of Id2 within the thymus, the role of this transcription factor at peripheral sites requires further work.

Building upon our previous data, we sought to examine iNKT subsets amongst GFP<sup>-</sup> and GFP<sup>+</sup> cells and thus indicating whether these cells express Id2. To achieve this, iNKT1, iNKT2 and iNKT17 subsets were characterised amongst cells isolated from thymus, mLN and pLN of Id2-eGFP mice, where the live reporting of Id2 might overcome the limits of cre induction. Total iNKT cells were first shown in the thymus using the CD1d-tetramer (CD1d<sup>+</sup> TCRβ<sup>+</sup>) and subsequent gating identified the GFP expression of these cells (Figure 5.4A; upper panel). Gating controls used cells isolated from the corresponding tissue of a WT mouse (shown in grey). Once again, iNKT subsets were defined amongst GFP<sup>-</sup> and GFP<sup>+</sup> cells using PLZF and RORγt (Figure 5.4A; upper panel). This gating strategy was applied to cells isolated from the mLN (middle panel) and pLN (lower panel) (Figure 5.4A). Observations from these FACS plots demonstrate all three subsets of iNKT could be identified in these tissues amongst both GFP<sup>-</sup> and GFP<sup>+</sup> populations. However, it should be noted that the expression of GFP in these mice is low and therefore gating on GFP<sup>+</sup> is not clear. Furthermore, the GFP<sup>-</sup> and GFP<sup>+</sup> cells are not distinct and suggest homogenous low expression of GFP by all cells. Based on previously published research it is likely that all iNKT cells are GFP<sup>+</sup> and not just a proportion.(77)

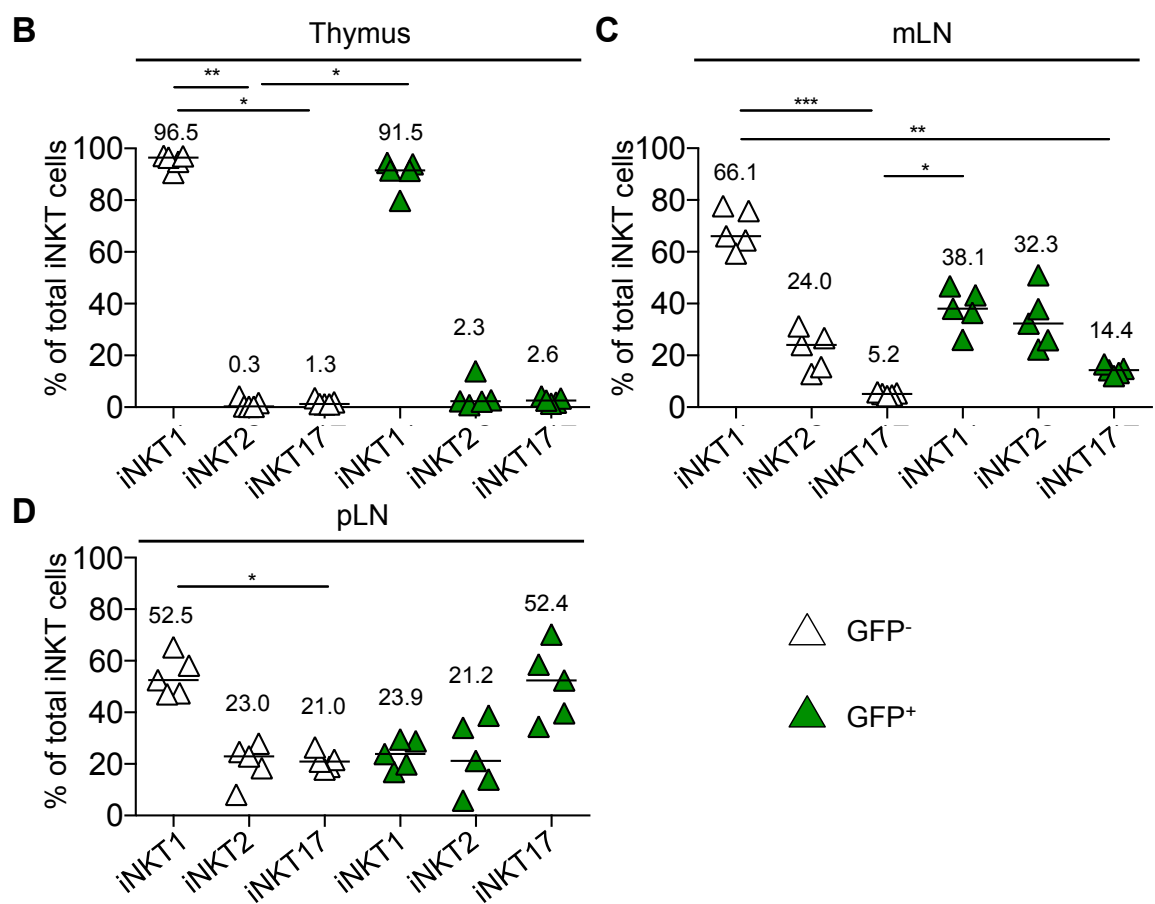
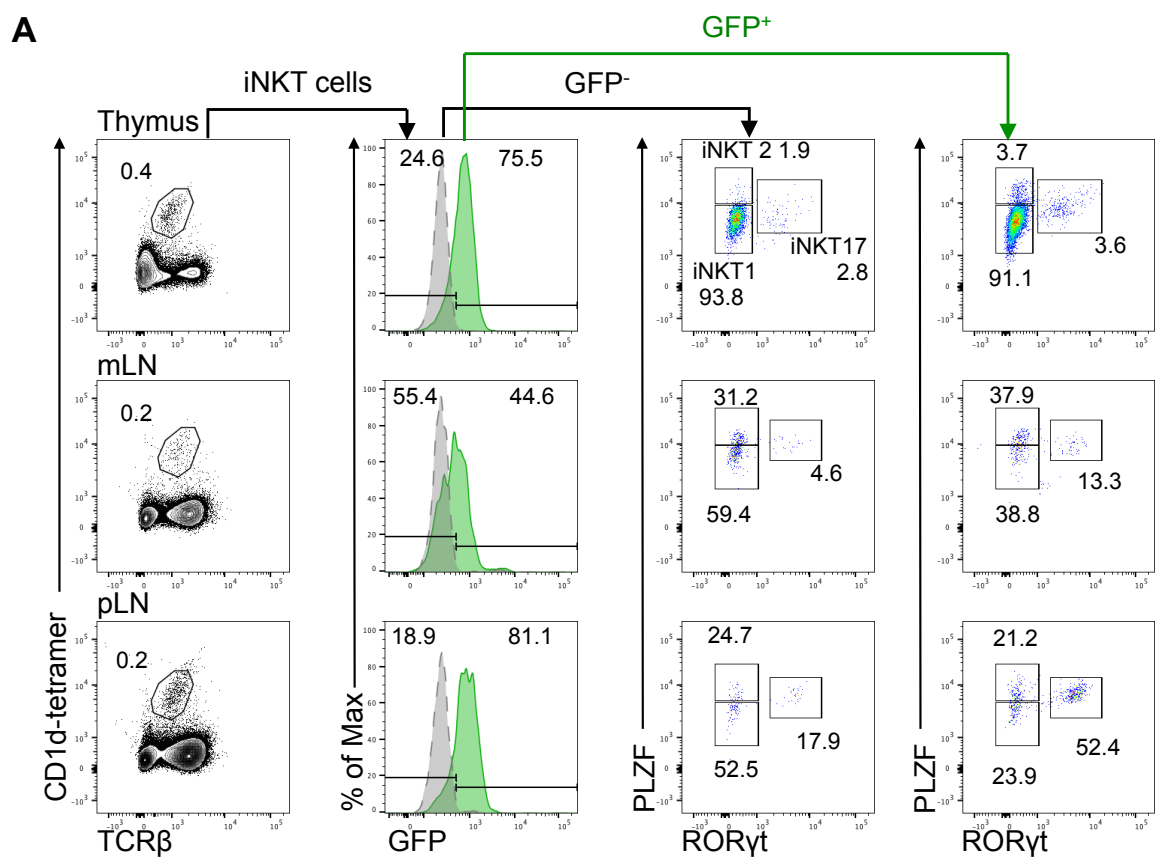
The proportions of iNKT1, iNKT2 and iNKT17 subsets amongst GFP<sup>-</sup> and GFP<sup>+</sup> cells were enumerated and compared within each tissue (Figure 5.4B-D). Consistent with

**Figure 5.4 Id2 is expressed by iNKT1, iNKT2 and iNKT17 cells in the thymus and is maintained in peripheral lymph nodes**

To directly assess the expression of Id2 by iNKT subsets in the thymus, mLN and pLN, cells isolated from these tissues were assessed in Id2-eGFP reporter mice. Samples were analysed using flow cytometry and total numbers calculated per whole tissue. Pooled peripheral lymph nodes consisted of cells isolated from the axillary, cervical and inguinal lymph nodes to provide a sufficient number of cells for analysis. Data shown in white and green corresponds with GFP<sup>-</sup> and GFP<sup>+</sup> cells, respectively.

- A) Full gating strategy for the identification of iNKT1 (PLZF<sup>-</sup> RORγt<sup>-</sup>), iNKT2 (PLZF<sup>+</sup>RORγt<sup>-</sup>) and iNKT17 (PLZF<sup>-</sup> RORγt<sup>+</sup>) amongst GFP<sup>-</sup> (CD1d-tetramer<sup>+</sup> TCRβ<sup>+</sup> GFP<sup>-</sup>) and GFP<sup>+</sup> (CD1d-tetramer<sup>+</sup> TCRβ<sup>+</sup> GFP<sup>+</sup>) iNKT cells in the thymus (upper panel), mLN (middle panel) and pLN (lower panel) of Id2-eGFP mice.
- B) Proportion of iNKT1, iNKT2 and iNKT17 subsets amongst GFP<sup>-</sup> and GFP<sup>+</sup> iNKT cells in the thymus.
- C) Proportion of iNKT1, iNKT2 and iNKT17 subsets amongst GFP<sup>-</sup> and GFP<sup>+</sup> iNKT cells in the mLN.
- D) Proportion of iNKT1, iNKT2 and iNKT17 subsets amongst GFP<sup>-</sup> and GFP<sup>+</sup> iNKT cells in the pLN.

Kruskal-Wallis one-way ANOVA with post hoc Dunn's test was used (comparing three or more data sets) for statistical analysis where \*p<0.05, \*\*p<0.01, \*\*\*p<0.001, and \*\*\*\*p<0.0001. In all graphs the bar represents the median, n=5. Data shown from two independent experiments.





our findings in Figure 5.3, iNKT1 were the most abundant cells amongst iNKT cells in the thymus. Importantly, we observed no difference between the proportion of iNKT1 amongst GFP<sup>-</sup> and GFP<sup>+</sup> cells (Figure 5.4B). Concerning iNKT cells of the mLN, iNKT1 cells were the most abundant subset amongst GFP<sup>-</sup> cells while iNKT subsets arising for GFP<sup>+</sup> cells indicate no significant difference in their proportion (Figure 5.4C). The results regarding the pLN prove most interesting. While the proportions of iNKT1 are the most abundant amongst GFP<sup>-</sup> cells, the proportions of these subsets appears the opposite amongst GFP<sup>+</sup> cells where iNKT17 cells have the greater proportion (Figure 5.4D). Overall, our investigations show Id2 to be expressed by all iNKT cells at peripheral sites while Id2 expression in the thymus was largely restricted to iNKT1 cells. Whether Id2 influences the function of these cells will be explored next.

To widen our understanding of the link between Id2 and cytokine production amongst iNKT cell subsets, Id2<sup>creERT2</sup> x ROSA26<sup>RFP</sup> mice were administered tamoxifen by oral gavage for 5 consecutive days and cells isolated from the thymus, mLN and spleen were used for analysis. Total iNKT cells were assessed for the production of IL-4 and IFN $\gamma$  following cell culture in the presence of PMA, ionomycin and BFA (Figure 5.5). In keeping with our previous approach, total iNKT cells were identified as CD1d-tetramer<sup>+</sup> TCR $\beta$ <sup>+</sup> cells in the thymus and subsequent gating defined these cells by their expression of RFP and their capability of producing IL-4 and IFN $\gamma$  (Figure 5.5A). This gating strategy was applied to cells of the mLN and pLN (Figure 5.5A). The proportion of IL-4 and IFN $\gamma$  production was enumerated and compared within each tissue (Figure 5.5B-D). These data demonstrated cells that produced both IL-4 and

IFN $\gamma$  (IL-4<sup>+</sup> IFN $\gamma$ <sup>+</sup>) to be the most abundant amongst RFP<sup>-</sup> and RFP<sup>+</sup> cells in all three tissues (Figure 5.5B-D). Moreover, no significant difference between the proportions of cells producing only IL-4 or IFN $\gamma$  was observed within each tissue (Figure 5.5B-D). Figure 5.4 demonstrated the proportion of iNKT17 cells to increase in GFP<sup>+</sup> iNKT cells compared to those that were GFP<sup>-</sup>. However, IL-17A, a key cytokine produced by iNKT17 cells, was not assessed within Figure 5.5. Future work would aim to investigate whether the production of IL-17A amongst iNKT17 cells differed between GFP<sup>-</sup> and GFP<sup>+</sup> cells. Overall, these data highlight no clear difference in the function of cells that fate-map or do not fate-map to Id2. As previously discussed, it is likely that all iNKT cells express Id2 and the efficiency of cre induction is the reason for the split in iNKT populations that either fate-map or do not-fate map to Id2. This idea is supported by this data where no differences are observed between iNKT cells that fate map to Id2 and those that do not.

### **5.2.3 $\gamma\delta$ T cells of multiple developmental lineages express Id2**

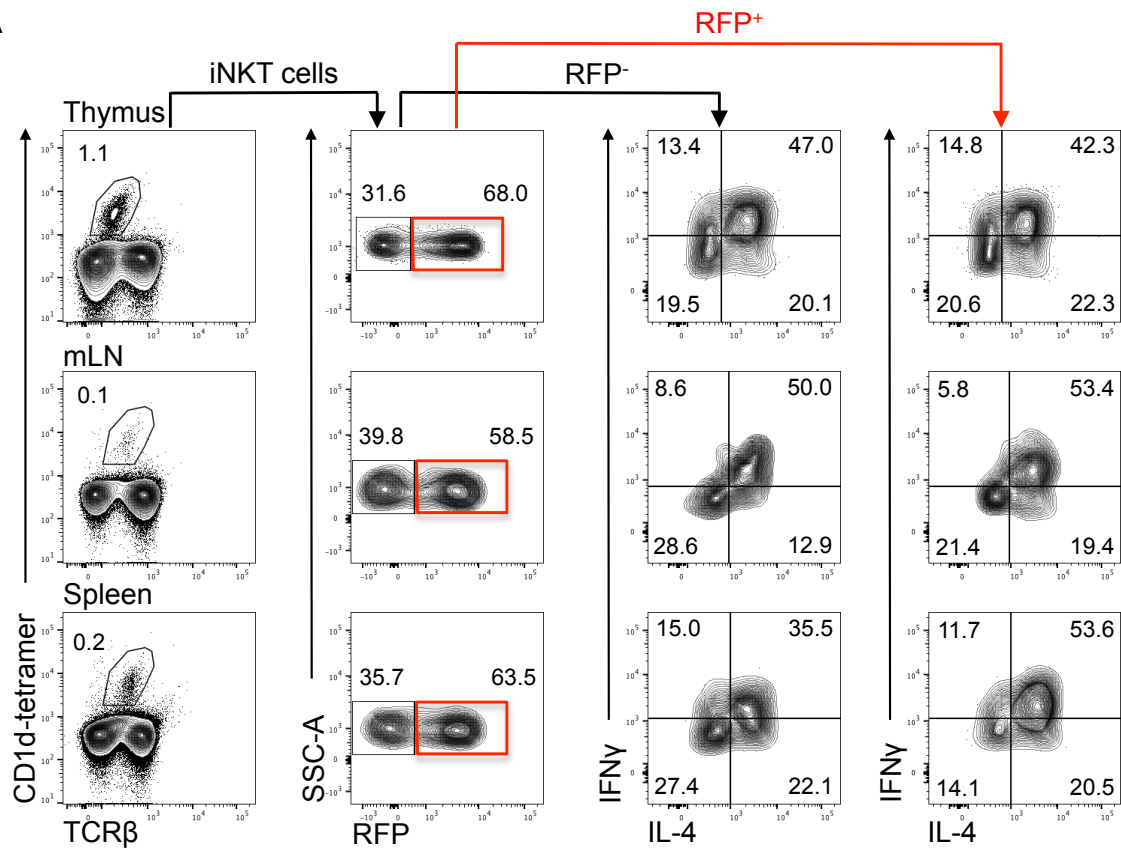
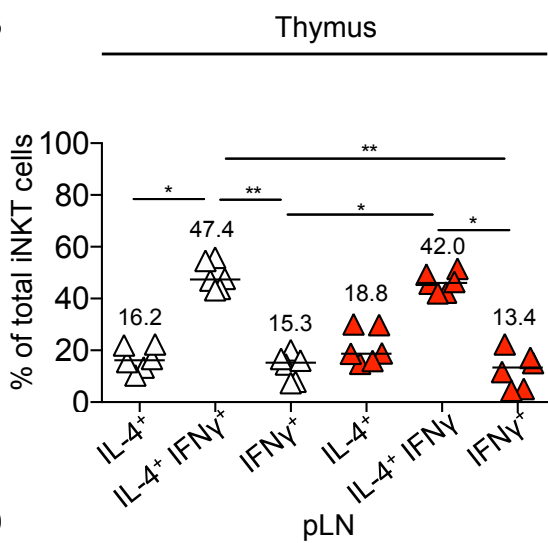
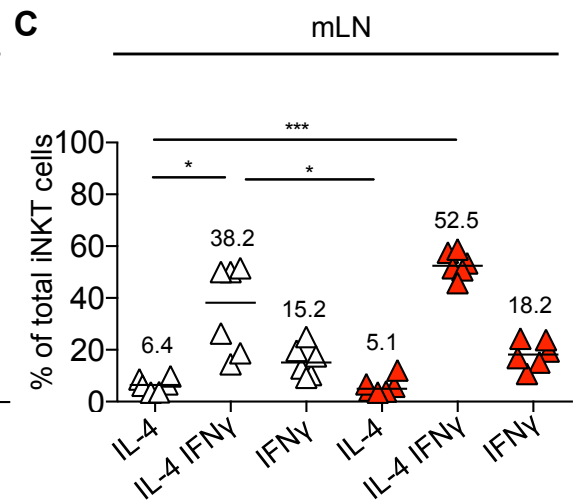
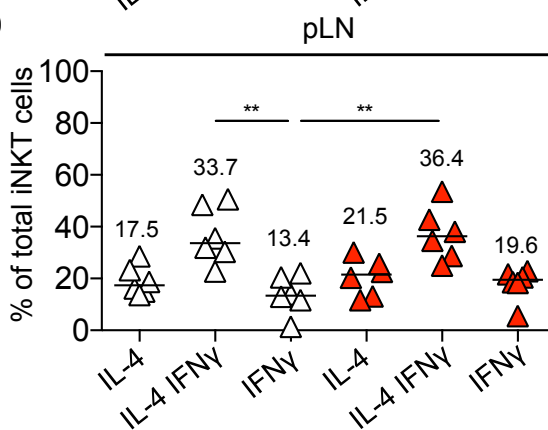
The data described within Figure 5.1 demonstrate  $\gamma\delta$  T cells to arise from RFP<sup>+</sup> cells in both the mLN and thymus; thus indicating their current or previous expression of Id2. However, the proportion of  $\gamma\delta$  T cells amongst RFP<sup>+</sup> cells is greater in the thymus than the mLN. It is possible this change could reflect a requirement for Id2 in the thymus during  $\gamma\delta$  T cell development or RFP<sup>+</sup>  $\gamma\delta$  T cells exiting the thymus and migrating to tissues other than the mLN. This section of work aims to examine the expression of Id2 amongst  $\gamma\delta$  T cells in the thymus and at peripheral sites. Moreover, this work aims to determine whether  $\gamma\delta$  T cells of a certain developmental lineage require Id2.

**Figure 5.5 The fate-mapping of iNKT cells to Id2 does not affect the ability of these cells to produce IL-4 or IFN $\gamma$**

To investigate the correlation between Id2 and the capability of iNKT cells to produce IFN $\gamma$  and IL-4, iNKT cells from the thymus, mLN and spleen of Id2<sup>creERT2</sup> x ROSA26<sup>RFP</sup> mice were assessed. Administration of tamoxifen by oral gavage on five consecutive days was performed and tissues were analysed 3 days later. Samples were analysed using flow cytometry and total numbers calculated per whole tissue. Data shown in red corresponds with RFP<sup>+</sup> cells.

- A) Full gating strategy for the identification of RFP<sup>-</sup> and RFP<sup>+</sup> cells amongst IFN $\gamma$ <sup>+</sup> and IL-4<sup>+</sup> iNKT cells (CD1d-tetramer<sup>+</sup> TCR $\beta$ <sup>+</sup>) in the thymus (upper panel), mLN (middle panel) and spleen (lower panel) of Id2<sup>creERT2</sup> x ROSA26<sup>RFP</sup> mice.
- B) Proportion of IFN $\gamma$  and IL-4 expression amongst RFP<sup>-</sup> and RFP<sup>+</sup> iNKT cells in the thymus.
- C) Proportion of IFN $\gamma$  and IL-4 expression amongst RFP<sup>-</sup> and RFP<sup>+</sup> iNKT cells in the mLN.
- D) Proportion of IFN $\gamma$  and IL-4 expression amongst RFP<sup>-</sup> and RFP<sup>+</sup> iNKT cells in the spleen.

Kruskal-Wallis one-way ANOVA with post hoc Dunn's test was used (comparing three or more data sets) for statistical analysis where \*p<0.05, \*\*p<0.01, \*\*\*p<0.001, and \*\*\*\*p<0.0001. In all graphs the bar represents the median, n=6. Data shown from two independent experiments.

**A****B****C****D**

△ RFP<sup>-</sup>  
 ▲ RFP<sup>+</sup>

$\gamma\delta$  T cells can be divided into three main classes based on their effector function.(65) The proceeding investigations will focus on two of these subclasses that are defined by their ability to produce IL-17 or IFN $\gamma$ .(68) It is well established that  $\gamma\delta$  T cells emigrate the thymus in a naïve state and obtain their effector function following priming in peripheral lymph nodes. However, programming of  $\gamma\delta$  T cell effector fate is predominantly performed within the thymus prior to their migration into the periphery.(68) Moreover, this commitment of  $\gamma\delta$  T cells to IFN $\gamma$  or IL-17 lineages results from developmental waves based on different V $\gamma$  segment usage.(67,68) Based on the Garman nomenclature,  $\gamma\delta$  T cells that express either V $\gamma$ 1.1, V $\gamma$ 3 or V $\gamma$ 5 segments primarily develop towards the IFN $\gamma$  producing lineage while  $\gamma\delta$  T cells that express the V $\gamma$ 4 segment developing into IL-17 producing cells. Interestingly, those  $\gamma\delta$  T cells that expression the V $\gamma$ 2 segment are capable of developing into either IFN $\gamma$  or IL-17 producing cells.(68,69)

Data published by Sumira *et al.* (2017) demonstrated TCR $\gamma\delta$  signal strength as another factor that influenced the developmental pathways of  $\gamma\delta$  T cells and, ultimately, the functional capabilities of these cells.(206) This research illustrated strong TCR $\gamma\delta$  signaling characterised the development of IFN $\gamma$ -producing  $\gamma\delta$  T cells and the inhibition of the development of cells capable of IL-17A. In contrast, IL-17A-producing  $\gamma\delta$  T cells result from weak TCR $\gamma\delta$  signaling. Furthermore, CD44 and CD45RB can be used to pull apart these subsets amongst mature  $\gamma\delta$  T cells (TCR $\gamma\delta^+$  CD24 $^-$ ).  $\gamma\delta$  T cells restricted to an IFN $\gamma$ -producing lineage are defined as CD44 $^{hi}$  CD45RB $^+$  while those restricted to an IL-17A-producing phenotype are described as CD44 $^{hi}$  CD45RB $^-$ . Studies that have investigated the involvement of Id2 in  $\gamma\delta$  T cell development are limited and therefore warrant further research.(66)

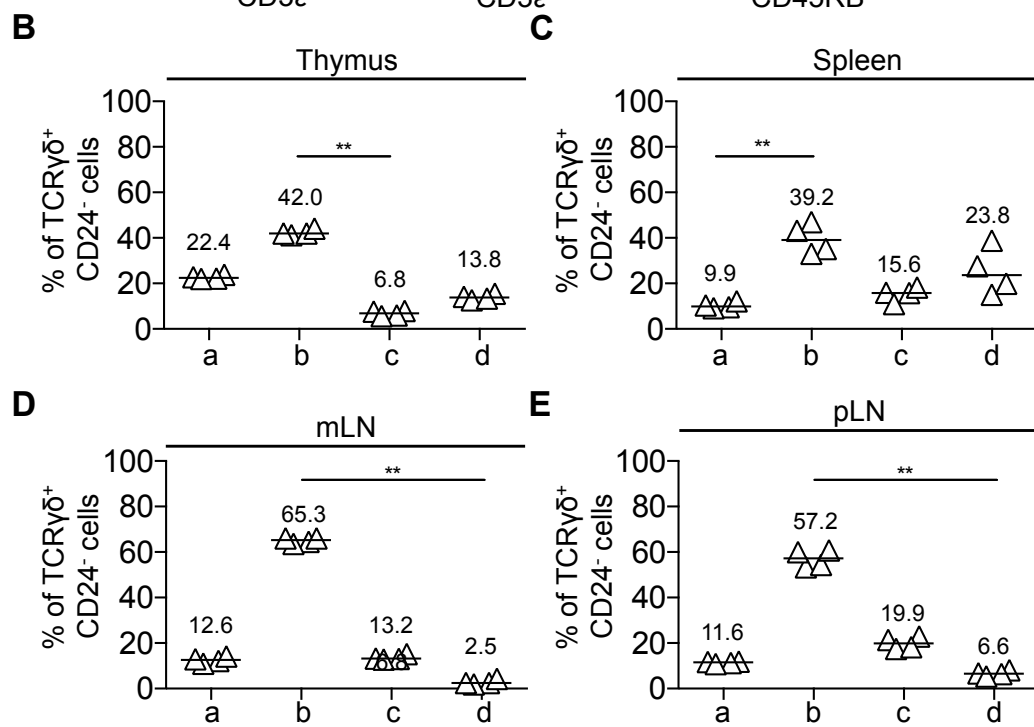
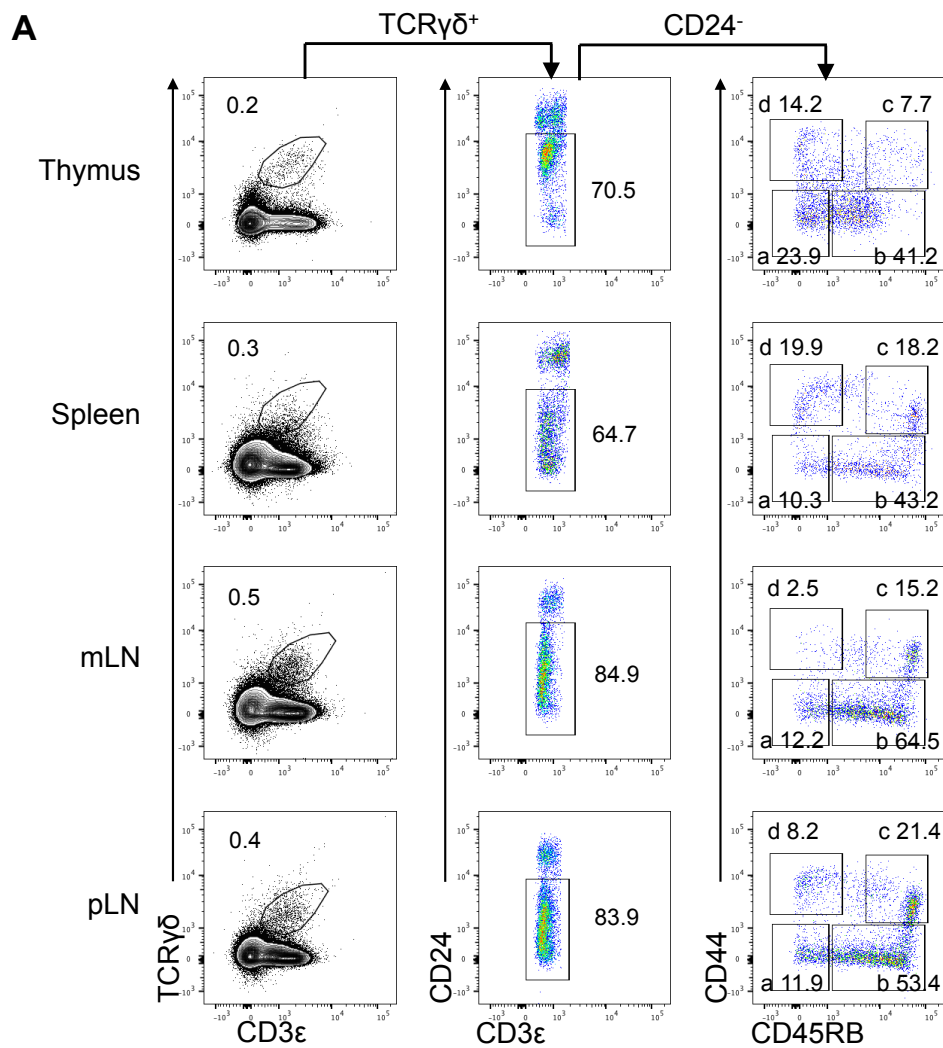
Prior to exploring the expression of Id2 amongst IFN $\gamma$  and IL-17A producing  $\gamma\delta$  T cells, we first sought to mimic the gating strategy previously published by Sumira *et al.* (2017) to identify these cells within our laboratory using WT mice (Figure 5.6). (206) To perform this, cells were isolated from the thymus, spleen, mLN and pLN of WT mice and mature  $\gamma\delta$  T cells (TCR $\gamma\delta^+$  CD3 $\epsilon^+$  CD24 $^-$ ) were assessed for their expression of CD44 and CD45RB. The study undertaken by Sumira *et al.* (2017) utilized cells of the thymus and peripheral lymph and, as such, we decided to isolate cells from these tissues within our investigation. (206) Using cells isolated from the thymus, mature  $\gamma\delta$  T cells were identified as TCR $\gamma\delta^+$  CD3 $\epsilon^+$  CD24 $^-$  (Figure 5.6). Arising from these cells, four subsets were identified based on their expression of CD44 and CD45RB: CD44 $^{lo}$  CD45RB $^-$  (a), CD44 $^{lo}$  CD45RB $^+$  (b), CD44 $^{hi}$  CD45RB $^+$  (c) and CD44 $^{hi}$  CD45RB $^-$  (d). This gating strategy was later applied to cells isolated from the spleen, mLN and pLN, respectively (Figure 5.6). Each of these populations, 'a', 'b', 'c' and 'd', were enumerated and the proportions of each were compared within their tissue of origin (Figures 5.6B-E). Evidence from the thymus demonstrated all four subsets of mature  $\gamma\delta$  T cells to be present with CD44 $^{lo}$  CD45RB $^+$  (b) cells being the most abundant (Figure 5.6B). These findings were also true at peripheral sites where CD44 $^{lo}$  CD45RB $^+$  (b) cells were the most abundant in the spleen, mLN and pLN (Figure 5.6C-E). These findings are consistent with the work previously published by Sumira *et al.* (2017). (206) Figure 5.6 demonstrated CD44 $^{lo}$  CD45RB $^-$  (a), CD44 $^{lo}$  CD45RB $^+$  (b), CD44 $^{hi}$  CD45RB $^+$  (c) and CD44 $^{hi}$  CD45RB $^-$  (d) subsets could be identified amongst mature  $\gamma\delta$  T cells in the thymus and at peripheral sites.

**Figure 5.6  $\gamma\delta$  T cells can be classified based on their commitment to IL-17A-producing or IFN $\gamma$ -producing lineages**

Total  $\gamma\delta$  T cells associated with an IL-17A or IFN $\gamma$  restricted phenotype were characterised in the thymus, spleen, mLN and pLN of Id2-eGFP mice prior to determining the GFP expression amongst these cells. Samples were analysed using flow cytometry with total numbers calculated per whole tissue. Pooled peripheral lymph nodes consisted of cells isolated from the axillary, cervical and inguinal lymph nodes to provide a sufficient number of cells for analysis. Data shown in green corresponds with GFP<sup>+</sup> cells.

- A) Representative flow cytometry plots for the identification of CD44<sup>-</sup> CD45RB<sup>-</sup> (a), CD44<sup>-</sup> CD45RB<sup>+</sup> (b), CD44<sup>+</sup> CD45RB<sup>+</sup> (c) and CD44<sup>+</sup> CD45RB<sup>-</sup> (d) cells amongst total  $\gamma\delta$  T cells (TCR $\gamma\delta$ <sup>+</sup> CD24<sup>-</sup>) in the thymus, spleen, mLN and pLN.
- B) Proportion of CD44<sup>-</sup> CD45RB<sup>-</sup> (a), CD44<sup>-</sup> CD45RB<sup>+</sup> (b), CD44<sup>+</sup> CD45RB<sup>+</sup> (c) and CD44<sup>+</sup> CD45RB<sup>-</sup> (d) cells amongst total  $\gamma\delta$  T cells (TCR $\gamma\delta$ <sup>+</sup> CD24<sup>-</sup>) in the thymus.
- C) Proportion of CD44<sup>-</sup> CD45RB<sup>-</sup> (a), CD44<sup>-</sup> CD45RB<sup>+</sup> (b), CD44<sup>+</sup> CD45RB<sup>+</sup> (c) and CD44<sup>+</sup> CD45RB<sup>-</sup> (d) cells amongst total  $\gamma\delta$  T cells (TCR $\gamma\delta$ <sup>+</sup> CD24<sup>-</sup>) in the spleen.
- D) Proportion of CD44<sup>-</sup> CD45RB<sup>-</sup> (a), CD44<sup>-</sup> CD45RB<sup>+</sup> (b), CD44<sup>+</sup> CD45RB<sup>+</sup> (c) and CD44<sup>+</sup> CD45RB<sup>-</sup> (d) cells amongst total  $\gamma\delta$  T cells (TCR $\gamma\delta$ <sup>+</sup> CD24<sup>-</sup>) in the mLN.
- E) Proportion of CD44<sup>-</sup> CD45RB<sup>-</sup> (a), CD44<sup>-</sup> CD45RB<sup>+</sup> (b), CD44<sup>+</sup> CD45RB<sup>+</sup> (c) and CD44<sup>+</sup> CD45RB<sup>-</sup> (d) cells amongst total  $\gamma\delta$  T cells (TCR $\gamma\delta$ <sup>+</sup> CD24<sup>-</sup>) in the pLN.

Kruskal-Wallis one-way ANOVA with post hoc Dunn's test was used (comparing three or more data sets) for statistical analysis where \*\*p<0.01. In all graphs the bar represents the median, n=4. Data for all time points shown from one independent experiment.





Following from this, we sought to identify whether the proportions of these subsets differed when gating on GFP<sup>+</sup>  $\gamma\delta$  T cells only. To achieve this, CD44<sup>lo</sup> CD45RB<sup>-</sup> (a), CD44<sup>lo</sup> CD45RB<sup>+</sup> (b), CD44<sup>hi</sup> CD45RB<sup>+</sup> (c) and CD44<sup>hi</sup> CD45RB<sup>-</sup> (d) subsets were assessed amongst GFP<sup>+</sup>  $\gamma\delta$  T cells isolated from the thymus, spleen, mLN and pLN of Id2-eGFP reporter mice. The gating strategy utilised in Figure 5.6 was adapted so that Id2 expression could be assessed. Mature, GFP<sup>+</sup>  $\gamma\delta$  T cells were identified in all tissues as TCR $\gamma\delta$ <sup>+</sup> CD3 $\epsilon$ <sup>+</sup> GFP<sup>+</sup> CD24<sup>-</sup> cells and subsets 'a', 'b', 'c' and 'd' were identified based on their expression of CD44 and CD45RB (Figure 5.7A). Gating controls for GFP expression used cells isolated from the thymus of a WT mouse (Figure 5.7B).

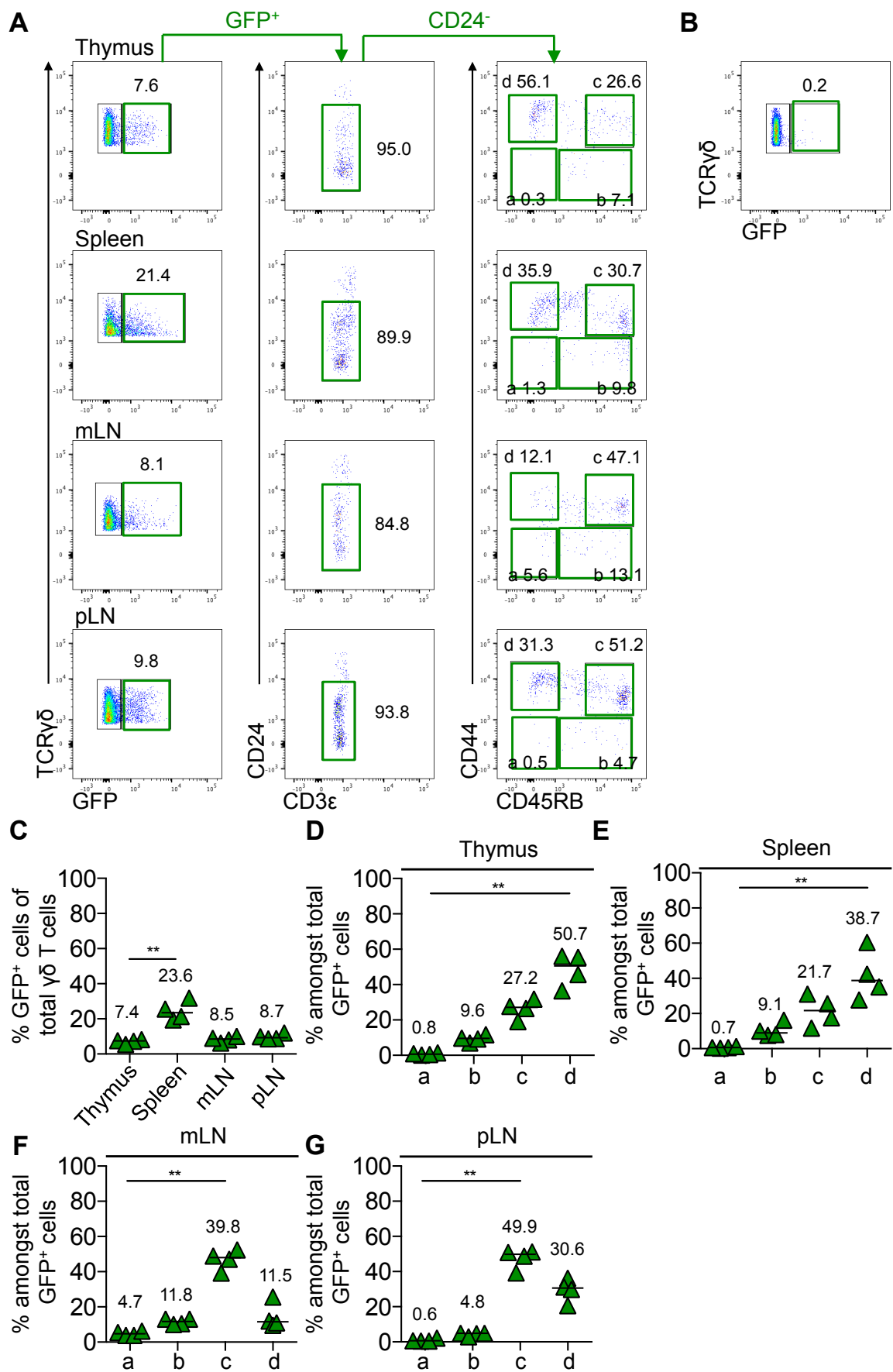
Following enumeration, the proportion of GFP expressed by  $\gamma\delta$  T cells was compared across tissues (Figure 5.7C). This revealed the expression of GFP by  $\gamma\delta$  T cells in the spleen to be much greater than other tissues (Figure 5.7C). To address our original question of whether the proportion of CD44<sup>lo</sup> CD45RB<sup>-</sup> (a), CD44<sup>lo</sup> CD45RB<sup>+</sup> (b), CD44<sup>hi</sup> CD45RB<sup>+</sup> (c) and CD44<sup>hi</sup> CD45RB<sup>-</sup> (d) subsets changed following prior gating on GFP<sup>+</sup> cells, these subsets were compared within each tissue. In the thymus, CD44<sup>hi</sup> CD45RB<sup>-</sup> (d) cells account for approximately half GFP<sup>+</sup>  $\gamma\delta$  T cells. Furthermore, CD44<sup>hi</sup> CD45RB<sup>-</sup> (d) cells are significantly higher compared to CD44<sup>lo</sup> CD45RB<sup>-</sup> (a), which were negligible (Figure 5.7D). Interestingly, CD44<sup>hi</sup> CD45RB<sup>+</sup> (c) cells account for approximately one quarter of GFP<sup>+</sup>  $\gamma\delta$  T cells (Figure 5.7D) while this population were the least abundant when looking at total  $\gamma\delta$  T cells (Figure 5.6A-B). Concerning the spleen, the proportions of CD44<sup>lo</sup> CD45RB<sup>-</sup> (a),

**Figure 5.7 Id2 is expressed in  $\gamma\delta$  T cells of both the IL-17A-producing and IFN $\gamma$ -producing lineage**

$\gamma\delta$  T cells associated with an IL-17A or IFN $\gamma$  restricted phenotype were characterised in the thymus, spleen, mLN and pLN of Id2-eGFP mice to identify cells that express Id2. Samples were analysed using flow cytometry with total numbers calculated per whole tissue. Pooled peripheral lymph nodes consisted of cells isolated from the axillary, cervical and inguinal lymph nodes to provide a sufficient number of cells for analysis. Data shown in green corresponds with GFP<sup>+</sup> cells.

- A) Representative flow cytometry plots for the identification of CD44<sup>-</sup> CD45RB<sup>-</sup> (a), CD44<sup>-</sup> CD45RB<sup>+</sup> (b), CD44<sup>+</sup> CD45RB<sup>+</sup> (c) and CD44<sup>+</sup> CD45RB<sup>-</sup> (d) cells amongst GFP<sup>+</sup>  $\gamma\delta$  T cells (TCR $\gamma\delta$ <sup>+</sup> GFP<sup>+</sup> CD24<sup>-</sup>) in the thymus, spleen, mLN and pLN. Cells were pre-gated on TCR $\gamma\delta$ <sup>+</sup> CD3 $\epsilon$ <sup>+</sup> cells.
- B) Gating controls for GFP expression were based on cells isolated from the thymus of a WT mouse.
- C) Comparison of the proportion of GFP<sup>+</sup>  $\gamma\delta$  T cells in the thymus, spleen, mLN and pLN.
- D) Proportion of CD44<sup>-</sup> CD45RB<sup>-</sup> (a), CD44<sup>-</sup> CD45RB<sup>+</sup> (b), CD44<sup>+</sup> CD45RB<sup>+</sup> (c) and CD44<sup>+</sup> CD45RB<sup>-</sup> (d) cells amongst GFP<sup>+</sup>  $\gamma\delta$  T cells (TCR $\gamma\delta$ <sup>+</sup> GFP<sup>+</sup> CD24<sup>-</sup>) in the thymus.
- E) Proportion of CD44<sup>-</sup> CD45RB<sup>-</sup> (a), CD44<sup>-</sup> CD45RB<sup>+</sup> (b), CD44<sup>+</sup> CD45RB<sup>+</sup> (c) and CD44<sup>+</sup> CD45RB<sup>-</sup> (d) cells amongst GFP<sup>+</sup>  $\gamma\delta$  T cells (TCR $\gamma\delta$ <sup>+</sup> GFP<sup>+</sup> CD24<sup>-</sup>) in the spleen.
- F) Proportion of CD44<sup>-</sup> CD45RB<sup>-</sup> (a), CD44<sup>-</sup> CD45RB<sup>+</sup> (b), CD44<sup>+</sup> CD45RB<sup>+</sup> (c) and CD44<sup>+</sup> CD45RB<sup>-</sup> (d) cells amongst GFP<sup>+</sup>  $\gamma\delta$  T cells (TCR $\gamma\delta$ <sup>+</sup> GFP<sup>+</sup> CD24<sup>-</sup>) in the mLN.
- G) Proportion of CD44<sup>-</sup> CD45RB<sup>-</sup> (a), CD44<sup>-</sup> CD45RB<sup>+</sup> (b), CD44<sup>+</sup> CD45RB<sup>+</sup> (c) and CD44<sup>+</sup> CD45RB<sup>-</sup> (d) cells amongst GFP<sup>+</sup>  $\gamma\delta$  T cells (TCR $\gamma\delta$ <sup>+</sup> GFP<sup>+</sup> CD24<sup>-</sup>) in the pLN.

Kruskal-Wallis one-way ANOVA with post hoc Dunn's test was used (comparing three or more data sets) for statistical analysis where \*\*p<0.01. In all graphs the bar represents the median, n=4. Data for all time points shown from one independent experiment.



CD44<sup>lo</sup> CD45RB<sup>+</sup> (b), CD44<sup>hi</sup> CD45RB<sup>+</sup> (c) and CD44<sup>hi</sup> CD45RB<sup>-</sup> (d) subsets amongst GFP<sup>+</sup>  $\gamma\delta$  T cells appeared similar to that of the thymus with CD44<sup>hi</sup> CD45RB<sup>-</sup> (d) and CD44<sup>hi</sup> CD45RB<sup>+</sup> (c) cells being most abundant, respectively (Figure 5.7D-E). Analysis of these populations within the mLN demonstrated CD44<sup>hi</sup> CD45RB<sup>+</sup> (c) to be the most abundant subset (Figure 5.7F) and was also true in cells isolated from the spleen (Figure 5.7G). In all tissues, CD44<sup>lo</sup> CD45RB<sup>-</sup> (a) cells accounted for the smallest proportion of  $\gamma\delta$  T cells (Figure 5.7D-G).

Either CD44<sup>hi</sup> CD45RB<sup>+</sup> (c) or CD44<sup>hi</sup> CD45RB<sup>-</sup> (d)  $\gamma\delta$  T cells were the largest populations arising from GFP<sup>+</sup>  $\gamma\delta$  T cells in the thymus, spleen, mLN and pLN. Interestingly, it is these two subsets that have been associated with an IFN $\gamma$  or IL-17A-producing restricted phenotype. To investigate the usage of V $\gamma$ 1 and V $\gamma$ 2 expression amongst CD44<sup>hi</sup> CD45RB<sup>+</sup> (c) or CD44<sup>hi</sup> CD45RB<sup>-</sup> (d) GFP<sup>+</sup>  $\gamma\delta$  T cells, the expression of these  $\gamma$ -chains was assessed amongst these subsets in Id2-eGFP reporter mice (Figure 5.8). Representative flow cytometry plots illustrating V $\gamma$ 1<sup>+</sup>, V $\gamma$ 1<sup>-</sup> V $\gamma$ 2<sup>-</sup> and V $\gamma$ 2<sup>+</sup> cells amongst either CD44<sup>hi</sup> CD45RB<sup>+</sup> (c) or CD44<sup>hi</sup> CD45RB<sup>-</sup> (d) GFP<sup>+</sup>  $\gamma\delta$  T cells in the thymus, spleen, mLN and pLN is shown in Figure 5.8A. First assessing the expression of these  $\gamma$ -chains in the thymus, V $\gamma$ 1<sup>+</sup> cells are the most abundant amongst CD44<sup>hi</sup> CD45RB<sup>+</sup> (c) cells while the greatest proportion of cells amongst the CD44<sup>hi</sup> CD45RB<sup>-</sup> (d) lacked expression of both V $\gamma$ 1 and V $\gamma$ 2. However, the proportion of these V $\gamma$ 1<sup>-</sup> V $\gamma$ 2<sup>-</sup> cells was not significantly greater than V $\gamma$ 2<sup>+</sup> cells, which accounted for approximately one third of the CD44<sup>hi</sup> CD45RB<sup>-</sup> (d) subset.

At peripheral lymphoid sites,  $\gamma$ -chain usage was much more variable amongst CD44<sup>hi</sup> CD45RB<sup>+</sup> (c) and CD44<sup>hi</sup> CD45RB<sup>-</sup> (d) subsets. Of the CD44<sup>hi</sup> CD45RB<sup>+</sup> (c) cells in the spleen, the proportion of V $\gamma$ 2<sup>+</sup> cells was significantly greater than V $\gamma$ 1<sup>-</sup> V $\gamma$ 2<sup>-</sup> cells

but comparable to  $V\gamma 1^+$  cells (Figure 5.8C). However, analysis  $\gamma$ -chain usage amongst  $CD44^{hi} CD45RB^-$  (d) cells from the same tissue demonstrated the majority of these cells to lack the expression of both  $V\gamma 1$  and  $V\gamma 2$  (Figure 5.8C). Amongst the cells isolated from the mLN,  $V\gamma 1^+$  cells were predominant amongst  $CD44^{hi} CD45RB^+$  (c) cells while  $CD44^{hi} CD45RB^-$  (d) cells consisted of mainly  $V\gamma 1^- V\gamma 2^-$  cells (Figure 5.8D). The results for  $\gamma$ -chain usage amongst  $CD44^{hi} CD45RB^+$  (c) cells in the pLN were comparable to those of the mLN with the majority of these cells expressing  $V\gamma 1$  (Figure 5.8E). Amongst  $CD44^{hi} CD45RB^-$  (d) cells in the pLN, comparable proportions of  $V\gamma 1^- V\gamma 2^-$  and  $V\gamma 2^+$  were identified while the proportion of  $V\gamma 1^+$  cells was negligible (Figure 5.8E). Interestingly, the highest proportion of cells amongst the  $CD44^{hi} CD45RB^-$  (d) subset expressing  $V\gamma 2$  only was identified in the pLN (Figure 5.8E).

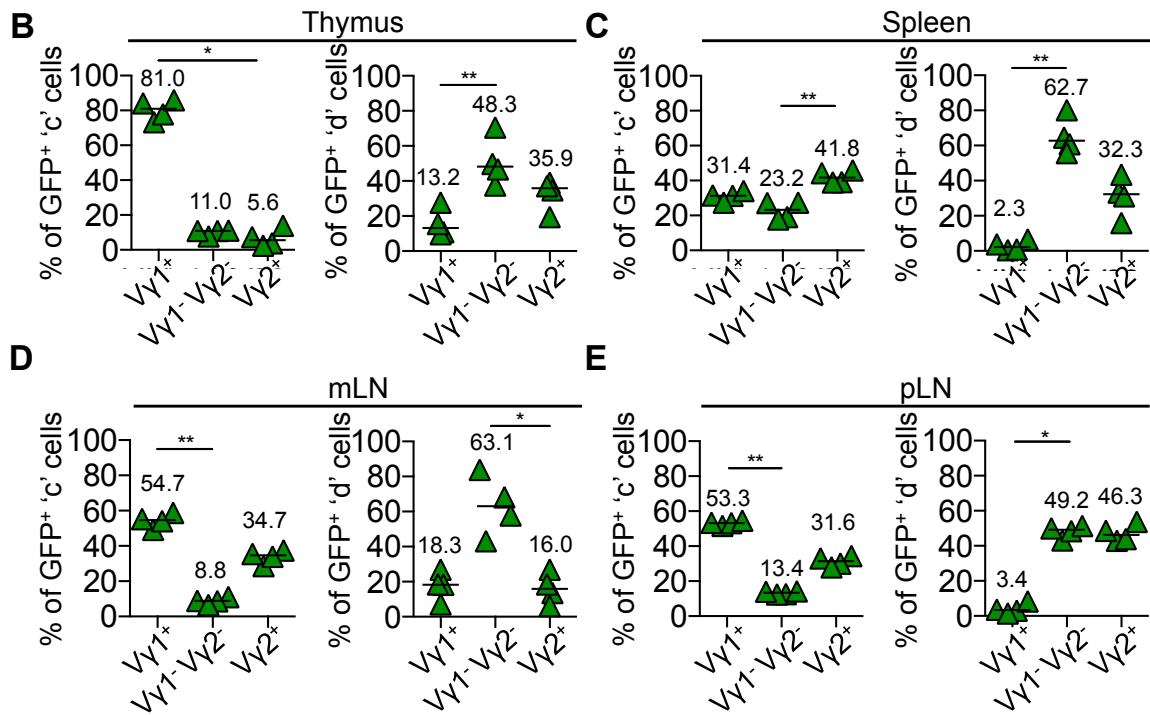
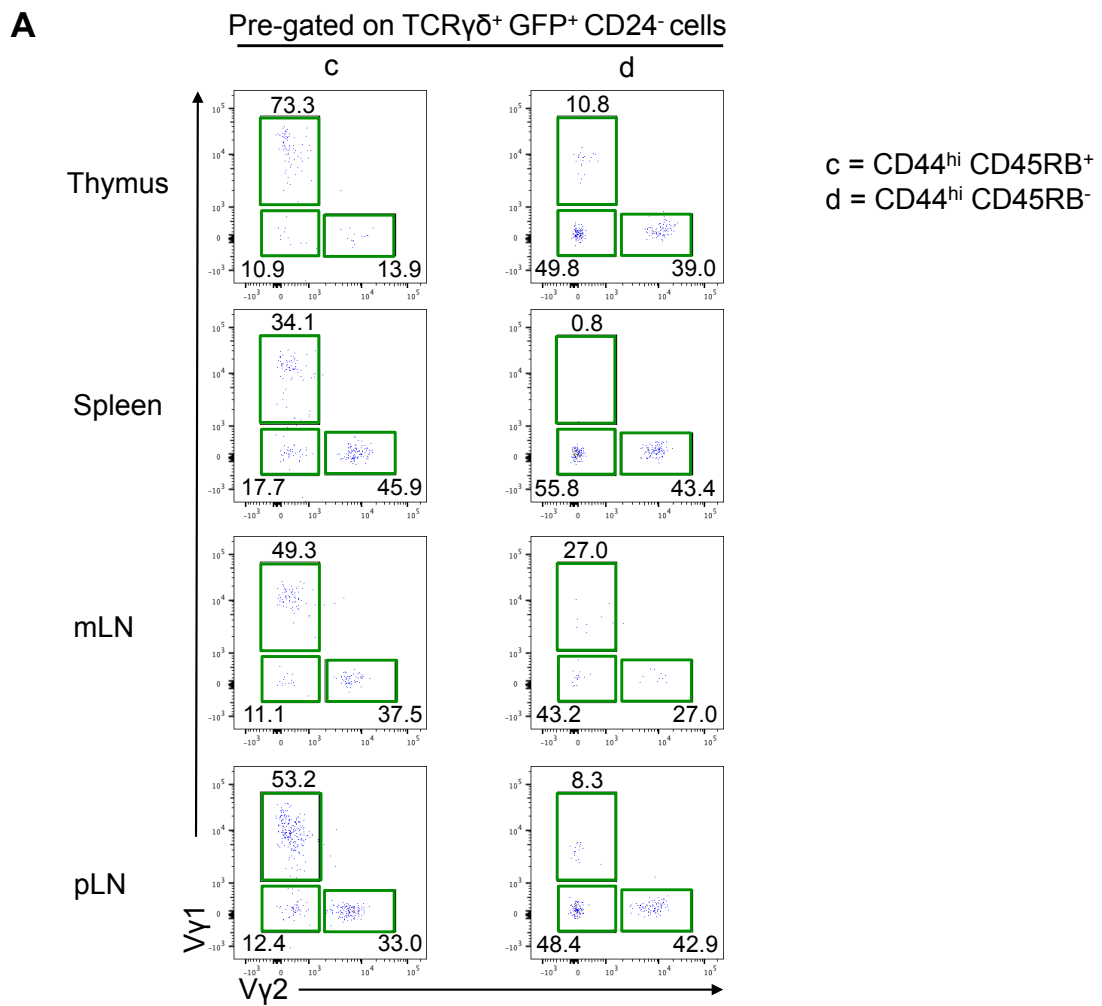
Collectively, these data demonstrate  $\gamma\delta$  T cells restricted to either an IL-17A-producing or IFN $\gamma$ -producing lineage to be present in the thymus, spleen and peripheral lymph nodes of an adult WT mouse. Using Id2-eGFP reporter mice, we revealed Id2 expression in both  $CD44^{hi} CD45RB^+$  (c) and  $CD44^{hi} CD45RB^-$  (d) populations, representing the IL-17A-producing and IFN $\gamma$ -producing cells respectively. In addition, we demonstrated the majority of the GFP $^+$  cells amongst the  $CD44^{hi} CD45RB^+$  (c) population to be  $V\gamma 1^+$ . While in the spleen there were comparable proportions of GFP $^+$  cells that were  $V\gamma 1^+$ ,  $V\gamma 1^- V\gamma 2^-$  and  $V\gamma 2^+$ . The majority of GFP $^+$  cells amongst the  $CD44^{hi} CD45RB^-$  (d) population were negative for both  $V\gamma 1$  and  $V\gamma 2$  in all tissues, suggesting the use of other  $V\gamma$  segments by these cells.

**Figure 5.8 V $\gamma$ -segment usage amongst Id2<sup>+</sup>  $\gamma\delta$  T cells varies depending on location and effector function**

To investigate V $\gamma$ 1 and V $\gamma$ 2 segment usage amongst GFP<sup>+</sup> CD44<sup>+</sup> CD45RB<sup>+</sup> and CD44<sup>+</sup> CD45RB<sup>-</sup>  $\delta$ -T cells, cells isolated from the thymus, spleen, mLN and pLN of Id2-eGFP mice were assessed. Samples were analysed using flow cytometry with total numbers calculated per whole tissue. Pooled peripheral lymph nodes consisted of cells isolated from the axillary, cervical and inguinal lymph nodes to provide a sufficient number of cells for analysis. Data shown in green corresponds with GFP<sup>+</sup> cells.

- A) Representative flow cytometry plots for the identification of V $\gamma$ 1 and V $\gamma$ 2 expression amongst CD44<sup>+</sup> CD45RB<sup>+</sup> (c) and CD44<sup>+</sup> CD45RB<sup>-</sup> (d) GFP<sup>+</sup>  $\gamma\delta$  T cells (TCR $\gamma\delta$ <sup>+</sup> GFP<sup>+</sup> CD24<sup>-</sup>) in the thymus, spleen, mLN and pLN. Cells were pre-gated on TCR $\gamma\delta$ <sup>+</sup> GFP<sup>+</sup> CD24<sup>-</sup> cells.
- B) Proportion of V $\gamma$ 1<sup>+</sup>, V $\gamma$ 1<sup>-</sup> V $\gamma$ 2<sup>-</sup> and V $\gamma$ 2<sup>+</sup> cells amongst GFP<sup>+</sup> CD44<sup>+</sup> CD45RB<sup>+</sup> (c) and CD44<sup>+</sup> CD45RB<sup>-</sup> (d)  $\gamma\delta$  T cells (TCR $\gamma\delta$ <sup>+</sup> GFP<sup>+</sup> CD24<sup>-</sup>) in the thymus.
- C) Proportion of V $\gamma$ 1<sup>+</sup>, V $\gamma$ 1<sup>-</sup> V $\gamma$ 2<sup>-</sup> and V $\gamma$ 2<sup>+</sup> cells amongst GFP<sup>+</sup> CD44<sup>+</sup> CD45RB<sup>+</sup> (c) and CD44<sup>+</sup> CD45RB<sup>-</sup> (d)  $\gamma\delta$  T cells (TCR $\gamma\delta$ <sup>+</sup> GFP<sup>+</sup> CD24<sup>-</sup>) in the spleen.
- D) Proportion of V $\gamma$ 1<sup>+</sup>, V $\gamma$ 1<sup>-</sup> V $\gamma$ 2<sup>-</sup> and V $\gamma$ 2<sup>+</sup> cells amongst GFP<sup>+</sup> CD44<sup>+</sup> CD45RB<sup>+</sup> (c) and CD44<sup>+</sup> CD45RB<sup>-</sup> (d)  $\gamma\delta$  T cells (TCR $\gamma\delta$ <sup>+</sup> GFP<sup>+</sup> CD24<sup>-</sup>) in the mLN.
- E) Proportion of V $\gamma$ 1<sup>+</sup>, V $\gamma$ 1<sup>-</sup> V $\gamma$ 2<sup>-</sup> and V $\gamma$ 2<sup>+</sup> cells amongst GFP<sup>+</sup> CD44<sup>+</sup> CD45RB<sup>+</sup> (c) and CD44<sup>+</sup> CD45RB<sup>-</sup> (d)  $\gamma\delta$  T cells (TCR $\gamma\delta$ <sup>+</sup> GFP<sup>+</sup> CD24<sup>-</sup>) in the pLN.

Kruskal-Wallis one-way ANOVA with post hoc Dunn's test was used (comparing three or more data sets) for statistical analysis where \*p<0.05 and \*\*p<0.01. In all graphs the bar represents the median, n=4. Data for all time points shown from one independent experiment.



#### 5.2.4 Id2 expression is restricted to an IL-17A-producing lineage in the neonatal thymus

Following our investigations within adult tissue, we sought to assess the expression of Id2 amongst  $\gamma\delta$  T cells in neonatal mice. Supplementary data presented by Sumira *et al.* (2017) described CD44 and CD45RB expression amongst neonatal mice at day 3 and 5 post-birth.(206) At both of these stages, CD44<sup>hi</sup> CD45RB<sup>-</sup> (d) cells were the most abundant, closely followed by CD44<sup>hi</sup> CD45RB<sup>+</sup> (c) cells. Additionally, this work characterised IL-17A and IFN $\gamma$  production by these cells at day 5. Consistent with their previous work in adult tissue, CD44<sup>hi</sup> CD45RB<sup>-</sup> (d) cells produced IL-17A while CD44<sup>hi</sup> CD45RB<sup>+</sup> (c) cells produced IFN $\gamma$ . To address this, CD44<sup>lo</sup> CD45RB<sup>-</sup> (a), CD44<sup>lo</sup> CD45RB<sup>+</sup> (b), CD44<sup>hi</sup> CD45RB<sup>+</sup> (c) and CD44<sup>hi</sup> CD45RB<sup>-</sup> (d) subsets amongst GFP<sup>-</sup> and GFP<sup>+</sup>  $\gamma\delta$  T cells in neonatal Id2-eGFP reporter mice were assessed. Mature  $\gamma\delta$  T cells (TCR $\gamma\delta$ <sup>+</sup> CD24<sup>-</sup>) were first identified amongst total cells and the gates for CD44<sup>lo</sup> CD45RB<sup>-</sup> (a), CD44<sup>lo</sup> CD45RB<sup>+</sup> (b), CD44<sup>hi</sup> CD45RB<sup>+</sup> (c) and CD44<sup>hi</sup> CD45RB<sup>-</sup> (d) subsets were set based on CD44 and CD45RB expression (Figure 5.9; upper panels). This gating strategy was adapted to include GFP so that CD44<sup>lo</sup> CD45RB<sup>-</sup> (a), CD44<sup>lo</sup> CD45RB<sup>+</sup> (b), CD44<sup>hi</sup> CD45RB<sup>+</sup> (c) and CD44<sup>hi</sup> CD45RB<sup>-</sup> (d) subsets amongst GFP<sup>-</sup> and GFP<sup>+</sup> cells were identified (Figure 5.9; middle and lower panels, respectively). Comparison of the proportion of CD44<sup>lo</sup> CD45RB<sup>-</sup> (a), CD44<sup>lo</sup> CD45RB<sup>+</sup> (b), CD44<sup>hi</sup> CD45RB<sup>+</sup> (c) and CD44<sup>hi</sup> CD45RB<sup>-</sup> (d) cells amongst GFP<sup>-</sup>  $\gamma\delta$  T cells demonstrated the CD44<sup>hi</sup> CD45RB<sup>-</sup> (d) subset to be the most abundant amongst these cells (Figure 5.9B). Interestingly, the proportion of the CD44<sup>hi</sup> CD45RB<sup>-</sup> (d) subset increased amongst GFP<sup>+</sup>  $\gamma\delta$  T cells, demonstrating the importance of Id2 in the development of these cells (Figure 5.9C). The CD44<sup>lo</sup> CD45RB<sup>-</sup> (a), CD44<sup>lo</sup>



CD45RB<sup>+</sup> (b), CD44<sup>hi</sup> CD45RB<sup>+</sup> (c) subsets, however, comprised of less than 10% of the GFP<sup>+</sup>  $\gamma\delta$  T cells (Figure 5.9C). Given the abundance of the CD44<sup>hi</sup> CD45RB<sup>-</sup> (d) subset amongst GFP<sup>+</sup>  $\gamma\delta$  T cells, we sought to determine the usage of V $\gamma$ 1 and V $\gamma$ 2 amongst these cells (Figure 5.9D-E). Using the same gating strategy demonstrated in adult tissue, V $\gamma$ 1 and V $\gamma$ 2 expression amongst CD44<sup>hi</sup> CD45RB<sup>-</sup> (d) cells was assessed (Figure 5.9D). This data demonstrated the majority of GFP<sup>+</sup>  $\gamma\delta$  T cells amongst the CD44<sup>hi</sup> CD45RB<sup>-</sup> (d) to lack the expression of both V $\gamma$ 1 and V $\gamma$ 2 (Figure 5.9E). The availability of Id2-eGFP mice at this time resulted in the few data points within this experiment. Future research would aim to repeat this investigation with a greater number of mice.

#### **5.2.5 Id2 expression is greater in T effector memory (Tem) cells when compared to their naïve counterparts**

We have previously illustrated  $\alpha\beta$  T cells to be numerically the most abundant cells arising from RFP<sup>+</sup> cells in both the mLN and thymus (Figure 5.1). Despite this, only a small fraction of these  $\alpha\beta$  T cells were shown to fate-map to Id2 (Figure 5.2). Therefore, we aimed to discover more about the expression of Id2 amongst  $\alpha\beta$  T cells and how Id2 influenced the function of these cells.

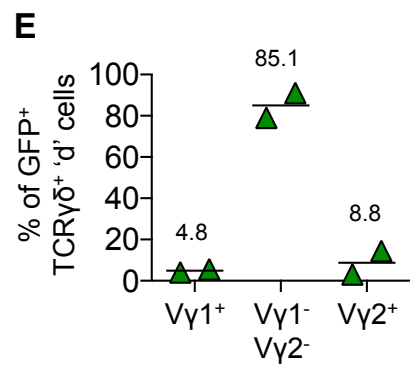
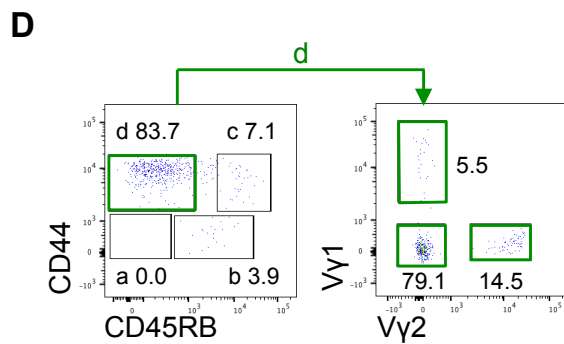
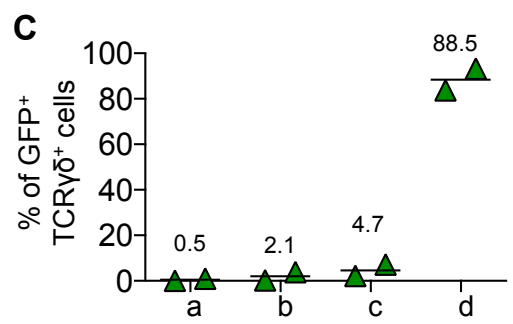
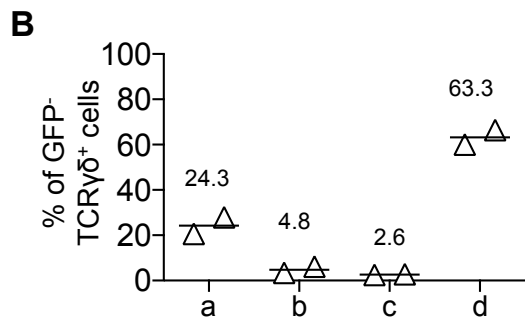
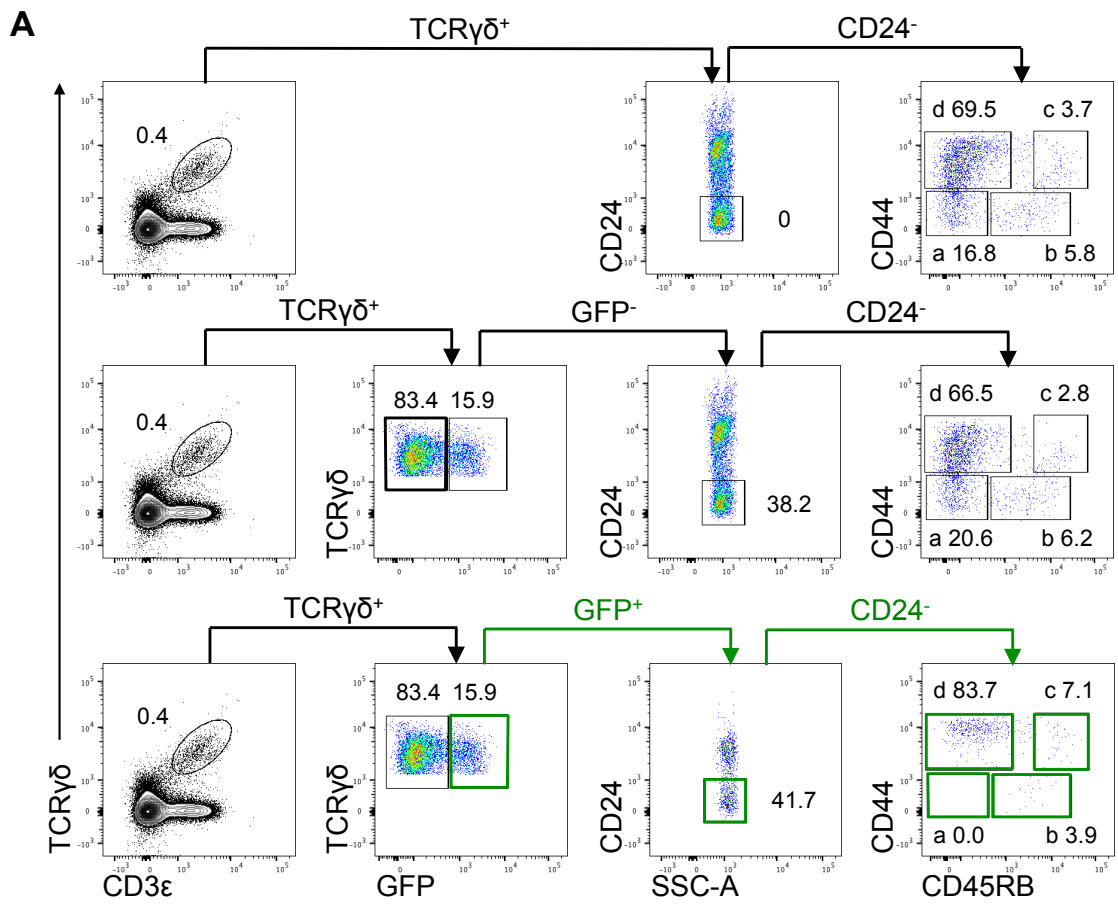
It has previously been shown that Id2 is up regulated in CD4 effector T cells and is required for their differentiation into Th1 cells.(196) As such, we hypothesised the expression of Id2 might be greater in T effector memory (Tem) cells compared to naïve T cells due to the transient activation Tem cells. To test this, CD4 T cells isolated from the mLN of Id2-eGFP mice were assessed for their expression of CD44 and CD62L. These markers were used to separate naïve T cells (CD44<sup>lo</sup> CD62L<sup>+</sup>) from Tem cells (CD44<sup>hi</sup> CD62L<sup>-</sup>) in the mLN of these mice and expression of GFP

**Figure 5.9  $\gamma\delta$  T cells expressing Id2 in the neonatal thymus are predominantly of the IL-17A-producing lineage**

To investigate the expression of Id2 amongst  $\gamma\delta$  T cells associated with IL-17A or IFN $\gamma$  production in the thymus, cells were isolated from this tissue in 4 day old neonatal Id2-eGFP reporter mice. Samples were analysed using flow cytometry with total numbers calculated per whole thymus. Data shown in green corresponds with GFP<sup>+</sup> cells.

- A) Representative flow cytometry plots for the identification of CD44<sup>-</sup> CD45RB<sup>-</sup> (a), CD44<sup>-</sup> CD45RB<sup>+</sup> (b), CD44<sup>+</sup> CD45RB<sup>+</sup> (c) and CD44<sup>+</sup> CD45RB<sup>-</sup> (d) cells amongst total (upper panels, GFP<sup>-</sup> (middle panels), and GFP<sup>+</sup> (lower panels)  $\gamma\delta$  T cells (TCR $\gamma\delta$ <sup>+</sup> CD24<sup>-</sup>) in the thymus.
- B) Proportion of CD44<sup>-</sup> CD45RB<sup>-</sup> (a), CD44<sup>-</sup> CD45RB<sup>+</sup> (b), CD44<sup>+</sup> CD45RB<sup>+</sup> (c) and CD44<sup>+</sup> CD45RB<sup>-</sup> (d) cells amongst GFP<sup>-</sup>  $\gamma\delta$  T cells in the thymus.
- C) Proportion of CD44<sup>-</sup> CD45RB<sup>-</sup> (a), CD44<sup>-</sup> CD45RB<sup>+</sup> (b), CD44<sup>+</sup> CD45RB<sup>+</sup> (c) and CD44<sup>+</sup> CD45RB<sup>-</sup> (d) cells amongst GFP<sup>+</sup>  $\gamma\delta$  T cells in the thymus.
- D) Representative flow cytometry plots showing V $\gamma$ 1 and V $\gamma$ 2 expression amongst TCR $\gamma\delta$ <sup>+</sup> GFP<sup>+</sup> CD24<sup>-</sup> CD44<sup>+</sup> CD45RB<sup>-</sup> (d) cells in the thymus.
- E) Proportion of V $\gamma$ 1<sup>+</sup>, V $\gamma$ 1<sup>-</sup> V $\gamma$ 2<sup>-</sup> and V $\gamma$ 2<sup>+</sup> cells amongst amongst TCR $\gamma\delta$ <sup>+</sup> GFP<sup>+</sup> CD24<sup>-</sup> CD44<sup>+</sup> CD45RB<sup>-</sup> (d) cells in the thymus.

Kruskal-Wallis one-way ANOVA with post hoc Dunn's test was used (comparing three or more data sets) for statistical analysis. In all graphs the bar represents the median, n=2. Data for all time points shown from one independent experiments.



from each subset was assessed (Figure 5.10A). Gating controls for GFP expression was based on cells isolated from the mLN of a WT mouse (Figure 5.10B). This study illustrated proportion of GFP expressed, and therefore Id2 expression, to be greater in Tem cells compared to naïve T cells (Figure 5.10C).

#### **5.2.6 Id2 is expressed by $\alpha\beta$ and $\gamma\delta$ T cells in effector tissue**

Our investigations so far have focused on the expression of Id2 amongst T cell populations in lymphoid tissue. However, evidence has shown  $\alpha\beta$  T cells to up regulate Id2 while completing effector functions during a Th1 immune response.(196) As such, we investigated the expression of Id2 amongst  $\alpha\beta$  and  $\gamma\delta$  T cells in the small intestine of Id2-eGFP mice. The small intestine is encompassed within the gut where immune cells are constantly exposed to antigens from the surrounding microbiome. As such, immune cells have a crucial role in maintaining immune homoeostasis within this tissue. Furthermore, our previous figure identified some Tem cells as expressers of Id2. Given that Tem spend most of their time in tissue, we hypothesised that the small intestine would be an appropriate effector tissue to investigate Id2 expression amongst  $\alpha\beta$  and  $\gamma\delta$  T cells.

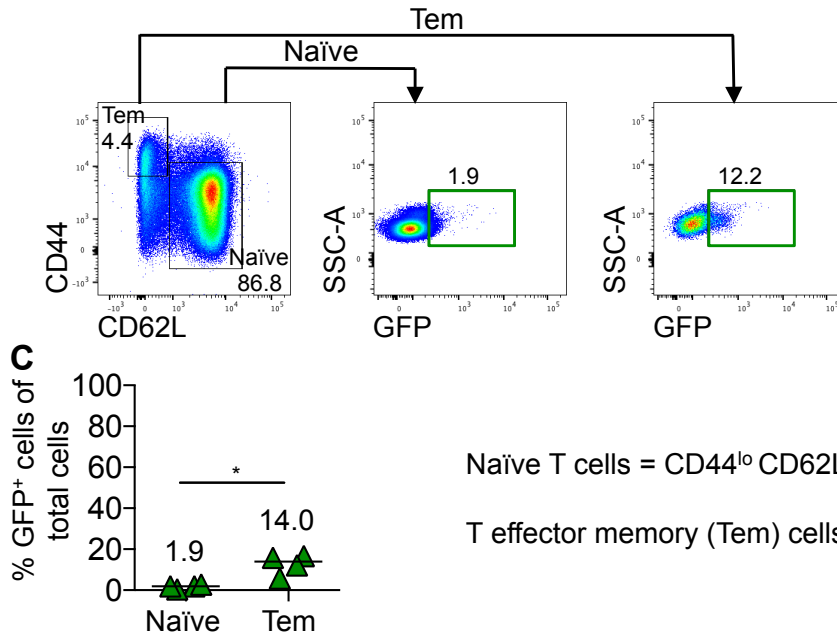
As shown within the representative FACS plots, both  $\alpha\beta$  and  $\gamma\delta$  T cells could be clearly identified within the small intestine using antibodies against TCR $\beta$  and TCR $\gamma\delta$ , respectively, prior to assessing GFP expression amongst these cells (Figure 5.11A). TCR $\beta$  and TCR $\gamma\delta$  subsets were pre-gated on live CD45<sup>+</sup> cells to identify lymphocyte populations in this non-lymphoid tissue. Gating controls for GFP utilised cells isolated from the small intestine of a WT mouse (Figure 5.11B). Upon enumeration, the proportion and total number of  $\alpha\beta$  T cells were significantly greater than that of  $\gamma\delta$  T cells in this tissue. However, comparison of GFP expression

**Figure 5.10 Id2 expression is greater in T effector memory cells compared to naïve T cells in peripheral lymphoid tissue**

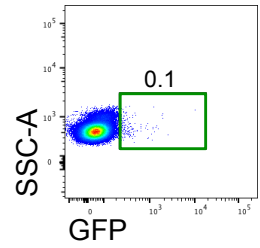
To examine the expression of Id2 in naïve and T effector memory (Tem) cells in peripheral lymphoid tissue, CD4 T cells isolated from the mLN of Id2-eGFP were assessed based on their expression of CD44 and CD62L. Samples were analysed by flow cytometry and total numbers were calculated per whole mLN. Data shown in green corresponds with GFP<sup>+</sup> cells.

- A) Representative FACS plots illustrating the level of GFP expressed by naïve (CD44<sup>lo</sup> CD62L<sup>+</sup>) and Tem cells (CD44<sup>hi</sup> CD62L<sup>-</sup>) in the mLN.
- B) Gating controls for GFP expressed used cells isolated from the mLN of a WT mouse.
- C) Comparison of the proportion of GFP expressed by naïve and Tem cell in the mLN.

Mann-Whitney U (nonparametric, two-tailed) test was used for statistical analysis where \*p<0.05. In all graphs the bar represents the median, n=4. Data for all time points shown from two independent experiments.

**A**Pre-gated on CD4<sup>+</sup> TCRβ<sup>+</sup> cells**B**

WT Control



amongst these two subsets revealed GFP expression to be greater amongst  $\gamma\delta$  T cells when compared to the proportion of GFP expressed by  $\alpha\beta$  T cells (Figure 5.11F). While the proportion of GFP expressed by  $\gamma\delta$  T cells was greater than that of  $\alpha\beta$  T cells, we sought to pursue a greater understanding of  $\alpha\beta$  T cells where there was already a growing interest in the expression of Id2 in these cells within the literature.(196,200,201)

The expression of GFP was successfully identified amongst both  $CD4^+$  and  $CD8^+$   $\alpha\beta$  T cell populations, as demonstrated by the representative FACS plots in Figure 5.11E. Gating controls for GFP expression utilised cells isolated from the thymus of a WT mouse (Figure 5.11F). Enumeration of these subsets demonstrated the majority of  $\alpha\beta$  T cells in this tissue to be  $CD4^+$  (Figure 5.11G). Furthermore, the expression of GFP amongst  $CD4^+$   $\alpha\beta$  T cells was significantly greater than that of  $CD8^+$   $\alpha\beta$  T cells (Figure 5.11H).

### **5.2.7 Investigation of Id2 expression following immunisation with Lm-2W1S**

Previously, we have illustrated Id2 to be expressed amongst effector T cell populations in lymphoid tissue (Figure 5.11). Moreover, our studies in the small intestine have demonstrated the expression of Id2 by  $CD4^+$  T cells to be increased at effector sites. Following on from these findings, we wanted to examine the expression of Id2 amongst specific  $CD4^+$  effector T cell subsets. Therefore, we sought to investigate the expression of Id2 in these cells using a well-established model of a Th1 immune response.

Immunisation of mice with *Listeria monocytogenes* (*L. monocytogenes*) provides a highly reproducible model for studying the adaptive immune response. This uses an

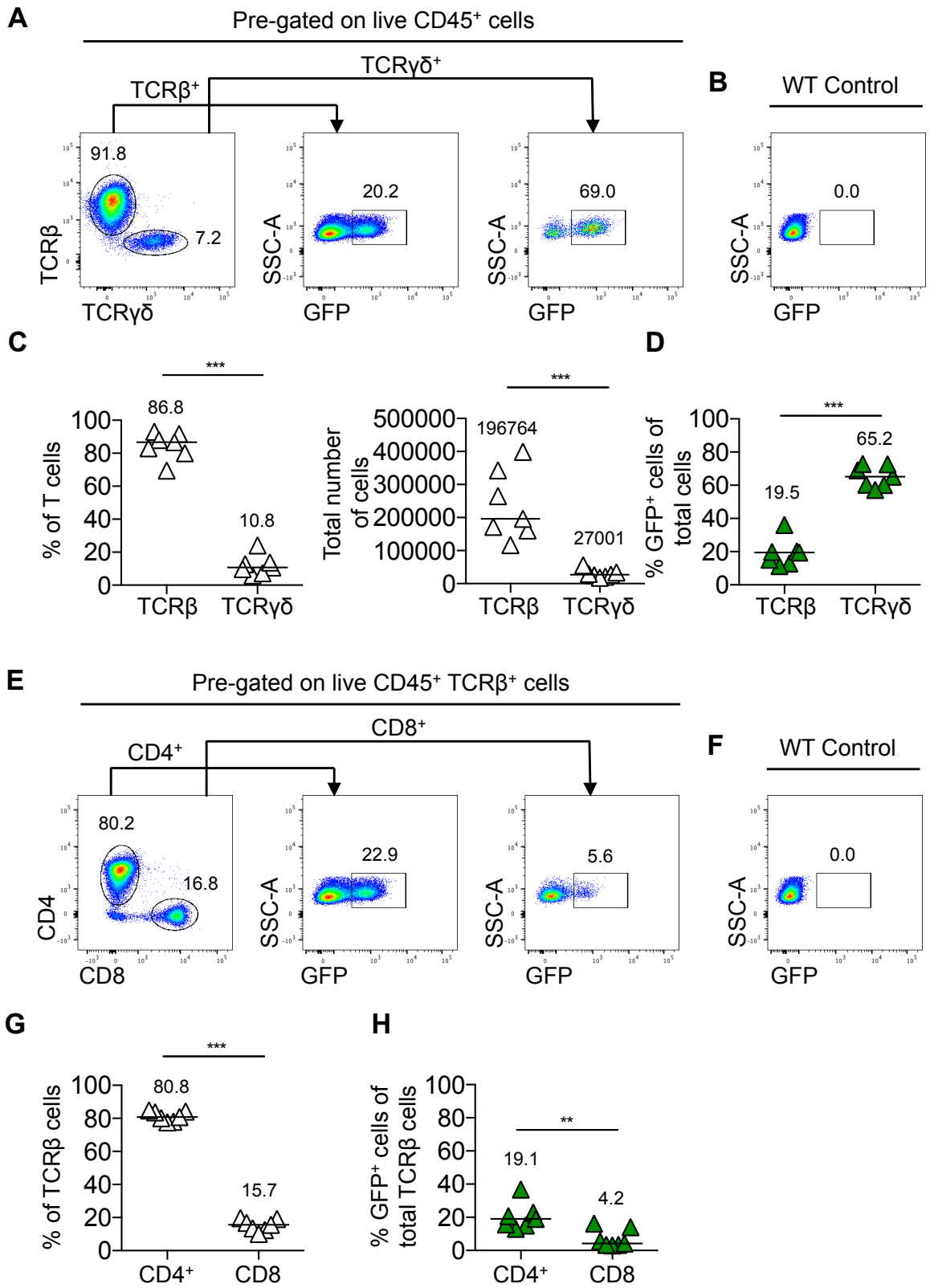
### Figure 5.11 Id2 is expressed by both $\alpha\beta$ and $\gamma\delta$ T cells in the small intestine

To investigate the expression of Id2 amongst  $\alpha\beta$  T cells and  $\gamma\delta$  T cells in effector tissue, cells were isolated from small intestine in Id2-eGFP reporter mice. Samples were analysed using flow cytometry with total numbers calculated per whole small intestine. Data shown in green corresponds with GFP<sup>+</sup> cells.

- A) Representative flow cytometry plots for the identification of GFP<sup>+</sup> cells amongst  $\alpha\beta$  T cell (TCR $\beta$ <sup>+</sup>) and  $\gamma\delta$  T cells (TCR $\gamma\delta$ <sup>+</sup>) in the small intestine. All cells were pre-gated on live CD45<sup>+</sup> cells.
- B) Gating control for GFP based on the expression of GFP in a WT mouse.
- C) Proportion and total number of  $\alpha\beta$  T cells and  $\gamma\delta$  T cells amongst all T cells in the small intestine.
- D) Proportion of GFP<sup>+</sup> cells amongst  $\alpha\beta$  T cells and  $\gamma\delta$  T cells in the small intestine.
- E) Representative flow cytometry plots for the identification of GFP<sup>+</sup> cells amongst CD4<sup>+</sup> and CD8<sup>+</sup>  $\alpha\beta$  T cells in the small intestine. All cells were pre-gated on live CD45<sup>+</sup> TCR $\beta$ <sup>+</sup> cells.
- F) Gating control for GFP based on the expression of GFP in a WT mouse.
- G) Proportion of CD4<sup>+</sup> and CD8<sup>+</sup> cells amongst  $\alpha\beta$  T cells (TCR $\beta$ <sup>+</sup>) in the small intestine.
- H) Proportion of GFP<sup>+</sup> cells amongst CD4<sup>+</sup> and CD8<sup>+</sup>  $\alpha\beta$  T cells in the small intestine.

Mann-Whitney U (nonparametric, two-tailed) test was used for statistical analysis where \*\*p<0.01 and \*\*\*p<0.001. In all graphs the bar represents the median, n=7. Data for all time points shown from two independent experiments.





attenuated strain of *L. monocytogenes* that has been engineered so that a fusion protein containing a region of Ovalbumin (OVA) and the 2W1S peptide under the *hly* promoter is secreted.(207) The availability of MHC class II tetramers has enabled the tracking of a population of CD4<sup>+</sup> T cells that are specific for 2W1S from initiation of the primary response through to the memory response.(208) The 2W1S peptide is highly immunogenic and following immunisation undergoes processing by antigen presenting cells and is presented on MHC class II molecules. These tetramers make it possible to identify CD4<sup>+</sup> T cell populations that have a TCR specific for 2W1S. We sought to track the expression of Id2 in effector T cell populations as they undergo clonal expansion in response to *Listeria monocytogenes* (*L. monocytogenes*). Within the proceeding investigations, CD4<sup>+</sup> T cells with a TCR specific for 2W1S were identified in the spleen or peripheral lymph nodes using a 2W1S:I-A<sup>b</sup> MHC class II tetramer that was conjugated to either APC or PE.

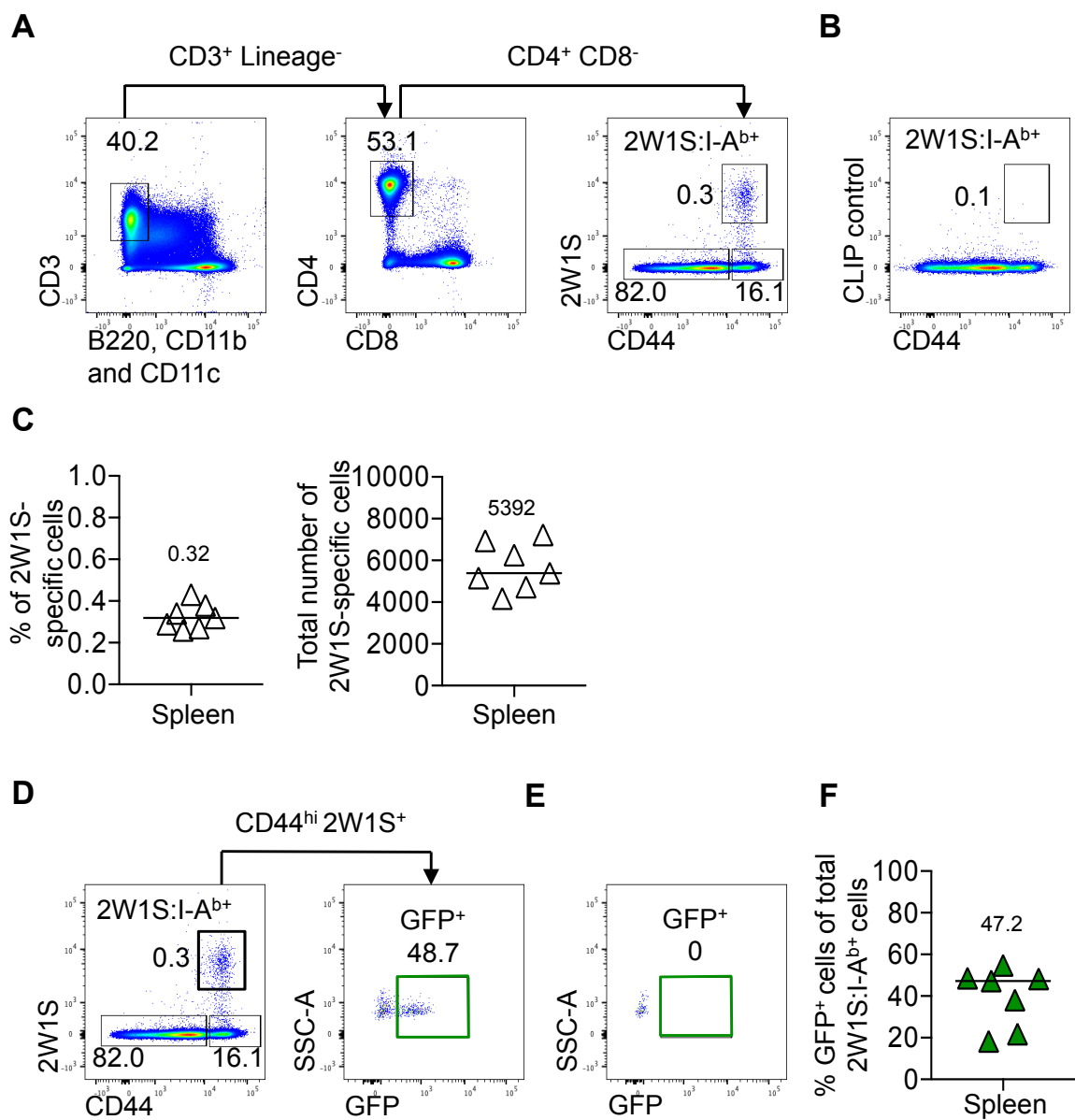
Our initial experiments assessed 2W1S-specific T cells in the spleen of Id2-eGFP mice 7 days post-immunisation with Lm-2W1S. 2W1S-specific CD4<sup>+</sup> effector T cells were identified as CD3<sup>+</sup> B220<sup>-</sup> CD11b<sup>-</sup> CD11c<sup>-</sup> CD4<sup>+</sup> CD44<sup>hi</sup> 2W1S:I-A<sup>b</sup> (Figure 5.12A). Gating controls for 2W1S-specific T cells used cells isolated from the spleen of an Id2-eGFP mouse 7 days post-immunisation with Lm-2W1S that was incubated with class II-associated invariant peptide (CLIP) (Figure 5.9B). Enumeration of these cells demonstrated 2W1S-specific T cells to account for less than 1% of CD4<sup>+</sup> T cells, which equated to approximately 5000 cells (Figure 5.12C). To determine the expression of Id2 amongst these cells, 2W1S-specific T cells were assessed for their expression of GFP (Figure 5.12D). Gating controls for GFP expression used cells isolated from the spleen of a WT mouse (Figure 5.12E). Although the expression of

**Figure 5.12 Analysis of Id2 expression by effector CD4<sup>+</sup> T cell subsets following immunisation with Lm-2W1S**

To investigate Id2-expression following the induction of a Th1 immune response, CD4<sup>+</sup> effector T cells were assessed in the spleen of Id2-eGFP mice 7 days post-immunisation with Lm-2W1S. Samples were analysed using flow cytometry and total numbers calculated per whole spleen. Data shown in green corresponds with GFP<sup>+</sup> cells.

- A) Gating strategy for the identification of 2W1S-specific CD4<sup>+</sup> effector T cells, defined as CD3<sup>+</sup> Lineage<sup>-</sup> CD4<sup>+</sup> CD44<sup>hi</sup> 2W1S:I-A<sup>b+</sup>, in the spleen of Id2-eGFP mice 7 days post-immunisation with Lm-2W1S.
- B) Representative FACS plot for class II-associated invariant peptide (CLIP) control in the spleen of Id2-eGFP mice 7 days post-immunisation with Lm-2W1S.
- C) Proportion and total number of 2W1S-specific T cells amongst the CD4<sup>+</sup> effector T cell population.
- D) Representative FACS plots showing the expression of GFP amongst the 2W1S-specific CD4<sup>+</sup> effector T cell population.
- E) GFP expression amongst the 2W1S-specific CD4<sup>+</sup> effector T cell population was controlled using cells isolated from the spleen of WT mice.
- F) Proportion of GFP<sup>+</sup> cells amongst the 2W1S-specific CD4<sup>+</sup> effector T cell population.

Mann-Whitney U (non-parametric, two-tailed) test was used (comparing two data sets) was used for statistical analysis where \*p<0.05, \*\*p<0.01, \*\*\*p<0.001, and \*\*\*\*p<0.0001. In all graphs the bar represents the median, n=9. Data shown from two independent experiments.



GFP was varied amongst 2W1S-specific T cells, as demonstrated by the range of data points, a median proportion of GFP<sup>+</sup> cells of almost 50% was identified (Figure 5.12F).

Responding T cell populations can be divided into three subsets based on their expression of CXCR5 and PD-1: CXCR5<sup>-</sup> PD-1<sup>-</sup> (Tem), CXCR5<sup>+</sup> PD-1<sup>-</sup> (Tcm) and CXCR5<sup>+</sup> PD-1<sup>+</sup> (Tfh).(209) To investigate the expression of Id2 amongst CXCR5<sup>-</sup> PD-1<sup>-</sup>, CXCR5<sup>+</sup> PD-1<sup>-</sup> and CXCR5<sup>+</sup> PD-1<sup>+</sup> subsets, Id2-eGFP mice were immunised with Lm-2W1S and cells isolated from the spleen 7 days post-immunisation were assessed. Representative FACS plots for the identification of CXCR5<sup>-</sup> PD-1<sup>-</sup>, CXCR5<sup>+</sup> PD-1<sup>-</sup> and CXCR5<sup>+</sup> PD-1<sup>+</sup> subsets amongst total 2W1S-specific T cells is shown in Figure 5.13A. Of these cells, CXCR5<sup>-</sup> PD-1<sup>-</sup> and CXCR5<sup>+</sup> PD-1<sup>-</sup> cells were the most abundant with both the proportion and total number of these cells being significantly greater than CXCR5<sup>+</sup> PD-1<sup>+</sup> cells (Figure 5.13B-C). The GFP expression amongst these cells was later assessed. Representative FACS plots for the expression of GFP amongst CXCR5<sup>-</sup> PD-1<sup>-</sup>, CXCR5<sup>+</sup> PD-1<sup>-</sup> and CXCR5<sup>+</sup> PD-1<sup>+</sup> cells is shown in Figure 5.9D. Enumeration of GFP expression amongst these subsets demonstrates Id2 to be restricted to the CXCR5<sup>-</sup> PD-1<sup>-</sup> subset whereby GFP is expressed by almost 70% of these cells (Figure 5.13E).

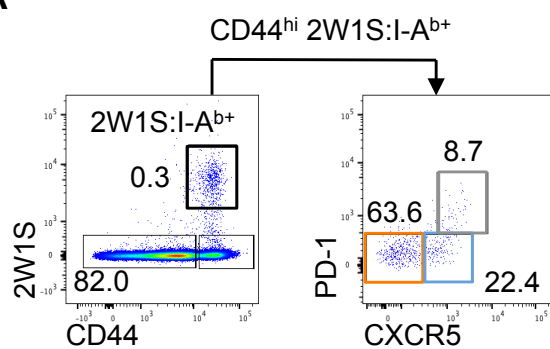
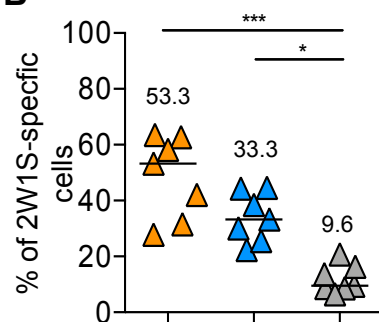
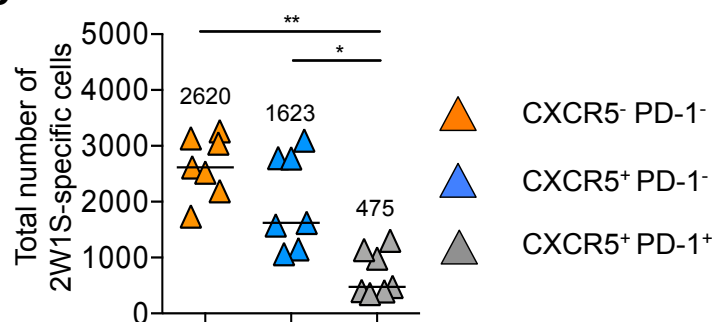
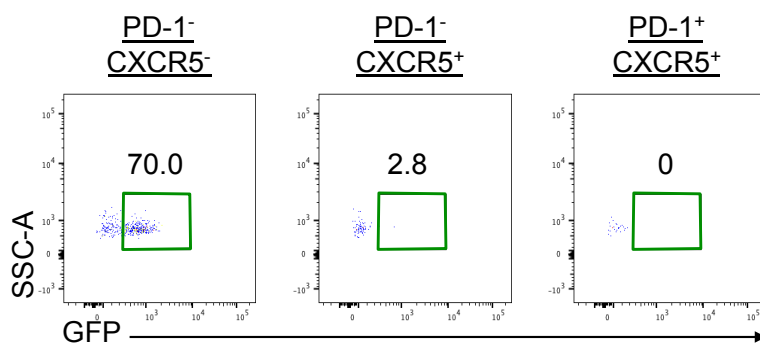
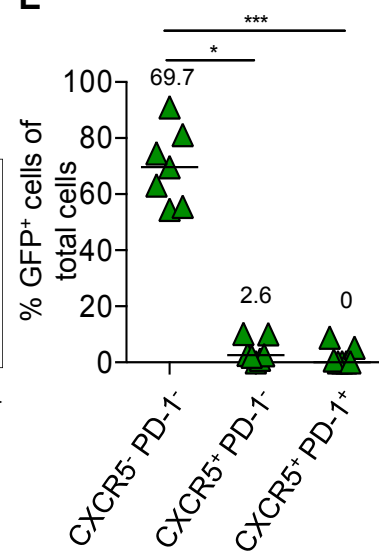
Overall, these data demonstrate Id2 to be expressed amongst CD4<sup>+</sup> effector T cells as they respond to Lm-2W1S. Building upon this data, we sought to investigate whether the expression of Id2 varied at different stages of the immune response. To achieve this, 2W1S-specific T cells from the spleen of Id2-eGFP reporter mice were assessed 4, 7, 11 and 21 days post-immunisation with Lm-2W1S. Representative FACS plots illustrating the identification of CD44<sup>+</sup> 2W1S-specific T cells and their

**Figure 5.13 Id2 expression is restricted to CXCR5<sup>-</sup> Th1 effector CD4<sup>+</sup> T cells 7 days post-immunisation with Lm-2W1S**

Responding T cell populations can be divided into three subsets based on their expression of CXCR5 and PD-1. To investigate whether Id2 expression was restricted to CXCR5<sup>-</sup> cells, Id2-eGFP mice were immunised with Lm-2W1S and cells isolated from the spleen 7 days later were characterised based on their expression of CXCR5 and PD-1. Samples were analysed by flow cytometry and total numbers calculated per whole spleen. Data shown in orange, blue and grey corresponds to CXCR5<sup>-</sup> PD-1<sup>-</sup>, CXCR5<sup>+</sup> PD-1<sup>-</sup> and CXCR5<sup>+</sup> PD-1<sup>+</sup> cells, respectively. Data shown in green corresponds with GFP<sup>+</sup> cells.

- A) Representative FACs plots for the identification of CXCR5<sup>-</sup> PD-1<sup>-</sup>, CXCR5<sup>+</sup> PD-1<sup>-</sup> and CXCR5<sup>+</sup> PD-1<sup>+</sup> cells amongst 2W1S-specific CD4<sup>+</sup> effector T cell populations, identified as CD3<sup>-</sup> Lineage<sup>-</sup> CD4<sup>+</sup> CD44<sup>hi</sup> 2W1S:I-A<sup>b+</sup> cells. Lineage channel consists of antibodies against B220, CD3, CD5, CD11b and CD11c.
- B) Proportion of CXCR5<sup>-</sup> PD-1<sup>-</sup>, CXCR5<sup>+</sup> PD-1<sup>-</sup> and CXCR5<sup>+</sup> PD-1<sup>+</sup> cells amongst 2W1S-specific CD4<sup>+</sup> effector T cell populations.
- C) Total number of CXCR5<sup>-</sup> PD-1<sup>-</sup>, CXCR5<sup>+</sup> PD-1<sup>-</sup> and CXCR5<sup>+</sup> PD-1<sup>+</sup> cells amongst 2W1S-specific CD4<sup>+</sup> effector T cell populations.
- D) Representative FACs plots showing the expression of GFP by CXCR5<sup>-</sup> PD-1<sup>-</sup> (left panel), CXCR5<sup>+</sup> PD-1<sup>-</sup> (middle panel) and CXCR5<sup>+</sup> PD-1<sup>+</sup> (right panel) cells amongst 2W1S-specific CD4<sup>+</sup> effector T cell populations.
- E) Proportion of GFP<sup>+</sup> cells amongst CXCR5<sup>-</sup> PD-1<sup>-</sup>, CXCR5<sup>+</sup> PD-1<sup>-</sup> and CXCR5<sup>+</sup> PD-1<sup>+</sup> subsets.

Kruskal-Wallis one-way ANOVA with post hoc Dunn's test was used (comparing three or more data sets) for statistical analysis \*p<0.05, \*\*p<0.01, \*\*\*p<0.001, and \*\*\*\*p<0.0001. In all graphs the bar represents the median, n=9. Data shown from two independent experiments.

**A****B****C****D****E**

expression of GFP at day 4, 7, 11 and 21 post-immunisation with Lm-2W1S is shown in Figure 5.14A and were pre-gated on CD3<sup>+</sup> Lineage<sup>-</sup> CD4<sup>+</sup> cells. Gating controls for 2W1S expression used cells isolated from the spleen of Id2-eGFP mice at 4, 7 and 11 days post-immunisation with Lm-2W1S following incubation with a CLIP control (Figure 5.14B). Gating controls for GFP expression used cells isolated from the spleen of WT mice at 4, 7, 11 and 21 days post-immunisation with Lm-2W1S (Figure 5.14C). Enumeration of the proportion and total number of 2W1S-specific T cells at these time points demonstrated 2W1S-specific T cells to be most abundant between days 7 and 11 (Figure 5.14D-E). However, the proportion of GFP expressed amongst 2W1S-specific T cells was comparable on all days investigated (Figure 5.14F).

The data described thus far provides evidence to support the expression of Id2 by CD4<sup>+</sup> effector T cells in response to immunization with Lm-2W1S immunisation. However, this data does not indicate the function of Id2 amongst these cells. Previous studies have shown Id2 to be up regulated in Th1 cells that express Tbet (Shaw 2016). Therefore, we sought to determine the effect of Tbet deletion amongst CD4<sup>+</sup> effector T cell function using our model of a Th1 immune response. To achieve this, we first established pilot experiments combining our techniques of immunisation with Lm-2W1S and tamoxifen administration by oral gavage in Id2<sup>creERT2</sup>xROSA26<sup>RFP</sup>, Id2<sup>creERT2</sup>Tbx21<sup>F/F</sup>xROSA26<sup>RFP</sup> and CD4<sup>creERT2</sup>Tbx21<sup>F/F</sup>xROSA26<sup>RFP</sup> mice. Immunisation of mice with Lm-2W1S initiated a Th1 immune response by CD4<sup>+</sup> effector T cells while the administration of tamoxifen induced the expression of the Cre recombinase transgene within our transgenic mouse models and enable identification of cells that fate map to either Id2 or CD4 by expression of RFP.

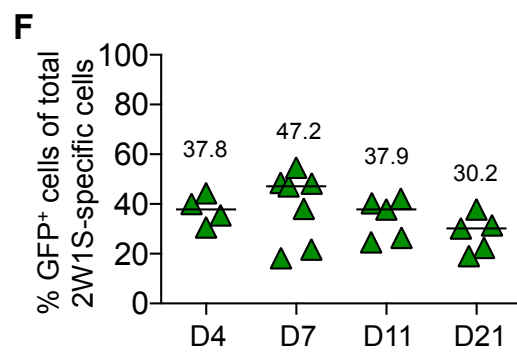
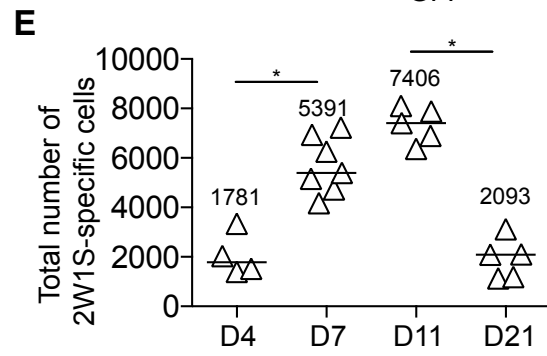
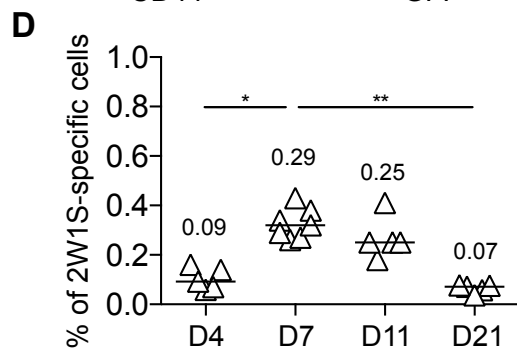
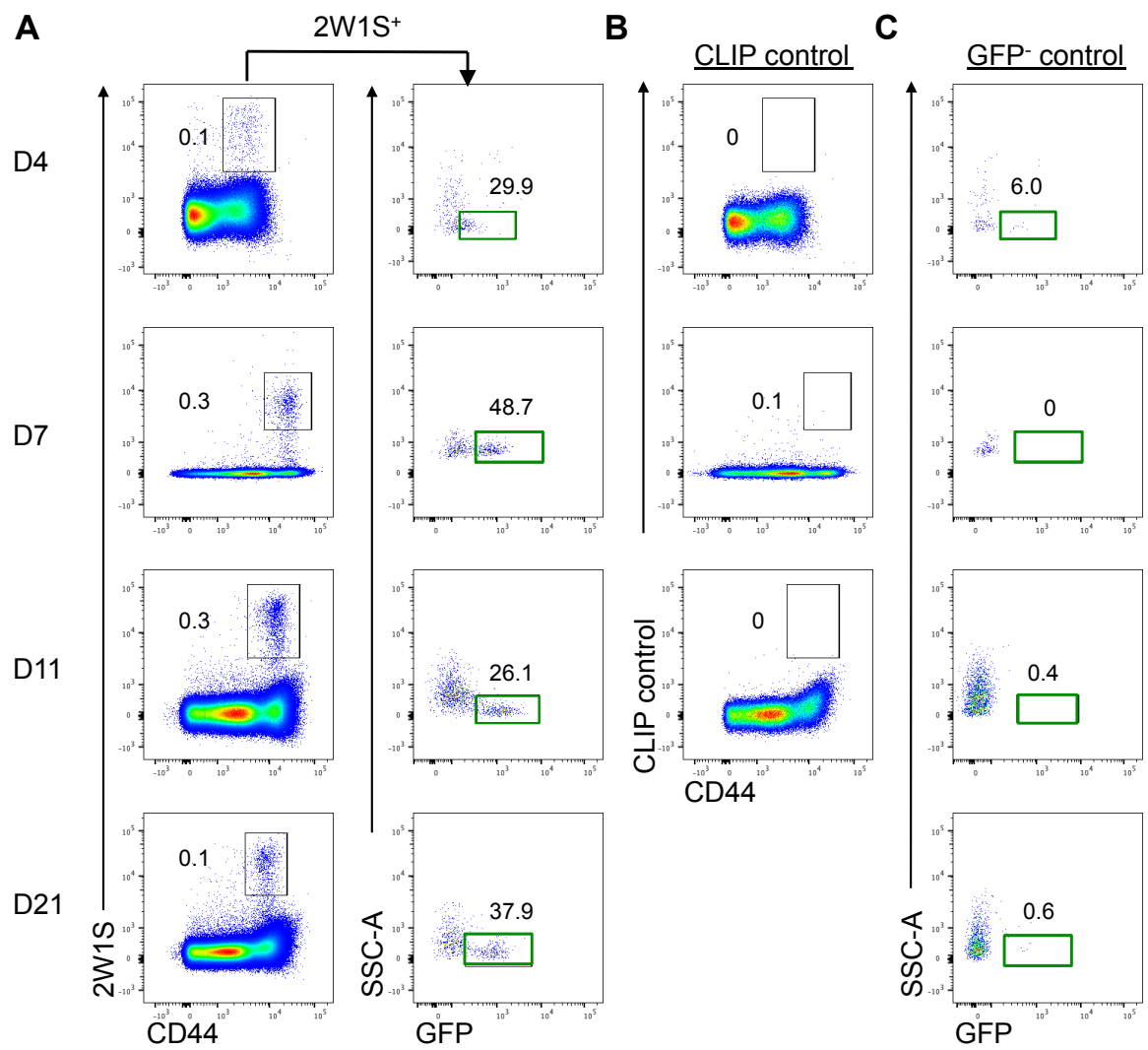


**Figure 5.14 Increasing Id2 expression corresponds with the increasing number of 2W1S-specific CD4<sup>+</sup> T cells in response to Lm-2W1S immunisation**

To investigate Id2 expression at different stages of the immune response, cells from the spleen of Id2-eGFP mice were assessed at 4, 7, 11 and 21 days post-immunisation with Lm-2W1S. Samples were analysed using flow cytometry with total numbers calculated per whole spleen. Data shown in green corresponds with GFP<sup>+</sup> cells.

- A) Representative FACs plots for the identification of GFP<sup>+</sup> cells amongst 2W1S-specific CD4<sup>+</sup> T cells, identified as CD3<sup>-</sup> Lineage<sup>-</sup> CD4<sup>+</sup> CD44<sup>hi</sup> 2W1S:I-A<sup>b</sup> cells, in the spleen of Id2-eGFP mice at day 4 (D4), day 7 (D7), day 11 (D11) and day 21 (D21) post-immunisation with Lm-2W1S.
- B) CLIP control staining for 2W1S<sup>+</sup> cells amongst CD4<sup>+</sup> T cells at day 4, 7 and 11 post-immunisation with Lm-2W1S. All cells isolated from the spleen at D21 were used for staining with the 2W1S:I-A<sup>b</sup> tetramer given their low numbers at this time point.
- C) Gating controls for GFP expression based on cells isolated from the spleen of WT mice.
- D) Proportion of 2W1S-specific cells amongst CD4<sup>+</sup> T cells at day 4, 7, 11 and 21 post-immunisation with Lm-2W1S.
- E) Total number of 2W1S-specific cells amongst CD4<sup>+</sup> T cells at day 4, 7, 11 and 21 post-immunisation with Lm-2W1S.
- F) Proportion of GFP<sup>+</sup> cells amongst 2W1S-specific CD4<sup>+</sup> T cells at day 4, 7, 11 and 21 post-immunisation with Lm-2W1S.

Kruskal-Wallis one-way ANOVA with post hoc Dunn's test was used (comparing three or more data sets) for statistical analysis where \*p<0.05 and \*\*p<0.01. In all graphs the bar represents the median, n=5 (D4, D11 and D21) and n=9 (D7). Data for all time points shown from two independent experiments.



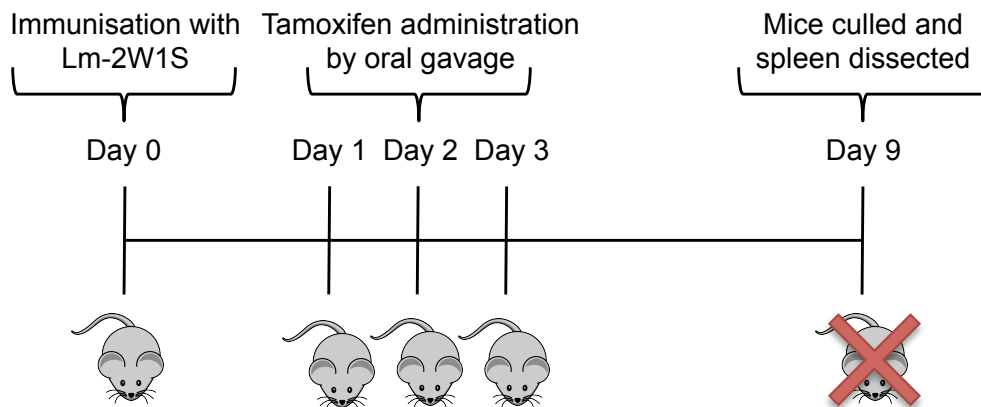
The evidence presented in Figure 5.14 demonstrated Id2 to be expressed amongst CD4<sup>+</sup> effector T cells at 4, 7, 11 and 21 days following immunisation with Lm-2W1S. However, these data did not inform us of which stage of the immune response the gene for Id2 is switched on. Furthermore, our earlier investigations used Id2-eGFP mice that enabled identification of current Id2 expression. In contrast, the proportion of Id2 expressed in our fate-mapping model is influenced by the efficiency of labeling these cells following tamoxifen administration (as previously described in Chapter 3). Therefore, we designed two pilot approaches to capture the expression of Id2 amongst CD4<sup>+</sup> effector T cells in response to Lm-2W1S, termed method 1, were immunised with Lm-2W1S on day 0 and administered tamoxifen by oral gavage on days 1, 2, and 3. The mice were culled on day 9 and cells isolated from the spleen were assessed (Figure 5.15A). It was hypothesised that administering tamoxifen at these time points would capture CD4<sup>+</sup> T cells as they initiate an immune response against Lm-2W1S. In our second approach, termed method 2, mice were immunised with Lm-2W1S on day 0 and were administered tamoxifen by oral gavage on days 6, 7 and 8. The mice were culled on day 12 and cells isolated from the spleen were assessed (Figure 5.15B). Data shown in Figure 5.14 demonstrated the expansion of 2W1S-specific CD4<sup>+</sup> effector T cells between day 7 and day 11 following immunization with Lm-2W1S. As such, it was hypothesised that administration of tamoxifen at days 6, 7 and 8 would capture these cells as they undergo clonal expansion. These results of these approaches are illustrated in Figure 5.16.

Representative FACS plots demonstrate 2W1S-specific T cells to be identified in the spleen of CD4<sup>creERT2</sup>Tbx21<sup>F/F</sup>xROSA26<sup>RFP</sup>, Id2<sup>creERT2</sup>xROSA26<sup>RFP</sup> and Id2<sup>creERT2</sup>Tbx21<sup>F/F</sup>xROSA26<sup>RFP</sup> mice following the experimental approach described

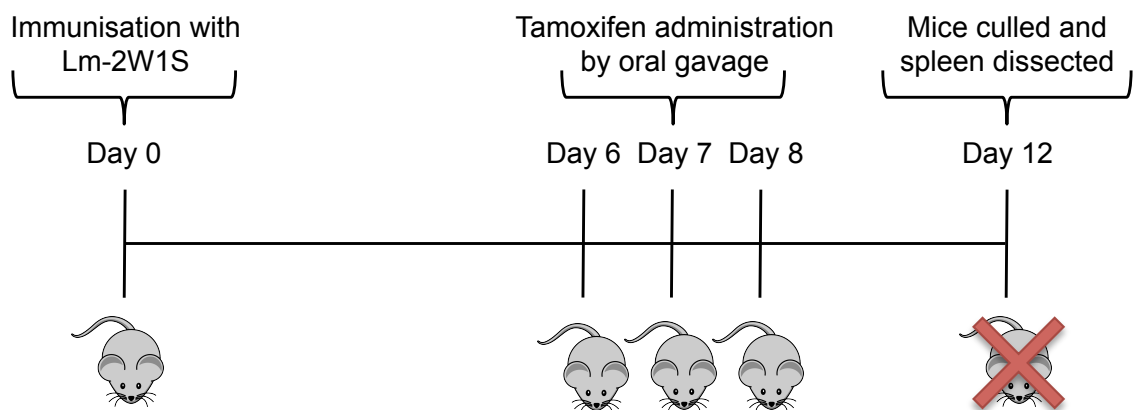
### **5.15 Experimental design for investigating Id2 expression amongst CD4<sup>+</sup> effector T cells during a Th1 response**

To compare the expression of Id2 amongst CD4<sup>+</sup> effector T cells during a Th1 immune response, Id2<sup>creERT2</sup>xROSA26<sup>RFP</sup> and Id2<sup>creERT2</sup>Tbx21<sup>F/F</sup>xROSA26<sup>RFP</sup> mice were immunised with Lm-2W1S and subsequently administered tamoxifen by oral gavage using two different approaches. A) Method 1. Mice were immunised with Lm-2W1S on day 0 and administered tamoxifen by oral gavage on days 1, 2 and 3 before culling on day 9 and the spleen dissected for analysis. B) Method 2 Mice were immunised with Lm-2W1S on day 0 and administered tamoxifen by oral gavage on days 6, 7, and 8 before culling on day 12 and the spleen dissected for analysis.

**A** Method 1



**B** Method 2



in method 1 (Figure 5.16A). A proportion of RFP<sup>+</sup> cells corresponding to Id2 expression can also be observed amongst the 2W1S-specific cells identified in these mice (Figure 5.16A). The CD4<sup>creERT2</sup>Tbx21<sup>F/F</sup>xROSA26<sup>RFP</sup> mouse was included to provide evidence of our model working. Cells shown in these FACS plots were pre-gated on CD3<sup>+</sup> B220<sup>-</sup> CD11b<sup>-</sup> CD11c<sup>-</sup> cells. Gating controls for 2W1S-specific cells were based on cells isolated from the spleen of Id2<sup>creERT2</sup>xROSA26<sup>RFP</sup> mouse and incubated with a CLIP control (Figure 5.16B). Gating controls for RFP expression were based on cells isolated from the spleen of Id2<sup>creERT2</sup>xROSA26<sup>RFP</sup> mice in the absence of the gene for Cre recombinase (Figure 5.16C).

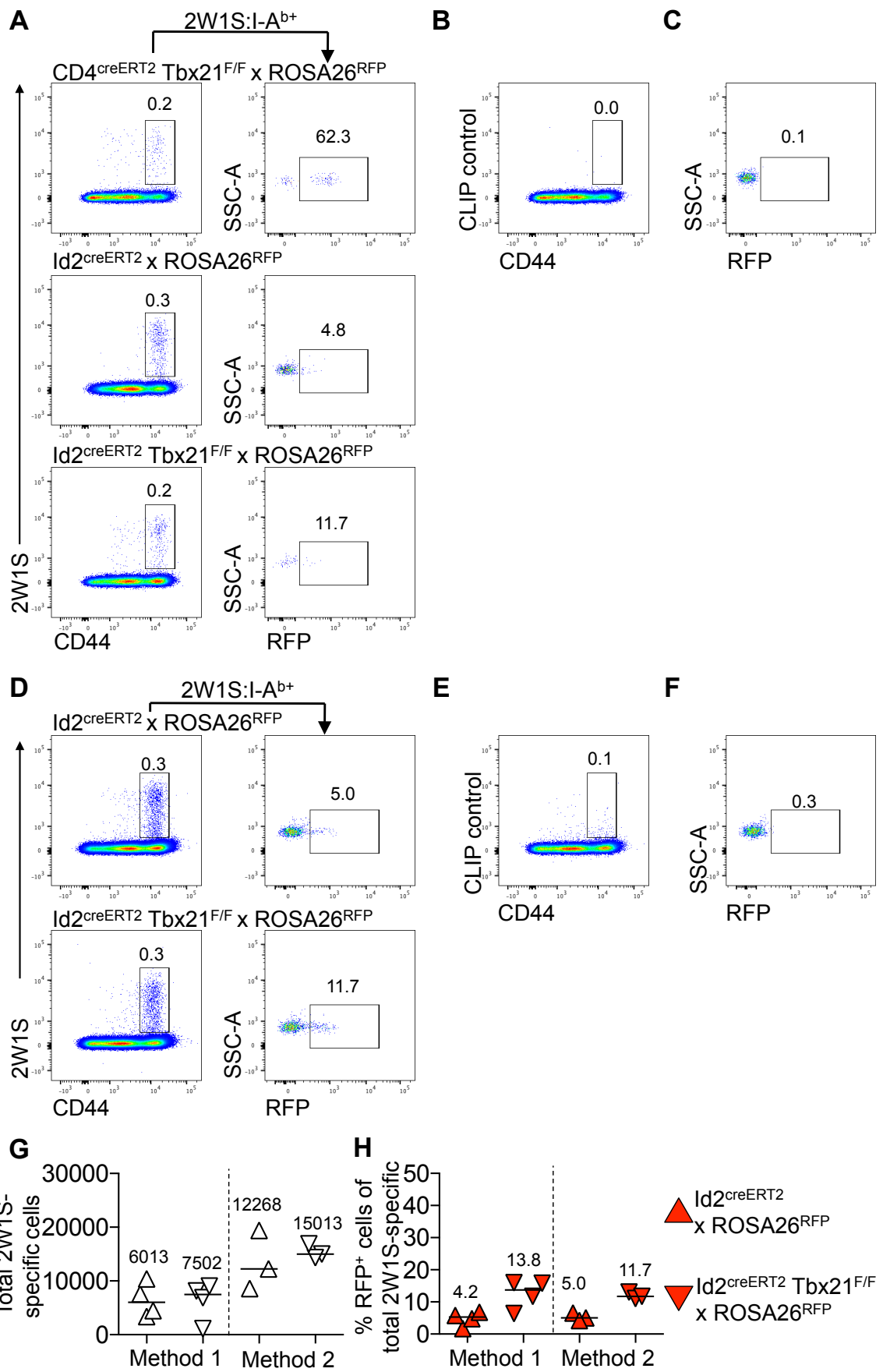
Representative FACS plots demonstrate 2W1S-specific cells to be identified in the spleen of Id2<sup>creERT2</sup>xROSA26<sup>RFP</sup> and Id2<sup>creERT2</sup>Tbx21<sup>F/F</sup>x ROA26<sup>RFP</sup> mice following the experimental approach described in method 2 (Figure 5.16D). A proportion of RFP<sup>+</sup> cells corresponding to Id2 expression can also be observed amongst the 2W1S-specific cells identified in these mice (Figure 5.16D). CD4<sup>creERT2</sup>Tbx21<sup>F/F</sup>xROSA26<sup>RFP</sup> mice were absent from this methodology due to the availability of these mice. Control gating for 2W1S-specific cells and RFP expression were determined using the methods described above and their FACS plots shown in Figure 5.16E and 5.16F, respectively. Statistical comparison of the total number of 2W1S-specific cells in the spleen of Id2<sup>creERT2</sup>xROSA26<sup>RFP</sup> and Id2<sup>creERT2</sup>Tbx21<sup>F/F</sup>x ROA26<sup>RFP</sup> mice following either method 1 or method 2 demonstrate no significant difference amongst these mice (Figure 5.16F). However, comparison of the median of the total number of cells between these two methods identify elevated numbers in both mouse strains following treatment as described in method 2 (Figure 5.16G). While, statistically, there is no significant difference between the proportion of RFP

### 5.16 Id2 expression can be detected amongst CD4<sup>+</sup> effector T cells in the spleen following immunisation with Lm-2W1S

To compare the expression of Id2 amongst CD4<sup>+</sup> effector T cells during a Th1 immune response, Id2<sup>creERT2</sup>xROSA26<sup>RFP</sup> and Id2<sup>creERT2</sup>Tbx21<sup>F/F</sup>xROSA26<sup>RFP</sup> mice were immunised with Lm-2W1S and subsequently administered tamoxifen by oral gavage using two different approaches. In method 1, mice were immunised with Lm-2W1S on day 0 and administered tamoxifen on days 1, 2 and 3 before culling on day 9. In method 2, mice were immunised with Lm-2W1S on day 0 and administered tamoxifen on days 6, 7, and 8 before culling on day 12. Cells isolated from the spleen were assessed in both methods. Cells were analysed by flow cytometry and total numbers calculated per whole spleen. Data shown in red corresponds with RFP expression.

- A) Representative FACS plots for the identification of 2W1S-specific RFP<sup>+</sup> T cells in the spleen following treatment as described in method 1. Cells were pre-gated on CD3<sup>+</sup> B220<sup>-</sup> CD11b<sup>-</sup> CD11c<sup>-</sup> CD4<sup>+</sup> cells. CD4<sup>creERT2</sup> Tbx21<sup>F/F</sup> x ROSA26<sup>RFP</sup> mice were used as a positive control RFP expression amongst total CD4<sup>+</sup> T cells.
- B) Representative FACS plot for the CLIP control in the spleen of Id2<sup>creERT2</sup>xROSA26<sup>RFP</sup> mice following treatment as described in method 1.
- C) Gating controls for RFP<sup>+</sup> cells were based on RFP expression in mLN (left) and thymus (right) of Id2<sup>ERT2</sup> x ROSA26<sup>RFP</sup> mice that are absent of the gene for Cre recombinase following treatment as described in method 1.
- D) Representative FACS plots for the identification of 2W1S-specific RFP<sup>+</sup> T cells in the spleen following treatment as described in method 2. Cells were pre-gated on CD3<sup>+</sup> B220<sup>-</sup> CD11b<sup>-</sup> CD11c<sup>-</sup> CD4<sup>+</sup> cells.
- E) Representative FACS plot for the CLIP control in the spleen of Id2<sup>creERT2</sup>xROSA26<sup>RFP</sup> mice following treatment as described in method 2.
- F) Gating controls for RFP<sup>+</sup> cells were based on RFP expression in mLN (left) and thymus (right) of Id2<sup>ERT2</sup> x ROSA26<sup>RFP</sup> mice that are absent of cre following treatment as described in method 2.
- G) Comparison of the total number of 2W1S-specific T cells in the spleen of Id2<sup>creERT2</sup>xROSA26<sup>RFP</sup> and Id2<sup>creERT2</sup>Tbx21<sup>F/F</sup>xROSA26<sup>RFP</sup> mice following treatment as per method 1 or method 2.
- H) Comparison of the proportion of RFP<sup>+</sup> cells amongst 2W1S-specific T cells in the spleen of Id2<sup>creERT2</sup>xROSA26<sup>RFP</sup> and Id2<sup>creERT2</sup>Tbx21<sup>F/F</sup>xROSA26<sup>RFP</sup> mice following treatment as per method 1 or method 2.

Kruskal-Wallis one-way ANOVA with post hoc Dunn's test was used (comparing three or more data sets) for statistical analysis. In all graphs the bar represents the median, n=5 (method 1) and n=3 (method 2). Data for all time points shown from one independent experiment.





expressed amongst these cells in both mouse strains and across methods, comparison of the median values amongst these mice show a rise in RFP expression in the spleen of  $Id2^{creERT2}Tbx21^{F/F} \times ROSA26^{RFP}$  in comparison to  $Id2^{creERT2} \times ROSA26^{RFP}$  (Figure 5.16H). Of course, these experiments were preliminary to future work and the availability of mice limited the sample sizes used. Overall, these data demonstrate that  $Id2$  expression can be assessed amongst  $CD4^+$  effector T cells that are specific for Lm-2W1S.

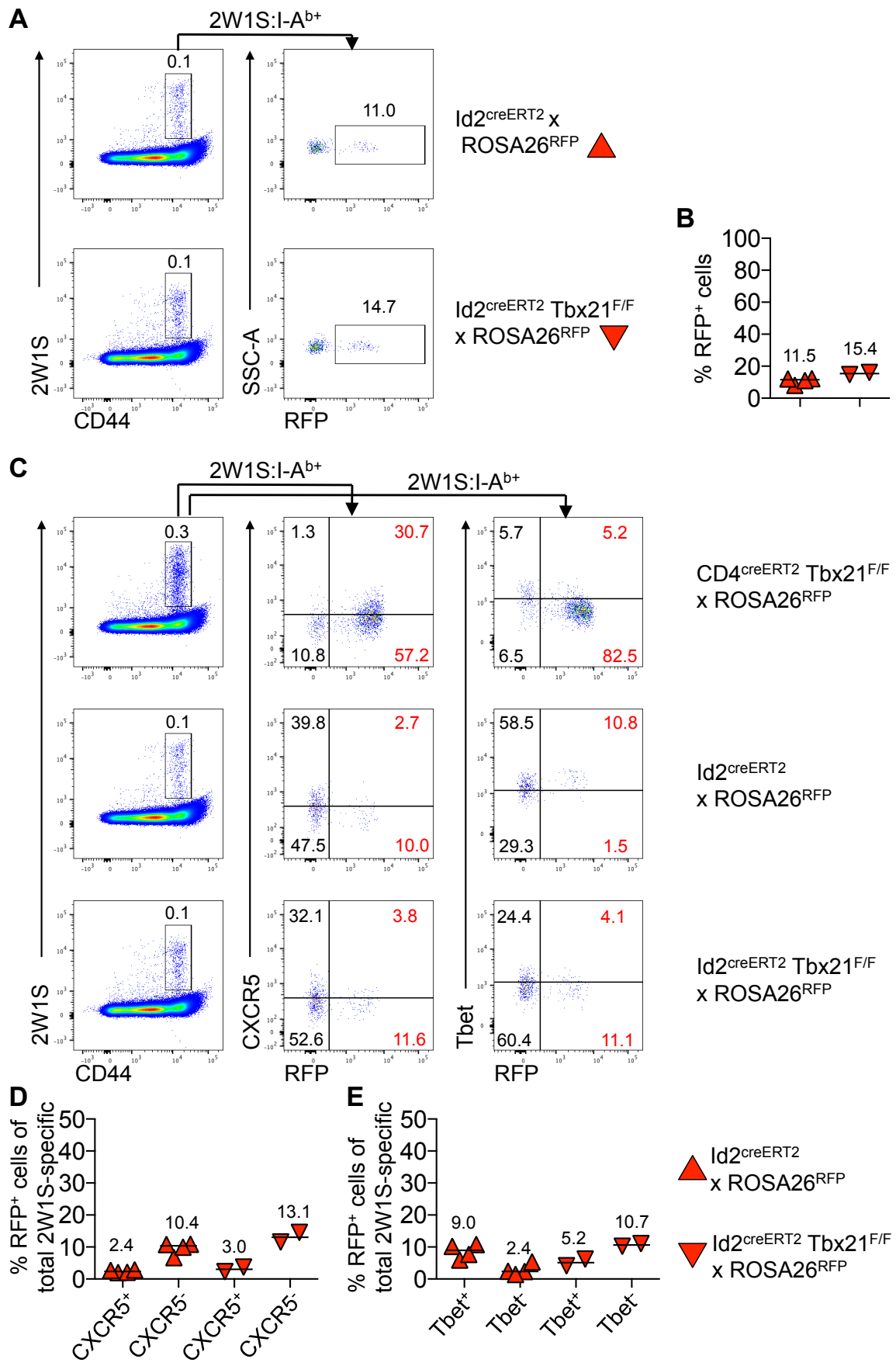
Given the progress of these pilot experiments, we next attempted to optimise our methodology and expand our staining panel so that Tbet expression amongst Th1 effector T cells could be identified. Building upon the approach described in method 2,  $CD4^{creERT2}Tbx21^{F/F} \times ROSA26^{RFP}$ ,  $Id2^{creERT2} \times ROSA26^{RFP}$  and  $Id2^{creERT2}Tbx21^{F/F} \times ROSA26^{RFP}$  mice were immunised with Lm-2W1S on day 0 and administered tamoxifen for a prolonged period on days 4, 5, 6 and 7. Mice were culled on day 14 and cells pooled from the spleen and the axillary, cervical and inguinal lymph nodes (peripheral lymph nodes; pLN) were assessed. Firstly, cells were identified as per the gating strategy used in Figure 5.16 and RFP expression amongst 2W1S-specific T cells in  $Id2^{creERT2} \times ROSA26^{RFP}$  and  $Id2^{creERT2}Tbx21^{F/F} \times ROSA26^{RFP}$  mice was shown (Figure 5.17A) Enumeration of the proportion of RFP expressed was identified to be greater than 10% in both mice (Figure 5.17B). These findings were consistent with our preliminary experiments whereby RFP expression could be identified amongst  $CD4^+$  effector T cells that were specific for 2W1S. Following from this, we assessed the expression of CXCR5 and Tbet expression in relation to RFP (Figure 5.17C-E).

### 5.17 Tbet can be deleted amongst CD4<sup>+</sup> effector T cells in the spleen and pLN following Cre induction with tamoxifen

To determine whether Tbet can be deleted amongst 2W1S-specific CD4<sup>+</sup> effector T cells that fate-map to Id2, Id2<sup>creERT2</sup>xROSA26<sup>RFP</sup> and Id2<sup>creERT2</sup>Tbx21<sup>F/F</sup>xROSA26<sup>RFP</sup> mice were immunised with Lm-2W1S and subsequently administered tamoxifen by oral gavage. Cells isolated from the spleen and pLN were analysed by flow cytometry. Total numbers calculated from pooling the cells isolated from the spleen and peripheral lymph nodes. Data shown in red corresponds with RFP expression.

- A) Representative FACS plots for the identification of 2W1S-specific RFP<sup>+</sup> T cells in the spleen of Id2<sup>creERT2</sup>xROSA26<sup>RFP</sup> and Id2<sup>creERT2</sup>Tbx21<sup>F/F</sup>xROSA26<sup>RFP</sup> mice. Mice were immunised with Lm-2W1S on day 0, administered tamoxifen on days 4, 5, 6 and 7, and culled on day 14. Cells were pre-gated on CD3<sup>+</sup> B220<sup>-</sup> CD11b<sup>-</sup> CD11c<sup>-</sup> CD4<sup>+</sup> cells.
- B) Proportion of RFP<sup>+</sup> cells amongst 2W1S-specific T cells in the spleen and pLN.
- C) Representative FACS plots for the identification of RFP, CXCR5 and Tbet expression amongst 2W1S-specific T cells in the spleen and pLN of Id2<sup>creERT2</sup>xROSA26<sup>RFP</sup> and Id2<sup>creERT2</sup>Tbx21<sup>F/F</sup>xROSA26<sup>RFP</sup> mice. CD4<sup>creERT2</sup> Tbx21<sup>F/F</sup> x ROA26<sup>RFP</sup> mice were used as a positive control for Tbet deletion amongst total CD4<sup>+</sup> T cells.
- D) Comparison of the proportion of RFP expressed by CXCR5<sup>+</sup> and CXCR5<sup>-</sup> cells amongst 2W1S-specific T cells.
- E) Comparison of the proportion of RFP expressed by Tbet<sup>+</sup> and Tbet<sup>-</sup> cells amongst 2W1S-specific T cells.

Kruskal-Wallis one-way ANOVA with post hoc Dunn's test was used (comparing three or more data sets) for statistical analysis. In all graphs the bar represents the median, n=4 and n=2 for Id2<sup>creERT2</sup>xROSA26<sup>RFP</sup> and Id2<sup>creERT2</sup>Tbx21<sup>F/F</sup>xROSA26<sup>RFP</sup>, respectively. Data for all time points shown from one independent experiment.



Using cells pooled from the spleen and pLN of CD4<sup>creERT2</sup>Tbx21<sup>F/F</sup>xROSA26<sup>RFP</sup> mice, RFP<sup>+</sup> cells were shown to be CXCR5<sup>-</sup> and Tbet<sup>-</sup> (Figure 5.17C). This demonstrates the majority of Tbet deleted on cells fate-mapped to CD4. This gating strategy was applied to cells pooled from the spleen and pLN of Id2<sup>creERT2</sup>xROSA26<sup>RFP</sup> and Id2<sup>creERT2</sup>Tbx21<sup>F/F</sup>x ROA26<sup>RFP</sup> mice (Figure 5.17C). Here, the majority of RFP<sup>+</sup> cells amongst the 2W1S<sup>+</sup> population in Id2<sup>creERT2</sup>xROSA26<sup>RFP</sup> express Tbet. However, in Id2<sup>creERT2</sup>Tbx21<sup>F/F</sup>x ROA26<sup>RFP</sup> mice, the majority of RFP<sup>+</sup> cells arising from the 2W1S<sup>+</sup> are Tbet<sup>-</sup>; demonstrating the successful deletion of Tbet from this subset (Figure 5.17C). Enumeration of these data demonstrates the proportion of RFP expressed by 2W1S-specific T cells to be greatest amongst CXCR5<sup>-</sup> cells (Figure 5.17D). Moreover, these data illustrate the proportion of RFP expressed by 2W1S-specific T cells to be greater amongst Tbet<sup>-</sup> cells of Id2<sup>creERT2</sup>Tbx21<sup>F/F</sup>x ROA26<sup>RFP</sup> mice (Figure 5.17E). However, repeat analysis is required to determine whether these data to be statistically significant.

### 5.3 Discussion

Throughout our earlier investigations it was observed that the majority of cells in the thymus that expressed Id2 were not ILC. Therefore, we aimed to characterise the expression of Id2 amongst cells other than ILC, both in the thymus and at peripheral sites. Early on within our fate-mapping investigations it was apparent that while  $\alpha\beta$  T cells were the most abundant cells arising from RFP<sup>+</sup> cells, only a small proportion of total  $\alpha\beta$  T cells expressed Id2. Notably, the greatest proportion of RFP<sup>+</sup> cells arose from iNKT cells and was true of both the thymus and mLN. Moreover, the proportion of RFP<sup>+</sup> cells amongst the iNKT cell population was comparable to that of ILC. Given that all ILC express Id2 due to the indispensable requirement for this transcription factor during development, it was inferred that all iNKT cells also expressed Id2. The ability to label all cells in a tamoxifen inducible Cre-LoxP system is technically challenging and is affected by the efficiency of our model. Therefore, the efficiency of Cre induction can account for the fewer than 100% of ILC, and ultimately iNKT cells, which express RFP in our model.

Continuing with our study of iNKT cells, we were able to identify iNKT1, iNKT2 and iNKT17 subsets in the thymus of WT mice in proportions similar to those previously described.<sup>(57)</sup> We later demonstrated Id2 expression amongst all iNKT subsets using reporter mice that was maintained in peripheral lymph nodes. Although all iNKT subsets, to at least some extent, were shown to arise from Id2-expressing cells in the thymus, the majority of these were iNKT1 cells. However, this is reflective of the composition of iNKT cells within this tissue as shown in the WT data. Moreover, in both WT and Id2 reporter experiments it was not possible to include an antibody against Tbet within our antibody panel due to the limited choice of conjugate

fluorochrome. Instead, we relied on PLZF and ROR $\gamma$ t to separate these populations from total iNKT cells. To strengthen our findings, these iNKT subsets could be further characterised by their expression of NK1.1. While NK1.1 is not a substitute for Tbet, its inclusion would provide further evidence to support the identification of iNKT1 cells given NK1.1 is not expressed by either iNKT2 or iNKT17 cells.(57) Overall, we concluded in Id2 reporter mice that all iNKT subsets expressed Id2. However, this does not explain why some of these cells were arising from the Id2-negative proportion of iNKT cells. We propose this difference is due to the brightness of GFP on the cell surface. In our investigations, there was weak expression of GFP that was difficult to pull apart from the non-Id2 expressing cells despite including a suitable control. Furthermore, if the cells present were truly GFP<sup>-</sup> then they are likely to show as a distinct population. While there were some limitations to our experiments, our findings were consistent with other studies.(77)

Our data demonstrated Id2 expression by iNKT1, iNKT2 and iNKT17 subsets was maintained in peripheral lymph nodes. Until now, the expression of Id2 by iNKT cells in the periphery had been assessed predominantly in the liver and spleen. These investigations illustrated a drastic reduction in absolute numbers of iNKT cells within the liver in the absence of Id2, while numbers of these cells in the spleen and thymus were normal.(56) We sought to examine the effect of Id2 on the function of iNKT cells, again using mice that fate mapped to Id2. These data illustrated no difference in the capability of iNKT cells to produce IL-4 or IFN $\gamma$  whether regardless of their Id2 expression. As previously mentioned, the ability to identify all cells that fate map to Id2 is reliant on the efficiency of the Cre-LoxP system. The fact no difference is observed between non-fate mapped and fate mapped cells in our experiment support

the idea that these are all the same cells. Previously, our data in Id2 reporter mice had shown the greatest proportion of Id2 to be expressed by iNKT17 cells in the pooled peripheral lymph nodes. While it would be interesting to assess the association between Id2 expression and the capability of these cells to produce IL-17, we would hypothesise that no difference would be observed between cells that fate map or do not fate map to Id2 in our model.

It had previously been reported that strength of TCR $\gamma\delta$  signalling restricted the development of IL-17A producing  $\gamma\delta$  T cells and instead influenced the development of IFN $\gamma$  producing cells.(206) It was evident in the prenatal thymus that these two pathways could be segregated base on the expression of either V $\gamma$ 5 or V $\gamma$ 6.(206) The expression of V $\gamma$ 5 at the prenatal stage generated IFN $\gamma$  producing  $\gamma\delta$  T cells while cells of the IL-17A pathway expressed V $\gamma$ 6. However, following birth, the expression of V $\gamma$ 1, V $\gamma$ 2/3 and V $\gamma$ 4 was detected in both pathways in the postnatal and adult thymus.(206)

Building upon our previous data where we demonstrated Id2 to be expressed by a small proportion of  $\gamma\delta$  T cells in the thymus, we sought to examine the expression of Id2 amongst the IFN $\gamma$  and IL-17 pathways.(206) Using the same strategy as Sumaria *et al.* (2017), we successfully identified cells akin to IFN $\gamma$  (CD44<sup>+</sup> CD45RB<sup>+</sup>) and IL-17A (CD44<sup>+</sup> CD45RB<sup>-</sup>) producing cells in the thymus and at peripheral sites. This was followed by the assessment of these populations arising from GFP<sup>+</sup> cells in Id2-eGFP reporter mice. However, we revealed Id2 to be expressed by all  $\gamma\delta$  T cells investigated and its expression was not restricted to either IFN $\gamma$  or IL-17A lineage.

We later illustrated the expression of Id2 based on V $\gamma$ 1 or V $\gamma$ 2 segment usage amongst CD44<sup>+</sup> CD45RB<sup>+</sup> and CD44<sup>+</sup> CD45RB<sup>-</sup> populations. While it would have been interesting to examine the expression of all  $\gamma$ -chains associated with these cells, such as V $\gamma$ 4, V $\gamma$ 5 and V $\gamma$ 6, we were limited by the availability of antibodies that fit with our existing antibody panel. We demonstrated the majority GFP<sup>+</sup> CD44<sup>+</sup> CD45RB<sup>+</sup> cells in peripheral tissues to be either V $\gamma$ 1<sup>+</sup> or V $\gamma$ 2<sup>+</sup> cells. However, GFP<sup>+</sup> CD44<sup>+</sup> CD45RB<sup>-</sup> cells were either V $\gamma$ 2<sup>+</sup> or V $\gamma$ 1<sup>-</sup> V $\gamma$ 2<sup>-</sup>. Although this indicates differences in  $\gamma$ -chain usage amongst these cells, these data does not demonstrate a restriction between Id2 and specific  $\gamma$ -chain usage. Instead, the differences in  $\gamma$ -chain usage between CD44<sup>+</sup> CD45RB<sup>+</sup> and CD44<sup>+</sup> CD45RB<sup>-</sup> cells are likely to be associated to the functions of these cells and not Id2 itself. This could be assessed in future experiments by comparing  $\gamma$ -chain usage amongst CD44<sup>+</sup> CD45RB<sup>+</sup> and CD44<sup>+</sup> CD45RB<sup>-</sup> populations in WT and Id2-eGFP reporter mice.

Our data in the neonatal thymus revealed the majority of GFP<sup>+</sup>  $\gamma\delta$  T cells to be CD44<sup>+</sup> CD45RB<sup>-</sup> cells, representing those restricted to the IL-17A lineage. Moreover, it was identified that these cells were V $\gamma$ 1<sup>-</sup> V $\gamma$ 2<sup>-</sup>. However, the slight variation in the CD24<sup>-</sup> gate in the neonatal thymus compared to our adult data must be acknowledged here. Cells isolated from the adult tissues comprised of CD24<sup>+</sup>, CD24<sup>lo</sup> and CD24<sup>-</sup> cells and therefore it was not entirely clear where to position the CD24<sup>-</sup> gate, whilst in the neonatal thymus the CD24<sup>-</sup> and CD24<sup>+</sup> cells were much more distinct. However, our data in the neonatal thymus was limited by the availability of Id2-eGFP mice. Future investigations would seek to repeat this experiment to provide greater reliability in our findings.



Further ideas to strengthen these data include examining the expression of V $\gamma$ 4, V $\gamma$ 5 and V $\gamma$ 6 amongst Id2-expressing populations. Moreover,  $\gamma\delta$  T cells were shown to segregate in the prenatal thymus based on their expression of V $\gamma$ 5 and V $\gamma$ 6. It would be interesting to determine the expression of Id2 in these cells during the prenatal window. Collectively, our data demonstrated Id2 to be expressed by mature  $\gamma\delta$  T cells regardless of lineage restriction. Returning to what is known about other innate-populations, such as iNKT cells, where Id2 expression is increased with maturation, it would be interesting to explore the stage at which Id2 is switched on in  $\gamma\delta$  T cells.

Moving away from innate populations, we later explored the expression of Id2 in effector T cell populations where previous work had shown Id2 to reinforce Th1 differentiation and restriction of a Tfh cell fate.(196) Fitting with these reports, our initial findings demonstrated Id2 to be negligible among naïve CD4<sup>+</sup> T cells while Id2 expression was elevated amongst CD4<sup>+</sup> T cells at effector sites, such as the small intestine, using Id2-eGFP reporter mice. Id2 expression was also identified in CD8<sup>+</sup> T cells in the small intestine, although to a lesser extent than CD4<sup>+</sup> T cells. Due to restrictions in time during our investigations it was not possible to explore either of these subsets in this tissue further. However, if time had permitted it would have been interesting to further characterise Id2 expression amongst both CD4<sup>+</sup> and CD8<sup>+</sup> cells in the small intestine. Firstly, it would be interesting to see whether Id2 was associated with a specialised group of CD8<sup>+</sup> T cells in the small intestine, termed intraepithelial lymphocytes. Further investigations could use CD8 $\alpha$ , CD69 and CD103, which are commonly used to identify this homogenous cell population.(210) In addition, Treg are a population of CD4<sup>+</sup> T cells that are fundamental in ensuring immune homeostasis.(204,211) These cells are characterised by their expression of

FoxP3, which is fundamental in maintaining their suppressive properties.(204,212) Moreover, the expression of FoxP3 enables discrimination of these cells from other T cell subsets.(204) Recently, it was shown that Id2 expression mediates the plasticity of Treg whereby increased Id2 expression in an inflammatory environment favours an ex-FoxP3 Th17 cell phenotype.(204) As such, further investigating the relationship between Id2 and the phenotype and function of Treg in the small intestine would be an interesting avenue to pursue. Interestingly, the majority of  $\gamma\delta$  T cells isolated from the small intestine also expressed Id2. Further to this, the expression of Id2 amongst  $\gamma\delta$  T cells at this effector site was greater than that previously observed in lymphoid tissues. While these data indicates a role for Id2 in the effector response of  $\gamma\delta$  T cells, this was not explored within this thesis.

We successfully identified Id2 expression amongst antigen-specific CD4<sup>+</sup> T cells in the spleen. Moreover, the expression of Id2 was restricted to Th1 effector T cells, agreeing with previously published work by Shaw *et al.* (2016).(196) However, we used an alternative approach compared to this work by Shaw *et al.* (2016). We next used our model to assess changes in Id2 expression across this antigen-specific immune response between day 4 and day 21 post-immunisation. We examined the expression of Id2 a several time points post-immunisation with Lm-2W1S and demonstrated GFP expression to be greatest at day 7. Previous studies by Pepper *et al.* (2011) have demonstrated the number of antigen-specific T cells to peak at day 7, illustrating the increase in Id2 expression coincides with the clonal expansion of antigen-specific T cells.(213) Collectively, these data demonstrated Id2 to be upregulated in antigen-specific CD4<sup>+</sup> T cells and orchestrated the differentiation of the Th1 effector subsets. While these data are not entirely novel, our findings are

consistent with the published literature and provide us with confidence in our own findings.

The final, and likely the most experimental part of our studies, attempted to delete Tbet amongst antigen-specific T cells that expressed Id2 to determine the effect on Th1 cell function. While these experiments were limited by the time available, we successfully deleted Tbet in this context as shown by the absence of this transcription factor amongst the majority of RFP<sup>+</sup> cells in our final experiments. However, our data demonstrated a small proportion of RFP<sup>+</sup> cells that were Tbet<sup>+</sup>, illustrating the technical challenges faced within our investigations. It is clear from our data that the fluorochrome conjugated to the anti-Tbet antibody is not very bright and is owing to the limited availability of anti-Tbet antibodies that would fit within our antibody panel. As a result of this, the Tbet<sup>+</sup> and Tbet<sup>-</sup> cells are not highly distinct. An attempt to improve Tbet staining in this context could be made in future experiments by incubating cells with the intracellular antibodies for a longer period of time. In addition to this caveat, the ability to target antigen-specific cells in this context is also technically challenging. While our previous experiments had demonstrated Id2 expression to be greater at day 7, these experiments were performed in reporter mice, which illustrate the live expression of Id2. Our fate-mapping model, however, identifies cells that are currently or have previously expressed Id2, during or just before the window of tamoxifen administration. Therefore, it is more difficult to label the target cells. Initially, we administered tamoxifen to these mice by oral gavage on days 1, 2 and 3 post-immunisation with Lm-2W1S prior to the rapid proliferation of antigen-specific T cells between days 3 and 7.(213) However, this only labelled ~5% of antigen-specific T cells that expressed Id2. Adapting our methodology slightly, we

administered tamoxifen by oral gavage on days 6, 7 and 8, where we have previously observed the greater proportion of Id2 expression in reporter mice. Given that the time taken for Id2 to exert its effect is not known, it was not unreasonable for us to attempt to target the antigen-specific T cells across these time points. However, this also resulted in only ~5% of Id2 expressing antigen-specific cells to be labelled. Interestingly, for reasons unknown, the proportion of Id2 expressing antigen specific cells of Id2<sup>CreERT2</sup> Tbx21<sup>F/F</sup> xROSA26<sup>RFP</sup> mice was greater than that observed in Id2<sup>CreERT2</sup> xROSA26<sup>RFP</sup>.

Our final investigations attempted to target these cells by extending the duration at which mice were administered tamoxifen. While labelling efficiency did not meet the level observed in reporter mice, this was increased to ~11% and ~15% in Id2<sup>CreERT2</sup> Tbx21<sup>F/F</sup> xROSA26<sup>RFP</sup> and Id2<sup>CreERT2</sup> xROSA26<sup>RFP</sup> mice, respectively. It was within these mice that we also assessed Tbet expression and observed successful deletion of this transcription factor. Unfortunately, giving time restraints, we were unable to take these investigations further. Subsequent work hoped to explore the effect of Tbet deletion on the function of antigen-specific Th1 cells by assessing IFN $\gamma$  in these cells. Within the literature, it was shown that deletion of Id2 amongst effector T cells inhibited the differentiation of Th1 cells and instead restricted cells to a Tfh effector lineage. Based on these findings we would anticipate the absence of Tbet to reduce the ability of these cells to produce IFN $\gamma$ . Moreover, it would be interesting to reassess the CXCR5 PD-1 phenotype of the antigen-specific T cells. Based on published literature, it would not be unreasonable to suggest these cells to have a Tfh phenotype and upregulate Bcl-6.(196,213)

Collectively, the data presented within this chapter illustrated Id2 to be expressed by  $\gamma\delta$  T cells and iNKT cells following their maturation in the thymus and this expression was maintained in peripheral sites. However, Id2 is largely absent from naïve CD4<sup>+</sup> T cells but is rapidly upregulated following initiation of the adaptive immune response. In this context, we were able to track the expression of Id2 amongst antigen-specific CD4<sup>+</sup> T cells by immunising Id2-eGFP reporter mice with Lm-2W1S with GFP<sup>+</sup> expression peaking at day 7. Finally, we demonstrated Id2 expression to be restricted to Th1 effector T cells and established a model whereby Tbet could be conditionally deleted in Id2-expressing cells. Whether the deletion of Tbet in this context affects the function of these requires further investigation. Together, these data illustrated the differences in Id2 expression between innate and effector populations. However, further work is required to define the roles of Id2 in either context.

## **CHAPTER 6: GENERAL DISCUSSION**

## 6.1 Overview

The thymus is responsible for the establishment of self-tolerant T cells with the ability to respond to a variety of antigens and initiate the adaptive immune response. Failure to eliminate self-reactive T cells during this process can lead to the development of autoimmune diseases, such as rheumatoid arthritis, and therefore the establishment of immune tolerance is of utmost importance.(214) The capability to complete this function is a result of the unique microenvironments within the thymus, which is split into two main components: the parenchyma and the stroma. While the parenchyma consists mainly of T lymphocytes, the thymic stroma consists of specialist thymic epithelial cells (TEC). Although these are discussed as two entities, the development of multiple T cell populations within this tissue is a result of bidirectional signalling between cells of the stroma, such as the cortical and medullary TEC, and developing thymocytes.(215) Thus, there is a requirement for cells to interact with each other within the thymus in order to support their own development.

Indeed, this bidirectional relationship between developing thymocytes and the thymic stroma is important across the life span of the thymus. This is highlighted in the involution of the ageing thymus, which is characterised by a reduction in thymic tissue mass and cellularity, in addition to a loss in tissue organisation.(113) Together, this results in reduced naïve T cell output with a decline in T cell diversity that is thought to contribute to the increased susceptibility of older individuals to infection and autoimmune disease, as well as cancer.(113) Although it is widely appreciated that the thymus involutes with age, the mechanisms that contribute to this process are less well understood. However, there is evidence to support the idea that thymic

involution is a result of defects in both developing thymocytes and the thymic stroma; both having an effect on the bidirectional relationship.(112)

The complex mechanisms that govern thymopoiesis have been described in earlier chapters of this thesis. However, it is important to acknowledge the important role of the bone marrow that provides the continual supply of progenitors required by the thymus.(113) Therefore, any changes in the bone marrow as a result of ageing will also impact on the functioning of the thymus. Evidence has shown that haematopoietic stems cells in the ageing bone marrow have increased bias towards the myeloid lineage compared to the lymphoid lineage.(216) This is thought to contribute to involution of the thymus during ageing due to the reduced influx of thymic progenitors to this tissue.(113)

To examine the significance of ILC populations in the thymus it is important to review our findings in the context of the thymus at different stages of life. As previously mentioned, the stromal compartment has a crucial role in thymopoiesis where it promotes the proliferation and differentiation of developing thymocytes through the provision of key signals. This is largely influenced by cTEC and mTEC that comprise the majority of the thymic stroma.(217) Therefore, any changes amongst the niches that exist within the thymus will impact the on the function of the thymus. This raises the question of what the importance of ILC is throughout development. It was demonstrated from our own investigations that ILC3, namely LTi cells, are the main population of ILC in the embryonic thymus and persist following birth. These cells are known to support the maturation of mTEC in the embryonic thymus through the provision of RANKL.(98) However, ILC2 soon became the main population of ILC within the neonatal thymus and this persisted into adulthood. We identified ILC2 in



the medulla of the neonatal and adult thymus, where others have previously identified ILC3 in the embryonic thymus. Moreover, ILC2 isolated from the WT thymus were unable to provide RANKL and instead were capable of producing type-2 cytokines associated with these cells at peripheral sites; indicating distinct functions amongst ILC in the thymus. However, the relevance of these findings in the wider field has yet to be discussed. Here, we review our findings in the context of current literature to determine the significance of ILC within the thymus across ontogeny.

It has become evident over recent years that that functional diversity exists amongst ILC populations. This includes, but is not restricted to, their role in the maintenance of immune homeostasis, particularly at barrier sites and within lymphoid organs.(72) These barrier sites comprise of epithelia that have an underappreciated function in the maintenance of immunity where they provide first line defence to invading pathogens.(218) In addition, there is extensive evidence to support ILC function at these sites, particularly in the lung, where ILC2 are numerous and play a key role in maintain epithelial function.(130) The role of ILC3 in the maintenance of immune homeostasis has also been extensively studied. Recently, ILC3 have been proposed to act as “communication hubs” in the small intestine where they are capable of responding to a number of different signals from their surrounding microenvironment.(219) These signals are integrated into complex intracellular mechanisms that result in different immune outputs. Therefore, how ILC3 respond to the signals influences the maintenance of immune homeostasis at these sites.(219)

Within this thesis, we hypothesised that ILC populations would also support the epithelial niches in the thymus. Previously, published research described the communication between LT $\alpha$ i cells and TEC that supported the development and

maintenance of the thymic microenvironment in the embryo.(98) Therefore, it was not unreasonable for us to explore the idea that ILC could have other supportive roles within the thymus, which consists of vast epithelial networks. However, the work of Rossi *et al.* (2007) was published greater than 10 years ago and preceded our realisation of multiple ILC populations. As a result, we built upon our extensive understanding of ILC populations and their function within the periphery to undertake a detailed assessment of ILC populations within the thymus. In addition, we interrogated the function of these cells to understand how they might support homeostasis within the thymus.

## **6.2 ILC3 support epithelial development in the embryonic and neonatal thymus**

Building on the initial studies by Rossi *et al.* (2007), we observed ILC3 within the embryonic thymus and later identified these cells within the neonatal thymus. Our data also demonstrated other ILC subsets to be evident in the embryonic thymus. This is owing to the advancement of our understanding of how to identify these cells since the preceding work. The number of ILC3 within the neonatal thymus of WT mice was sufficient for assessment of their function *ex vivo* and it was identified in these studies that ILC3 were capable of expressing RANKL. Based on the previous work by Rossi *et al.* (2007) we inferred that ILC3 provided RANKL to immature mTEC to support their maturation, however this was not assessed directly within our investigations. One solution includes the use of advanced imaging techniques, such as multiphoton laser scanning microscopy, which enables live imaging of cell-to-cell interactions. However, this would not be without its technical challenges. Throughout our investigations it was essential for the rib cage to be pulled apart so that the thymus could be accessed, and given the close proximity of the thymus to the heart,

risked damaged to the cardiovascular system. This is not an ideal scenario for multiphoton laser scanning microscopy where a live animal is required. Furthermore, the thymus is a dense cellular network and given ILC are a rare population in comparison to T cells it would be difficult to identify them in this context. More so because of the similarity between ILC and developing T cells, which was one of the main challenges faced throughout our studies.

Furthermore, ILC3 are not the sole providers of RANKL within the developing thymus as published literature has shown this signal to be jointly provided by invariant  $V\gamma 5^+$  DETC.(99) This raises the question to whether the role of LTi cells in providing RANKL is redundant. This could be addressed by assessing these cells in *Rag*<sup>-/-</sup> *Rorc*<sup>-/-</sup> mice. Moreover, primitive lymphoid anlagen comprise LTi cells where they provide lymphotoxin and TNF signals that stimulate the chemokines and adhesion molecules required for lymphoid tissue development. Together, these data support a role for LTi cells in the embryonic and neonatal thymus prior to the decline of ILC3 in the adult thymus. While these data support a role for ILC3 in the embryonic and early neonatal thymus, the number and proportion of these cells then rapidly and substantially fall. As such, it is hard to ascribe a function to ILC3 in the adult thymus where there are so few cells that they are almost absent.

### **6.3 Postnatal changes in thymic ILC3 populations**

Evidence with the literature has identified ILC3 within the adult thymus where they are indicated as key provider of IL-22 and support the regeneration of the thymus following injury. We utilised several *in vivo* models to characterise the ILC composition in the adult thymus and all of these demonstrated that very few ILC3 were present in this tissue. We enumerated these cells and discovered less than 50

to exist within the adult thymus. Therefore, it is difficult for us to understand how these cells contribute to homeostasis in the adult. Moreover, the numbers of ILC3 we observed were several orders of magnitude lower than those described by Dudakov *et al.* (2012).(100) Therefore, it is possible that the authors misidentified these cells, particularly as their gating strategy was not entirely clear. One example of this is evident in the literature concerning the discovery of a regulatory ILC population that was present in the mouse and human intestine.(220) This study used IL-10 reporter mice to identify a novel subset of ILC that suppressed the action of ILC1 and ILC3 through the provision of IL-10.(220) However, this was later disproved. In a subsequent study, the production of IL-10 by regulatory ILC was assessed in mice from three independent mouse vendors and discovered these cells to be absent. Furthermore, regulatory ILC were absent in two models of inflammation. Interestingly, a minute population of ILC2 within this tissue were demonstrated to be the provider of IL-10.(221)

To provide further confidence in our own data we assessed the ILC composition of the thymus following sub-lethal irradiation. While Dudakov *et al.* (2012) suggested radio-resistance amongst the ILC population, we observed completed depletion of all ILC.(100) Further to this, published data reported an increase in IL-22 production in irradiated mice that was attributed to ILC3. We were unable to detect either ILC3 or IL-22 producing ILC3 in the irradiated thymus and, given the number detected in the non-irradiated thymus, this was unsurprising. Moreover, we adapted our gating strategy within this investigation to match that of the publication, rather than use the established gating strategy from our own laboratory. In addition, investigations using *Rorc*<sup>-/-</sup> mice are not without their limitations. We had made several attempts to extend

the thymic recovery period following sub-lethal irradiation. However, *Rorc*<sup>-/-</sup> are severely immunocompromised and have a greater incidence of thymic tumours making this difficult.

#### **6.4 ILC2 is the dominant ILC population post-birth**

Our identification of ILC2 within the thymus is likely the most interesting aspect of our investigations. We demonstrated ILC2 to be present at all stages of thymic development with their number gradually increasing up to 2 weeks post-birth where the numbers are maintained in the adult thymus. Furthermore, we demonstrated ILC2 isolated from the neonatal thymus to be capable of producing IL-5 and IL-13 following *ex vivo* culture. While it is likely that ILC2 in the adult thymus are capable of producing IL-13, an artefact in our investigations limited our analysis and further investigation is required. Finally, the use of confocal microscopy illustrated the presence of these cells in the thymic medulla. Here, we discuss the potential roles of ILC2 in the thymus based on the results described within this thesis. Some of these roles have previously been described within chapter 4 and include the direct effects of IL-13 on thymocytes, the influence of the IL-4/IL-13 receptor complex on the fate of early haematopoietic progenitors, and the activation of medullary epithelium by IL-4 or IL-13 and its influence on T cell egress and will not be discussed again here.(165,190,191)

Our current understanding of ILC2 proposes that these cells are capable of monitoring surrounding tissues and can become activated in response to perturbations in immune homeostasis.(218) IL-25 and IL-33 are some of the key molecules involved in ILC2 activation and cause subsequent IL-5, IL-9 and IL-13 production. Tuft cells are a source of IL-25 and frequent epithelial sites where they

support others cells. Previous evidence has shown Tuft cell-derived IL-25 is sufficient to activate ILC2 in the small intestine. More recently, cells of similar morphology to Tuft cells have been identified in the thymic medulla and it was later confirmed through RNA-sequencing and strict phenotyping that these cells comprised a *bona fide* population of Tuft cells. Moreover, these cells made up to 10% of cells in the thymic medulla.(135,136,222) Single cell sequencing technology has demonstrated thymic Tuft to be a distinct subset of mTEC, known as mTEC Group IV, which are functionally distinct to other mTECs yet closely related to Tuft cells of the intestinal tract. Given Tuft cells in the small intestine are capable of activating ILC2 through the provision of IL-25, we hypothesis these Tuft cells support the type-2 immune environment that supports the function of ILC2.(135,136,222)

The use of single-cell sequencing is becoming more commonplace within immunology and is capable of providing a greater understanding of the molecular mechanisms that govern immune cells. In the example above, this method identified a close relationship of the novel thymic Tuft cells with those described within the small intestine. However, other studies have now used these methods to study other immune cells where a distinct phenotype and function is already described. Classical dendritic cells, for example, can be divided into two distinct subsets, cDC1 and cDC2, based on their phenotype and ability to prime CD4 or CD8 T cells, respectively. Using single-cell sequencing, it has now been discovered that cDC1 populations consist of two populations that arose from two distinct developmental pathways. The cDC2A population is Tbet<sup>+</sup> and has a role in the anti-inflammatory response while cDC2B are RORγt<sup>+</sup> and have pro-inflammatory capabilities.(223) Moreover, single cell sequencing technologies have been used to compare the transcriptomic and

epigenetic landscape of ILCs from the small intestine.(86) These methods could be applied to ILC of the thymus to provide a greater understanding of their molecular identity.

ILC3 are not the only subset of ILC that have been implicated in the restoration of damaged tissues. While the restorative function of ILC2 have not been described within the thymus, there is evidence to suggest a role for ILC2 in this context at peripheral sites, including the lung, skin and small intestine.(131,187,188) Given that ILC2 are the main ILC subset within the adult thymus it is not unreasonable to suggest they are involved in tissue repair. While ILC2 are not a producer of IL-22 they are producers of amphiregulin.(87) Whether ILC2 in the thymus have the potential to produce amphiregulin has yet to be determined.

Since undertaking our research there have been several studies that demonstrate ILC2 have the potential to arise from within the thymus.(102,104,105) This is unsurprising given the thymus is a rich source of IL-7 and Notch signals that are required for ILC2 differentiation.(104) This has been addressed *in vivo* through the manipulation of E protein activity.(104) As previously discussed, Id2 is essential for ILC development where it inhibits the activity of E proteins that are critical in the development of B and T lymphocytes.(75) In the context of these investigations, inhibition of E protein activity in the thymus resulted in a substantial increase in ILC2.(104) Together, these findings support the biological significance of Id2 in inhibiting E protein activity and supporting ILC development. These findings have opened an interesting avenue for ILC research in the thymus. It would be important to discover whether the increase in ILC2 we describe post-birth is a result of reduced

E protein activity and whether these cells are of a thymic origin. There is also scope for determining whether ILC3 also have the potential to develop intrathymically.

We have previously described the important bidirectional relationship that exists between the developing thymocytes and the thymic stroma. Moreover, ILC3 have been shown to support the maturation of the stromal compartment by providing important RANKL signals to developing mTEC populations.(98) Involution of the thymus is widely reported as a feature of ageing and is thought to be a result of defects in both the developing thymocytes and the surrounding stromal compartment.(113) However, whether ILC3, which support the stromal compartment, have a role in this breakdown has yet to be determined. It is quite possible that the decline in ILC3 post-birth and into the adult contribute to involution of the thymus by removing the supportive signals required by mTEC. However, it is thought that CD4<sup>+</sup> T cells become a key provider of RANKL in the adult thymus. More recently, iNKT cells have also been implicated in the provision of RANKL in this context.(210) Therefore, it is more likely that ILC3 function becomes redundant in this tissue in the adult.

The evidence shown within our research supports a role for either ILC3 or ILC2 during different stages of thymic development. However, there are still arguments in the literature to support the redundancy of these cells, particularly when translated into humans. One study observed the effect of ILC deficiency in a cohort of patients with Severe Combined Immunodeficiency (SCID). ILC were shown to be absent in a cohort of patients with SCID who had a mutation in the gene encoding either the  $\gamma$ -chain cytokine receptor subunit, IL-2R $\alpha$ , or tyrosine kinase, JAK3. Treatment of these patients with haematopoietic stem cell transplantation (HSCT) resulted in the



reconstitution of T cells but ILC number remained lower than that of healthy controls. Patients with ILC deficiency were not associated with increased susceptibility to disease therefore redundancy of ILC was suggested when the function of T and B lymphocytes is preserved.(224)

## **6.5 Other lymphocytes**

It was apparent from our studies that the majority of cells that expressed Id2 within the thymus were not ILC. Therefore, we sought to determine the biological significance of this transcriptional regulator amongst other subsets. Following further assessment we revealed  $\alpha\beta$  T cells to be the most abundant cells expression Id2. However, this observation was unsurprising given the thymus contains a vast number of  $\alpha\beta$  T cells in the developing thymus. Therefore, it was more useful to assess the proportion of Id2 expressed, which revealed that only a small proportion of  $\alpha\beta$  T cells in the thymus expressed Id2. It had previously been shown that Id2 was upregulated by effector  $CD4^+$  T cells where it was required for the differentiation into Th1 cells.(196) This was consistent with our own data and provides insight into the biological significance of Id2 in these cells. Id2 is a transcriptional regulator of the E proteins where it acts to limit their activity.(75) E protein activity, namely E2A and HEB, is required for development down a T cell lineage; therefore it is unsurprisingly that  $\alpha\beta$  T cells in the thymus express little Id2.(225) However, our data, and that of others, illustrate an important role for Id2 in  $\alpha\beta$  T cells in the periphery where it acts to reinforce T cell differentiation into Th1 cells and support their effector immune response.(196)

The developmental stage at which Id2 is expressed in cells is an important factor when considering the biological significance of Id2 expression amongst lymphocyte

populations. It is understood that iNKT cells diverge from the DP stage of T cell development following successful positive selection.(226) Moreover, up until this stage, these cells follow the same developmental pathway of similar T cell lineages that arise from the CLP under the action of E proteins.(227) Therefore, it would not be beneficial for these cells to express Id2 early in T cell development. Our findings, much like that of others, identified Id2 expression by all mature iNKT subsets in the thymus and this expression was maintained in peripheral lymph nodes.(77) While we observed two distinct populations of iNKT cells that fate-mapped to Id2 and those that did not, there was no difference in the function of these cells and is likely a result of the efficiency of our inducible Cre to label cells. Interestingly, the role of Id2 has been explored in hepatic iNKT cells where it functioned to support the survival of these lymphocytes.(228) In the context of our own findings, it is likely the significance of Id2 in iNKT cells is to support the maintenance and survival of these cells.

We also identified a small fraction of  $\gamma\delta$  T cells that expressed Id2 in the thymus of Id2 reporter mice. However, this was not restricted to a specific lineage associated with effector function.(206) Further work is required to determine when Id2 is switched on during  $\gamma\delta$  T cell development. This includes the assessment of Id2 expression amongst  $V\gamma 5^+$  and  $V\gamma 6^+$   $\gamma\delta$  T cells in the thymus where the IL-17A and IFN $\gamma$ -associated lineages have been reported to segregate.(206) Together, we have shown Id2 to be expressed amongst multiple innate-like populations. While further work is required to determine whether Id2 has a unique function in these cells that otherwise have similar effector functions.

## 6.6 Further limitations

One drawback of our investigations included the technically challenging aspect of identifying Id2 expression using both reporter and fate mapping models. The difficulty in identifying all Id2-expressing cells was evident within our investigations where we did not observe 100% Id2 expression amongst ILC. This is a result of combined low reporter gene expression with a weak fluorochrome. Furthermore, expression will always be less than 100% when using an inducible Cre system. Furthermore, these challenges could be extended to the study of other lymphocyte populations. Recently, a novel Id2<sup>RFP</sup> reporter mouse was developed for the study of ILC progenitors and improved the way ILC could be interrogated *in vivo*.(229) As expected, these data illustrated Id2 expression amongst all ILC subsets, including splenic NK cells, liver NK cells and ILC1, lung ILC2 and ILC3 in the small intestine. Furthermore, this evidence demonstrated near to 100% of these cells to express Id2. Importantly, the authors observed poor expression of Id2 in CD4<sup>+</sup> and CD8<sup>+</sup> T cells in the spleen and its complete absence in B cells. The strength of this model was confirmed through comparison of Id2 expression with endogenous Id2 mRNA, which mirrored the results.(229)

## 6.6 Concluding remarks

Throughout this study we have used several *in vivo* models to illustrate the ILC composition of the thymus. While, as first hypothesised, LT<sub>i</sub> cells that comprise the ILC3 subset were present in the embryonic and neonatal thymus, the number of ILC3 decreased in the adult thymus. Within these investigations, we were the first to identify ILC2 within the embryonic thymus, albeit in a smaller proportion than ILC3. Interestingly, the number of ILC2 increased in the neonatal thymus where they were



present in comparable numbers to ILC3. However, while the number of ILC3 rapidly declined in the adult thymus, this coincided with an increase in ILC2, which become the dominant ILC population within this tissue. Our subsequent investigations provided evidence to support the provision of RANKL by thymic ILC3 in the neonatal stage. However, our findings indicated a role for ILC3 in the adult thymus is unlikely given the very few cells observed in this tissue. It was evident through our *ex vivo* studies that ILC2 of the neonatal and adult thymus were capable of producing type-2 cytokines. Moreover, the use of confocal imaging supported the idea of thymic ILC2 to be located in the thymic medulla. Together, our data provided evidence of ILC2 and ILC3 within the thymus where they have similar roles in supporting the thymic epithelium. Within our final body of work we characterised the expression of Id2 amongst other lymphocyte populations. These data illustrated similarities between ILC and other innate-like populations, such as iNKT cells, where all mature cells constitutively expressed Id2. Further to this, we identified Id2 amongst  $\gamma\delta$  T cells, however this was not attributed to particular effector function. Finally, we demonstrated Id2 to be absent in naïve T cells but its expression was upregulated at effector sites. Moreover, our evidence indicates Id2 expression to be restricted to Th1 effector T cells and supported the requirement of Id2 during differentiation of these cells.

### **Papers arising from this thesis**

Jones R, Cosway EJ, Willis C, White AJ, Jenkinson WE, Fehling HJ, et al. Dynamic changes in intrathymic ILC populations during murine neonatal development. *Eur J Immunol.* 2018;1–11.

## Research Article

**Dynamic changes in intrathymic ILC populations during murine neonatal development**

Rhys Jones<sup>1</sup>, Emilie J. Cosway<sup>1</sup>, Claire Willis<sup>1</sup>, Andrea J. White<sup>1</sup>, William E. Jenkinson<sup>1</sup>, Hans J. Fehling<sup>2</sup>, Graham Anderson<sup>1</sup>  and David R. Withers<sup>1</sup> 

<sup>1</sup> Institute of Immunology & Immunotherapy, College of Medical and Dental Sciences, University of Birmingham, Birmingham, UK

<sup>2</sup> Institute of Immunology, University of Ulm, Ulm, Germany

Members of the innate lymphoid cell (ILC) family have been implicated in the development of thymic microenvironments and the recovery of this architecture after damage. However, a detailed characterization of this family in the thymus is lacking. To better understand the thymic ILC compartment, we have utilized multiple *in vivo* models including the fate mapping of inhibitor of DNA binding-2 (Id2) expression and the use of Id2 reporter mice. Our data demonstrate that ILCs are more prominent immediately after birth, but were rapidly diluted as the T-cell development program increased. As observed in the embryonic thymus, CCR6<sup>+</sup>NKp46<sup>−</sup> lymphoid tissue inducer (LTi) cells were the main ILC3 population present, but numbers of these cells swiftly declined in the neonate and ILC3 were barely detectable in adult thymus. This loss of ILC3 means ILC2 are the dominant ILC population in the thymus. Thymic ILC2 were able to produce IL-5 and IL-13, were located within the medulla, and did not result from ILC3 plasticity. Furthermore, in WT mice, thymic ILC2 express little RANKL (receptor activator of nuclear factor kappa-B ligand) arguing that functionally, these cells provide different signals to LTi cells in the thymus. Collectively, these data reveal a dynamic switch in the ILC populations of the thymus during neonatal development.

**Keywords:** Innate lymphoid cells · Lymphoid tissue · Neonate · RORγt · Thymus



Additional supporting information may be found online in the Supporting Information section at the end of the article.

**Introduction**

Innate lymphoid cells (ILC) have been described in many tissues [1, 2] and it seems likely that this family of cells is present essentially throughout the body. However, it is clear that the precise composition of these cells is often highly tissue specific and also developmentally regulated. Within the embryo, lymphoid tissue inducer (LTi) cells comprise the RORγt-dependent group 3 ILC

(ILC3) population and these cells appear, required for the establishment of secondary lymphoid tissues such as lymph nodes and Peyer's patches [3], through orchestrating recruitment of lymphocytes to the developing anlagen after LTi cell:stromal cell interactions [4]. Notably, LTi cells were also identified within the embryonic thymus where they again interact with stroma to establish a lymphoid microenvironment, in this case providing receptor activator of nuclear factor kappa-B ligand (RANKL) to developing medullary thymic epithelial cells (mTEC) [5]. Thus in both primary and secondary lymphoid tissues, members of the ILC3 family play a key role in the generation of tissue microenvironments that

Correspondence: Dr. David R. Withers  
e-mail: d.withers@bham.ac.uk

© 2018 The Authors. *European Journal of Immunology* published by WILEY-VCH Verlag GmbH & Co. KGaA, Weinheim.  
This is an open access article under the terms of the Creative Commons Attribution License, which permits use, distribution and reproduction in any medium, provided the original work is properly cited.

www.eji-journal.eu

support lymphocyte maturation and subsequent responses. Given the importance of lymphoid tissue microenvironments to normal function, recovery of such architecture is rapidly induced following damage and ILC3 have also been implicated in this process in both primary and secondary lymphoid tissue [6, 7]. Recovery of splenic architecture after viral infection was impaired in *Rorc*<sup>−/−</sup> mice [6], while ILC3 have been identified as a key source of IL-22 after radiation induced thymic damage [7]. While the ILC compartment of secondary lymphoid tissues has been described in several studies [8, 9], characterization of ILC populations in the thymus has not been performed in detail, perhaps impeded by the phenotypic similarities between ILC and developing thymocytes. In addition to the descriptions of ILC3, ILC2 have also been identified in both mouse and human thymus [10–13], although their location within the tissue and their function remain unclear. Furthermore, whether the ILC populations in the thymus change over time has not been addressed. Here we have undertaken a detailed characterization of thymic ILC from birth through to adulthood using several *in vivo* models to ensure discrimination of ILC from developing thymocytes. While we could clearly detect ILC3 with an LT $\alpha$  cell phenotype in embryonic and neonatal thymus, surprisingly we found that ILC3 rapidly declined in number after birth. In contrast, ILC2 gradually increased in the thymus over time. These cells were located within the medulla of the thymus, were functional in terms of their capacity to make IL5 and IL-13, and lacked expression of RANKL, a molecule thought to be critical for LT $\alpha$  cell function in the developing thymus. Collectively, our data reveal that while ILC3 function to establish the thymic medulla, ILC2 become the dominant ILC population within the thymus after birth and likely support normal thymic function through type 2 cytokine release.

## Results

### ILC populations in the neonatal thymus

LT $\alpha$  cells were originally identified within the embryonic thymus more than 10 years ago [5]. Since the discovery of LT $\alpha$  cells, it is now understood that these cells belong to the ILC family, with inclusion in this family dependent upon a clearly described phenotype and function [2]. Given these advances, we wanted to reexamine the ILC populations within the embryonic thymus and asked whether any other ILC populations beyond LT $\alpha$  cells were present. To do this, we established fetal thymic organ cultures using embryonic day 16 thymi. After 7 days in culture, fetal thymic organ cultures were disaggregated and ILC populations were assessed by flow cytometry. ILC were defined as IL-7 $\alpha$ <sup>+</sup>Lin<sup>−</sup>CD8 $\alpha$ <sup>−</sup> intracellular CD3<sup>−</sup> (CD3i<sup>−</sup>) cells with ILC2 and ILC3 identified on the basis of expression of the transcription factors GATA-3 and ROR $\gamma$ t (Supporting Information Fig. 1). In addition to a clear LT $\alpha$  cell population (ROR $\gamma$ t<sup>+</sup>CCR6<sup>+</sup>NKp46<sup>−</sup>CD4<sup>+/−</sup>), a smaller, but distinct population of ROR $\gamma$ t<sup>−</sup>GATA-3<sup>+</sup> ILC2 was evident, indicating that multiple ILC populations or at least their progenitors exist within the embryonic thymus after *ex vivo* culture condition.

To understand whether these embryonic ILC populations were maintained after birth, we characterized ILC populations in the thymus at different ages (Fig. 1A). The neonatal thymus contained a mixture of ILC3 and ILC2 populations in similar proportions during the first week of life; however, by 2 weeks of age, the proportion of ILC that expressed ROR $\gamma$ t had decreased sharply and very few ILC3 (<5% ILC population) were detected from this age onwards (Fig. 1A and B). The proportion of ILC among total thymocytes was highest at birth (~0.05% of total thymocytes) but then rapidly declined, such that by 2 weeks of age, ILC formed a tiny (<0.001%) proportion of all thymocytes (Fig. 1C). Total numbers of ILC had actually increased between birth and 2 weeks of age (Fig. 1D), largely due to an increase in the total number of ILC2 (Fig. 1E). Total numbers of ILC3 had declined by 2 weeks of age and we could detect <50 ILC3 within an entire adult thymus (Fig. 1E). Having identified ILC2 and ILC3 populations, we additionally stained for expression of T-bet to identify ILC1 in the thymus. At 7 and 14 days postbirth, a distinct ILC1 population was evident (Fig. 1F–H), demonstrating that the neonatal thymus contains all the ILC subsets. Notably, a population of ILC based on IL-7 $\alpha$  expression in the absence of expression of an extensive panel of lineage markers was also observed (Fig. 1F–H), consistent with a recent report identifying such cells in multiple tissues [14]. In this report, prolonged enzymatic digestion was shown to increase the frequency of these cells prompting concerns as to their exact nature; however, here the thymus was disaggregated using only mechanical means. Combined these data indicate that after birth, the ILC3 compartment is gradually lost while a small ILC2 population is maintained through to adult hood. Phenotypically, the ILC2 in the neonatal thymus expressed little KLRG-1, but did express ICOS and ST2, while the majority of the ILC3 compartment phenotypically resembled the CCR6<sup>+</sup>NKp46<sup>−</sup> LT $\alpha$  cells observed in the embryo (Fig. 1I and J and Supporting Information Fig. 2).

### Identification of ILCs in the adult thymus

ILC have a surface phenotype highly similar to T cells with the key exception of the TCR and associated signaling molecules. Given the variable expression of the TCR at different stages of thymocyte development, we considered that correct identification of ILC within adult thymus might be challenging using surface markers alone. Thus, we sought to confirm our initial data on ILC populations within the adult thymus and hypothesized that identification of cells that were fate mapped for inhibitor of DNA binding-2 (Id2) expression would facilitate identification of ILC, since Id2 is a key transcription factor expressed by ILC progenitors [15, 16] but largely absent in, and not required by, developing thymocytes [17]. To test this, we first assessed the ILC population detectable in the mesenteric lymph node (mLN) of Id2<sup>creERT2</sup> × ROSA<sup>mT/mG</sup> mice after tamoxifen administration by oral gavage (Fig. 2A). Comparing the ILC populations among total lymphocytes and those fate mapping for expression of Id2 (mGreen<sup>+</sup>), it was evident that prior gating on cells that were fate

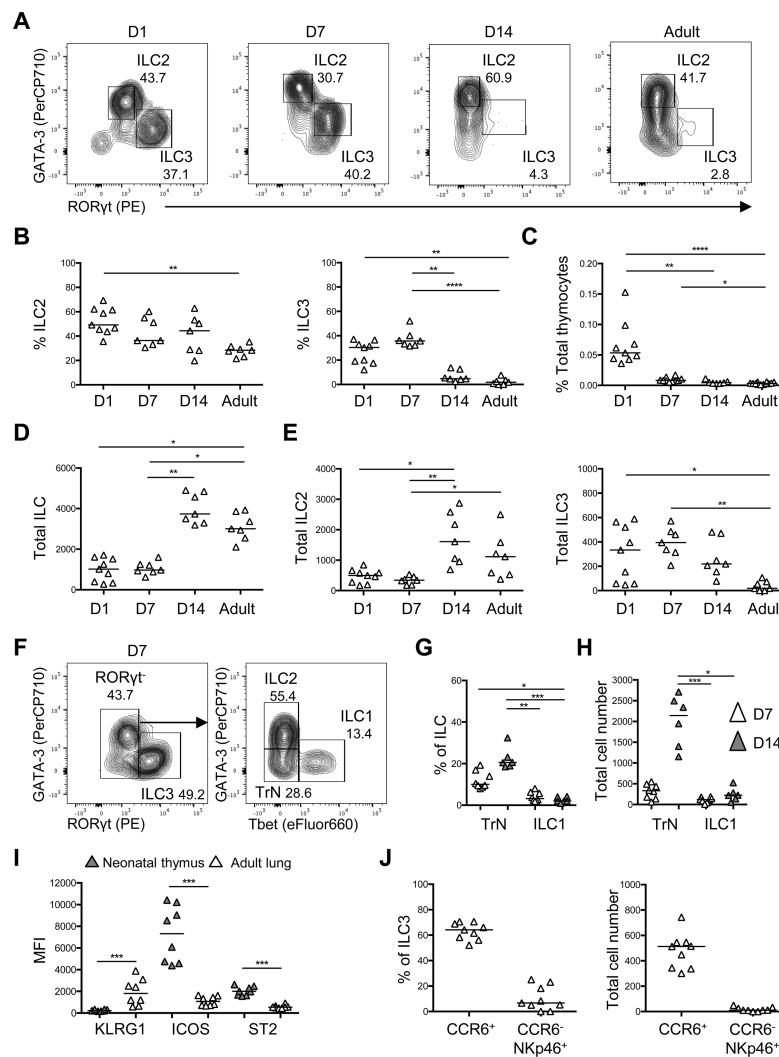


**Figure 1.** Characterization of thymic neonatal ILC populations. To assess the nature of ILC populations in the neonatal thymus, these cells were characterized at 1, 7, and 14 days postbirth and in adulthood (6–12 weeks) by flow cytometry. (A) Representative flow cytometry plots showing analysis of thymic ILC identified as CD8 $\alpha$ -CD3 $^+$ -IL-7R $\alpha$  $^+$ Lin $^-$  (B220, CD3, CD5, CD11b, and CD11c) cells with ILC2 (GATA-3 $^+$ ) and ILC3 (ROR $\gamma$  $^+$ ) gated. (B) The proportion of ILC2 and ILC3 as a percentage of the total thymic ILC population. (C) The proportion of ILC as a percentage of total thymocytes. The total number of ILC (D) and the total number of ILC2 and ILC3 (E) in the thymus at different ages. (F) Representative flow cytometry plots showing analysis of thymic ILCs identified as CD8 $\alpha$ -CD3 $^+$ -IL-7R $\alpha$  $^+$ extended-Lin $^-$  (B220, CD3, CD5, CD11b, CD11c, CD19, CD49b, CD123, F4/80, Fc $\epsilon$ R1, Gr-1, and Ter119) cells with ILC1 (Tbet $^+$ ), ILC2 (GATA-3 $^+$ ), ILC3 (ROR $\gamma$  $^+$ ), and "triple negative" ILC (TrN; GATA-3 $^-$ -ROR $\gamma$  $^-$ -Tbet $^-$ ) gated in the neonatal thymus at 7 days postbirth. The proportion (G) and total number (H) of "TrN" ILC and ILC1 in the neonatal thymus at 7 and 14 days postbirth. (I) The median fluorescence intensity (MFI) of KLRG1, ICOS, and ST2 expression by ILC2 isolated from neonatal thymus and adult lung. (J) The proportion and total number of CCR6 $^+$ NKp46 $^-$  and CCR6 $^+$ NKp46 $^+$  subsets in the neonatal thymus at 7 days postbirth. Mann-Whitney U-test (comparing two samples) or a one-way ANOVA (comparing three or more samples) was used for statistical analysis where \* $p$  < 0.05, \*\* $p$  < 0.01, \*\*\* $p$  < 0.001, and \*\*\*\* $p$  < 0.0001. In all graphs, the bar represents the median,  $n$  = 9 for day 1,  $n$  = 7 for day 7,  $n$  = 7 for day 14, and  $n$  = 7 for adulthood (apart from in F–H, where  $n$  = 8 for day 7 and  $n$  = 6 for day 14), with data (in panels B, C, D, E, G, H, I, and J) pooled from at least two independent experiments at each age. Full gating strategy for all flow cytometry data identifying thymic ILC populations is shown in Supporting Information Fig. 1A.



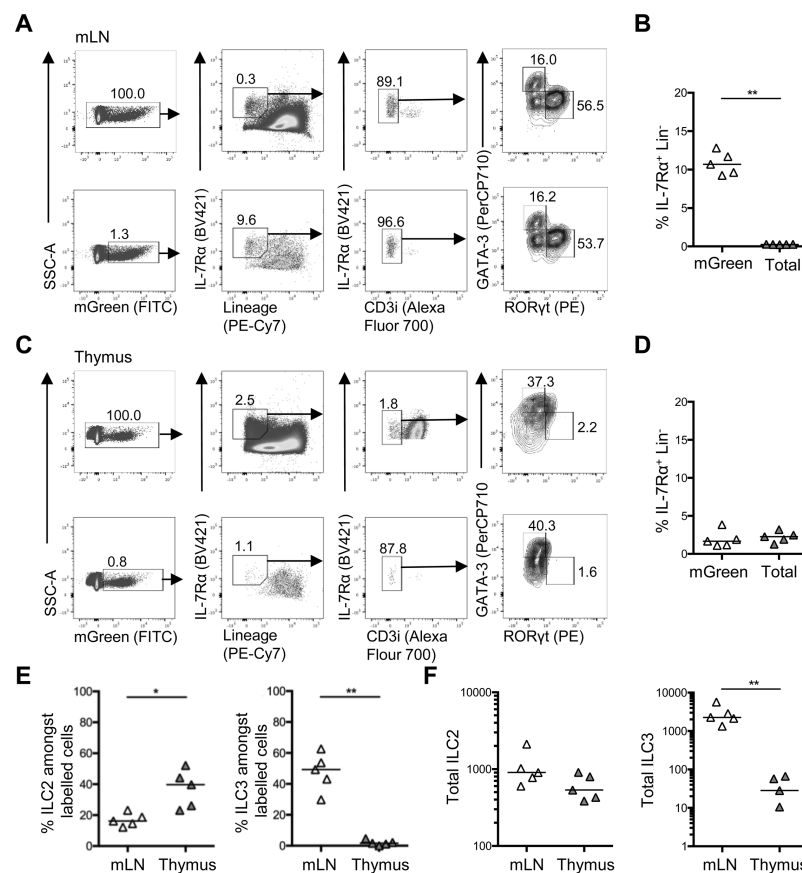


**Figure 2.** Analysis of thymic ILC populations through fate mapping Id2 expression. To aid identification of thymic ILC populations, Id2<sup>creERT2</sup> × ROSA<sup>mT/mG</sup> mice were used to fate map Id2 expression. Administration of tamoxifen by oral gavage on five consecutive days was performed and ILC populations in the thymus and mLN analyzed 3 days later by flow cytometry. (A) Full gating strategy for flow cytometry data showing analysis of IL-7Rα<sup>+</sup> Lin<sup>-</sup> CD3i<sup>-</sup> cells gated on all lymphocytes (upper panels) versus pre-gating on mGreen<sup>+</sup> Id2 fate-mapped cells (lower panels) among mLN cells. (B) The proportion of ILC in the mLN with and without gating on Id2 fate-mapped (mGreen<sup>+</sup>) cells. (C) Representative flow cytometry plots showing analysis of IL-7Rα<sup>+</sup> Lin<sup>-</sup> CD3i<sup>-</sup> cells from total cells (upper panels) versus pre-gating on mGreen<sup>+</sup> Id2 fate-mapped cells (lower panels) among thymus cells. (D) The proportion of ILC in the thymus with and without gating on Id2 fate-mapped (mGreen<sup>+</sup>) cells. The proportion (E) and total number (F) of ILC2 and ILC3 in the mLN and thymus of Id2<sup>creERT2</sup> × ROSA<sup>mT/mG</sup> mice. Mann-Whitney U-test was used for statistical analysis, where \**p* < 0.05 and \*\**p* < 0.01. In all graphs, the bar represents the median, *n* = 5, data (in panels B, D, E, and F) were pooled from two independent experiments.

mapped for Id2 expression increased the proportion of IL-7Rα<sup>+</sup> Lin<sup>-</sup> cells approximately 30-fold (Fig. 2B), indicating that this approach could indeed facilitate identification of ILC. Importantly, the proportions of ILC2 and ILC3 identified through these gating strategies remained highly comparable. We then applied this gating approach to the identification of thymic ILC, which revealed a small fate-mapped IL-7Rα<sup>+</sup> Lin<sup>-</sup> population in the thymus (Fig. 2C). While pre-gating on Id2-fate-mapped cells did not increase the proportion of ILC we identified, it did enable a more

clear demarcation of a distinct IL-7Rα<sup>+</sup> Lin<sup>-</sup> population (Fig. 2C and D). Analysis of the adult thymus in Id2<sup>creERT2</sup> × ROSA<sup>mT/mG</sup> mice after tamoxifen showed that ILC3 were indeed a tiny proportion (<5%) of the ILC population in the thymus (Fig. 2D and E). To enumerate these ILC populations, the efficiency of ILC fate mapping in the mLN was first calculated and then used to generate total numbers in the thymus assuming comparable cre induction. Using this quantitation, we could again detect a median of <50 ILC3 per adult thymus, while the total number of ILC2 in the thymus was

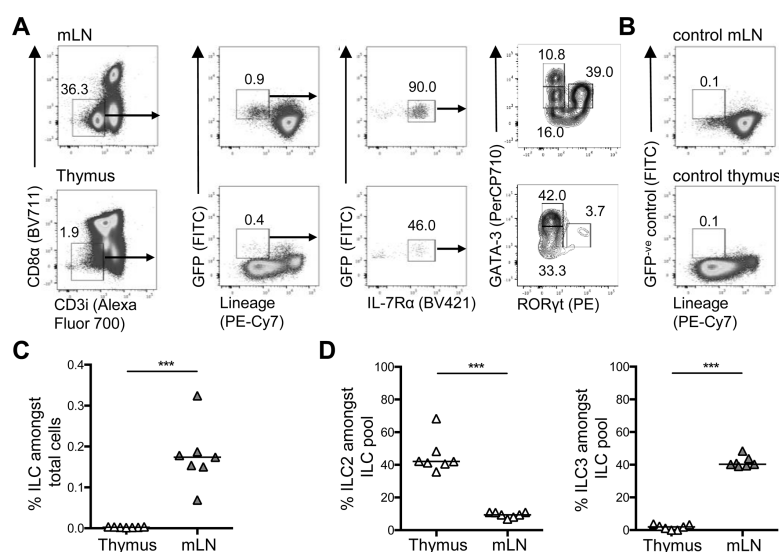


**Figure 3.** Analysis of thymic ILC in Id2-eGFP reporter mice. To directly assess Id2 expressing ILC populations in the thymus and mLN, these tissues from Id2-eGFP mice were analyzed by flow cytometry. (A) Full gating strategy for flow cytometry used to identify GATA3<sup>+</sup> ILC2 and RORγt<sup>+</sup> ILC3 among eGFP<sup>+</sup> cells isolated from the mLN and thymus. (B) Gating controls for eGFP<sup>+</sup> cells were based upon thymocytes from C57BL/6 WT mLN and thymus. (C) The percentage of eGFP<sup>+</sup> ILC (CD8α<sup>+</sup>CD3i<sup>+</sup>IL-7Rα<sup>+</sup>Lin<sup>+</sup> cells) as a proportion of total cells isolated from thymus and mLN. (D) The percentage of eGFP<sup>+</sup> ILC2 and ILC3 as a proportion of total ILC isolated from thymus and mLN. Mann-Whitney U-test was used for statistical analysis, where \*\*\**p* < 0.001, bars show medians, *n* = 7 for thymus and mLN. Data were pooled from two independent experiments.

comparable to that detected in the mLN (Fig. 2F). An alternative approach administering tamoxifen for a longer period of time via the diet enabled an increased proportion of ILC to be fate mapped, however, the data was comparable in terms of the ILC subsets identified within the thymus (Supporting Information Fig. 3). Collectively, these experiments reveal that fate mapping Id2 expression does enhance our ability to identify ILC and within the adult thymus, the majority of ILC are not ILC3, but rather GATA-3<sup>+</sup> ILC2.

While assessing the cells in the thymus that fate mapped for Id2 expression, it was evident that the vast majority of these cells were not ILC. Using Id2<sup>creERT2</sup> × ROSA26<sup>tdRFP</sup> mice given tamoxifen by oral gavage for 5 days, we identified that the majority of thymic cells that were fate mapped (RFP<sup>+</sup>) expressed TCRβ<sup>+</sup> (Supporting Information Fig. 4). Furthermore, it was observed that oral gavage with tamoxifen resulted in a substantial decline in thymocyte cellularity and double-positive thymocytes were found to be particularly sensitive to administration of tamoxifen in this manner (Supporting Information Fig. 5). Analysis of ILC within the mLN revealed only a modest decrease in these cells indicating that the very low numbers of ILC detected in the thymus of Id2<sup>creERT2</sup> × ROSA<sup>tdRFP</sup> mice were not solely due to the effects of tamoxifen treatment (Supporting Information Fig. 4).

To further analyze ILC populations using Id2 expression, but in the absence of tamoxifen administration, the ILC compartment in the mLN and thymus of Id2-eGFP reporters was assessed (Fig. 3A).

Cells isolated from WT mice (and thus eGFP<sup>+</sup>) were used to enable gating on eGFP<sup>+</sup> populations (Fig. 3B). In the mLN, gating on eGFP<sup>+</sup> cells enabled clear identification of ILC populations comparable to those described in the adult mLN [8]. Consistent with the data from Id2<sup>creERT2</sup> × ROSA<sup>tdRFP</sup> mice, only a very small population of eGFP<sup>+</sup>Lin<sup>+</sup> cells was detected in the thymus (Fig. 3A and C) and after gating on IL-7Rα<sup>+</sup> cells, ILC populations comparable to previous experiments were detected and arguing against an artefact of tamoxifen administration (Fig. 3A and D). Thus, using prior or current expression of Id2 to aid ILC identification, the data show that the adult thymus contains a small population of ILC in which ILC2 are far more numerous than ILC3.

### ILC2 are located in the thymic medulla

Having characterized the ILC populations of the thymus, we wanted to better understand the location of these cells and what signals within the thymic microenvironment impacted on their development and persistence. Analysis of ILC in sections of lymphoid tissue is challenging given the abundance of T cells, which likely surround ILC populations and hinder identification of non-T cells. Thus, we reasoned that it would be easier to identify ILC populations in the thymus using TCRα<sup>-/-</sup> mice and here we could clearly identify putative ILC2 (GATA-3<sup>+</sup>CD3<sup>+</sup>IL-7Rα<sup>+</sup>) scattered within the medulla using immunofluorescence (Fig. 4A). Analysis

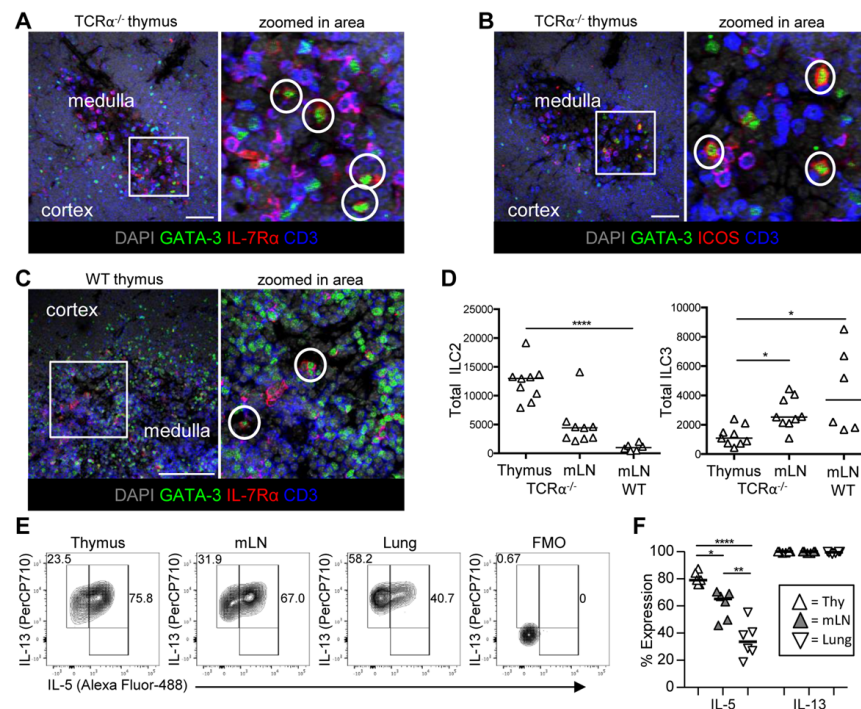


**Figure 4.** ILC2 reside within the medulla in the TCR $\alpha^{-/-}$  thymus. To investigate the location of ILC2 within the thymus, frozen sections of TCR $\alpha^{-/-}$  thymus were assessed for expression of (A) GATA-3, CD3, and IL-7R $\alpha$  and (B) GATA-3, CD3, and ICOS using immunofluorescence. Sections were counterstained with DAPI, data representative of tissue from three mice, putative ILC2 encircled in white. Scale bar: 50  $\mu$ m. (C) Sections of WT neonatal thymus assessed for expression of GATA-3, CD3, and IL-7R $\alpha$ . Sections were counterstained with DAPI, data representative of tissue from three mice, scale bar represents putative ILC2 encircled in white. Scale bar: 100  $\mu$ m. (D) Total numbers of ILC2 and ILC3 isolated from TCR $\alpha^{-/-}$  thymus, TCR $\alpha^{-/-}$  mLN, and WT mLN. (E) Representative flow cytometry plots showing expression of IL-5 versus IL-13 by ILC2 after ex vivo stimulation, alongside FMO control. Cells isolated from TCR $\alpha^{-/-}$  thymus, mLN, and lung were compared. (F) The proportion of ILC2 isolated from the thymus, mLN, or lung expressing IL-13 and IL-5 after ex vivo stimulation. Bars show medians,  $n = 9$  for TCR $\alpha^{-/-}$  thymus and TCR $\alpha^{-/-}$  mLN, and  $n = 6$  for WT mLN (C).  $n = 6$  for thymus, mLN, and lung (D, E, and F). Mann–Whitney  $U$ -test (comparing two samples) or a one-way ANOVA (comparing three or more samples) was used for statistical analysis, where \* $p < 0.05$ , \*\* $p < 0.01$ , \*\*\* $p < 0.001$ , and \*\*\*\* $p < 0.0001$ . Data were pooled from two independent experiments. Full gating strategy for all the flow cytometry data used to identify ILC in TCR $\alpha^{-/-}$  mice shown in Supporting Information Fig. 6A.

of ICOS expression identified a similar population (this time GATA-3 $^{+}$ CD3 $^{-}$ ICOS $^{+}$  cells) within the thymic medulla (Fig. 4B) providing further evidence that these cells were indeed ILC2. Staining of 7 day old WT thymus for expression of GATA-3 $^{+}$ , CD3 $^{-}$  and IL-7R $\alpha^{+}$  again identified putative ILC2 in the medulla indicating that this location was true of both TCR $\alpha^{-/-}$  and WT thymi (Fig. 4C). Flow cytometric analysis of the ILC populations within the TCR $\alpha^{-/-}$  thymus confirmed that the majority of ILC belonged to the ILC2 group (Fig. 4D). Thus, normal medullary development, which is impaired in the absence of single positive CD4 T cells, is not required for the predominance of ILC2 among ILC populations in the thymus. To confirm that thymic ILC2 were able to express the signature cytokines associated with ILC2 function, ex vivo stimulations were performed and expression of both IL-5 and IL-13 detected (Fig. 4E and F). As observed

in the mLN previously [8], ILC numbers were elevated within the TCR $\alpha^{-/-}$  thymus, but the vast majority remained ILC2 and the surface phenotype was consistent with that observed in the neonate (Supporting Information Fig. 6). The few thymic ILC that expressed ROR $\gamma$ t also expressed CCR6 and were a mixture of CD4 $^{+/-}$  cells, consistent with the LT1-like subset.

#### ILC2 expansion in the thymus is not due to ILC3 plasticity

Recent studies have identified plasticity among ILC populations, particularly within the ILC3 subset, where in vivo fate mapping studies have revealed that some ILC3 lose expression of ROR $\gamma$ t to become “ex-ILC3,” a population very similar to IFN $\gamma$  $^{+}$ Tb $\beta$  $^{+}$

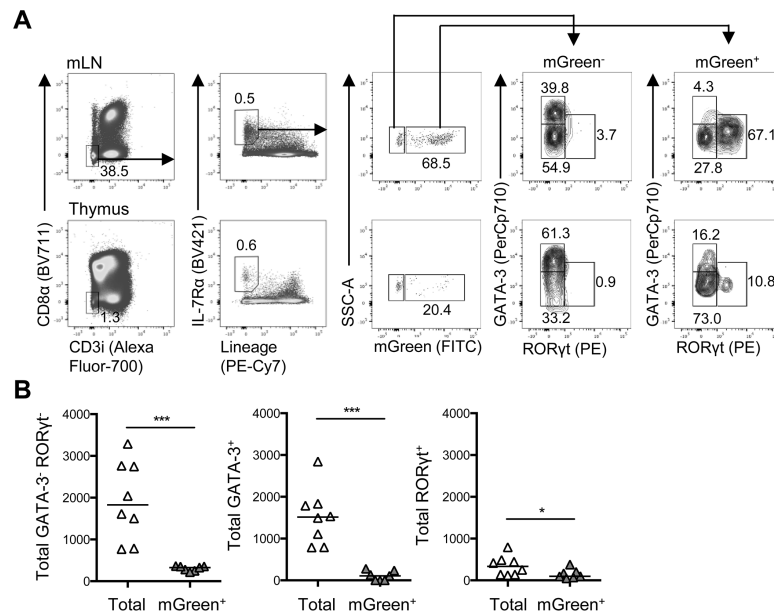


**Figure 5.** ILC3 plasticity does not account for increase in thymic ILC populations post birth. To test whether the loss of thymic ILC3 after birth could be attributed to differentiation to another ILC type, RORγt expression was fate mapped using *Rorc*<sup>cre</sup> × *ROSA*<sup>mT/mG</sup> mice and cells analyzed by flow cytometry. (A) Full gating strategy for flow cytometry data identifying mGreen<sup>+</sup> (fate mapped) and mGreen<sup>-</sup> populations among ILC (CD8<sup>-</sup>CD3i<sup>-</sup>IL-7Rα<sup>+</sup>Lin<sup>-</sup>) in the mLN and thymus. (B) Enumeration of thymic ILC showing putative ILC1 (GATA3<sup>+</sup>RORγt<sup>-</sup>), ILC2 (GATA3<sup>+</sup>), and ILC3 (RORγt<sup>+</sup>) comparing numbers of each population among total ILC versus mGreen<sup>+</sup> ILC. Mann-Whitney U-test was used for statistical analysis, where \**p* < 0.05. Bars show medians, *n* = 8, pooled from two independent experiments.

ILC1 [18]. Thus, it was conceivable that the loss of ILC3 in the thymus reflected plasticity during neonatal development with the RORγt-expressing ILC population switching to another fate. To test whether ILC3 populations in the thymus show evidence of plasticity, we fate mapped RORγt expression in thymic ILC using *Rorc*<sup>cre</sup> × *ROSA*<sup>mT/mG</sup> mice and looked at mGreen expression in the thymus and mLN. While the majority of ILC in the mLN were mGreen<sup>+</sup>, reflecting the large number of ILC3 in this tissue [8], only a minority of ILC (~20%) in the thymus were mGreen<sup>+</sup> (Fig. 5A). Analysis of RORγt expression at the protein level using intracellular flow cytometry revealed a clear “ex-ILC3” population in both the mLN and the thymus (mGreen<sup>+</sup> but RORγt<sup>-</sup>). Enumeration of the number of total versus mGreen<sup>+</sup> ILC populations made it clear that the vast majority of thymic ILC showed no evidence of previous expression at the *Rorc* locus, arguing against ILC3 plasticity accounting for the loss of ILC3 and the increase in ILC2 (Fig. 5B).

#### ILC expression of RANKL in the neonatal thymus

The data described here reveal that the ILC compartment of the thymus changes after birth with a substantial decline in ILC3 num-

ber and increased numbers of ILC2. Given the increase in ILC2 numbers that coincided with the loss of ILC3 and the evidence that ILC3 exist in the medulla [5], we postulated that ILC2 numbers might be enhanced in the absence of ILC3. To test this, we analyzed ILC populations in the thymus of WT and *Rorc*<sup>-/-</sup> mice. Within the adult thymus, ILC2 numbers were significantly enhanced (>2-fold) compared to WT controls (Fig. 6A). This increase in number was also evident in the neonate (Fig. 6B). While these data are consistent with competition for a medullary niche, the perturbations to T-cell development in *Rorc*<sup>-/-</sup> mice mean that ILC intrinsic versus T-cell-dependent effects cannot be distinguished. The ILC3 population in the thymus prebirth has been implicated in mTEC maturation through provision of RANKL. While after birth T cells are considered likely cellular providers of RANKL to mTEC, we assessed RANKL expression among neonatal thymic ILC3 and ILC2 to test whether ILC2 might provide RANKL after the decline in ILC3 numbers. Using adult mLN cells as a positive control for RANKL expression, robust RANKL expression was detected on neonatal ILC3, however there was very little detected on ILC2 (Fig. 6C–F). These data indicate that the expanding ILC2 population in the thymus do not take over the provision of RANKL to mTEC as ILC3 decline. Surprisingly, however, significantly enhanced expression of RANKL was detected on ILC2 in the neonatal thymi of *Rorc*<sup>-/-</sup>

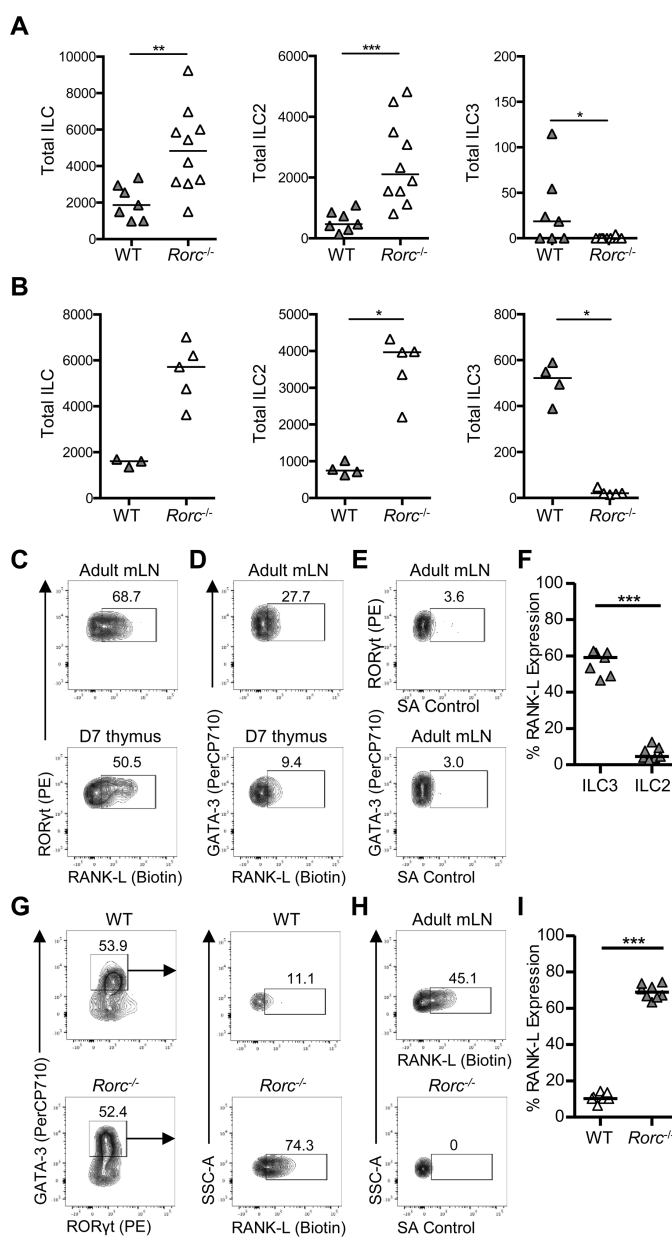


**Figure 6.** Neonatal ILC3, but not ILC2 express RANKL. To investigate the effect of *Rorc*<sup>-/-</sup> deletion on thymic ILC populations, ILC2 and ILC3 were enumerated in WT and *Rorc*<sup>-/-</sup> thymi. Numbers of ILC (IL-7Rα<sup>+</sup>Lin<sup>-</sup>CD8<sup>-</sup>CD3i<sup>-</sup>), ILC2 (GATA-3<sup>+</sup>), and ILC3 (RORγt<sup>+</sup>) detected in adult (A) and 7-day-old neonatal (B) thymus. *n* = 7 adult WT, 10 adult *Rorc*<sup>-/-</sup>, four neonatal WT, and five neonatal *Rorc*<sup>-/-</sup>. Expression of RANKL versus RORγt (C) and GATA-3 (D) by ILC (IL-7Rα<sup>+</sup>Lin<sup>-</sup>CD8<sup>-</sup>CD3i<sup>-</sup>) from adult mLN (upper panel) and neonatal thymus (lower panel) assessed by flow cytometry. (E) Staining control of SA-PECy7 only with ILC2 and ILC3 from adult mLN. (F) The percentage of ILC2 and ILC3 expressing RANKL in the neonatal thymus, *n* = 7. (G) Expression of RANKL by GATA-3<sup>+</sup> ILC2 from WT (upper panels) and *Rorc*<sup>-/-</sup> (lower panels) 14-day-old neonatal thymus. (H) Controls for RANKL showing positive staining of RANKL by ILC from the mLN and the negative control (SA-PECy7 only) for neonatal thymus. (I) The percentage of ILC2 isolated from WT and *Rorc*<sup>-/-</sup> neonatal thymus that express RANKL, *n* = 8. Mann-Whitney U-test was used for statistical analysis, where \*\**p* < 0.01, bars show medians. Data were pooled from two (A, C, D, and F) and one (B and G) independent experiments. Full gating strategy for all flow cytometry identifying thymic ILC populations is shown in Supporting Information Fig. 1A.

mice, suggesting that ILC2 can express RANKL when the thymic microenvironment is perturbed.

## Discussion

Here we provide the first detailed characterization of ILC in the thymus, utilizing several *in vivo* models to facilitate accurate identification of these cells. Building on the earlier observation that LT $\alpha$  cells populate the embryonic thymus and orchestrate mTEC maturation through RANK:RANKL interactions, we demonstrate that after birth, LT $\alpha$  cells decline during neonatal development while ILC2 increase in number and become the main ILC population present within the thymus. We provide evidence that thymic ILC2 are able to produce the signature cytokines IL-5 and IL-13 and reside in the medulla where they may compete for an environmental niche with ILC3. Finally, we show that thymic ILC2 do not express RANKL under normal conditions, and thus appear to have distinct functions to thymic LT $\alpha$  cells during embryonic development.

ILC have been characterized within most tissues; however, to date a clear description of the thymic ILC compartment has been lacking. Discrimination between ILC and developing thymocytes where TCR expression is reduced is technically challenging, but this problem was resolved through analyzing expression of Id2 given its fundamental role in ILC development and redundant role in  $\alpha\beta$  TCR $^+$  T cell development [17]. Using both fate mapping and reporting of Id2 expression, our data clearly identify thymic ILC, but reveal that these cells account for less than 0.05% of the hematopoietic compartment of the thymus after birth and less than 0.001% in the adult thymus. Thus, ILC are certainly a rare population in the thymus. Functionally, LT $\alpha$  cells in the embryonic thymus provide the RANKL signals required for mTEC maturation. It is now evident that RANKL can be provided by other cells in the developing embryonic thymus [19] and after birth, single-positive thymocytes alongside other T cell populations contribute to a complex network of signals governing mTEC development [20–22]. Thus, the loss of LT $\alpha$  cells in the neonatal thymus is consistent with changes in the cellular interactions that govern mTEC maturation. Our data would argue that while ILC2 reside within the medulla, they are unlikely to contribute to mTEC maturation via RANKL provision. Thus, the role for ILC in establishing thymic microenvironments is restricted to early embryonic development.

What then do ILC2 contribute to thymic function? Based on the array of studies in other tissues, it is reasonable to hypothesize that ILC2 in the thymus are a local source of type 2 cytokines. Type 2 cytokines from iNKT cells were recently shown to control thymic emigration of conventional thymocytes [23], and it is possible that ILC2 may also contribute to this cytokine milieu. Whether ILC2 have unique functions within the thymus, or redundancy with other innate populations also able to produce similar cytokines such as iNKT cells requires further study, including the specific deletion of ILC2 [24]. Since mice lacking ILC3 had increased numbers of ILC2 within the thymus, there may be intrathymic competition among ILC for residency within the tissue. However,

it is possible that the impaired T cell development caused by *Rorc* deficiency may also contribute to enhanced ILC2 numbers, particularly since a similar increase in thymic ILC2 was observed in the TCR $\alpha^{-/-}$  thymus, where numbers of single-positive thymocytes are obviously greatly reduced.

In summary, this study provides new insight into the changes that occur in ILC populations within the thymus during neonatal development. The challenge remains to determine unique *in vivo* roles for these cells, particularly within nonmucosal tissues.

## Materials and methods

### Mice

Mice were obtained from the University of Birmingham Biomedical Services Unit (BMSU) and were maintained in accordance with Home Office regulations. All mice were on a C57BL/6 background and strains included: WT, Id2<sup>creERT2</sup> [25]  $\times$  ROSA<sup>mT/mG</sup> [26], Id2<sup>creERT2</sup>  $\times$  ROSA26<sup>RFP</sup> [27], Id2-eGFP [28], *Rorc*<sup>-/-</sup> [29], *Rorc*<sup>cre</sup> [30]  $\times$  ROSA<sup>mT/mG</sup>, and TCR $\alpha^{-/-}$  [31]. Neonatal mice were culled at day 1, 7, and 14 postbirth, and adult mice were culled between 6 and 12 weeks of age.

### In vivo procedures

Tamoxifen was administered to Id2<sup>CreERT2</sup>  $\times$  ROSA<sup>mT/mG</sup> mice either by oral gavage (20mg/mL) once a day for five consecutive days and mice culled 3 days later or within diet for 3-week duration. Tamoxifen was administered to Id2<sup>CreERT2</sup>  $\times$  ROSA26<sup>RFP</sup> mice by oral gavage (20mg/mL) once a day for three consecutive days and mice analyzed the following day.

### Cell preparation

Thymus tissue was mechanically disaggregated between two glass slides. mLNs were cleaned of all fat, teased apart using fine forceps, and DNase I (0.025mg/mL, Roche Diagnostics) and collagenase dispase (0.25mg/mL, Roche Life Sciences) were used to digest tissue in Roswell Park Memorial Institute (RPMI). All cell suspensions were passed through a 70- $\mu$ m nylon strainer (Falcon®, Fisher scientific) using a syringe plunger.

### Fetal thymic organ cultures

The embryonic sack containing stage E16 mouse embryos was removed from a pregnant mouse following cervical dislocation. Each embryo was decapitated and cut along the breastbone to expose two thymic lobes, which were dissected under a light microscope in sterile conditions. Fetal thymic organ cultures were set up in optimal conditions as previously described by Jenkinson



and Anderson [32]. Thymic lobes were placed on an Isopore™ Membrane Filter (0.8 µm, Millipore) and positioned on top of a 1 cm<sup>2</sup> artwrap sponge within a small petri dish containing 2 mL DMEM (Sigma–Aldrich). Each petri dish was encapsulated within a sealed container containing 10 mL of H<sub>2</sub>O and incubated for 7 days at 37°C/5% CO<sub>2</sub>. Single cell suspension from thymus tissue was prepared as previously described.

### In vitro culture for RANKL expression

Thymocytes prepared from neonatal thymi were cultured in 1 mL of culture media (RPMI, 10% FBS, L-Glutamine, 100 IU/mL penicillin and 100 µg/mL streptomycin) overnight at 37°C/5% CO<sub>2</sub>. Wells were set up in duplicate for each sample with each well containing ~6 million cells. Duplicate wells were pooled following culture to provide a sufficient number of ILC for analysis.

### Flow cytometry

Cell surface staining was performed at 4°C for 30 min in FACS buffer (10% FBS, 2.5 mM EDTA in PBS). ILC were identified among CD8α<sup>−</sup> (clone 5.3–6.7, Biolegend), CD3i<sup>−</sup> (clone 17A2, Biolegend), IL-7Rα<sup>+</sup> (clone A7R34, Biolegend), B220<sup>−</sup> (clone RA3-6B2, eBioscience), CD11b<sup>−</sup> (clone M1/70, eBioscience), CD11c<sup>−</sup> (clone N418, eBioscience), CD3<sup>−</sup> (clone 145-2C11, eBioscience), and CD5<sup>−</sup> (clone 53–7.3, eBioscience). Thymic iNKT cells were identified as mCD1d/PBS57<sup>+</sup> and TCRβ<sup>+</sup> (clone H57-597, eBioscience). Intracellular cell staining was performed at room temperature for 1 h in permeabilization buffer (eBioscience). ILC2 and ILC3 subsets were identified using Abs against GATA3<sup>+</sup> (clone TWAJ, eBioscience) and RORγt<sup>+</sup> (clone AFKJS-9, eBioscience). Staining for RANKL expression was performed in two steps using biotinylated RANKL (clone: IK22/5, eBioscience) and streptavidin-PECy7 (Molecular Probes) at 4°C for 30 min in FACS buffer. Samples included SpheroTech Accucount blank particles to enable calculation of cell frequency and were acquired using a Fortessa (BD). Samples were analyzed using FlowJo (FlowJo, LLC). Full gating strategy for all flow cytometry data identifying thymic ILC populations is shown in Supporting Information Fig. 1A.

### Statistics

Flow cytometry data were analyzed and enumerated using FlowJo (v10.2) and Graphpad Prism 6 (v6 Mac OS X). An unpaired, nonparametric Mann–Whitney *U* statistical test was used where applicable. Where more than 2 data sets are compared a one-way ANOVA, nonparametric test was used. For each test, \**p* < 0.05, \*\**p* < 0.01, \*\*\**p* < 0.001, and \*\*\*\**p* < 0.0001. No bar present represents nonsignificant result.

**Acknowledgments:** We thank Gabrielle Belz for the provision of Id2-eGFP mice. The following tetramers were obtained through the NIH Tetramer Facility: mCD1d/PBS57. RJ and EJC are RACE ARUK funded PhD students. HJF has been supported by DFG-FE578/3. This work was additionally supported by a Senior Research Fellowship from the Wellcome Trust (110199/Z/15/Z) to DRW and MRC Programme award (MR/N000919/1) to GA.

**Conflict of interest:** The authors declare no financial or commercial conflict of interest.

### References

- Artis, D. and Spits, H., The biology of innate lymphoid cells. *Nature*. 2015. 517: 293–301.
- Spits, H., Artis, D., Colonna, M., Diefenbach, A., Di Santo, J. P., Eberl, G., Koyasu, S. et al., Innate lymphoid cells—a proposal for uniform nomenclature. *Nat. Rev. Immunol.* 2013. 13: 145–149.
- Eberl, G. and Littman, D. R., The role of the nuclear hormone receptor RORγt in the development of lymph nodes and Peyer's patches. *Immunol. Rev.* 2003. 195: 81–90.
- van de Pavert, S. A. and Mebius, R. E., New insights into the development of lymphoid tissues. *Nat. Rev. Immunol.* 2010. 10: 664–674.
- Rossi, S. W., Kim, M. Y., Leibbrandt, A., Parnell, S. M., Jenkinson, W. E., Glanville, S. H., McConnell, F. M. et al., RANK signals from CD4(+)3(−) inducer cells regulate development of Aire-expressing epithelial cells in the thymic medulla. *J. Exp. Med.* 2007. 204: 1267–1272.
- Scandella, E., Bolinger, B., Lattmann, E., Miller, S., Favre, S., Littman, D. R., Finke, D. et al., Restoration of lymphoid organ integrity through the interaction of lymphoid tissue-inducer cells with stroma of the T cell zone. *Nat. Immunol.* 2008. 9: 667–675.
- Dudakov, J. A., Hanash, A. M., Jenq, R. R., Young, L. F., Ghosh, A., Singer, N. V., West, M. L. et al., Interleukin-22 drives endogenous thymic regeneration in mice. *Science*. 2012. 336: 91–95.
- Mackley, E. C., Houston, S., Marriott, C. L., Halford, E. E., Lucas, B., Cerovic, V., Filbey, K. J. et al., CCR7-dependent trafficking of RORγt(+) ILCs creates a unique microenvironment within mucosal draining lymph nodes. *Nat. Commun.* 2015. 6: 5862.
- Hepworth, M. R., Monticelli, L. A., Fung, T. C., Ziegler, C. G., Grunberg, S., Sinha, R., Mantegazza, A. R. et al., Innate lymphoid cells regulate CD4+ T-cell responses to intestinal commensal bacteria. *Nature*. 2013. 498: 113–117.
- Gentek, R., Munneke, J. M., Helbig, C., Blom, B., Hazenberg, M. D., Spits, H. and Amsen, D., Modulation of signal strength switches notch from an inducer of T cells to an inducer of ILC2. *Front. Immunol.* 2013. 4: 334.
- Miyazaki, M., Miyazaki, K., Chen, K., Jin, Y., Turner, J., Moore, A. J., Saito, R. et al., The E-Id protein axis specifies adaptive lymphoid cell identity and suppresses thymic innate lymphoid cell development. *Immunity*. 2017. 46: 818–834.e4.
- Wang, H. C., Qian, L., Zhao, Y., Mengarelli, J., Adrianto, I., Montgomery, C. G., Urban, J. F. et al., Downregulation of E protein activity augments an ILC2 differentiation program in the thymus. *J. Immunol.* 2017. 198: 3149–3156.
- Wong, S. H., Walker, J. A., Jolin, H. E., Drynan, L. F., Hams, E., Camelo, A., Barlow, J. L. et al., Transcription factor RORα is critical for nuocyte development. *Nat. Immunol.* 2012. 13: 229–236.

- 14 Dutton, E. E., Camelo, A., Sleeman, M., Herbst, R., Carlesso, G., Belz, G. T. and Withers, D. R., Characterisation of innate lymphoid cell populations at different sites in mice with defective T cell immunity. *Wellcome Open Res.* 2017. 2: 117.
- 15 Constantinides, M. G., McDonald, B. D., Verhoef, P. A. and Bendelac, A., A committed precursor to innate lymphoid cells. *Nature.* 2014. 508: 397–401.
- 16 Klose, C. S., Flach, M., Mohle, L., Rogell, L., Hoyler, T., Ebert, K., Fabianke, C. et al., Differentiation of type 1 ILCs from a common progenitor to all helper-like innate lymphoid cell lineages. *Cell.* 2014. 157: 340–356.
- 17 Ikawa, T., Fujimoto, S., Kawamoto, H., Katsura, Y. and Yokota, Y., Commitment to natural killer cells requires the helix-loop-helix inhibitor Id2. *Proc. Natl. Acad. Sci. U S A.* 2001. 98: 5164–5169.
- 18 Klose, C. S., Kiss, E. A., Schwierzeck, V., Ebert, K., Hoyler, T., d'Hargues, Y., Goppert, N. et al., A T-bet gradient controls the fate and function of CCR6-RORgamma<sup>+</sup> innate lymphoid cells. *Nature.* 2013. 494: 261–265.
- 19 Roberts, N. A., White, A. J., Jenkinson, W. E., Turchinovich, G., Nakamura, K., Withers, D. R., McConnell, F. M., et al., Rank signaling links the development of invariant gammadelta T cell progenitors and Aire(+) medullary epithelium. *Immunity.* 2012. 36: 427–437.
- 20 Hikosaka, Y., Nitta, T., Ohgashi, I., Yano, K., Ishimaru, N., Hayashi, Y., Matsumoto, M. et al., The cytokine RANKL produced by positively selected thymocytes fosters medullary thymic epithelial cells that express autoimmune regulator. *Immunity.* 2008. 29: 438–450.
- 21 Akiyama, T., Shimo, Y., Yanai, H., Qin, J., Ohshima, D., Maruyama, Y., Asaumi, Y., The tumor necrosis factor family receptors RANK and CD40 cooperatively establish the thymic medullary microenvironment and self-tolerance. *Immunity.* 2008. 29: 423–437.
- 22 Abramson, J. and Anderson, G., Thymic Epithelial Cells. *Annu Rev Immunol.* 2017. 35: 85–118.
- 23 White, A. J., Baik, S., Parnell, S. M., Holland, A. M., Brombacher, F., Jenkinson, W. E. and Anderson, G., A type 2 cytokine axis for thymus emigration. *J Exp Med.* 2017. 214: 2205–2216.
- 24 Oliphant, C. J., Hwang, Y. Y., Walker, J. A., Salimi, M., Wong, S. H., Brewer, J. M., Englezakis, A. et al., MHCII-mediated dialog between group 2 innate lymphoid cells and CD4(+) T cells potentiates type 2 immunity and promotes parasitic helminth expulsion. *Immunity.* 2014. 41: 283–295.
- 25 Rawlins, E. L., Clark, C. P., Xue, Y. and Hogan, B. L., The Id2<sup>+</sup> distal tip lung epithelium contains individual multipotent embryonic progenitor cells. *Development.* 2009. 136: 3741–3745.
- 26 Muzumdar, M. D., Tasic, B., Miyamichi, K., Li, L. and Luo, L., A global double-fluorescent Cre reporter mouse. *Genesis.* 2007. 45: 593–605.
- 27 Luche, H., Weber, O., Nageswara Rao, T., Blum, C. and Fehling, H. J., Faithful activation of an extra-bright red fluorescent protein in "knock-in" Cre-reporter mice ideally suited for lineage tracing studies. *Eur J Immunol.* 2007. 37: 43–53.
- 28 Jackson, J. T., Hu, Y., Liu, R., Masson, F., D'Amico, A., Carotta, S., Xin, A. et al., Id2 expression delineates differential checkpoints in the genetic program of CD8alpha<sup>+</sup> and CD103<sup>+</sup> dendritic cell lineages. *EMBO J.* 2011. 30: 2690–2704.
- 29 Sun, Z., Unutmaz, D., Zou, Y. R., Sunshine, M. J., Pierani, A., Brenner-Morton, S., Mebius, R. E. et al., Requirement for RORgamma in thymocyte survival and lymphoid organ development. *Science.* 2000. 288: 2369–2373.
- 30 Eberl, G. and Littman, D. R., Thymic origin of intestinal alphabeta T Cells revealed by fate mapping of RORgamma<sup>+</sup> Cells. *Science.* 2004. 305: 248–251.
- 31 Mombaerts, P., Clarke, A. R., Rudnicki, M. A., Iacomini, J., Itoharu, S., Lafaille, J. J., Wang, L. et al., Mutations in T-cell antigen receptor genes alpha and beta block thymocyte development at different stages. *Nature.* 1992. 360: 225–231.
- 32 Robinson, J. H. and Owen, J. J., Pillars article: generation of T-cell function in organ culture of fetal mouse thymus I. Mitogen responsiveness. 1975. *J Immunol.* 2008. 181: 7437–7444.

**Abbreviations:** Id2: inhibitor of DNA binding-2 · ILC: innate lymphoid cells · LTi: lymphoid tissue inducer · mLN: mesenteric lymph node · mTEC: medullary thymic epithelial cells · RANKL: receptor activator of nuclear factor kappa-B ligand

**Full correspondence:** Dr. David Withers, Institute of Immunology & Immunotherapy (III), College of Medical and Dental Sciences, University of Birmingham, Birmingham, B15 2TT, UK  
Fax: +44 (0)121 414 3599  
e-mail: d.withers@bham.ac.uk

Received: 24/1/2018  
Revised: 19/4/2018  
Accepted: 25/5/2018  
Accepted article online: 31/5/2018



## **References**

1. Parkin J, Cohen B. Overview of the immune system. *Lancet*. 2001;357:1777–89.
2. Leonard WJ. Cytokines and immunodeficiency diseases. *Nature*. 2001;1:200–8.
3. Wolf AJ, Underhill DM. Peptidoglycan recognition by the innate immune system. Vol. 18, *Nature Reviews Immunology*. Nature Publishing Group; 2018. p. 243–54.
4. Janeway CA, Medzhitov R. Innate Immune Recognition. *Annu Rev Immunol*. 2002 Apr;20(1):197–216.
5. Clark R, Kupper T. Old meets new: The interaction between innate and adaptive immunity. *J Invest Dermatol*. 2005;
6. Hepworth MR, Monticelli LA, Fung TC, Ziegler CGK, Grunberg S, Sinha R, et al. Innate lymphoid cells regulate CD4 + T-cell responses to intestinal commensal bacteria. *Nature*. 2013;498(7452):113–7.
7. Colonna M. Innate Lymphoid Cells: Diversity, Plasticity, and Unique Functions in Immunity. Vol. 48, *Immunity*. Cell Press; 2018. p. 1104–17.
8. Boehm T, Swann JB. Thymus involution and regeneration: Two sides of the same coin? *Nat Rev Immunol*. 2013;13(11):831–8.
9. Pellicci DG, Koay HF, Berzins SP. Thymic development of unconventional T cells: how NKT cells, MAIT cells and  $\gamma\delta$  T cells emerge. *Nat Rev Immunol*. 2020;
10. Vivier E, Artis D, Colonna M, Diefenbach A, Di Santo JP, Eberl G, et al. Innate Lymphoid Cells: 10 Years On. *Cell*. 2018;174(5):1054–66.
11. Vaidya HJ, Briones Leon A, Blackburn CC. FOXP1 in thymus organogenesis and development. Vol. 46, *European Journal of Immunology*. Wiley-VCH Verlag; 2016. p. 1826–37.
12. Blackburn CC, Manley NR. Developing a new paradigm for thymus organogenesis. *Nat Rev Immunol*. 2004;4(4):278–89.
13. Gordon J, Wilson VA, Blair NF, Sheridan J, Farley A, Wilson L, et al. Functional evidence for a single endodermal origin for the thymic epithelium. *Nat Immunol*. 2004;5(5):546–53.
14. Romano R, Palamaro L, Fusco A, Giardino G, Gallo V, Del Vecchio L, et al. FOXP1: A master regulator gene of thymic epithelial development program. Vol. 4, *Frontiers in Immunology*. 2013.
15. Anderson G, Takahama Y. Thymic epithelial cells: Working class heroes for T cell development and repertoire selection. *Trends Immunol*. 2012;33(6):256–63.

16. Sheikh A, Abraham N. Interleukin-7 Receptor Alpha in Innate Lymphoid Cells: More Than a Marker. *Front Immunol.* 2019;10(December).
17. Shah DK, Zúñiga-Pflücker JC. An Overview of the Intrathymic Intricacies of T Cell Development. *J Immunol.* 2014;192(9):4017–23.
18. Lind EF, Prockop SE, Porritt HE, Petrie HT. Mapping precursor movement through the postnatal thymus reveals specific microenvironments supporting defined stages of early lymphoid development. *J Exp Med.* 2001;194(2):127–34.
19. Rossi FMV, Corbel SY, Merzaban JS, Carlow DA, Gossens K, Duenas J, et al. Recruitment of adult thymic progenitors is regulated by P-selectin and its ligand PSGL-1. *Nat Immunol.* 2005;6(6):626–34.
20. Calderón L, Boehm T. Three chemokine receptors cooperatively regulate homing of hematopoietic progenitors to the embryonic mouse thymus. *Proc Natl Acad Sci U S A.* 2011;108(18):7517–22.
21. Liu C, Saito F, Liu Z, Lei Y, Uehara S, Love P, et al. Coordination between CCR7- and CCR9-mediated chemokine signals in prevascular fetal thymus colonization. *Blood.* 2006;108(8):2531–9.
22. Patra AK, Avots A, Zahedi RP, Schüler T, Sickmann A, Bommhardt U, et al. An alternative NFAT-activation pathway mediated by IL-7 is critical for early thymocyte development. *Nat Immunol.* 2013;14(2):127–35.
23. Ribeiro AR, Rodrigues PM, Meireles C, Di Santo JP, Alves NL. Thymocyte Selection Regulates the Homeostasis of IL-7–Expressing Thymic Cortical Epithelial Cells In Vivo. *J Immunol.* 2013;
24. Germain RN. T-cell development and the CD4-CD8 lineage decision. *Nat Rev Immunol.* 2002;2(5):309–22.
25. Foxwell BMJ, Beadling C, Guschin D, Kerr I, Cantrell D. Interleukin-7 can induce the activation of Jak 1, Jak 3 and STAT 5 proteins in murine T cells. *Eur J Immunol.* 1995;25(11):3041–6.
26. Lin J-X, Leonard WJ. The role of Stat5a and Stat5b in signaling by IL-2 family cytokines. *Oncogene.* 2000;19:2566.
27. Spits H, Artis D, Colonna M, Diefenbach A, Di Santo JP, Eberl G, et al. Innate lymphoid cells-a proposal for uniform nomenclature. *Nat Rev Immunol.* 2013;13:145–9.
28. Ciofani M, Zúñiga-Pflücker JC. The thymus as an inductive site for T lymphopoiesis. *Annu Rev Cell Dev Biol.* 2007;23:463–93.
29. Ciofani M, Zúñiga-Pflücker JC. Determining  $\gamma \delta$  versus  $\alpha \beta$  T cell development. *Nat Rev Immunol.* 2010;10(9):657–63.
30. Takaba H, Takayanagi H. The Mechanisms of T Cell Selection in the Thymus. *Trends Immunol.* 2017;38(11):805–16.

31. Dash P, Fiore-Gartland AJ, Hertz T, Wang GC, Sharma S, Souquette A, et al. Quantifiable predictive features define epitope-specific T cell receptor repertoires. *Nature*. 2017;547(7661):89–93.
32. Starr TK, Jameson SC, Hogquist KA. Positive and negative selection of T cells. *Annu Rev Immunol*. 2003;21:139–76.
33. Ripen AM, Nitta T, Murata S, Tanaka K, Takahama Y. Ontogeny of thymic cortical epithelial cells expressing the thymoproteasome subunit  $\beta 5t$ . *Eur J Immunol*. 2011;41(5):1278–87.
34. Nitta T, Murata S, Sasaki K, Fujii H, Ripen AM, Ishimaru N, et al. Thymoproteasome Shapes Immunocompetent Repertoire of CD8<sup>+</sup> T Cells. *Immunity*. 2010;32(1):29–40.
35. Nitta T, Ohigashi I, Nakagawa Y, Takahama Y. Cytokine crosstalk for thymic medulla formation. *Curr Opin Immunol*. 2011;23(2):190–7.
36. Gommeaux J, Grégoire C, Nguessan P, Richelme M, Malissen M, Guerder S, et al. Thymus-specific serine protease regulates positive selection of a subset of CD4<sup>+</sup> thymocytes. *Eur J Immunol*. 2009;39(4):956–64.
37. Viret C, Lamare C, Guiraud M, Fazilleau N, Bour A, Malissen B, et al. Thymus-specific serine protease contributes to the diversification of the functional endogenous CD4 T cell receptor repertoire. *J Exp Med*. 2011;208(1):3–11.
38. Lucas B, Germain RN. Unexpectedly complex regulation of CD4/CD8 coreceptor expression supports a revised model for CD4<sup>+</sup>CD8<sup>+</sup> thymocyte differentiation. *Immunity*. 1996;5(5):461–77.
39. Ueno T, Saito F, Gray DHD, Kuse S, Hieshima K, Nakano H, et al. CCR7 signals are essential for cortex-medulla migration of developing thymocytes. *J Exp Med*. 2004;200(4):493–505.
40. Lkhagvasuren E, Sakata M, Ohigashi I, Takahama Y. Lymphotoxin  $\beta$  Receptor Regulates the Development of CCL21-Expressing Subset of Postnatal Medullary Thymic Epithelial Cells. *J Immunol*. 2013;190(10):5110–7.
41. Klein L, Kyewski B, Allen PM, Hogquist KA. Positive and negative selection of the T cell repertoire: What thymocytes see (and don't see). *Nat Rev Immunol*. 2014;14(6):377–91.
42. DeVoss JJ, LeClair NP, Hou Y, Grewal NK, Johannes KP, Lu W, et al. An Autoimmune Response to Odorant Binding Protein 1a Is Associated with Dry Eye in the Aire<sup>-</sup>Deficient Mouse. *J Immunol*. 2010;184(8):4236–46.
43. Anderson MS, Venzani ES, Klein L, Chen Z, Berzins SP, Turley SJ, et al. Projection of an immunological self shadow within the thymus by the aire protein. *Science* (80- ). 2002;298(5597):1395–401.
44. Fujikado N, Mann AO, Bansal K, Romito KR, Ferre EMN, Rosenzweig SD, et al. Aire Inhibits the Generation of a Perinatal Population of Interleukin-17A-Producing  $\gamma\delta$  T Cells to Promote Immunologic Tolerance. *Immunity*. 2016;45(5):999–1012.

45. Takaba H, Morishita Y, Tomofuji Y, Danks L, Nitta T, Komatsu N, et al. Fezf2 Orchestrates a Thymic Program of Self-Antigen Expression for Immune Tolerance. *Cell*. 2015;163(4):975–87.
46. Cosway EJ, Lucas B, James KD, Parnell SM, Carvalho-Gaspar M, White AJ, et al. Redefining thymus medulla specialization for central tolerance. *J Exp Med*. 2017;214(11):3183–95.
47. Sakaguchi S. Regulatory T cells: Key controllers of immunologic self-tolerance. *Cell*. 2000;101(5):455–8.
48. Owen DL, Mahmud SA, Sjaastad LE, Williams JB, Spanier JA, Simeonov DR, et al. Thymic regulatory T cells arise via two distinct developmental programs. *Nat Immunol*. 2019;20(2):195–205.
49. Vignali DAA, Collison LW, Workman CJ. How regulatory T cells work. *Nat Rev Immunol*. 2008;8(7):523–32.
50. Kimura MY, Pobezinsky LA, Guinter TI, Thomas J, Adams A, Park JH, et al. IL-7 signaling must be intermittent, not continuous, during CD8 + T cell homeostasis to promote cell survival instead of cell death. *Nat Immunol*. 2013;14(2):143–51.
51. Li J, Wu D, Jiang N, Zhuang Y. Combined Deletion of Id2 and Id3 Genes Reveals Multiple Roles for E Proteins in Invariant NKT Cell Development and Expansion. *J Immunol*. 2013;191(10):5052–64.
52. Chiu YH, Park SH, Benlagha K, Forestier C, Jayawardena-Wolf J, Savage PB, et al. Multiple defects in antigen presentation and T cell development by mice expressing cytoplasmic tail-truncated CD1d. *Nat Immunol*. 2002;
53. Elewaut D, Lawton AP, Nagarajan NA, Maverakis E, Khurana A, Höning S, et al. The Adaptor Protein AP-3 Is Required for CD1d-Mediated Antigen Presentation of Glycosphingolipids and Development of Vα14i NKT Cells. *J Exp Med*. 2003;
54. Pellicci DG, Hammond KJL, Uldrich AP, Baxter AG, Smyth MJ, Godfrey DI. A natural killer T (NKT) cell developmental pathway involving a thymus-dependent NK1.1-CD4+ CD1d-dependent precursor stage. *J Exp Med*. 2002;
55. Hammond K, Cain W, Van Driel I, Godfrey D. Three day neonatal thymectomy selectively depletes NK1.1+ T cells. *Int Immunol*. 1998;
56. Das R, Sant'Angelo DB, Nichols KE. Transcriptional control of invariant NKT cell development. *Immunol Rev*. 2010;238(1):195–215.
57. Lee YJ, Holzapfel KL, Zhu J, Jameson SC, Hogquist KA. Steady-state production of IL-4 modulates immunity in mouse strains and is determined by lineage diversity of iNKT cells. *Nat Immunol*. 2013;14(11):1146–54.
58. Georgiev H, Ravens I, Benarafa C, Förster R, Bernhardt G. Distinct gene expression patterns correlate with developmental and functional traits of iNKT subsets. *Nat Commun*. 2016 Oct 10;7.

59. Vomhof-DeKrey EE, Yates J, Leadbetter EA. Invariant NKT cells provide innate and adaptive help for B cells. *Curr Opin Immunol*. 2014;28(1):12–7.
60. Smyth MJ, Wallace ME, Nutt SL, Yagita H, Godfrey DI, Hayakawa Y. Sequential activation of NKT cells and NK cells provides effective innate immunotherapy of cancer. *J Exp Med*. 2005;201(12):1973–85.
61. Semmling V, Lukacs-Kornek V, Thaiss CA, Quast T, Hochheiser K, Panzer U, et al. Alternative cross-priming through CCL17-CCR4-mediated attraction of CTLs toward NKT cell-licensed DCs. *Nat Immunol*. 2010;11(4):313–20.
62. Santo C De, Salio M, Masri SH, Lee LY, Dong T, Speak AO, et al. \*  
OWBSJBOU / , 5 DFMMT SFEVDF UIF JNNVOPTVQQSFTTJWF BDUJWJUZ  
PG JOGMVFO [ B " WJSVTmJOEVD FE NZFMPJE EFSJWFE TVQQSFTTPS.  
2008;2(24):4036–48.
63. Kawakami K, Yamamoto N, Kinjo Y, Miyagi K, Nakasone C, Uezu K, et al. Critical role of V $\alpha$ 14<sup>+</sup> natural killer T cells in the innate phase of host protection against *Streptococcus pneumoniae* infection. *Eur J Immunol*. 2003;33(12):3322–30.
64. Advertisement Start. *Vet Surg*. :9.
65. Fahl SP, Coffey F, Wiest DL. Origins of  $\gamma\delta$  T Cell Effector Subsets: A Riddle Wrapped in an Enigma. *J Immunol*. 2014;193(9):4289–94.
66. Zhang B, Lin Y-Y, Dai M, Zhuang Y. Id3 and Id2 Act as a Dual Safety Mechanism in Regulating the Development and Population Size of Innate-like  $\gamma\delta$  T Cells. *J Immunol*. 2014 Feb 1;192(3):1055–63.
67. Ito K, Bonneville M, Takagaki Y, Nakanishi N, Kanagawa O, Krecko EG, et al. Different  $\gamma\delta$  T-cell receptors are expressed on thymocytes at different stages of development. *Proc Natl Acad Sci U S A*. 1989;86(2):631–5.
68. Jee MH, Johansen JD, Buus TB, Petersen TH, Gadsbøll ASØ, Woetmann A, et al. Increased production of IL-17A-producing  $\gamma\delta$  T cells in the thymus of filaggrin-deficient mice. *Front Immunol*. 2018 May 8;9(MAY).
69. Garman RD, Doherty PJ, Raulet DH. Diversity, rearrangement, and expression of murine T cell gamma genes. Vol. 45, *Cell*. 1986.
70. Ribot JC, deBarros A, Pang DJ, Neves JF, Peperzak V, Roberts SJ, et al. CD27 is a thymic determinant of the balance between interferon- $\gamma$ - and interleukin 17-producing  $\gamma\delta$  T cell subsets. *Nat Immunol*. 2009;10(4):427–36.
71. Do J, Fink PJ, Li L, Spolski R, Robinson J, Leonard WJ, et al. Cutting Edge: Spontaneous Development of IL-17–Producing  $\gamma\delta$  T Cells in the Thymus Occurs via a TGF- $\beta$ 1–Dependent Mechanism. *J Immunol*. 2010;184(4):1675–9.
72. Artis D, Spits H. The biology of innate lymphoid cells. Vol. 517, *Nature*. Nature Publishing Group; 2015. p. 293–301.
73. Zhu J, Yamane H, Paul WE. Differentiation of Effector CD4 T Cell Populations.

- Annu Rev Immunol. 2010;28(1):445–89.
74. Fang D, Zhu J. Dynamic balance between master transcription factors determines the fates and functions of CD4 T cell and innate lymphoid cell subsets. *J Exp Med*. 2017;214(7):1861–76.
  75. Eberl G, Colonna M, Santo JPD, McKenzie ANJ. Innate lymphoid cells: A new paradigm in immunology. *Science* (80- ). 2015;348(6237).
  76. Boos MD, Yokota Y, Eberl G, Kee BL. Mature natural killer cell and lymphoid tissue-inducing cell development requires Id2-mediated suppression of E protein activity. *J Exp Med*. 2007 May;204(5):1119–30.
  77. D’Cruz LM, Stradner MH, Yang CY, Goldrath AW. E and Id Proteins Influence Invariant NKT Cell Sublineage Differentiation and Proliferation. *J Immunol*. 2014 Mar 1;192(5):2227–36.
  78. Wang LH, Baker NE. E Proteins and ID Proteins: Helix-Loop-Helix Partners in Development and Disease. *Dev Cell*. 2015;35(3):269–80.
  79. Murre C, McCaw PS, Vaessin H, Caudy M, Jan LY, Jan YN, et al. Interactions between heterologous helix-loop-helix proteins generate complexes that bind specifically to a common DNA sequence. *Cell*. 1989;58(3):537–44.
  80. Vonarbourg C, Mortha A, Bui VL, Hernandez PP, Kiss EA, Hoyler T, et al. Regulated expression of nuclear receptor ROR $\gamma$ t confers distinct functional fates to NK cell receptor-expressing ROR $\gamma$ t<sup>+</sup> innate lymphocytes. *Immunity*. 2010 Nov 24;33(5):736–51.
  81. Klose CSN, Kiss EA, Schwierzeck V, Ebert K, Hoyler T, D’Hargues Y, et al. A T-bet gradient controls the fate and function of CCR6-ROR $\gamma$ t<sup>+</sup>innate lymphoid cells. *Nature*. 2013;494:261–6.
  82. Rankin LC, Groom JR, Chopin M, Herold MJ, Walker JA, Mielke LA, et al. The transcription factor T-bet is essential for the development of NKp46 + innate lymphocytes via the Notch pathway. *Nat Immunol*. 2013;14(4):389–95.
  83. Viant C, Rankin LC, Girard-Madoux MJH, Seillet C, Shi W, Smyth MJ, et al. Transforming growth factor- $\beta$  and Notch ligands act as opposing environmental cues in regulating the plasticity of type 3 innate lymphoid cells. *Sci Signal*. 2016;9(426).
  84. Huang Y, Guo L, Qiu J, Chen X, Hu-Li J, Siebenlist U, et al. IL-25-responsive, lineage-negative KLRG1<sup>hi</sup> cells are multipotential “inflammatory” type 2 innate lymphoid cells. *Nat Immunol*. 2015;16(2):161–9.
  85. Zhang K, Xu X, Pasha MA, Siebel CW, Costello A, Haczku A, et al. Cutting Edge: Notch Signaling Promotes the Plasticity of Group-2 Innate Lymphoid Cells. *J Immunol*. 2017;198(5):1798–803.
  86. Gury-BenAri M, Thaïs CA, Serafini N, Winter DR, Giladi A, Lara-Astiaso D, et al. The Spectrum and Regulatory Landscape of Intestinal Innate Lymphoid Cells Are Shaped by the Microbiome. *Cell*. 2016 Aug 25;166(5):1231–1246.e13.

87. Klose CSN, Artis D. Innate lymphoid cells as regulators of immunity, inflammation and tissue homeostasis. *Nat Immunol.* 2016;17(7):765–74.
88. Dutton EE, Carlesso G, Belz GT, Sleeman M, Herbst R, Camelo A, et al. Characterisation of innate lymphoid cell populations at different sites in mice with defective T cell immunity. *Wellcome Open Res.* 2018;2(117):1–24.
89. Mackley EC, Milling S, Marriott CL, Lucas B, Maizels RM, Hepworth MR, et al. CCR7-dependent trafficking of RORγ<sup>+</sup> ILCs creates a unique microenvironment within mucosal draining lymph nodes. *Nat Commun.* 2015;6(5862):1–12.
90. Spits H, Di Santo JP. The expanding family of innate lymphoid cells: Regulators and effectors of immunity and tissue remodeling. *Nat Immunol.* 2011;12(1):21–7.
91. Kerfoot SM, Yaari G, Patel JR, Johnson KL, Gonzalez DG, Kleinstein SH, et al. Germinal Center B Cell and T Follicular Helper Cell Development Initiates in the Interfollicular Zone. *Immunity.* 2011;
92. Li J, Zhang Y, Zhang L. Discovering susceptibility genes for allergic rhinitis and allergy using a genome-wide association study strategy. *Current Opinion in Allergy and Clinical Immunology.* 2015.
93. Halim TYF, Krauß RH, Sun AC, Takei F. Lung Natural Helper Cells Are a Critical Source of Th2 Cell-Type Cytokines in Protease Allergen-Induced Airway Inflammation. *Immunity.* 2012;
94. Hepworth MR, Fung TC, Masur SH, Kelsen JR, McConnell FM, Dubrot J, et al. Group 3 innate lymphoid cells mediate intestinal selection of commensal bacteria-specific CD4<sup>+</sup> T cells. *Science (80- ).* 2015;348(6238):1031–5.
95. Buonocore S, Ahern PP, Uhlig HH, Ivanov II, Littman DR, Maloy KJ, et al. Innate lymphoid cells drive interleukin-23-dependent innate intestinal pathology. *Nature.* 2010;
96. Kim MY, Gaspal FMC, Wiggett HE, McConnell FM, Gulbranson-Judge A, Raykundalia C, et al. CD4<sup>+</sup>CD3<sup>-</sup> accessory cells costimulate primed CD4 T cells through OX40 and CD30 at sites where T cells collaborate with B cells. *Immunity.* 2003;
97. Kim M-Y, Anderson G, White A, Jenkinson E, Arit W, Martensson I-L, et al. OX40 Ligand and CD30 Ligand Are Expressed on Adult but Not Neonatal CD4<sup>+</sup> CD3<sup>-</sup> Inducer Cells: Evidence That IL-7 Signals Regulate CD30 Ligand but Not OX40 Ligand Expression . *J Immunol.* 2005;
98. Rossi SW, Leibbrandt A, Lane PJL, Kim M-Y, Jenkinson WE, Parnell SM, et al. RANK signals from CD4<sup>+</sup> 3<sup>-</sup> inducer cells regulate development of Aire-expressing epithelial cells in the thymic medulla. *J Exp Med.* 2007;204(6):1267–72.
99. Roberts NA, White AJ, Jenkinson WE, Turchinovich G, Nakamura K, Withers DR, et al. Rank Signaling Links the Development of Invariant γδ T Cell

- Progenitors and Aire + Medullary Epithelium. *Immunity*. 2012 Mar 23;36(3):427–37.
100. Dudakov JA, Hanash AM, Jenq RR, Young LF, Ghosh A, Singer N V., et al. Interleukin-22 drives endogenous thymic regeneration in mice. *Science* (80- ). 2012;335(6077):91–5.
  101. Dudakov JA, Mertelsmann AM, O'Connor MH, Jenq RR, Velardi E, Young LF, et al. Loss of thymic innate lymphoid cells leads to impaired thymopoiesis in experimental graft-versus-host disease. *Blood*. 2017;130(7):933–42.
  102. Gentek R, Munneke JM, Helbig C, Blom B, Hazenberg MD, Spits H, et al. Modulation of Signal Strength Switches Notch from an Inducer of T Cells to an Inducer of ILC2. *Front Immunol*. 2013;4(October).
  103. Miyazaki M, Miyazaki K, Chen K, Jin Y, Turner J, Moore AJ, et al. The E-Id Protein Axis Specifies Adaptive Lymphoid Cell Identity and Suppresses Thymic Innate Lymphoid Cell Development. *Immunity*. 2017 May 16;46(5):818-834.e4.
  104. Wang H-C, Qian L, Zhao Y, Mengarelli J, Adrianto I, Montgomery CG, et al. Downregulation of E Protein Activity Augments an ILC2 Differentiation Program in the Thymus. *J Immunol*. 2017 Apr 15;198(8):3149–56.
  105. Qian L, Bajana S, Georgescu C, Peng V, Wang HC, Adrianto I, et al. Suppression of ILC2 differentiation from committed T cell precursors by E protein transcription factors. *J Exp Med*. 2019;216(4):884–99.
  106. Shi J, Petrie HT. Activation Kinetics and Off-Target Effects of Thymus-Initiated Cre Transgenes. *PLoS One*. 2012;7(10).
  107. Robinson JH, Owen JJT. Generation of T cell function in organ culture of foetal mouse thymus. I. Mitogen responsiveness. *Clin Exp Immunol*. 1976;23(2):347–54.
  108. Anderson G, Jenkinson EJ. Bringing the Thymus to the Bench. *J Immunol*. 2008;181(11):7435–6.
  109. Haeryfar SMM, Hoskin DW. Thy-1: More than a Mouse Pan-T Cell Marker. *J Immunol*. 2004;173(6):3581–8.
  110. Ashton-Rickardt PG, Van Kaer L, Schumacher TNM, Ploegh HL, Tonegawa S. Peptide contributes to the specificity of positive selection of CD8+ T cells in the thymus. *Cell*. 1993;73(5):1041–9.
  111. Jenkinson EJ, Franchi LL, Kingston R, Owen JJT. Effect of deoxyguanosine on lymphopoiesis in the developing thymus rudiment in vitro: Application in the production of chimeric thymus rudiments. *Eur J Immunol*. 1982;12(7):583–7.
  112. Linton PJ, Dorshkind K. Age-related changes in lymphocyte development and function. *Nat Immunol*. 2004;5(2):133–9.
  113. Palmer DB. The effect of age on thymic function. *Front Immunol*. 2013;4(OCT):1–6.



114. Kinsella S, Dudakov JA. When the Damage Is Done: Injury and Repair in Thymus Function. *Front Immunol.* 2020;11(August):1–12.
115. Taub DD, Longo DL. Insights into thymic aging and regeneration. *Immunol Rev.* 2005;205:72–93.
116. Xiao S, Shterev ID, Zhang W, Young L, Shieh J-H, Moore M, et al. Sublethal Total Body Irradiation Causes Long-Term Deficits in Thymus Function by Reducing Lymphoid Progenitors. *J Immunol.* 2017;199(8):2701–12.
117. Lemischka IR, Raulet DH, Mulligan RC. Developmental potential and dynamic behavior of hematopoietic stem cells. *Cell.* 1986;
118. Wang Y, Schulte BA, LaRue AC, Ogawa M, Zhou D. Total body irradiation selectively induces murine hematopoietic stem cell senescence. *Blood.* 2006;107(1):358–66.
119. Mombaerts P, Clarke a R, Rudnicki M a, Iacomini J, Itohara S, Lafaille JJ, et al. Mutations in T-cell antigen receptor genes alpha and beta block thymocyte development at different stages. *Nature.* 1992;360(6401):225–31.
120. Sun Z, Unutmaz D, Zho Y, Sunshine M j, Pierani A, Brenner-Morton S, et al. Requirement for RORgamma in Thymocyte Survival and Lymphoid Organ Development. *Science (80- ).* 2000;288(5475):2369–73.
121. Rawlins EL, Clark CP, Xue Y, Hogan BLM. The Id2+ distal tip lung epithelium contains individual multipotent embryonic progenitor cells. *Development.* 2009;136(22):3741–5.
122. Muzumdar D m, Tasic B, Miyamichi K, Li L, Luo L. A Global Double-Fluorescent Cre Reporter Mouse. *Genesis.* 2007;45(6):418–26.
123. Luche H, Weber O, Rao TN, Blum C, Fehling HJ. Faithful activation of an extra-bright red fluorescent protein in “knock-in” Cre-reporter mice ideally suited for lineage tracing studies. *Eur J Immunol.* 2007;37(1):43–53.
124. Jackson JT, Hu Y, Liu R, Masson F, D’Amico A, Carotta S, et al. Id2 expression delineates differential checkpoints in the genetic program of CD8 $\alpha$ +and CD103+dendritic cell lineages. *EMBO J.* 2011;30(13):2690–704.
125. Eberl G. Thymic Origin of Intestinal T Cells Revealed by Fate Mapping of ROR t+ Cells. *Science (80- ).* 2004;305(5681):248–51.
126. Zhong ZA, Sun W, Chen H, Zhang H, Lay YAE, Lane NE, et al. Optimizing tamoxifen-inducible Cre/loxP system to reduce tamoxifen effect on bone turnover in long bones of young mice. *Bone.* 2015;81:614–9.
127. Kim H, Kim M, Im S-K, Fang S. Mouse Cre-LoxP system: general principles to determine tissue-specific roles of target genes. *Lab Anim Res.* 2018;34(4):147.
128. Robinson JH, Owen JJT. Pillars Article: Generation of T-cell Function in Organ Culture of Foetal Mouse Thymus. I. Mitogen Responsiveness. *J Immunol.* 2008 Dec 1;181(11):7437 LP – 7444.

129. Jones R, Cosway EJ, Willis C, White AJ, Jenkinson WE, Fehling HJ, et al. Dynamic changes in intrathymic ILC populations during murine neonatal development. *Eur J Immunol*. 2018;48(9):1–11.
130. Wallrapp A, Riesenfeld SJ, Burkett PR, Abdulnour REE, Nyman J, Dionne D, et al. The neuropeptide NMU amplifies ILC2-driven allergic lung inflammation. *Nature*. 2017;549(7672):351–6.
131. Monticelli LA, Sonnenberg GF, Abt MC, Alenghat T, Ziegler CGK, Doering TA, et al. Innate lymphoid cells promote lung-tissue homeostasis after infection with influenza virus. *Nat Immunol*. 2011;12(11):1045–54.
132. Van De Pavert SA, Mebius RE. New insights into the development of lymphoid tissues. *Nat Rev Immunol*. 2010;10(9):664–74.
133. Eberl G, Littman DR. The role of the nuclear hormone receptor ROR $\gamma$ t in the development of lymph nodes and Peyer's patches. *Immunol Rev*. 2003;195:81–90.
134. Scandella E, Bolinger B, Lattmann E, Miller S, Favre S, Littman DR, et al. Restoration of lymphoid organ integrity through the interaction of lymphoid tissue-inducer cells with stroma of the T cell zone. *Nat Immunol*. 2008;9(6):667–75.
135. Miller CN, Proekt I, von Moltke J, Wells KL, Rajpurkar AR, Wang H, et al. Thymic tuft cells promote an IL-4-enriched medulla and shape thymocyte development. Vol. 559, *Nature*. Nature Publishing Group; 2018. p. 627–31.
136. Bornstein C, Nevo S, Giladi A, Kadouri N, Pouzolles M, Gerbe F, et al. Single-cell mapping of the thymic stroma identifies IL-25-producing tuft epithelial cells. Vol. 559, *Nature*. Nature Publishing Group; 2018. p. 622–6.
137. Gasteiger G, Fan X, Dikiy S, Lee SY, Rudensky AY. Tissue residency of innate lymphoid cells in lymphoid and nonlymphoid organs. *Science* (80- ). 2015 Nov 20;350(6263):981–5.
138. Diefenbach A, Colonna M, Koyasu S. Development, differentiation, and diversity of innate lymphoid cells. *Immunity*. 2014 Sep 18;41(3):354–65.
139. Robinette ML, Colonna M. Immune modules shared by innate lymphoid cells and T cells. *J Allergy Clin Immunol*. 2016;138(5):1243–51.
140. Pai S-Y, Truitt ML, Ting C-N, Leiden JM, Glimcher LH, Ho I-C. Dana-Farber Cancer Institute and Children's Hospital van Oers. Vol. 19, *Immunity*. 2003.
141. Hosoya T, Maillard I, Engel JD. From the cradle to the grave: Activities of GATA-3 throughout T-cell development and differentiation. *Immunol Rev*. 2010 Nov;238(1):110–25.
142. Zhong C, Zhu J. Small-Molecule ROR $\gamma$ t Antagonists: One Stone Kills Two Birds. Vol. 38, *Trends in Immunology*. Elsevier Ltd; 2017. p. 229–31.
143. Eberl G, Marmon S, Sunshine MJ, Rennert PD, Choi Y, Littmann DR. An essential function for the nuclear receptor ROR $\gamma$ t in the generation of fetal

- lymphoid tissue inducer cells. *Nat Immunol.* 2004 Jan;5(1):64–73.
144. Robinette ML, Fuchs A, Cortez VS, Lee JS, Wang Y, Durum SK, et al. Transcriptional programs define molecular characteristics of innate lymphoid cell classes and subsets. *Nat Immunol.* 2015;16(3):306–17.
  145. Krueger A, Zięta N, Łyszkiewicz M. T Cell Development by the Numbers. Vol. 38, *Trends in Immunology*. Elsevier Ltd; 2017. p. 128–39.
  146. Wilford G, Huntington ND. Regulation of murine natural killer cell development. *Front Immunol.* 2017;8(FEB):1–9.
  147. Constantinides MG, McDonald BD, Verhoef PA, Bendelac A. A committed precursor to innate lymphoid cells. *Nature.* 2014;508(7496):397–401.
  148. Flach M, Veiga-Fernandes H, Busslinger M, Domingues RG, Pfeifer D, Fabiunke C, et al. Differentiation of Type 1 ILCs from a Common Progenitor to All Helper-like Innate Lymphoid Cell Lineages. *Cell.* 2014;157:340–56.
  149. Yokota Y, Kawamoto H, Fujimoto S, Katsura Y, Ikawa T. Commitment to natural killer cells requires the helix-loop-helix inhibitor Id2. *Proc Natl Acad Sci.* 2001;98(9):5164–9.
  150. Dougherty T. Effect of Hormones on Lymphatic Tissue. *Physiol Rev.* 1952;32(4):379–401.
  151. Sciumé G, Hirahara K, Takahashi H, Laurence A, Villarino A V., Singleton KL, et al. Distinct requirements for T-bet in gut innate lymphoid cells. *J Exp Med.* 2012 Dec 17;209(13):2331–8.
  152. Bernink JH, Krabbendam L, Germar K, de Jong E, Gronke K, Kofoed-Nielsen M, et al. Interleukin-12 and -23 Control Plasticity Of Cd127+ Group 1 And Group 3 Innate Lymphoid Cells In The Intestinal Lamina Propria. *Immunity.* 2015 Jul 21;43(1):146–60.
  153. Halim TYF, MacLaren A, Romanish MT, Gold MJ, McNagny KM, Takei F. Retinoic-Acid-Receptor-Related Orphan Nuclear Receptor Alpha Is Required for Natural Helper Cell Development and Allergic Inflammation. *Immunity.* 2012;37(3):463–74.
  154. Salimi M, Barlow JL, Saunders SP, Xue L, Gutowska-Owsiak D, Wang X, et al. A role for IL-25 and IL-33-driven type-2 innate lymphoid cells in atopic dermatitis. *J Exp Med.* 2013 Dec;210(13):2939–50.
  155. Sonnenberg GF, Monticelli LA, Elloso MM, Fouser LA, Artis D. CD4+ lymphoid tissue inducer cells promote innate immunity in the gut. 2011;34(1):122–34.
  156. Locksley RM, Heinzel FP, Sadick MD, Holaday BJ, Gardner KD. Murine cutaneous leishmaniasis : Susceptibility correlates with differential expansion of helper T-cell subsets. *Ann l'Institut Pasteur - Immunol.* 1987;138(5):744–9.
  157. Gessner A, Blum H, Röllinghoff M. Differential Regulation of IL-9-Expression after Infection with *Leishmania major* in Susceptible and Resistant Mice. *Immunobiology.* 1993;189(5):419–35.

158. Dzhagalov I, Phee H. How to find your way through the thymus: A practical guide for aspiring T cells. Vol. 69, Cellular and Molecular Life Sciences. 2012. p. 663–82.
159. Ioannidis V, Beermann F, Clevers H, Held W. The  $\beta$ -catenin – TCF-1 pathway ensures CD4 + CD8 + thymocyte survival © 2001 Nature Publishing Group <http://immunol.nature.com>. 2001;2(8).
160. Overgaard NH, Jung J-W, Steptoe RJ, Wells JW. CD4 + /CD8 + double-positive T cells: more than just a developmental stage? . J Leukoc Biol. 2015 Jan;97(1):31–8.
161. Mombaerts P, Clarke AR, Rudnicki MA, Iacomini J, Itohara S, Lafaille J, et al. Mutations in T cell receptor genes  $\alpha$  and  $\beta$  block thymocyte development at different stages. Nature. 1992;360(November):225–31.
162. Hayashi S, McMahon AP. Efficient recombination in diverse tissues by a tamoxifen-inducible form of Cre: A tool for temporally regulated gene activation/inactivation in the mouse. Dev Biol. 2002;244(2):305–18.
163. Chalfie M, Tu Y, Euskirchen G, Ward WW, Prasher DC. Green fluorescent protein as a marker for gene expression. Science (80- ). 1994;263:802–5.
164. Engelbertsen D, Lichtman AH. Innate lymphoid cells in atherosclerosis. Eur J Pharmacol. 2017 Dec 5;816:32–6.
165. Cupedo T. ILC2: at home in the thymus. Vol. 48, European Journal of Immunology. Wiley-VCH Verlag; 2018. p. 1441–4.
166. Lai AY, Kondo M. Identification of a bone marrow precursor of the earliest thymocytes in adult mouse. Proc Natl Acad Sci U S A. 2007;104(15):6311–6.
167. Schwarz BA, Sambandam A, Maillard I, Harman BC, Love PE, Bhandoola A. Selective Thymus Settling Regulated by Cytokine and Chemokine Receptors. J Immunol. 2007;178(4):2008–17.
168. Sambandam A, Maillard I, Zediak VP, Xu L, Gerstein RM, Aster JC, et al. Notch signaling controls the generation and differentiation of early T lineage progenitors. Nat Immunol. 2005;6(7):663–70.
169. Yang Q, Monticelli LA, Saenz SA, Chi AWS, Sonnenberg GF, Tang J, et al. T Cell Factor 1 Is Required for Group 2 Innate Lymphoid Cell Generation. Immunity. 2013;38(4):694–704.
170. Wojciechowski J, Lai A, Kondo M, Zhuang Y. E2A and HEB Are Required to Block Thymocyte Proliferation Prior to Pre-TCR Expression. J Immunol. 2007;178(9):5717–26.
171. Von Burg N, Chappaz S, Baerenwaldt A, Horvath E, Bose Dasgupta S, Ashok D, et al. Activated group 3 innate lymphoid cells promote T-cell-mediated immune responses. Proc Natl Acad Sci U S A. 2014;111(35):12835–40.
172. Paclik D, Stehle C, Lahmann A, Hutloff A, Romagnani C. ICOS regulates the pool of group 2 innate lymphoid cells under homeostatic and inflammatory

- conditions in mice. *Eur J Immunol*. 2015;45(10):2766–72.
173. White AJ, Withers DR, Parnell SM, Scott HS, Finke D, Lane PJL, et al. Sequential phases in the development of Aire-expressing medullary thymic epithelial cells involve distinct cellular input. *Eur J Immunol*. 2008 Apr;38(4):942–7.
  174. Raifer H, Mahiny AJ, Bollig N, Petermann F, Hellhund A, Kellner K, et al. Unlike  $\alpha\beta$  T cells,  $\gamma\delta$  T cells, LTi cells and NKT cells do not require IRF4 for the production of IL-17A and IL-22. *Eur J Immunol*. 2012 Dec;42(12):3189–201.
  175. Ivanov II, McKenzie BS, Zhou L, Tadokoro CE, Lepelley A, Lafaille JJ, et al. The Orphan Nuclear Receptor ROR $\gamma$ t Directs the Differentiation Program of Proinflammatory IL-17+ T Helper Cells. *Cell*. 2006 Sep 22;126(6):1121–33.
  176. He Z, Zhang J, Huang Z, Du Q, Li N, Zhang Q, et al. Sumoylation of ROR $\gamma$ t regulates TH17 differentiation and thymocyte development. *Nat Commun*. 2018 Nov 19;9(1):4870.
  177. Takatori H, Kanno Y, Watford WT, Tato CM, Weiss G, Ivanov II, et al. Lymphoid tissue inducer–like cells are an innate source of IL-17 and IL-22. *J Exp Med*. 2009;206(1):35–41.
  178. Bando JK, Colonna M. Innate lymphoid cell function in the context of adaptive immunity. *Nat Immunol*. 2016;17(7):783–9.
  179. Sobacchi C, Menale C, Villa A. The RANKL-RANK axis: A bone to thymus round trip. *Front Immunol*. 2019;10(MAR):1–10.
  180. Bichele R, Kisand K, Peterson P, Laan M. TNF superfamily members play distinct roles in shaping the thymic stromal microenvironment. *Mol Immunol*. 2016;72:92–102.
  181. Bernink JH, Germar K, Spits H. The role of ILC2 in pathology of type 2 inflammatory diseases. *Current Opinion in Immunology*. 2014.
  182. Roediger B, Kyle R, Le Gros G, Weninger W. Dermal group 2 innate lymphoid cells in atopic dermatitis and allergy. *Current Opinion in Immunology*. 2014.
  183. Neill DR, Wong SH, Bellosi A, Flynn RJ, Daly M, Langford TKA, et al. Nuocytes represent a new innate effector leukocyte that mediates type-2 immunity. *Nature*. 2010;
  184. Chang YJ, Kim HY, Albacker LA, Baumgarth N, McKenzie ANJ, Smith DE, et al. Innate lymphoid cells mediate influenza-induced airway hyper-reactivity independently of adaptive immunity. *Nat Immunol*. 2011;
  185. Roediger B, Kyle R, Yip KH, Sumaria N, Guy T V., Kim BS, et al. Cutaneous immunosurveillance and regulation of inflammation by group 2 innate lymphoid cells. *Nat Immunol*. 2013;
  186. Monticelli LA, Sonnenberg GF, Abt MC, Alenghat T, Ziegler CGK, Doering TA, et al. Innate lymphoid cells promote lung-tissue homeostasis after infection with influenza virus. *Nat Immunol*. 2011;12(11):1045–54.

187. Monticelli LA, Osborne LC, Noti M, Tran S V., Zaiss DMW, Artis D. IL-33 promotes an innate immune pathway of intestinal tissue protection dependent on amphiregulin-EGFR interactions. *Proc Natl Acad Sci U S A*. 2015 Aug 25;112(34):10762–7.
188. Rak GD, Osborne LC, Siracusa MC, Kim BS, Wang K, Bayat A, et al. IL-33-Dependent Group 2 Innate Lymphoid Cells Promote Cutaneous Wound Healing. *J Invest Dermatol*. 2016;136(2):487–96.
189. Bennett AR, Farley A, Blair NF, Gordon J, Sharp L, Blackburn CC. Identification and characterization of thymic epithelial progenitor cells. *Immunity*. 2002;16(6):803–14.
190. Barik S, Miller MM, Cattin-Roy AN, Ukah TK, Chen W, Zaghouani H. IL-4/IL-13 Signaling Inhibits the Potential of Early Thymic Progenitors To Commit to the T Cell Lineage. *J Immunol*. 2017;199(8):2767–76.
191. White AJ, Baik S, Parnell SM, Holland AM, Brombacher F, Jenkinson WE, et al. A type 2 cytokine axis for thymus emigration. *J Exp Med*. 2017;214(8):2205–16.
192. Ghaedi M, Takei F. Development of Group 2 Innate Lymphoid Cells. *Encycl Immunobiol*. 2016;1(11c):149–55.
193. Oliphant CJ, Hwang YY, Walker JA, Salimi M, Wong SH, Brewer JM, et al. MHCII-mediated dialog between group 2 innate lymphoid cells and CD4+ T cells potentiates type 2 immunity and promotes parasitic helminth expulsion. *Immunity*. 2014;41(2):283–95.
194. Wong SH, Walker JA, Jolin HE, Drynan LF, Hams E, Camelo A, et al. Transcription factor ROR $\alpha$  is critical for nuocyte development. *Nat Immunol*. 2012;13(3):229–36.
195. Cording S, Medvedovic J, Lécuyer E, Aychek T, Déjardin F, Eberl G. Mouse models for the study of fate and function of innate lymphoid cells. *Eur J Immunol*. 2018;48(8):1271–80.
196. Shaw LA, Bélanger S, Omilusik KD, Cho S, Scott-Browne JP, Nance JP, et al. Id2 reinforces TH 1 differentiation and inhibits E2A to repress TFH differentiation. *Nat Immunol*. 2016 Jun 21;17(7):834–43.
197. Cannarile MA, Lind NA, Rivera R, Sheridan AD, Camfield KA, Wu BB, et al. Transcriptional regulator Id2 mediates CD8+ T cell immunity. *Nat Immunol*. 2006;7(12):1317–25.
198. Knell J, Best JA, Lind NA, Yang E, D’Cruz LM, Goldrath AW. Id2 Influences Differentiation of Killer Cell Lectin-like Receptor G1 hi Short-Lived CD8 + Effector T Cells . *J Immunol*. 2013;190(4):1501–9.
199. Omilusik KD, Nadsombati MS, Shaw LA, Yu B, Justin Milner J, Goldrath AW. Sustained Id2 regulation of E proteins is required for terminal differentiation of effector CD8 + T cells. *J Exp Med*. 2018;215(3):773–83.
200. Frias AB, Hyzny EJ, Buechel HM, Beppu LY, Xie B, Jurczak MJ, et al. The

- Transcriptional Regulator Id2 Is Critical for Adipose-Resident Regulatory T Cell Differentiation, Survival, and Function. *J Immunol.* 2019 Aug 1;203(3):658–64.
201. Masson F, Minnich M, Olshansky M, Bilic I, Mount AM, Kallies A, et al. Id2-Mediated Inhibition of E2A Represses Memory CD8 + T Cell Differentiation . *J Immunol.* 2013;190(9):4585–94.
  202. Khan IA, Hwang S, Moretto M. *Toxoplasma gondii*: CD8 T cells cry for CD4 help. *Front Cell Infect Microbiol.* 2019;9(MAY):1–8.
  203. Lin Y-Y, Jones-Mason ME, Inoue M, Lasorella A, Iavarone A, Li Q-J, et al. Transcriptional Regulator Id2 Is Required for the CD4 T Cell Immune Response in the Development of Experimental Autoimmune Encephalomyelitis. *J Immunol.* 2012;189(3):1400–5.
  204. Hwang SM, Sharma G, Verma R, Byun S, Rudra D, Im SH. Inflammation-induced Id2 promotes plasticity in regulatory T cells. *Nat Commun.* 2018;9(1):1–13.
  205. Fujii SI, Shimizu K, Smith C, Bonifaz L, Steinman RM. Activation of natural killer T cells by  $\alpha$ -galactosylceramide rapidly induces the full maturation of dendritic cells in vivo and thereby acts as an adjuvant for combined CD4 and CD8 T cell immunity to a coadministered protein. *J Exp Med.* 2003;198(2):267–79.
  206. Sumaria N, Grandjean CL, Silva-Santos B, Pennington DJ. Strong TCR $\gamma\delta$  Signaling Prohibits Thymic Development of IL-17A-Secreting  $\gamma\delta$  T Cells. *Cell Rep.* 2017 Jun 20;19(12):2469–76.
  207. Ertelt JM, Rowe JH, Johanns TM, Lai JC, McLachlan JB, Way SS. Selective Priming and Expansion of Antigen-Specific Foxp3 – CD4 + T Cells during *Listeria monocytogenes* Infection . *J Immunol.* 2009;182(5):3032–8.
  208. Rees W, Bender J, Teague TK, Kedl RM, Crawford F, Marrack P, et al. An inverse relationship between T cell receptor affinity and antigen dose during CD4+ T cell responses in vivo and in vitro. *Proc Natl Acad Sci U S A.* 1999;96(17):9781–6.
  209. Pepper M, Linehan JL, Pagán AJ, Zell T, Dileepan T, Cleary PP, et al. Different routes of bacterial infection induce long-lived T H 1 memory cells and short-lived T H 17 cells. *Nat Immunol.* 2010;11(1):83–9.
  210. White AJ, Lucas B, Jenkinson WE, Anderson G. Invariant NKT Cells and Control of the Thymus Medulla. *J Immunol.* 2018;200(10):3333–9.
  211. Josefowicz SZ, Lu LF, Rudensky AY. Regulatory T cells: Mechanisms of differentiation and function. *Annu Rev Immunol.* 2012;30:531–64.
  212. Hori S, Nomura T, Sakaguchi S. Control of regulatory T cell development by the transcription factor Foxp3. *J Immunol.* 2017;
  213. Pepper M, Pagán AJ, Igyártó BZ, Taylor JJ, Jenkins MK. Opposing Signals from the Bcl6 Transcription Factor and the Interleukin-2 Receptor Generate T Helper 1 Central and Effector Memory Cells. *Immunity.* 2011 Oct 28;35(4):583–

95.

- 214. McInnes IB, Schett G. The Pathogenesis of Rheumatoid Arthritis.
- 215. James KD, Jenkinson WE, Anderson G. T-cell egress from the thymus: Should I stay or should I go? Vol. 104, *Journal of Leukocyte Biology*. John Wiley and Sons Inc.; 2018. p. 275–84.
- 216. Beerman I, Maloney WJ, Weissmann IL, Rossi DJ. Stem cells and the aging hematopoietic system. *Curr Opin Immunol*. 2010;22(4):500–6.
- 217. Anderson G, Jenkinson EJ. Lymphostromal interactions in thymic development and function. *Nat Rev Immunol*. 2001;1(1):31–40.
- 218. Ting H-A, von Moltke J. The Immune Function of Tuft Cells at Gut Mucosal Surfaces and Beyond. *J Immunol*. 2019;202(5):1321–9.
- 219. Withers DR, Hepworth MR. Group 3 innate lymphoid cells: Communications hubs of the intestinal immune system. Vol. 8, *Frontiers in Immunology*. Frontiers Media S.A.; 2017.
- 220. Wang S, Xia P, Chen Y, Qu Y, Xiong Z, Ye B, et al. Regulatory Innate Lymphoid Cells Control Innate Intestinal Inflammation. *Cell*. 2017;171(1):201–216.e18.
- 221. Bando JK, Gilfillan S, Di Luccia B, Fachi JL, Sécca C, Cella M, et al. ILC2s are the predominant source of intestinal ILC-derived IL-10. *J Exp Med*. 2020 Feb 3;217(2).
- 222. Minton K. Introducing ... thymic tuft cells. *Nat Rev Immunol*. 2018;18(9):542.
- 223. Brown CC, Gudjonson H, Pritykin Y, Deep D, Lavallée VP, Mendoza A, et al. Transcriptional Basis of Mouse and Human Dendritic Cell Heterogeneity. *Cell*. 2019 Oct 31;179(4):846–863.e24.
- 224. Vély F, Barlogis V, Vallentin B, Neven B, Piperoglou C, Ebbo M, et al. Evidence of innate lymphoid cell redundancy in humans. *Nat Immunol*. 2016;17(11):1291–9.
- 225. De Pooter RF, Kee BL. E proteins and the regulation of early lymphocyte development. *Immunol Rev*. 2010;238(1):93–109.
- 226. Gapin L. Development of invariant natural killer T cells. *Current Opinion in Immunology*. 2016.
- 227. Krovi SH, Gapin L. Invariant natural killer T cell subsets-more than just developmental intermediates. *Front Immunol*. 2018;9(JUN):1–17.
- 228. Monticelli LA, Yang Y, Knell J, D’Cruz LM, Cannarile MA, Engel I, et al. Transcriptional regulator Id2 controls survival of hepatic NKT cells. *Proc Natl Acad Sci U S A*. 2009;106(46):19461–6.
- 229. Xu W, Cherrier DE, Chea S, Vosshenrich C, Serafini N, Petit M, et al. An Id2RFP-Reporter Mouse Redefines Innate Lymphoid Cell Precursor Potentials. *Immunity*. 2019;50(4):1054–1068.e3.